

AD-A174 974

THE SCIENCE OF AND ADVANCED TECHNOLOGY FOR
COST-EFFECTIVE MANUFACTURE OF (U) PURDUE UNIV
LAFAYETTE IN SCHOOL OF INDUSTRIAL ENGINEERING

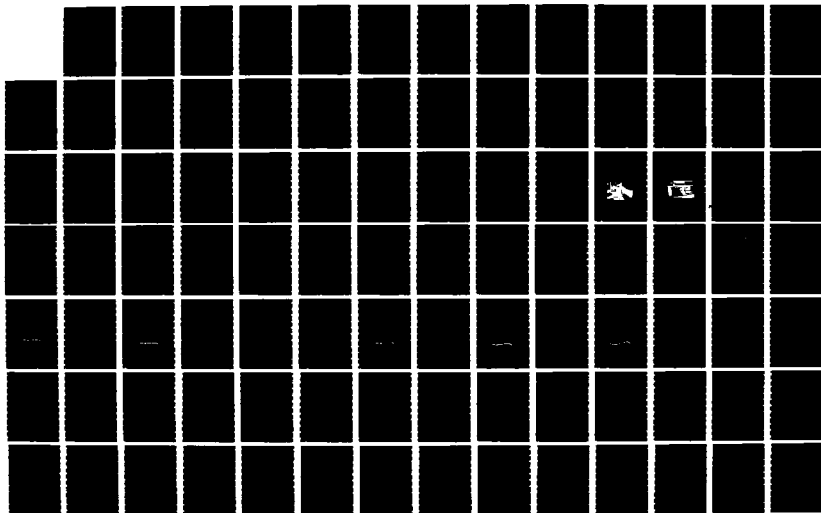
1/4

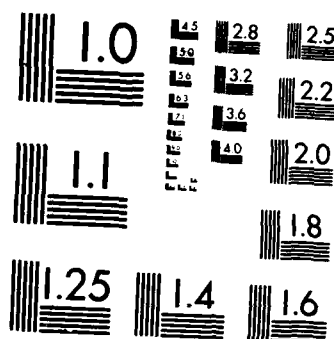
UNCLASSIFIED

S LEE ET AL NOV 86 N00014-83-K-0385

F/G 13/9

NL





XEROCOPY RESOLUTION TEST CHART
NATIONAL BUREAU OF STANDARDS-1963-A

AD-A174 974

DTIC FILE COPY

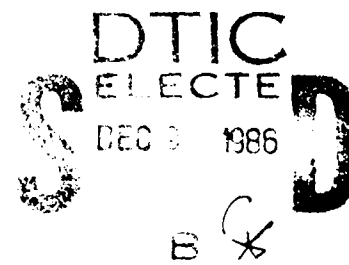
THE SCIENCE OF AND ADVANCED TECHNOLOGY FOR
COST-EFFECTIVE MANUFACTURE
OF HIGH PRECISION ENGINEERING PRODUCTS

ONR Contract No. 83K0385
FINAL REPORT
Vol. 6

ACCURACY IMPROVEMENT
OF A CNC MACHINING CENTER
BY USING
A TOUCH PROBE AND A METROLOGY PALLET

PREPARED BY
S.K. Lee and M.M. Barash

NOVEMBER 1986



Schools of
Industrial, Electrical and Mechanical Engineering
Purdue University
West Lafayette, Indiana 47907

DISTRIBUTION STATEMENT
Approved for public release
Distribution unlimited

86 11 26 002

REPORT DOCUMENTATION PAGE

1a REPORT SECURITY CLASSIFICATION None			1b RESTRICTIVE MARKINGS None		
2a SECURITY CLASSIFICATION AUTHORITY None			3 DISTRIBUTION / DISTRIBUTION OF REPORT DISTRIBUTION STATEMENT A Approved for public release; Distribution Unlimited		
2b DECLASSIFICATION / DOWNGRADING SCHEDULE None					
4 PERFORMING ORGANIZATION REPORT NUMBER(S) Final Report Vol. 6			5 MONITORING ORGANIZATION REPORT NUMBER(S)		
6a NAME OF PERFORMING ORGANIZATION PURDUE UNIVERSITY		6b OFFICE SYMBOL (If applicable)	7a NAME OF MONITORING ORGANIZATION Department of Defense Office of Naval Research		
6c ADDRESS (City, State, and ZIP Code) School of Industrial Engineering West Lafayette, Indiana 47907			7b ADDRESS (City, State, and ZIP Code) Arlington, VA 22217-5000		
8a NAME OF FUNDING / SPONSORING ORGANIZATION		8b OFFICE SYMBOL (If applicable) 614A	9 PROCUREMENT INSTRUMENT IDENTIFICATION NUMBER N00014-83-K-0385/12/12		
8c ADDRESS (City, State, and ZIP Code)			10 SOURCE OF FUNDING NUMBERS		
			PROGRAM ELEMENT NO ONR:433	PROJECT NO	TASK NO SRO-150
			WORK UNIT ACCESSION NO		
11 TITLE (Include Security Classification) ACCURACY IMPROVEMENT OF A CNC MACHINING CENTER BY USING A TOUCH PROBE AND A METROLOGY PALLET					
12 PERSONAL AUTHOR(S) Lee, S.K. and M. M. Barash					
13a TYPE OF REPORT Final		13b TIME COVERED FROM 1/83 TO 6/86	14 DATE OF REPORT (Year, Month, Day) November 1986		15 PAGE COUNT 299
16 SUPPLEMENTARY NOTATION					
17 COSATI CODES			18 SUBJECT TERMS (Continue on reverse if necessary and identify by block number)		
FIELD	GROUP	SUB GROUP	Precision engineering; Metrology; NC machine tools; Flexible Manufacturing Systems.		
13					
19 ABSTRACT (Continue on reverse if necessary and identify by block number)					
<p>Errors in the position of the tool tip in the work space of a machine tool are a major problem in precision engineering. The problem of determining these errors in a convenient and acceptable way for a certain thermal condition of a given machine tool has not yet been fully solved, for the unmanned manufacturing environment.</p> <p>To determine the errors in the position of the tool tip with a touch probe, a metrology pallet was used. The error model for touch probe application has been constructed using actual error measurements. An error calculation procedure, including the calibration of the metrology pallet on a machine tool, is formulated. Two approaches to obtaining error regression functions at a tool tip position have been formulated using one or two touch probes and the metrology pallet.</p> <p>A procedure for the decomposition of the probed errors into error components is set-up using the regression analysis. It establishes the relative contribution of each error component to the change in the resultant errors in the work space.</p> <p>(continued on back)</p>					
20 DISTRIBUTION AVAILABILITY OF ABSTRACT <input type="checkbox"/> UNCLASSIFIED/UNLIMITED <input checked="" type="checkbox"/> SAME AS RPT <input type="checkbox"/> DTIC USERS			21 ABSTRACT SECURITY CLASSIFICATION None		
22a NAME OF RESPONSIBLE INDIVIDUAL Dr. A. L. Meyrowitz			22b TELEPHONE (Include Area Code) 202-696-4302		22c OFFICE SYMBOL 433

(19) Continued

) A "dynamic" method of compensating the backlash is proposed using ANOVA (Analysis of Variance) analysis to determine the important factors affecting the backlash. Determination of probing intervals for the metrology pallet is done dynamically according to the thermal change of the machine tool using the drift error model obtained by General Method of Data Handling (GMDH) technique of Ivakhnenko.

Workpiece dimensional variations occurring when the temperature of the environment deviates from the calibration temperature can be compensated because the metrology pallet made of steel reflects this change.

A machining experiment has been conducted in a Flexible Manufacturing System environment to check the acceptability of the concept of using a touch probe and a metrology pallet for the compensation of errors in the work space of a machine tool. Around 50% of error reduction was obtained for the sample machining experiment.

THE SCIENCE OF AND ADVANCED TECHNOLOGY
FOR COST-EFFECTIVE MANUFACTURE
OF HIGH PRECISION ENGINEERING PRODUCTS

ONR Contract No. 83K0385
Final Report
Vol. 6

ACCURACY IMPROVEMENT
OF A CNC MACHINING CENTER
BY USING
A TOUCH PROBE AND A METROLOGY PALLET

Prepared by
S. K. Lee and M. M. Barash

November 1986

Schools of
Industrial, Electrical and Mechanical Engineering
Purdue University
West Lafayette, Indiana 47907

This report represents, with minor changes, the thesis submitted by Mr. Suk-Ho Lee to the Faculty of Purdue University for the award of the Degree of Doctor of Philosophy.

Research described in this report has been supported by the Office of Naval Research through Contract No. N83K0385 in the framework of the ONR Precision Engineering projects. M. M. Barash served as Major Professor for the thesis; he is a member of the faculty of the School of Industrial Engineering at Purdue University.

Work on the Precision Engineering project at Purdue University greatly benefited from the use of the technical facilities of the Purdue Computer Integrated Design, Manufacturing and Automation Center (CIDMAC) and the advice of the CIDMAC member companies*, which is gratefully acknowledged.

Accession For	
NTIS GRA&I	<input checked="" type="checkbox"/>
DTIC TAB	<input type="checkbox"/>
Unannounced	<input type="checkbox"/>
Justification	
PER LETTER	
By	
Distribution/	
Availability Codes	
Dist	Avail and/or Special
A-1	



Moshe M. Barash
Principal Investigator

C. Richard Liu
Principal Investigator

**DTIC
ELECTE
S DEC 9 1986 D
B**

*Member companies of CIDMAC are:

Cincinnati Milacron; TRW; Ransburg Corporation; Cummins Engine Co.; Control Data Corporation; ALCOA; Chrysler.

TABLE OF CONTENTS

	Page
LIST OF TABLES.....	v
LIST OF FIGURES.....	viii
ABSTRACT.....	xvi
1. INTRODUCTION.....	1
1.1 Problem Statement.....	1
1.2 Literature Survey.....	3
1.3 The Scope of the Study.....	12
2. ERROR ANALYSIS AND PREDICTION.....	15
2.1 Positioning Error.....	15
2.1.1 Positioning Error Prediction using GMDH.....	22
2.1.2 Repeatability and Thermal Drift.....	32
2.2 Backlash Analysis and Compensation.....	40
2.3 Angular Error Prediction using GMDH.....	46
3. METHODOLOGY.....	57
3.1 Volumetric Error Assessment.....	57
3.2 Mathematical Error Modeling for Touch Probe Application.....	64
3.3 Calculation of an Error.....	73
3.4 Calibration of the Metrology Pallet.....	76
3.5 Decomposition of the Resultant Error to Error Components.....	83
3.6 Determination of Measurement Points by a Touch Probe.....	87
4. ONE DIMENSIONAL EXPERIMENT AND ANALYSIS.....	89
4.1 Experimental Setup.....	89
4.2 Analysis and Results.....	91
4.3 Conclusion for One Dimensional Analysis.....	96

5. THREE DIMENSIONAL PROBING EXPERIMENT.....	98
5.1 Experimental Setup.....	101
5.1.1 Design of the Metrology Pallet.....	102
5.1.2 Construction of a Long Touch Probe.....	104
5.2 Experimental Procedure.....	108
5.2.1 Acquisition of Data.....	109
5.2.1.1 Acquisition of Probe Information Data.....	109
5.2.1.2 Acquisition of Temperature Data.....	112
6. ANALYSIS OF THREE DIMENSIONAL PROBING EXPERIMENT.....	119
6.1 Repeatability of a Touch Probe.....	119
6.2 Regression Prediction of Errors at Work Space.....	124
6.3 Determination of Probing Interval using GMDH.....	129
6.4 Decomposition of Resultant Error into Error Components.....	137
6.5 Determination of Measurement Points.....	147
7. MACHINING EXPERIMENT.....	156
7.1 Experimental Setup.....	156
7.1.1 Design of the Workpiece.....	157
7.1.2 Experimental Procedure.....	158
7.1.3 Machining Program Preparation.....	160
7.2 Analysis.....	162
8. CONCLUSIONS.....	172
9. RECOMMENDATIONS.....	176
LIST OF REFERENCES.....	179
APPENDICES	
Appendix 1 GMDH Modeling Technique.....	184
Appendix 2 Data for One Dimensional Error Analysis..	191
Appendix 3 Location of Temperature Points.....	201
Appendix 4 Data for Probing Experiment.....	207
Appendix 5 Repeatability Data for Probing Experiment	254
Appendix 6 Result of Decomposition Procedure.....	257
Appendix 7 Analysis Data for Machining Experiment...	268
Appendix 8 Project Staff in 1985-1986.	280

LIST OF TABLES

Table	Page
2.1 Output of 3-way anova analysis for backlash.....	44
2.2 Repeatability of a machining center according to thermal conditions, feed rates, positions, moving directions.....	54
2.3 Mean of the backlash of a machining center according to thermal conditions, feed rates, positions.....	55
4.1 Repeatability of a touch probe in the cold and the warmed-up condition when experimented for one dimensional analysis.....	96
5.1 Temperatures when the calibration probing is done...	108
6.1 Repeatability of a touch probe at the machine tool in the cold and the warmed-up condition when experimented for one dimensional analysis.....	120
6.2 Repeatability of the long probe in the cold condition.....	121
6.3 Repeatability of the long probe in the warm condition.....	122
6.4 Repeatability result of test no. 11 for three positions for a short and a long probes.....	127
6.5 Result of decomposition with the assumption of linear positioning error for test no. 11 using a short probe.....	148
6.6 Point numbers of outliers after the residual analysis for a long probe system.....	153
6.7 Variation of standard deviation of error regression function for a long and a short probes.....	154
6.8 Variation of MSE and confidence interval according to the number of points for test no. 11 of a short probe system.....	155

Table	Page
7.1 Variation of a tool diameter after each completion of machining 110 mm for 11 minutes.....	166
7.2 Machining error and its calculation using a pallet system.....	169
7.3 Error after compensation by a pallet system with cold machining error taken into account.....	170
7.4 Percentage error after compensation by a pallet system with and without the cold machining error taken into account.....	171
Appendix	
Table	
A.2.1 Part of output of 4-way ANOVA analysis program for backlash.....	199
A.3.1 Location of temperature points for x axis.....	201
A.3.2 Location of temperature points for y axis.....	202
A.3.3 Location of temperature points for z axis.....	203
A.4.1 Error data for three dimensional probing experiments with temperature information.....	210
A.5.1 Repeatability result of test no. 1 for three positions for a short and a long probes.....	254
A.5.2 Repeatability result of test no. 7 for three positions for a short and a long probes.....	254
A.5.3 Repeatability result of test no. 11 for three positions for a short and a long probes.....	255
A.5.4 Repeatability result of test no. 19 for three positions for a short and a long probes.....	255
A.5.5 Repeatability result of test no. 21 for three positions for a short and a long probes.....	256
A.6.1 The result of decomposition procedure for a short probe of test no. 11 with the quadratic assumption of positioning errors.....	258

Table	Page
A.6.2 The result of decomposition procedure for a long probe of test no. 11 with the quadratic assumption of positioning errors.....	259
A.6.3 The result of decomposition procedure for a long probe of test no. 11 with the linear assumption of positioning errors.....	260
A.6.4 The result of decomposition result when using two probes for test no. 11.....	261
A.6.5 FORTRAN program to calculate the coefficients of decomposed error component equations for a short probe approach.....	262

LIST OF FIGURES

Figure	Page
2.1 The cyclic error and the hysteresis with 0.1 mm increment.....	16
2.2 The Hewlett-Packard laser interferometer set-up for y axis positioning error measurement.....	17
2.3 The Hewlett-Packard laser display and the HP microcomputer system for data acquisition system.....	18
2.4 Positioning error measured three times for the whole y axis in increments of 10 mm and its hysteresis in the warm condition.....	21
2.5 Positioning error measured three times for the whole y axis in increments of 48 mm and its hysteresis in the cold condition.....	23
2.6 Positioning error measured three times for the whole y axis in increments of 48 mm and its hysteresis in the warm condition.....	25
2.7 Error change and its GMDH prediction for a whole day measurement with 48 mm increment.....	27
2.8 Error measurement after 230 minutes of movement with 1 mm increment.....	29
2.9 Error measurement after 230 minutes of movement with 10 mm increment.....	31
2.10 Error measurement after 860 minutes of movement with 1 mm increment.....	33
2.11 The GMDH prediction result of errors observed after 860 minutes for upward movement(3560 data points for training and 406 data points for checking).....	35
2.12 The GMDH prediction result of errors observed after 860 minutes for upward movement(3506 data points for training and 330 data points for checking).....	37

Figure	Page
2.13 The GMDH prediction result of errors observed after 860 minutes for upward movement(2700 data points for training and 606 data points for checking).....	39
2.14 The GMDH prediction result of errors observed after 740 minutes for upward movement.....	41
2.15 The GMDH prediction result of errors observed after 860 minutes for downward movement.....	43
2.16 The GMDH prediction result of errors observed after 740 minutes for downward movement.....	45
2.17 Thermal drift error after each trip of 20 mm and its change at top position.....	47
2.18 Drift error after a round trip of a short distance of 10 mm and its GMDH prediction for a bottom point.....	49
2.19 Drift error after a whole axis movement of 660 mm and its GMDH prediction for a bottom point.....	50
2.20 The GMDH prediction result on y axis drift error for a whole day experiment.....	51
2.21 The GMDH prediction result on y axis drift error with different set of experiment data for a whole day experiment.....	52
2.22 The GMDH prediction result on y axis drift error with different arrangement of input data.....	53
2.23 The result of the GMDH prediction on the x axis pitch error and its residual.....	56
3.1 The error components of x axis and their notations..	61
3.2 Non-orthogonality errors of moving axes with the assumption of the coincidence of the z moving axis with the z reference axis.....	63
3.3 The effect of the error components on the resultant work space error vector.....	65
3.4 One probe approach to obtain errors in the work space.....	70

Figure	Page
3.5 Two probe approach to obtain errors in the work space.....	72
3.6 The transform equations for the error of the probe tip position.....	74
3.7 Variation of a coordinate system at the machine because of the waviness of the surfaces, clamping forces, and so on.....	77
3.8 Differential change of a coordinate system with respect to x, y, and z axis at the machine.....	79
3.9 Four coordinate values from two extreme points used for calibration after homogeneous transformation....	80
4.1 The picture of the set-up for one dimensional experiment.....	90
4.2 The error after compensation in the cold condition for one dimensional experiment.....	94
4.3 The error after compensation in the warm condition for one dimensional experiment.....	95
5.1 The picture of the metrology pallet constructed with 34 measurement points.....	103
5.2 Temperature variation of metrology pallet without movement.....	105
5.3 Temperature variation of x axis without movement.....	107
5.4 Temperature variation of y axis without movement.....	110
5.5 Temperature variation of z axis without movement.....	111
5.6 The picture of the short probe and the long probe..	113
5.7 The picture of the information acquisition system for probing.....	114

Figure	Page
5.8 Temperature variation of metrology pallet with movement.....	115
5.9 Temperature variation of x axis with movement.....	116
5.10 Temperature variation of y axis with movement.....	117
5.11 Temperature variation of z axis with movement.....	118
6.1 The prediction result of x errors and residuals measurement origin by regression.....	126
6.2 The prediction result of y errors and residuals measurement origin by regression.....	128
6.3 The prediction result of relative z errors and residuals for the point no. 11 by regression.....	130
6.4 The prediction result of relative y errors and residuals for the point number 22 by regression....	132
6.5 GMDH prediction on x drift error of measurement origin using 21 set of data.....	134
6.6 GMDH prediction on x drift error of measurement origin using 20 set of data.....	136
6.7 GMDH prediction on x drift error of measurement origin using 18 set of data.....	138
6.8 GMDH prediction on x drift error of measurement origin using 11 set of data.....	140
6.9 GMDH prediction on y drift error of measurement origin using 20 set of data.....	142
6.10 GMDH prediction on z relative error of point 11 using 20 set of data.....	144
6.11 GMDH prediction on y relative error of point 22 using 21 set of data.....	146

Figure	Page
6.12 Results of GMDH prediction on x pitch error when calibration is done and test no. 11.....	149
6.13 Comparison between the GMDH prediction and the decomposed results for x pitch error.....	151
7.1 Workpiece prepared for machining experiment and the cutting tool.....	158
7.2 Workpiece being measured at the Zeiss coordinate measuring machine.....	160
7.3 The pictures of the machine controller.....	165
7.4 Error after the non-compensation machining and the compensation without cold machining errors.....	167
7.5 Error after the non-compensation machining and the compensation with cold machining errors.....	168
Appendix	
Figure	
A.1.1 Basic scheme of propagation of variables.....	186
A.1.2 Input to the GMDH algorithm.....	188
A.1.3 Construction of the new array Z to compute next generation of variables.....	190
A.2.1 Positioning error and its hysteresis for a whole y axis movement after 360 minutes with 1 mm increment.....	191
A.2.2 Positioning error and its hysteresis for a whole y axis movement after 490 minutes with 1 mm increment.....	192
A.2.3 Positioning error and its hysteresis for a whole y axis movement after 610 minutes with 1 mm increment.....	193
A.2.4 Positioning error and its hysteresis for a whole y axis movement after 740 minutes with 1 mm increment.....	194

Figure	Page
A.2.5 GMDH prediction on the drift error after each trip of 20 mm at 0 mm.....	195
A.2.6 GMDH prediction on the drift error after each trip of 20 mm at 5 mm(down).....	196
A.2.7 GMDH prediction on the drift error after each trip of 1320 mm at 660 mm.....	197
A.2.8 GMDH prediction on the drift error after each trip of 1320 mm at 330 mm.....	198
A.3.1 Location of temperature points of x axis.....	204
A.3.2 Location of temperature points of y axis.....	205
A.3.3 Location of temperature points of z axis.....	206
A.4.1 Numbering system for a pallet before residual analysis.....	207
A.4.2 Numbering system for a pallet after residual analysis.....	208
A.4.3 The regression result of x absolute errors of test 11 and residual for short probe.....	231
A.4.4 The regression result of x absolute errors of test 11 and residual for long probe.....	232
A.4.5 The regression result of y absolute errors of test 11 and residual for short probe.....	233
A.4.6 The regression result of y absolute errors of test 11 and residual for long probe.....	234
A.4.7 The regression result of z absolute errors of test 11 and residual for short probe.....	235
A.4.8 The regression result of z absolute errors of test 11 and residual for long probe.....	236

Figure	Page
A.4.9 The variation of x,y, and z errors for the measurement origin during three day experiment....	237
A.4.10 The regression result of x absolute errors of point 1 and residual for long probe.....	238
A.4.11 The regression result of x absolute errors of point 1 and residual for two probe.....	239
A.4.12 The regression result of y absolute errors of point 1 and residual for long probe.....	240
A.4.13 The regression result of y absolute errors of point 1 and residual for two probe.....	241
A.4.14 The regression result of z absolute errors of point 1 and residual for short probe.....	242
A.4.15 The regression result of z absolute errors of point 1 and residual for long probe.....	243
A.4.16 The variation of absolute error for point 11 during experiment.....	244
A.4.17 The variation of relative error for point 11 during experiment.....	245
A.4.18 The regression result of x absolute errors of point 11 and residual for short probe.....	246
A.4.19 The regression result of x absolute errors of point 11 and residual for long probe.....	247
A.4.20 The regression result of x absolute errors of point 11 and residual for two probe	248
A.4.21 The regression result of y absolute errors of point 11 and residual for short probe.....	249
A.4.22 The regression result of y absolute errors of point 11 and residual for long probe.....	250
A.4.23 The regression result of y absolute errors of point 11 and residual for two probe	251

Figure	Page
A.4.24 The regression result of z absolute errors of point 11 and residual for long probe.....	252
A.4.25 The variation of relative error for point 22 during experiment.....	253
A.7.1 Numbering system for corners of a workpiece for the machining experiment.....	268

ABSTRACT

Errors in the position of the tool tip in the work space of a machine tool are a major problem in precision engineering. The problem of determining these errors in a convenient and acceptable way for a certain thermal condition of a given machine tool has not yet been fully solved, for the unmanned manufacturing environment.

To determine the errors in the position of the tool tip with a touch probe, a metrology pallet was used. The error model for touch probe application has been constructed using actual error measurements.

An error calculation procedure, including the calibration of the metrology pallet on a machine tool, is formulated. Two approaches to obtaining error regression functions at a tool tip position have been formulated using one or two touch probes and the metrology pallet.

A procedure for the decomposition of the probed errors into error components is set-up using the regression analysis. It establishes the relative contribution of each error component to the change in the resultant errors in the work space.

A "dynamic" method of compensating the backlash is proposed using ANOVA(Analysis of Variance) analysis to determine the important factors affecting the backlash. Determination of probing intervals for the metrology pallet is done dynamically according to the thermal change of the machine tool using the drift error model obtained by General Method of Data Handling(GMDH) technique of Ivakhnenko.

Workpiece dimensional variations occurring when the temperature of the environment deviates from the calibration temperature can be compensated because the metrology pallet made of steel reflects this change.

A machining experiment has been conducted in a Flexible Manufacturing System environment to check the acceptability of the concept of using a touch probe and a metrology pallet for the compensation of errors in the work space of a machine tool. Around 50 % of error reduction was obtained for the sample machining experiment.

1 - INTRODUCTION

1.1 Problem Statement

Inaccuracy of the finished workpiece can be attributed to several factors. These factors are classified as follows:[1]

- 1.Geometric and kinematic errors of the machine tool.
- 2.Spindle errors of the machine tool.
- 3.Thermal effects on the machine tool and on the workpiece.
- 4.Static and dynamic loading.
- 5.Tool wear.
- 6.Errors due to work holding.

Among these factors, machine related errors consist of the major portion of the workpiece error. Geometric and kinematic errors exist when the machine is cold. Thermal errors are added as the machine warms up. A certain opinion was reported that thermal errors account for 50-70 percent of the total error in machine tools.[2]

There are two approaches to achieve improvement in the machine tool accuracy. The one is error avoidance and the other is error compensation. While the former has been by

no means completely achievable, the latter has been preferred as a convenient means to reduce the error. Software compensation of errors is generally achieved by storing the actually measured error values in computer memory (like look-up tables). This is limited by the computer memory and/or the input data measured. Because the thermal effect and other factors are varied, the measured data may not be able to represent the actual error all the time. Several trials [3,4,5] to measure and correct the errors have been done, but only to correct partial errors. As the machine continues to operate, the thermal condition and the whole error phenomenon change. The problem of determining the errors directly at the tool tip position for a certain thermal condition has not yet been fully solved.

The present study will attempt to provide an effective and easy means to detect the resultant errors directly at the tool tip in the work space as the thermal condition changes. This is achieved by using a touch probe system in conjunction with a metrology pallet.

A mathematical model is generated to represent the work space error using probed errors. This mathematical model leads to the model for the decomposition of the resultant error to its components along each axis. Therefore modeling the error component is necessary to compare with the decomposed result.

NC tape modification is the method to be used for the compensation. It is acceptable because most operations of a machining center need point-to-point positioning in relatively stable thermal conditions during the machining of a specific workpiece. While the study will concentrate on one type and size of machining center, the general idea extends to any type and size of machining center.

In order to validate the theory and the methodology developed in this study, a Cincinnati Milacron CNC machining center T-10, with its ACRAMATIC 900 controller, was used as a test machine. X and y travel range are 26 inches each and the maximum tool length allowable at the tool chain is 17 inches. Resolution of the machine is 1/10000 inch, which is also the limit for the position modification due to the compensation. This machine has a rotating pallet changer, which enables the simulation of an FMS environment.

1.2 Literature Survey

Static machine tool errors can be classified as belonging to two categories: geometric errors and thermal errors. The accuracy of the machine tool within the work space is greatly affected by the following geometric errors: positioning, straightness, squareness, and rotational errors like pitch, roll, and yaw errors. Geometric

errors change as the thermal condition of the machine tool changes. The heat from the spindle, the motors, the drive mechanisms, chips and so on is believed to contribute the most to the deterioration of the machine tool accuracy in the machining environment.[2] Also, the temperature change of the environment during the day is significant if there is no control of room temperature.

Many researchers have attempted to determine the errors in the position of the tool tip within the work space. Love and Scarr[6] analyzed the volumetric accuracy by determining the combined effects of errors in the measuring system and errors in geometric features, which showed the importance of the error concept within the work space.

Schultschik[3] investigated the problem of combining the measured error components which were dependent on both the coordinates and the offsets within the working volume. Mathematical rules were used for the systematic errors but not for the random errors. His analysis was based on the vector diagrams for the structure of the machine tool. Using a transformation matrix he presented the complete equation with a simplified presentation of the matrices including 18 errors within the axes, 5 errors of non-orthogonality, and 12 setting errors for the tool and the workpiece. But in common machining environments it is very

difficult to keep the temperature of the machine tool and the environment constant when measuring all these error components. Therefore it is very difficult to obtain the entire volumetric error "map" at a certain time in a certain thermal condition by combining the measured error components.

Systematic approaches to understand the problem of three-dimensional metrology were taken by Hocken et al.[7] They analyzed the three-dimensional measurement process using rigid body kinematics, the temporal modeling technique, and the multiple redundancy technique. The rigid body kinematics approach involved three coordinate systems: the space system, the table system, and the object system. They chose the minimum number of ideal reference frames necessary to characterize a machine and used matrix transformations to relate coordinates in these chosen frames. Temporal modeling was used to eliminate the drift and temporal variations in measured values by statistical methods. To eliminate the non-orthogonality and scale errors in the measurements the multiple redundancy method was used. The error "map" produced by this procedure for every component of the error was stored and used as a correction factor when the actual measurement was done. But this requires that the same thermal condition be applied as that, when the measurements were made. It needs tremendous time and efforts to measure the error components.

Thermal effects on the accuracy have also been looked into by several investigators.[8,9,10,11] In these studies the finite element technique was generally used to evaluate the deformation characteristics of machine tools. Then experimental data were used to evaluate the accuracy of predictions from numerical methods. However, due to the inaccuracy of information on heat sources and heat transfer at joints, computations to determine the thermal deformation behavior of machine tools provided no more than trend predictions.

Okushima [12] studied the reduction of the machining error caused by thermal deformation of machine tools using the coordinate system correction. The results indicated that the deformation and the loss in accuracy responded in the manner of a first order time lag to the heat generating rate and that there was no time lag between the thermal displacements and temperature elevations. Based on these results, they applied compensation by coordinate system correction using analog and digital techniques.

Sata [13] proposed the compensation method for the geometric error and the thermal deformation error. The geometric error of the machine tool was estimated in advance by using a standard master part fixed on the table. The relative displacement between the workpiece and the spindle caused by the thermal deformation of the machine

tool was evaluated during the operation, using a simplified finite element model of the structure, from temperature measurements taken from the machine tool. Master part and micrometer sets gave only the two-dimensional geometric errors. The accuracy of these sets may not be sufficient for them to be used for the purpose of error compensation. A simplified FEM model with a small number of temperature node information calculates the approximation of the spindle dimension variation. After finding the deformation error they fed the data to a minicomputer and modified the NC tape to compensate for the anticipated error.

The advantages of a 3-D probe system for numerically controlled machine tools were reported by Pfeifer and Furst.[14,15] The reduction of production uncertainties was obtained by adapting a 3-D probe system to a machine tool with suitable controls and unified interfaces. They found that in order to achieve accurate measurements, the random error of the unloaded machine tool and the 3-D probe must be small compared to the machining error. They concluded that systematic machining errors such as thermal displacements of the coordinate system and geometric errors of machine slideways could be compensated for.

As unmanned manufacturing has proceeded, sensors were reported to be one of the most important factors for flexible automation by Schaffer.[16]

One of the most significant developments has been the introduction of machine-mounted probes for setup work, part alignment, and a variety of in-process gaging operations. They can be handled by automatic tool changers and, when combined with software recently available for many CNC systems, can be automatically cycled through significant measuring routines.[17,18,19,20,21,22] Non contact probe has been developed to replace the contact probe on the coordinate measuring machine.[23]

Schultschik[24] analyzed the possibilities and limits of error feedback in automatic machining using a 3-D probe. He showed that the compensation of distance deviation between individual surfaces in the machining cycle is possible and can be included in the automatic sequence using CNC software. The reduction of certain machine errors and load effects is also described. The emphasis on the metrology in the Integrated Manufacturing System is done by Peters.[25] He reported a 95 % savings of time in his research which shows the importance of automatic measuring.

Sweet, Noller and Lee[26] performed statistical analysis to determine the location of a plane and a circle on the workpiece using a touch probe and suggested the possibility of using the probe for the determination of the workpiece location for compensation purpose.

Kearney & Trecker Co. is reported to be developing a continuous automatic compensation system, called the ADEC(Automatic Dynamic Error Compensation) system.[27] One end of a notched invar plate precisely calibrated by a laser is screwed to the machine bed for each of the three axes and a magnetic reader head was attached to the moving component to sense the positioning error and the change of the machine coordinate due to the thermal effects. This system is supposed to take care of the systematic positioning error and thermal effects on the positioning error of each axis, but not the Abbe offset error and rotational error components. A similar idea, using an invar bar, was mentioned in the proposal for research submitted to Office of Naval Research by Barash & Liu[28], by which the major research effort in precision engineering was launched at Purdue University.

Barash & Lee[29] suggested the adaptation of the touch probe for compensation of 3-dimensional resultant errors within the work space for the machining center using the pallet concept, which is applicable to Flexible Manufacturing Systems. They claimed that by intermittent probing of a precisely calibrated measurement pallet the systematic resultant errors within the work space and the thermal effects could be measured and compensated for. Also, the thermal drift was eliminated by probing the workpiece pallet whenever it was loaded on to the table.

While the combined error in the workspace is the major target of the studies[3,6,7,30], investigations on the error component have been done by many researchers.[31,32,33,34,35] Hemingray et.al[36,37] compared the existing testing method of the positioning accuracy. He suggested the necessity for more than adequate dealing with lost motion, cyclic error, and drift. Positioning error of a single cutting lathe is investigated by Vannerck et.al[38]. They showed that the most important feed error component is a cyclic one whose periodicity corresponds to the rotation of the lead screw. They show that this cyclic error is due to a periodical axial slip of the lead screw itself. They do not show any functional relationship of the error component for the compensation.

Kamyshev[39] analyzed the testing methods for the positioning accuracy of NC machine tools. The cumulative and periodic components are investigated and the non-identical measurement interval is found by determining the integral index of the systematic deviation.

Those complex error phenomenon lead to the uncertainty study of multi-axis machines.[40] One-, Two-, and Three-dimensional uncertainty for measurement by displacements of axes are proposed. The development of adequate calibrating systems and methods is recognized to be necessary. In addition, the research on the cause of uncertainty and its

control is needed. Knapp[41] proposed the circular test method to determine the influence of the single machine errors on the machined circular shape in two dimension.

Intensive research has been launched at Purdue University by the precision engineering group. Venugopal[42] showed the prediction capability of regression function on the thermal errors within the 80 % range. He proposed numerical methods for evaluating the errors exhibited by the slides of the machine. Liu and Ferreira[43] introduced the General Method of Data Handling(GMDH) technique of Russian engineer Ivakhnenko[44,45] on obtaining the self-organizing error compensation system. The algorithm was tested on the experiment data of the x pitch error. It showed the excellent prediction capability of the technique on the error.

Donmez[46] proposed a general methodology for the machine tool accuracy enhancement. He developed a general mathematical model to determine the total error at the cutting tool tip by using homogeneous coordinate transformations. A flexible and modular software compensation system was developed based on the models obtained by modeling the measured data for an entire thermal condition. Least squares curve fitting technique is used in modeling the error. A single-board microprocessor-based system translates errors into servo counts, which are injected

into the machine tool controller in real-time. While this system has the advantage of an accurate compensation capability, there may be some problems in applying the system. To obtain all the errors in the wide range of thermal conditions, a long period of measurement may be needed perhaps several months. The large thermal change of the environment including seasonal changes may invalidate the calibration result obtained by the previous error modeling.

Ferreira and Liu[47] proposed an analytical quadratic model for the geometric error of a machine tool. The assumption of the linear variation of individual errors gives the quadratic error model.

1.3 The Scope of the Study

As is seen in the above summary, there is a lack of a systematic approach to compensate easily for the work space error. The purpose of this research is to develop a general mathematical model and the methodology necessary to increase the accuracy of a CNC machining center by compensating for the systematic errors. A secondary goal is to validate the model and the methodology by doing the necessary experiments and analyses.

The objective is to obtain the position errors of the tool tip within a given work space under varying thermal conditions by using a touch probe. This study tries to

find an easy and clear way to obtain the resultant work space error by using a commercially available touch probe and a constructed metrology pallet. For obtaining the error "map" of a machine tool in the whole work space, the touch probe technique is used with a master metrology pallet. The master pallet has several measurement points and is mounted on the machine table at certain intervals to measure the thermal effects on the geometric and kinematic errors. Thermal drift is also eliminated by probing the workpiece pallet whenever it is loaded on the table.

Once a master pallet is calibrated, the differences between the calibrated measurements and the probed measurements can be used to compensate for thermal growth of the machine tool. Workpiece error due to the thermal change can be compensated because the master pallet will reflect this change.

The thesis is split into two broad parts: one dimensional analysis and three dimensional analysis. In Chapter 2, the one dimensional error analysis is completed. The positioning error and the angular error are modeled by the General Method of Data Handling (GMDH) technique of the Russian engineer Ivakhnenko[44]. The backlash phenomenon and the drift phenomenon are analyzed. In Chapter 3, the mathematical models for the probed work space error, the decomposition procedure and the calibration procedure are

developed. The one dimensional probing experiment is described in Chapter 4. In this chapter errors measured by the laser interferometer are compared with those measured by probing one dimensional metrology pallet to see the feasibility of the probing compensation system. Chapter 5 describes the three dimensional probing experiment, along with the construction of the long probe and the metrology pallet. In Chapter 6, the results of probing experiment are presented. The results of the determination of the probing interval and the decomposition procedure are explained. The results of the machining experiment are presented in Chapter 7. It demonstrates the capability of the error compensation by the metrology pallet and the touch probe system. In chapters 8 and 9, the conclusions and some recommendations are presented for the application of the results of one dimensional and three dimensional experiments.

2 - ERROR ANALYSIS AND PREDICTION

2.1 Positioning Error

The positioning error is composed of the systematic error, the cyclic error, and the hysteresis error including backlash. Thermal effects cause a large variation of errors and repeatability. Figure 2.1 shows the positioning error for the y axis measured for a range of 20 mm travel. The motion begins at y the coordinate of 140 mm and is made in 0.1 mm increments. The cyclic and the positioning error is measured by a laser interferometer. A laser head shoots a two frequency laser beam to the interferometer where one frequency beam is reflected to the laser head and the other frequency beam is deflected to the reflector. For the y axis positioning error measurement, the spindle moves along the y axis with the reflector mounted on the spindle. Two reflected beams go back to the laser head where the interference fringes are counted by the counting circuit. A microcomputer is connected to the display for the automatic data acquisition. Figure 2.2 is a picture of the Hewlett-Packard laser set-up for the y axis positioning and the cyclic error measurement. Figure 2.3 is a picture of the display and Hewlett-Packard microcomputer system for the

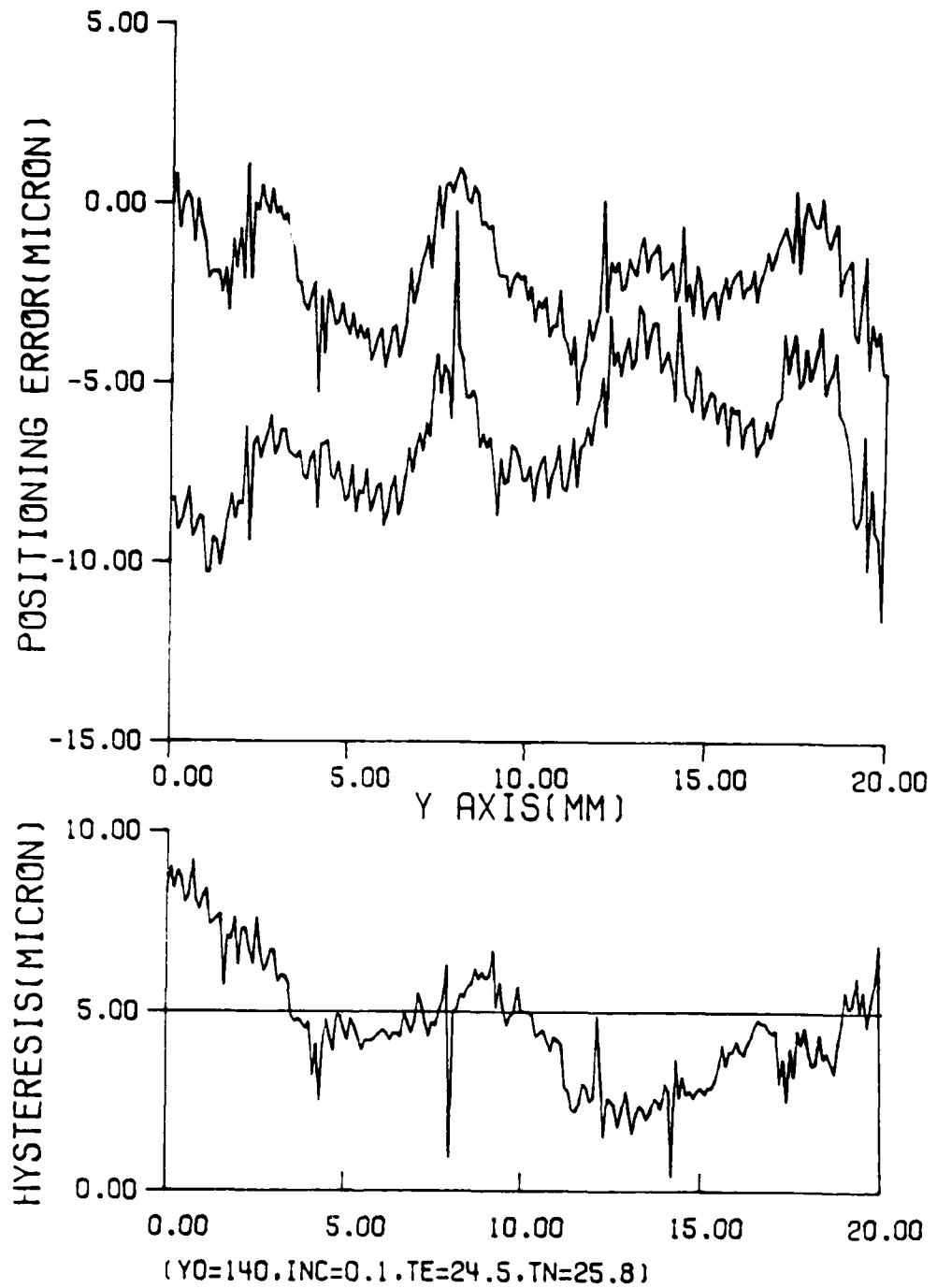


Figure 2.1 The cyclic error and the hysteresis with 0.1 mm increment.

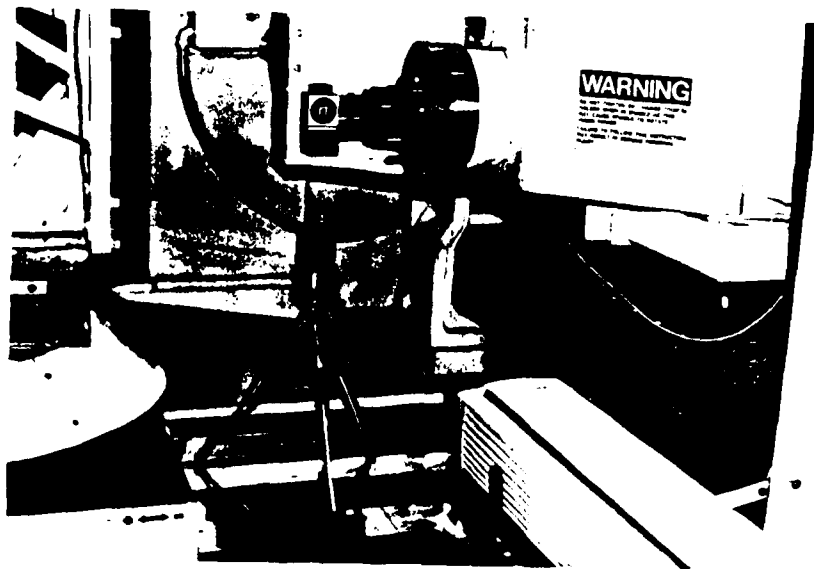


Figure 2.2 The Hewlett-Packard laser interferometer set-up for y axis positioning error measurement.

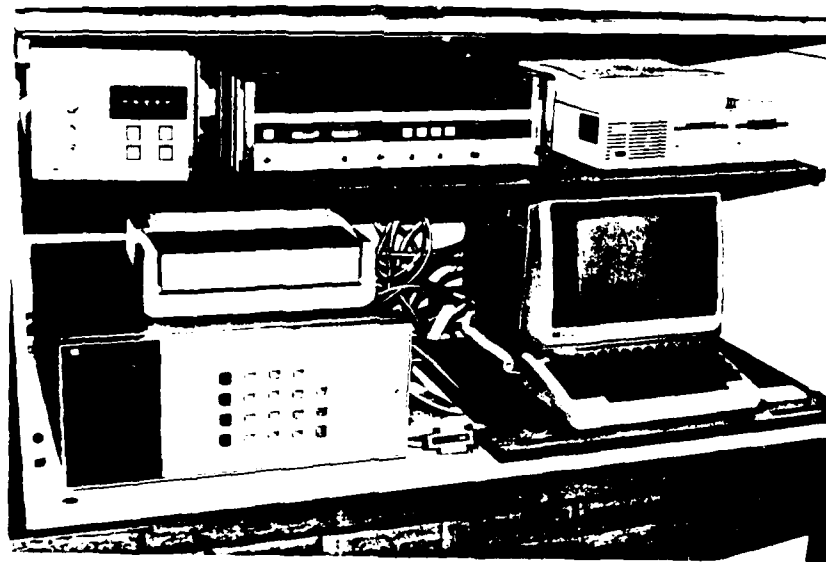


Figure 2.3 The Hewlett-Packard laser display and the HP microcomputer system for data acquisition system.

data acquisition system. This experiment is done when the machine is in the cold condition. The upper curve shows the errors resulting from upward motion and the lower curve shows the errors resulting from downward motion. The hysteresis between the upward and downward movement is also shown in figure 2.1.

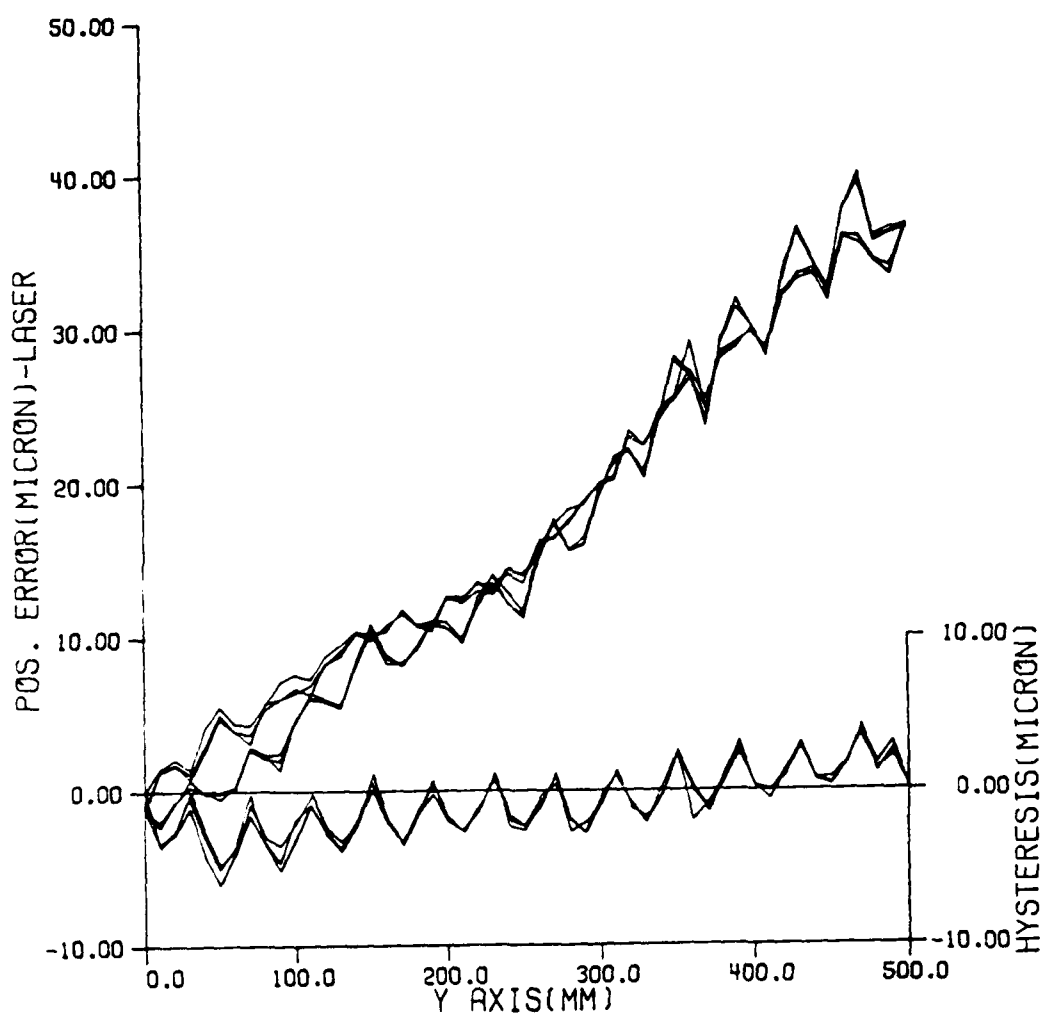
The period of the cyclic error and the hysteresis is 8 mm, which is equal to the pitch of the ball screw of the machine. The errors from the resolver feedback system and the drive system of the end bearing and the ball screw caused the cyclic phenomenon of the error and the hysteresis for the short distance. Continuous fluctuation along the cyclic error curve is caused by the resolution problem of the machine tool. The resolution of the experimented machine tool is $1/10000''$, which is a 2 or 3 micro meter resolution in the metric system. The resulting position does not reach the commanded position by 1 or less than 1 micro meter which causes a small magnitude of continuous fluctuation along the cyclic error curve. If the 1 micro meter resolution machine tool is tested, this shape of fluctuation can be reduced very much.

Several measurements at different positions and different thermal conditions are made for the cyclic error. The magnitudes of the cyclic error and the shape of hysteresis are not consistent at all positions and with the

change in the thermal condition of the machine tool. The period of the cyclic error for each case, however, is the same-8 mm.

Errors of various positions along the entire axis at intervals of 10 mm are shown in figure 2.4 in the warm condition. We can regard the increasing trend of the error along the axis as a systematic error. Every 4 measurements constitute one cycle of fluctuation. The positioning error, as also the hysteresis error, is repeated well for three cycles of measurement.

It is interesting to see the change of the systematic error trend as the thermal condition changes. To observe the thermal drift and the change of the systematic positioning error due to thermal effects, repeated traverses of the whole axis with different feed rates are made. Figure 2.5 shows the measurement of positioning error for the whole axis with the 48 mm increment in the cold condition. The three measurements show good repeatability of the machine axis and also a significant amount of repeated hysteresis error. This error curve does not include the cyclic error effect. Error increases nonlinearly from near 250 mm. The slope of the systematic error becomes sharper when the machine becomes warmer as shown in figure 2.6. Amount of hysteresis becomes smaller as the machine is warmed-up because of the reduced stick-slip phenomenon of



(Y0=140, INC=10, TE=26, TN=28.2)

Figure 2.4 Positioning error measured three times for the whole y axis in increments of 10 mm and its hysteresis in the warm condition.

the slideway.

2.1.1 Positioning Error Prediction Using GMDH Since the positioning error varies with the position and also the thermal condition of the machine tool, it can be modeled by the variables, position and temperatures of several important points of the machine tool. The GMDH technique which is described in appendix I is one of the better techniques for modeling error with several possible variables including varied temperature information. A major advantage of using the GMDH technique on error prediction is its ability to discern the most important variables, to predict the dependent variable. The experiment is set up to observe the capability of the GMDH technique to predict the systematic positioning error. The machine traverses the y axis continuously with the laser reflector mounted on the spindle as shown in figure 2.2. It simulates normal operating conditions. The data acquisition cycle is executed after a certain period of machine warm-up, which is about 1 hour. A sample result of a whole day experiment is shown in figure 2.7. Actual data for 7 measurements with 48 mm increment and the GMDH prediction are shown. The thermal drift is observed to be significant as the measurements are made continuously. The first 14 observations of figure 2.7 are made when the machine is in the cold condition and the last 14 observations when the machine is in the warm condition. From these 98 observations of 7

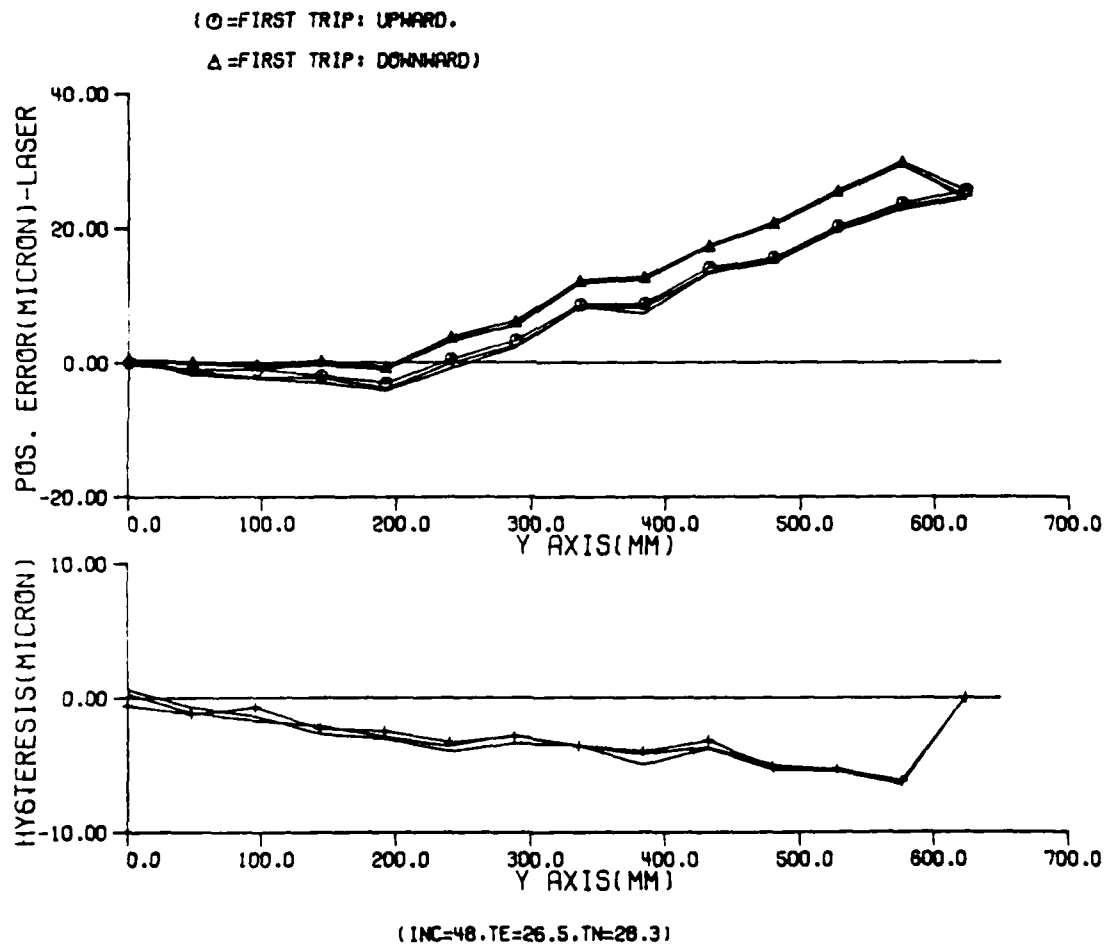


Figure 2.5 Positioning error measured three times for the whole y axis in increments of 48 mm and its hysteresis in the cold condition.

measurement cycles, 70 observations are used for a training set and 28 observations for a checking set. Computation is converged after one generation of computation. Position and one temperature point are the important variables remaining. Prediction residuals are within a 10 micro meter range. This result does not include the cyclic error effect since the obtained data represents systematic error components measured with a 48 mm increment. A whole day of measurement with a 1 mm increment is done to include the cyclic error component for the whole axis of 660 mm. Each laser data measurement is obtained 2 seconds after the axis stops. Figure 2.8 is the result of the error measurement cycle after 230 minutes of movement. The whole round trip measurement with a 1 mm increment needs more than 40 minutes to complete. To compare this measurement with the 10 mm increment in figure 2.4 with similar thermal conditions, error data with 10 mm interval is drawn in figure 2.9. Too much hysteresis between the starting and the ending point is caused by thermal effect compared with that of figure 2.4. A long measurement cycle causes significant changes in the thermal condition of the machine tool resulting in thermal error variation. Figure 2.10 is the measurement result for the round trip of the whole y axis after 860 minutes of movement. Appendix 2 contains the measurement results after 360 minutes, 490 minutes, 610 minutes, and 740 minutes in figures A.2.1, A.2.2, A.2.3,

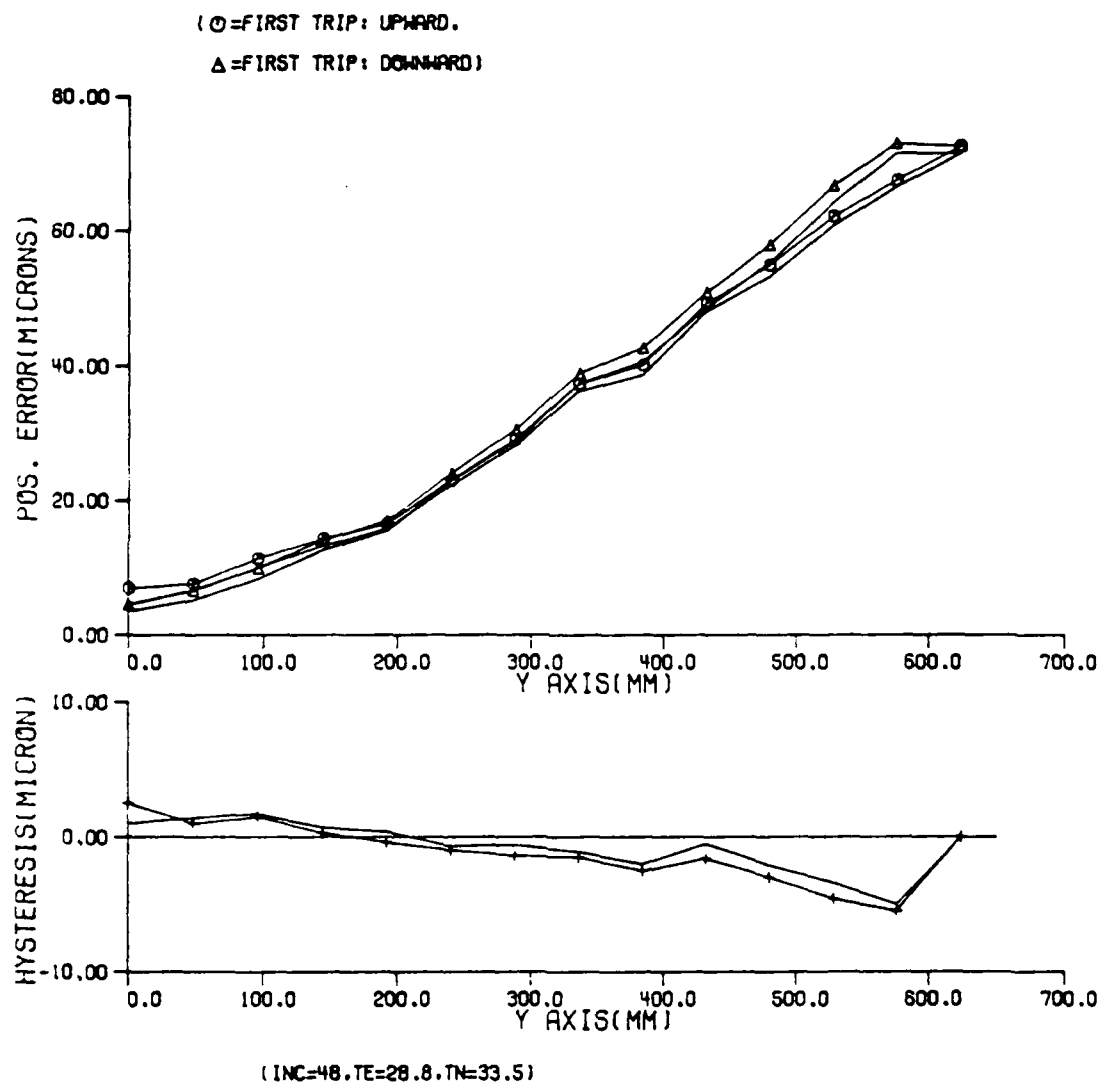


Figure 2.6 Positioning error measured two times for the whole y axis in increments of 48 mm and its hysteresis in the warm condition.

and A.2.4. One measurement cycle of 20 temperature data is done during the acquisition of each of the 48 laser error data for the experimental convenience. The same temperature information is assumed to be applicable to the 48 laser error data previously obtained.

GMDH modeling technique is applied separately to the upward motion and the downward motion, to eliminate the bias due to the backlash phenomenon. The backlash phenomenon can be compensated for by the method proposed later in this chapter. GMDH prediction on the last set of measured data for upward movement is shown in figure 2.11. It starts the measurement after 860 minutes of movement. Actual error measured from the cold condition ranges from around 30 micro meters to 120 micro meters. For GMDH modeling, 3506 data points are used for a training set and the last 460 data out of 3996 data points of 6 measurement cycles are used for a checking set. The values converged after the 1st generation of computation. The variables selected are the 4th and the 21st variables, which are the temperature from the point near the spindle motor and the axis coordinate. Predicted error ranges from around 30 micro meters to 125 micro meters and the residual error, between the actual and the predicted error, ranges mostly within plus and minus 5 micro meters. From the analysis of residual errors, it seems that most of the fluctuation of residual errors is from the cyclic effect of errors. Some

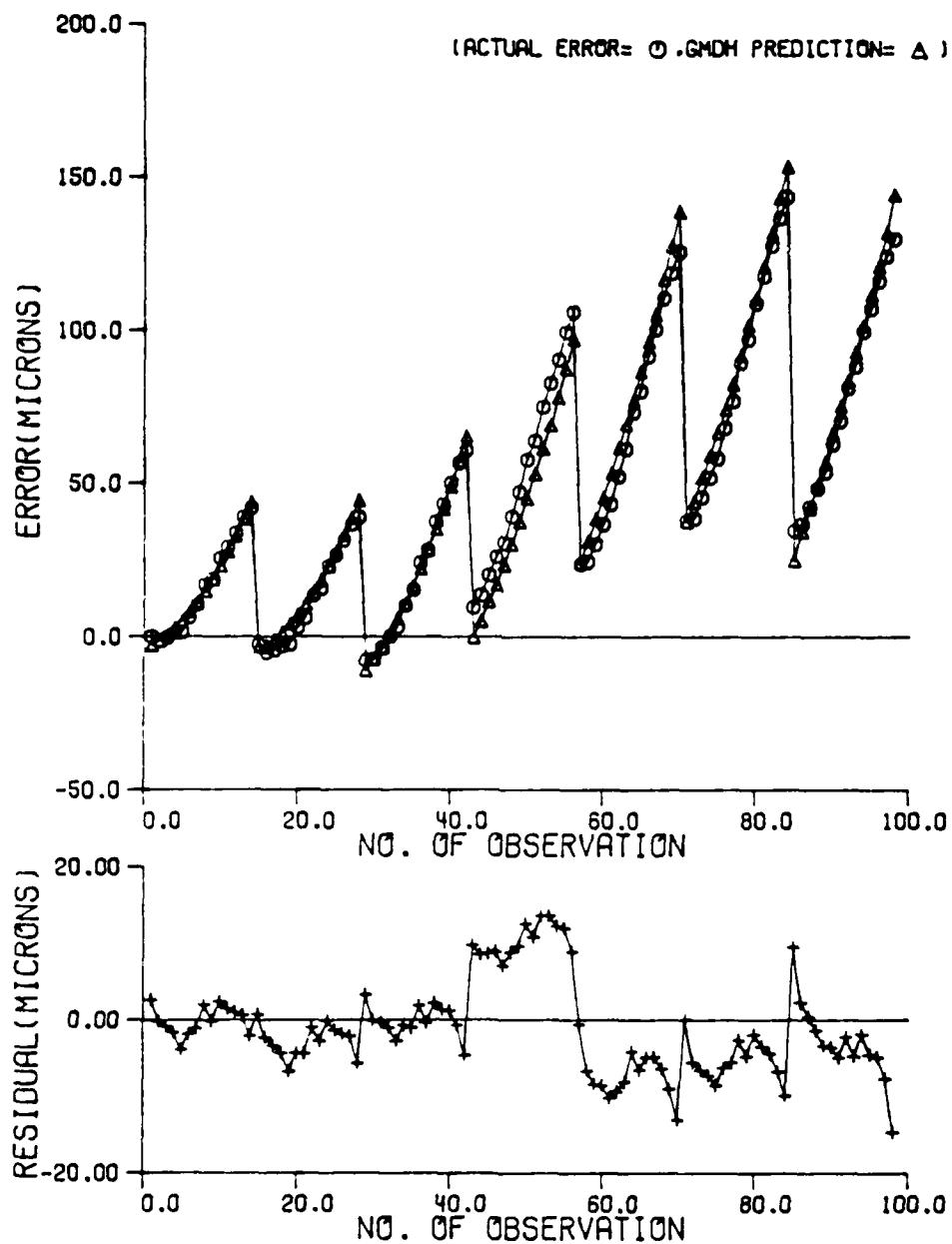


Figure 2.7 Error change and its GMDH prediction for a whole day measurement with 48 mm increments.

deviations are from irregularities in the machine slideway. A very good prediction, within 5 micro meters for 120 micro meters error with the axis coordinate and one temperature information, shows that the positioning error is mainly due to the thermal effect. This also tells that continuous temperature sensing of that specific point can be used for the compensation of positioning error.

The usage of the whole data for GMDH modeling, however, does not ensure that this modeling technique can predict all the errors which will be induced. Without the last 160 data points GMDH computation is done again. 3506 data points are used for a training set and 330 data points are used for a checking set. As shown in figure 2.12, the result is exactly the same as that of the previous computation shown in figure 2.11. Computation converged after the 1st generation of computation. The determined variables are the 4th and the 21st variables and the prediction values are exactly the same. This shows the prediction capability of GMDH modeling on the errors which are induced, with the temperature information of one point and the coordinate information.

The usage of only the first 5 sets of measurement data does not predict 661 error data very well for the whole 6th set of error measurements using GMDH modeling as shown in figure 2.13. 3306 error data points are used for the

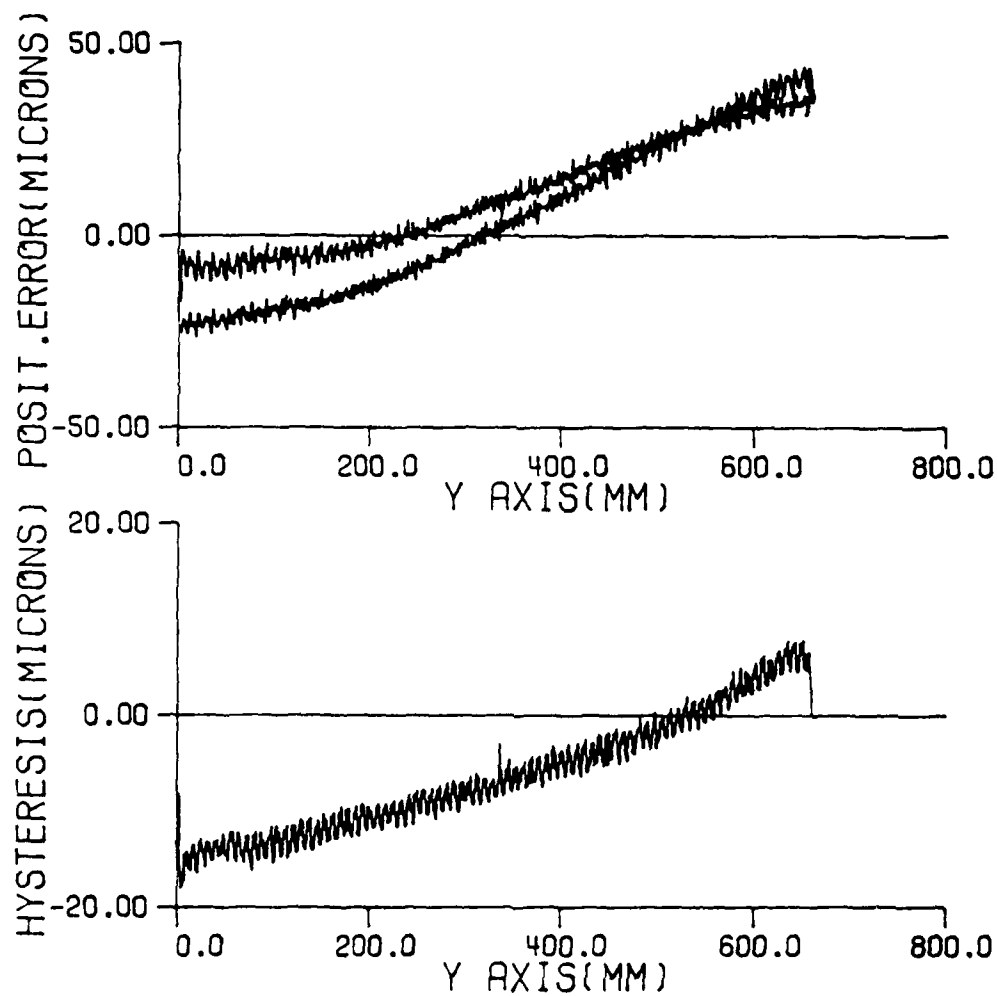


Figure 2.8 Error measurement after 230 minutes of movement with 1 mm increment.

prediction of the next 661 errors which will be induced for a movement of 120 minutes duration. The values converged after 1st generation of computation. Only two temperature information points without coordinate information turn out to be important. The determined variables are the 1st and the 2nd variables which represent temperature points on the lead screw motor and on the lead screw end bearing near the lead screw motor. Even though the GMDH computation determines these two temperature variables as optimum these two temperature information points do not predict the whole error of the 6th measurement set effectively. Predicted values are in a stepwise fashion because 48 error data points are assumed to have one set of the same temperature values. This analysis tells that sufficient information for the data input is necessary for the successful implementation of the GMDH technique for positioning error prediction. Figure 2.14 shows the result of GMDH prediction on 661 data points of the 5th data set measured after 740 minutes of upward movement analysis. 3560 data points are used for a training set and 430 data points are used for a checking set, which result in the same variables, the 4th and the 21st, being determined to be the cause of figure 2.11. This shows good predictability within 5 or 10 micrometer residual errors. For downward movement, the same procedure using GMDH modeling is applied. Figure 2.15 shows the prediction results of errors obtained after 860

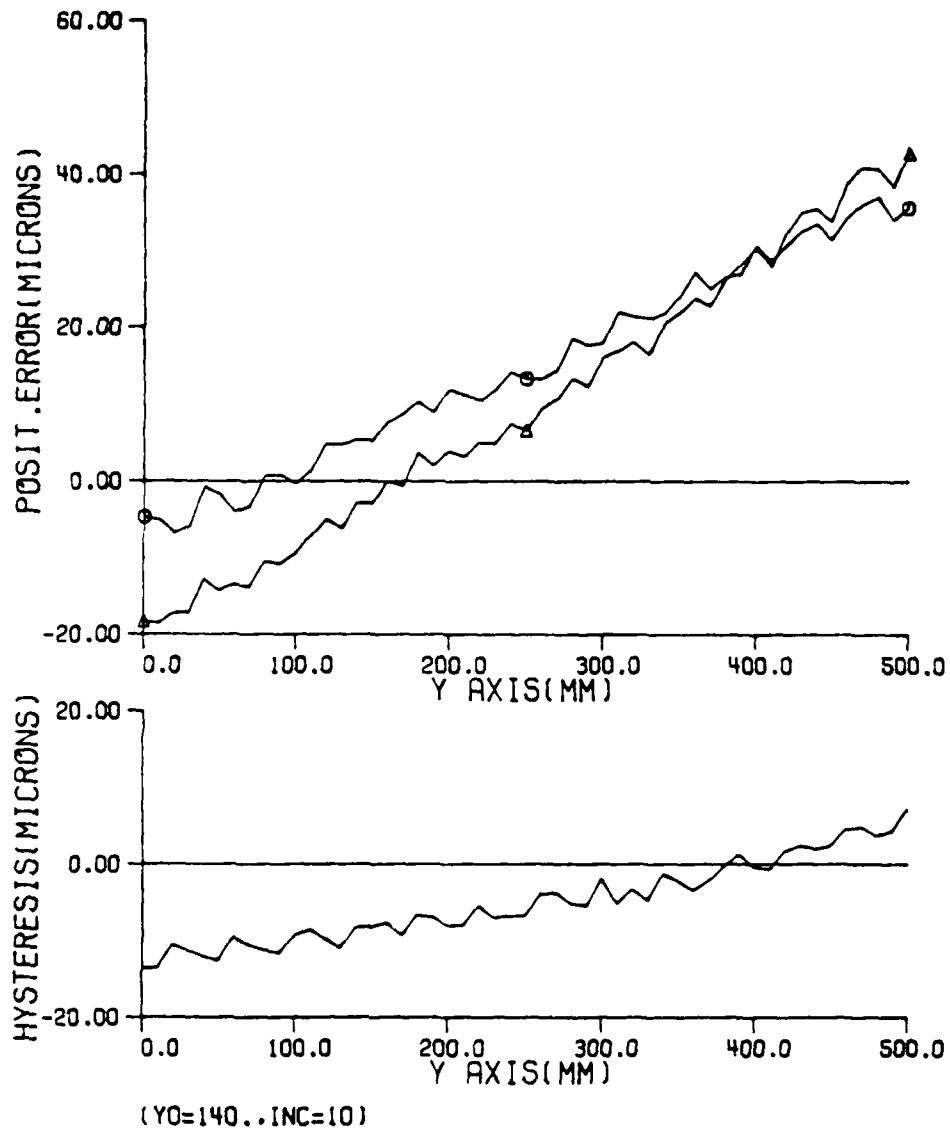


Figure 2.9 Error measurement after 230 minutes of movement drawn with 10 mm interval.

minutes of movement. Figure 2.16 are those obtained after 740 minutes of movement. In both cases 3560 data points are used for a training set and 436 data points are used for a checking set. The values converged after the 1st generation of computation in both cases. The variables selected are the 21st and the 4th variables, which are the axis coordinate and the temperature information from the point near the spindle motor the same as those of upward movement.

2.1.2 Repeatability and Thermal Drift Good repeatability is one of the most important factors in achieving a desired precision of the machined workpiece. One cause of poor repeatability is that the ball screw and the resolver feedback system experience continuous thermal effects as the machine members move.

Unidirectional repeatability is defined as the expected dispersion on each side of the mean resulting from a series of trials when approaching any given point under the same conditions according to the NMTBA[49]. The expected dispersion on each side of the mean is defined as 3σ , where

$$3\sigma = 3 \cdot [\sum (X_i - \bar{X})^2 / (n-1)]^{1/2}, \quad (2.11)$$

n is number of trials,

X_i , $i=1,2,\dots,n$ is the measurement data,

and \bar{X} is the mean of measured values.

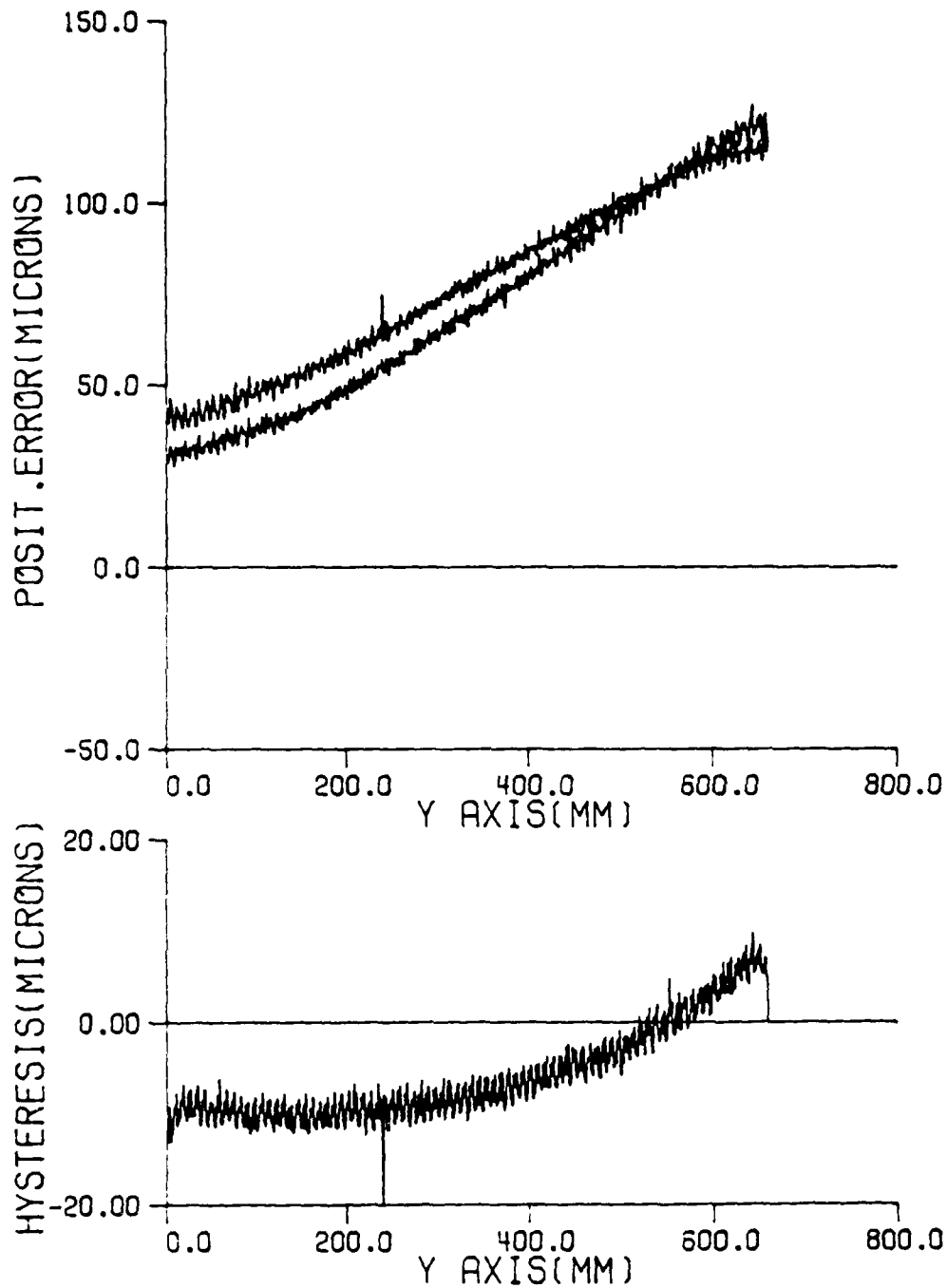
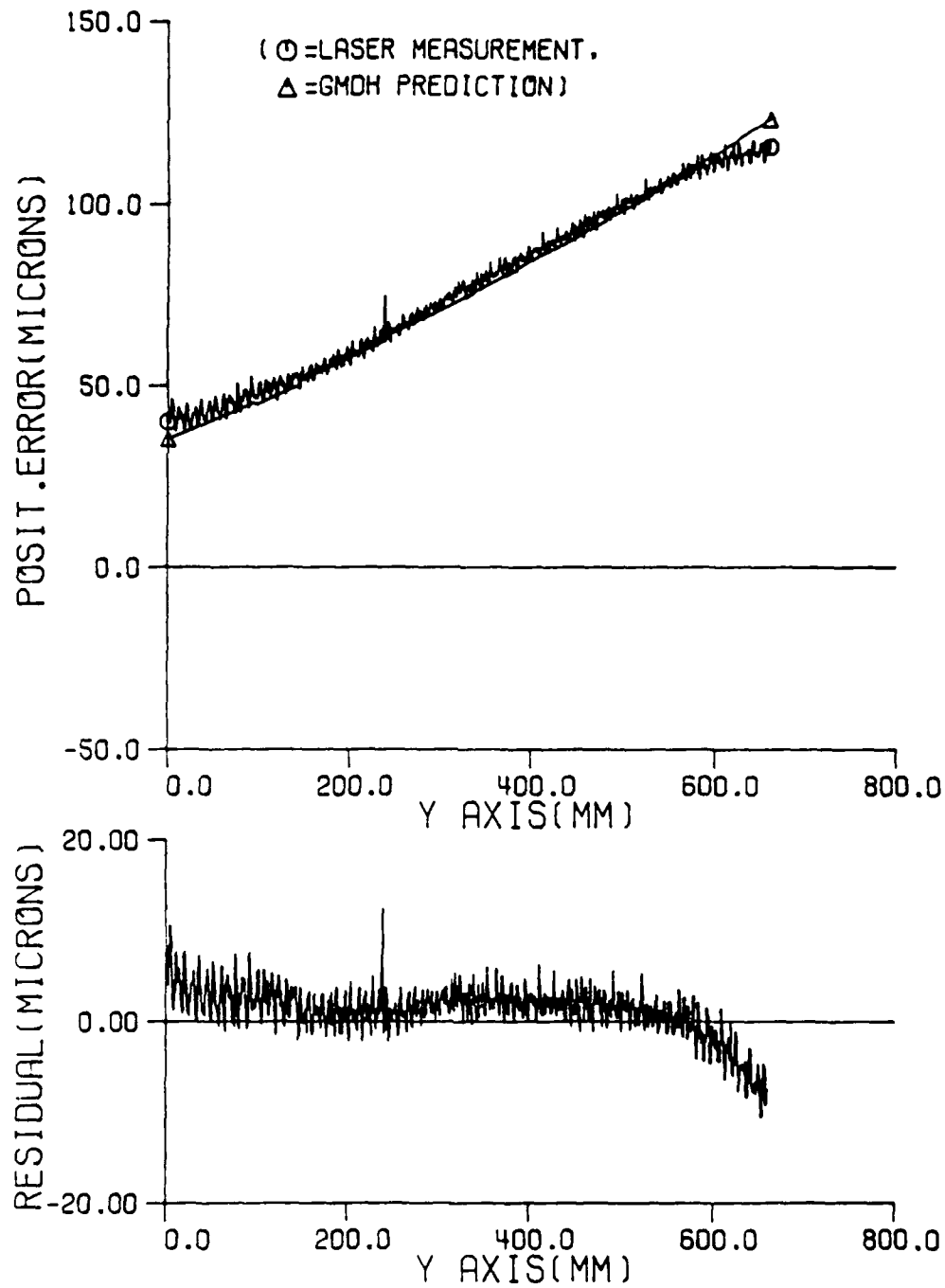


Figure 2.10 Error measurement after 860 minutes of movement with 1 mm increment.

The repeatability value increases as the thermal effects increase. This can also be seen in the repeated approach to a certain point after up and down movement of 10 mm as shown in figure 2.17. When in the cold condition, the magnitude of the error in repeated approaches after 20 mm trip to a certain position does not increase significantly, but when in the warm condition, the magnitude of the error shows an significant increasing trend. Figure 2.17 shows actual drift error after 20 mm of trip. It goes 5 mm up and 5 mm down. Then it goes 5 mm down and 5 mm up. At each position it stops for 5 seconds while the laser data and the temperature information for y axis are recorded in the computer. While short term measurement shows only the nature of random error change, continuous measurement shows the significant trend of error increase by thermal effects. For the measurement of repeatability, it is recommended to have 5 mm up and down movement for five or seven times not to have thermal effects. Application of the GMDH modeling to the drift error proves the good prediction capability of the GMDH technique using the temperature information. Figure 2.18 shows the result of GMDH prediction for fifty one observations. thirty one data points are used for training and twenty data points are used for checking. The values converged after one generation of computation. The prediction curve shows clear trend of increasing error and residuals show the random



(AFTER 860MIN,UP,N=3966,NT=3560,U=4,V=21)

Figure 2.11 The GMDH prediction result of errors observed after 860 minutes for upward movement(3560 data points for training and 406 data points for checking).

phenomenon. Appendix 2 has the prediction result of the thermal drift for the same experiment above, for the bottom point and for center point approaching downward in figures A.2.5 and A.2.6.

If the distance during one round trip is very long such as 1320 mm for a whole axis as shown in figure 2.19, we can see a continuous increase in the error when approaching a certain position. GMDH analysis is done on the thermal drift with thermal information of the machine tool for the bottom point. From fifty one observations, thirty one data points are used for training and twenty data points are used for checking. The values converged after one generation of computation. A similar result as for the short distance movement of figure 2.18 is obtained. The thermal variation of the ball screw and the machine structure causes significant increases in repeatability. The prediction results, for on the thermal drift of the same experiment for the top point at the y coordinate of 660 mm and center point of 330 mm, are shown in figures A.2.7 and A.2.8 of appendix 2.

For the whole day experiment above, several intermittent observations and several sets of continuous observations are used for the GMDH modeling on the drift error. Thirty two observations are used for a bottom point of y axis. Figure 2.20 shows the result of GMDH prediction.

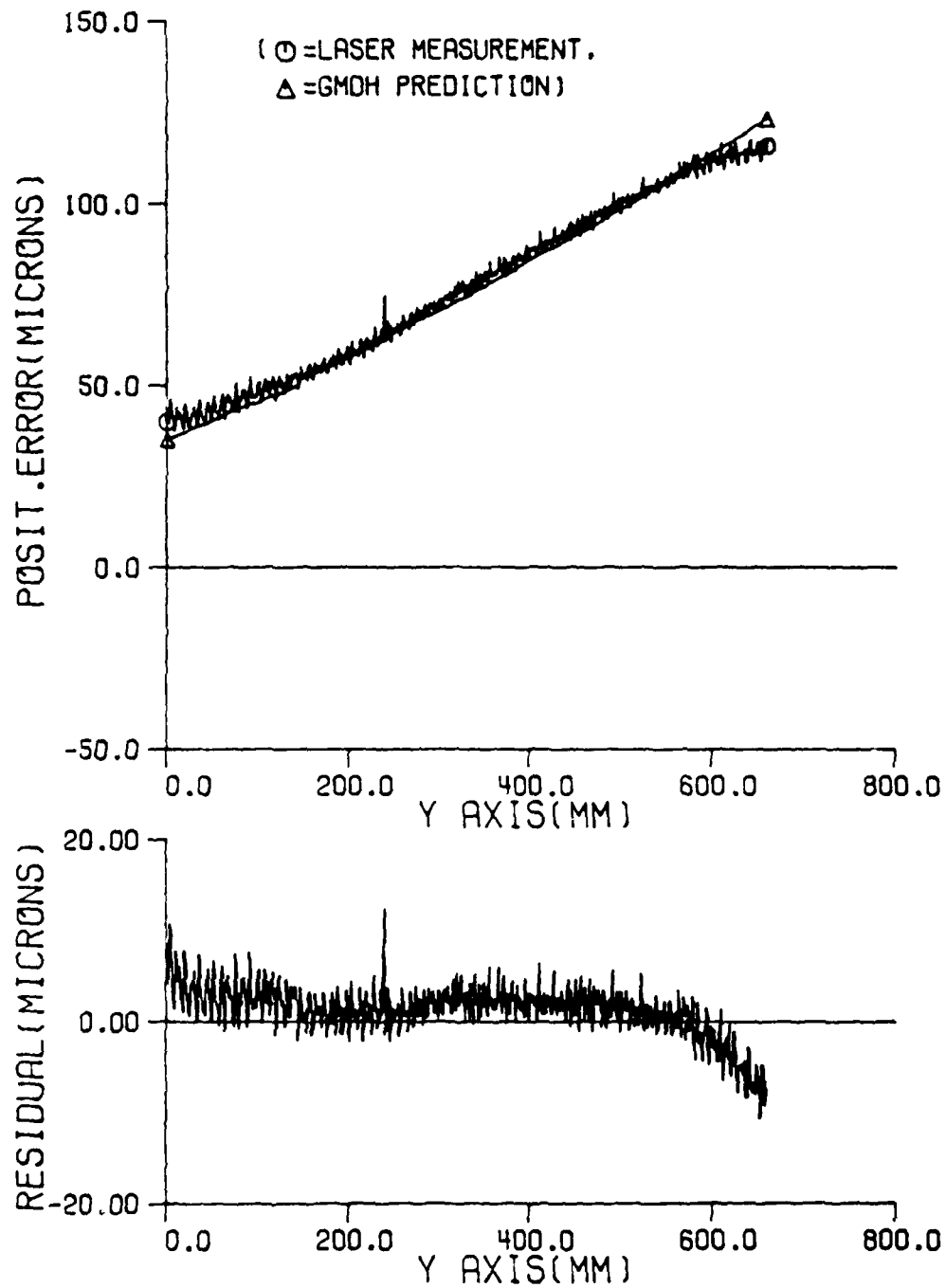


Figure 2.12 The GMDH prediction result of errors observed after 860 minutes for upward movement(3506 data points for training and 330 data points for checking).

Twenty five data points are used for a training set and seven data points are used for a checking set. Computation stop after one generation of computation, which gives only two important temperature variables. One is from the surface of ball screw nut and the other is from the middle of the column. Except for 2 or 3 points of 4 micro meter residual error, most points have residual errors within plus or minus 2 micro meters. This result shows that the drift error can be predicted using GMDH modeling technique with 2 points of temperature information.

Another set of data from a whole day experiment shows the prediction capability of GMDH modeling for the drift error. Figure 2.21 shows the prediction result of GMDH modeling for y axis drift error over a whole day of 12 hours. This is for the same point as in figure 2.20. The different operation from that of figure 2.20 gives different thermal drift phenomenon. Each observation was made at one hour interval. Temperature of the surface of the ball screw nut is also plotted. Even though the drift becomes negative because of no operation, for the observations number 4 and 5, the temperature of the ball screw nut increases continuously. This can say that the thermal drift cannot be predicted only by the temperature information of ball screw nut. The actual GMDH result shows that temperatures obtained from the ball screw nut and the top of the column near the guideway are found to be important

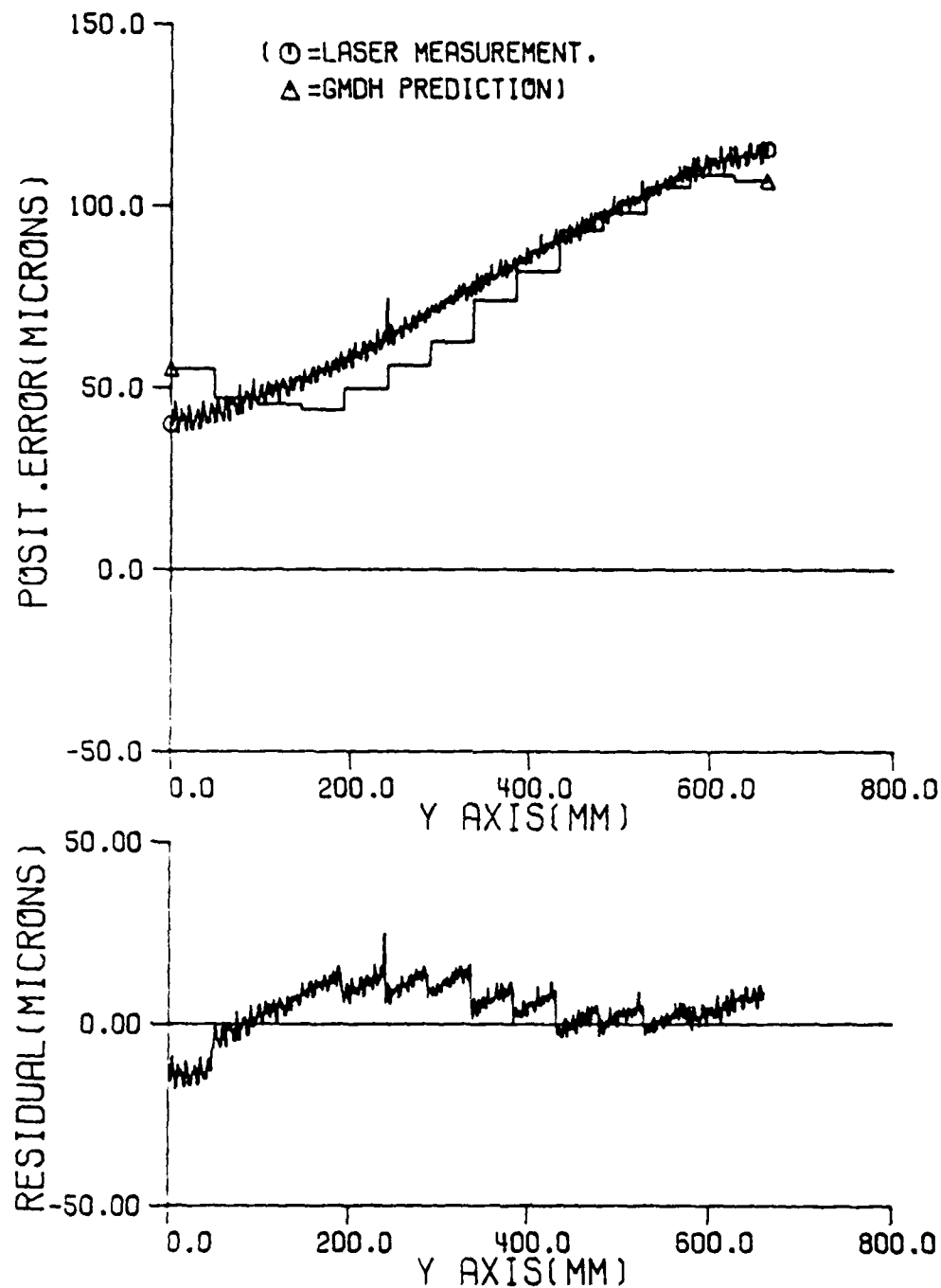


Figure 2.13 The GMDH prediction result of errors observed after 860 minutes for upward movement(2700 data points for training and 606 data points for checking).

after one generation of computation. Twelve data points are used for training and three data points are for checking. If the data input is arranged differently as shown in figure 2.22, the important variables are found to be different. The last two data are arranged to be placed before observation number 9. Temperatures from the ball screw nut and the bottom of the column near the guideway are selected after one generation of computation. Twelve data points are used for training and three data points are for checking as before. This shows that the GMDH technique is very sensitive to the data set and it is important to give data points in the same pattern as in the analysis, for the actual application.

Repeatability also varies with the position and other factors. To see the effect of position, moving direction, feed rate, and thermal condition on repeatability, the experiments are timed for just before the probing experiments of chapter 6.1 in the cold and the warmed-up condition. The laser measurement for the z axis repeatability test is done as shown at table 2.2, when the probe repeatability of chapter 6.1 is measured.

2.2 Backlash Analysis and Compensation

Nowadays, backlash of each axis is usually compensated for by software in CNC control. Most simple compensation

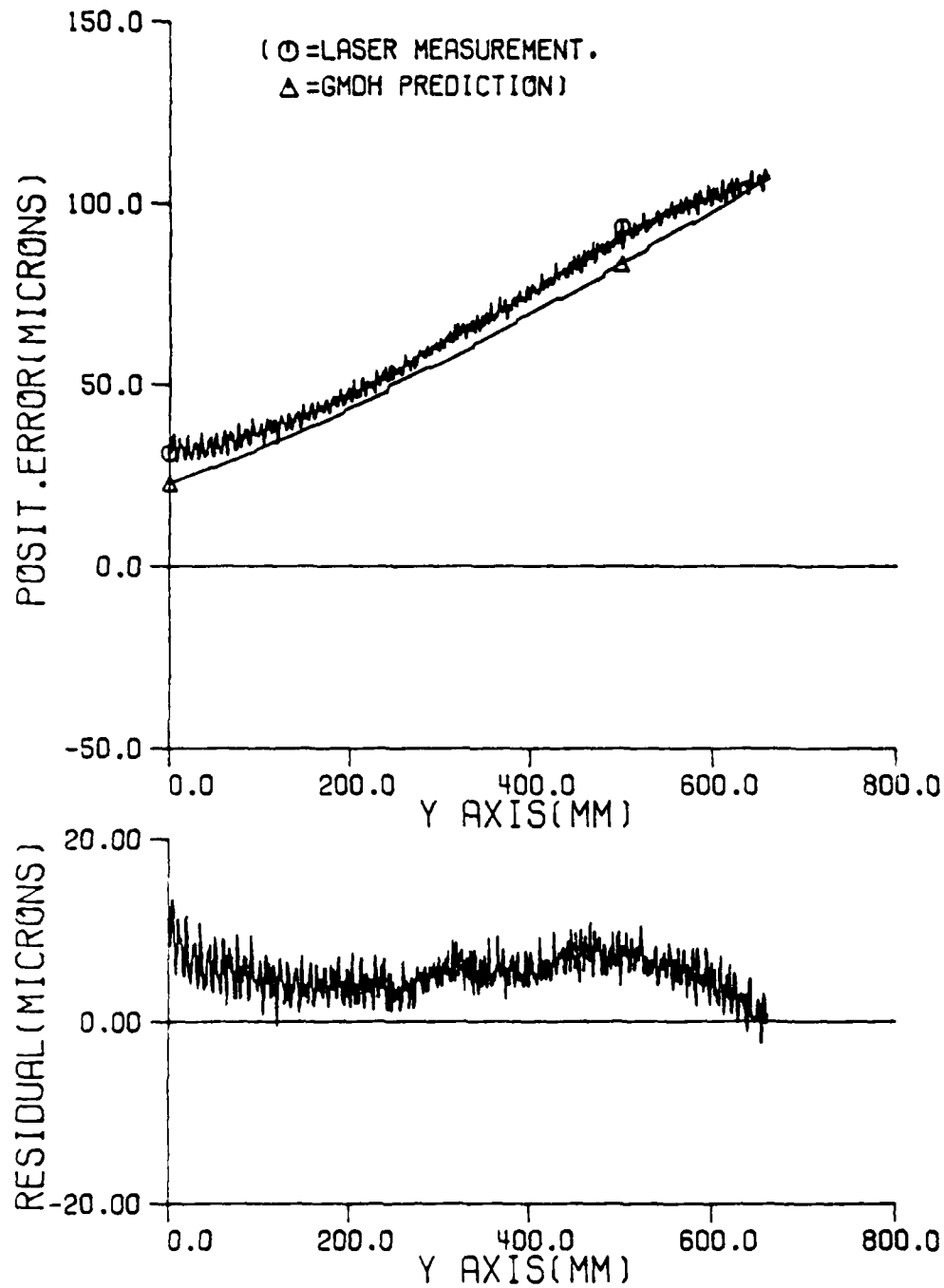


Figure 2.14 The GMDH prediction result of errors observed after 740 minutes for upward movement.

systems use the fixed value compensation approach. Backlash of a testing point at a certain thermal condition is measured. That value is fed into the controller manually. It is used for the compensation of backlash for all the thermal conditions and all the positions. There can be many factors that affect the backlash. Mechanical condition of the ball screw, end bearing of the screw, or another driving component can also be a factor, in addition to changes in the operating conditions. Under a certain mechanical condition, the operating condition is the only effect on the backlash. Thermal changes in the driving component lubrication and those of other operating conditions including speed, direction, position, and so on can cause the variation of the backlash. To figure out the dominant factor that affects the backlash, an experiment is set up. Thermal condition, position, speed, and moving direction are selected as experiment variables. Two thermal conditions, cold and warm, and three positions of z axis-650 mm, 690 mm, and 750 mm- are used for data observation. Two feed rates, 500 mm/min and 3000 mm/min, and two directions are also used for the observation. The result of 4-way(4 factor) Analysis of Variance(ANOVA) on the experiment data is shown at table A.2.1 of appendix 2.

From this result it is found that the moving direction does not affect the backlash. Excluding the moving direction factor gives 3-way ANOVA analysis shown in table 2.1.

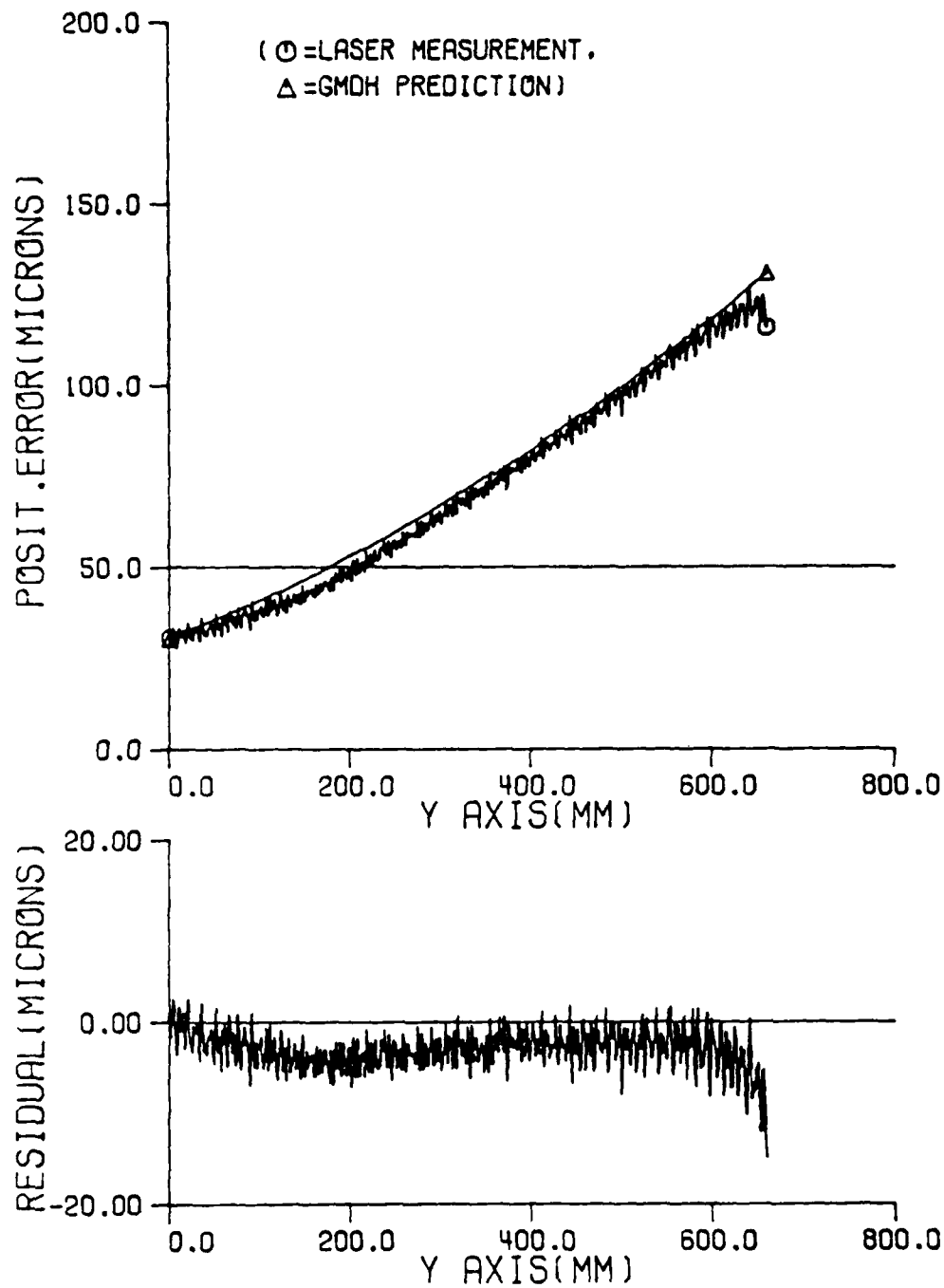


Figure 2.15 The GMDH prediction result of errors observed after 860 minutes for downward movement.

Table 2.1. Output of 3-way anova analysis for backlash

source of var.	sum of squares	df	mean square	f	signit of f
main effects	393.708	4	98.427	204.334	.001
thermal	354.780	1	354.780	736.521	.001
position	31.992	2	15.996	33.208	.001
feed	6.936	1	6.936	14.399	.001
2-way interact.	75.593	5	15.119	31.386	.001
thermal pos.	32.792	2	16.396	34.038	.001
thermal feed	.024	1	.024	.050	.824
position feed	42.777	2	21.389	44.402	.001
3-way interact.	61.783	2	30.891	64.131	.001
thermal pos. feed	61.783	2	30.891	64.131	.001
explained	531.085	11	48.280	100.230	.001
residual	109.827	228	.482		
total	640.912	239	2.682		

Feed rate does not significantly affect the backlash, but thermal condition and position have a significant effect at the 5 % significance. Even though position significantly affects the backlash, the difference between the mean of each position is relatively small compared with the resolution of the machine tool. A difference of $0.6 \mu\text{m}(0.00002")$ cannot be compensated for by a $2.5 \mu\text{m}(0.0001")$ resolution of the machine tool. Therefore thermal condition is the only factor to be considered for backlash compensation.

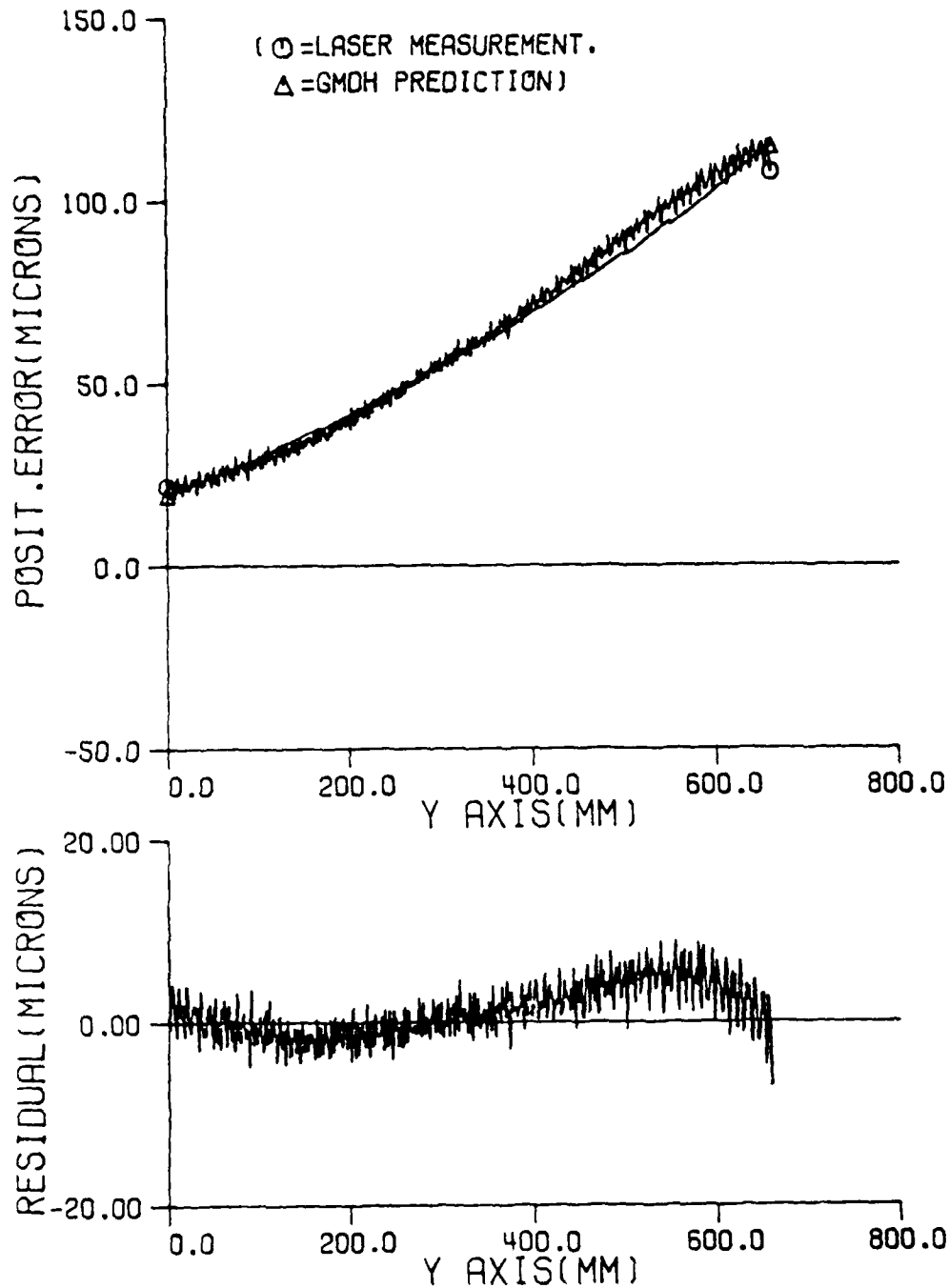


Figure 2.16 The GMDH prediction result of errors observed after 740 minutes for downward movement.

2.3 Angular Error Prediction using GMDH

The angular errors change as the thermal condition changes. The actual measurement of angular errors[42] shows some functional relationship between the temperature of certain points and the angular errors. The fact that there may be many possible variables including temperature points and the coordinates leads to its application of the GMDH technique to determine important variables to predict the angular errors.

For the pitch error of x axis, GMDH analysis is done to observe the prediction capability of the technique. This is used for the estimation of the pitch error for comparison with the decomposed error in chapter 6.4. Actual measurement data from reference 20 is used for the analysis. Ten repetitions of the measurement cycle using a 50 mm interval give 110 data points. Fifteen temperature points and the x coordinate are used as input variables. Pitch error varies between 0 arc seconds and -17 arc seconds for a whole day's experiment.

The values converged after the 1st generation of computation. The important variables selected are the x coordinate and the temperature point on the ball screw motor. Residual errors are within 2 arc seconds, except for two measurement cycles of near 4 arc seconds. This shows the excellent capability of the GMDH technique in the

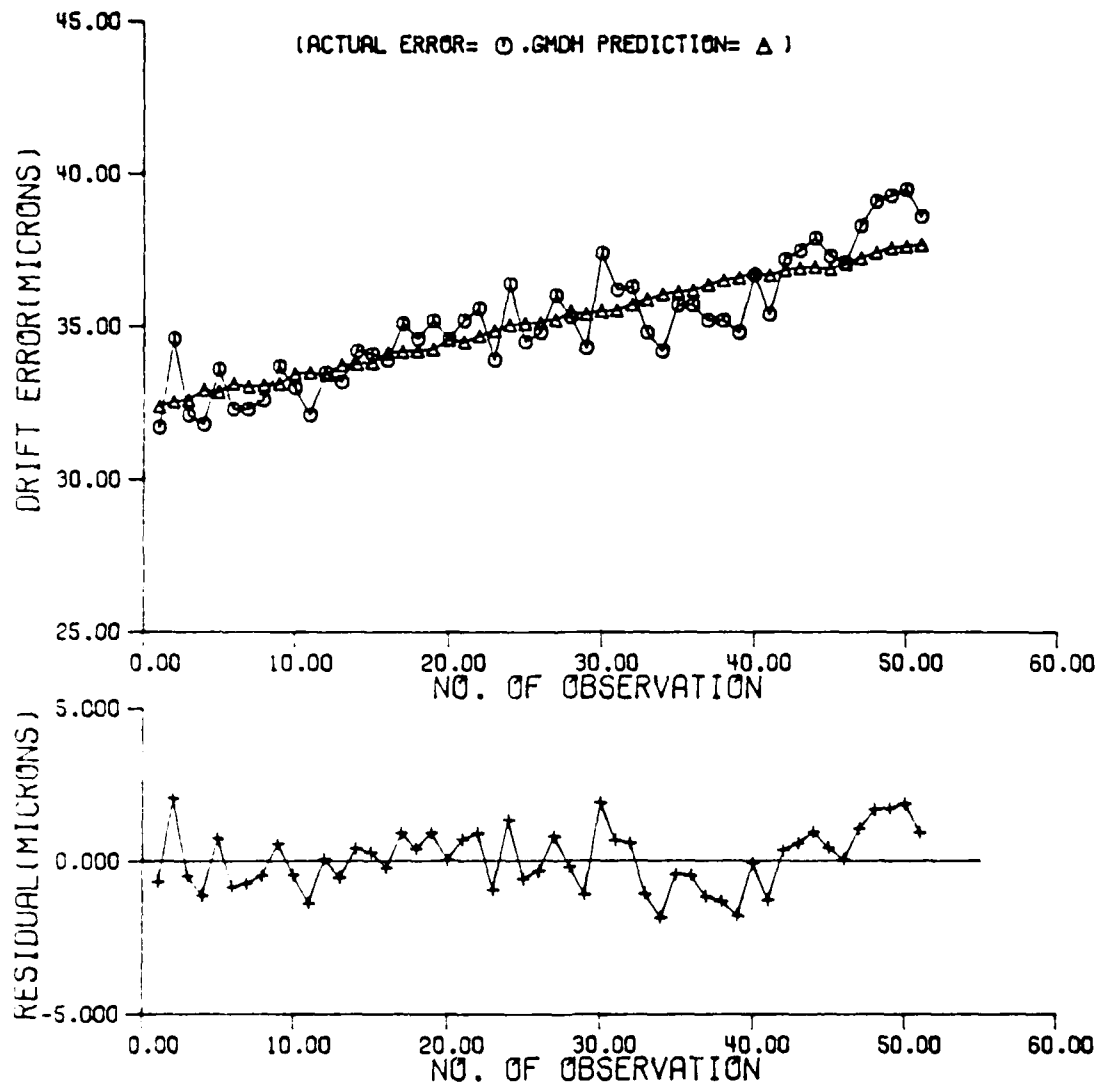


Figure 2.17 Thermal drift error after each trip of 20 mm and its change at top position.

prediction of angular errors with the temperature variables.

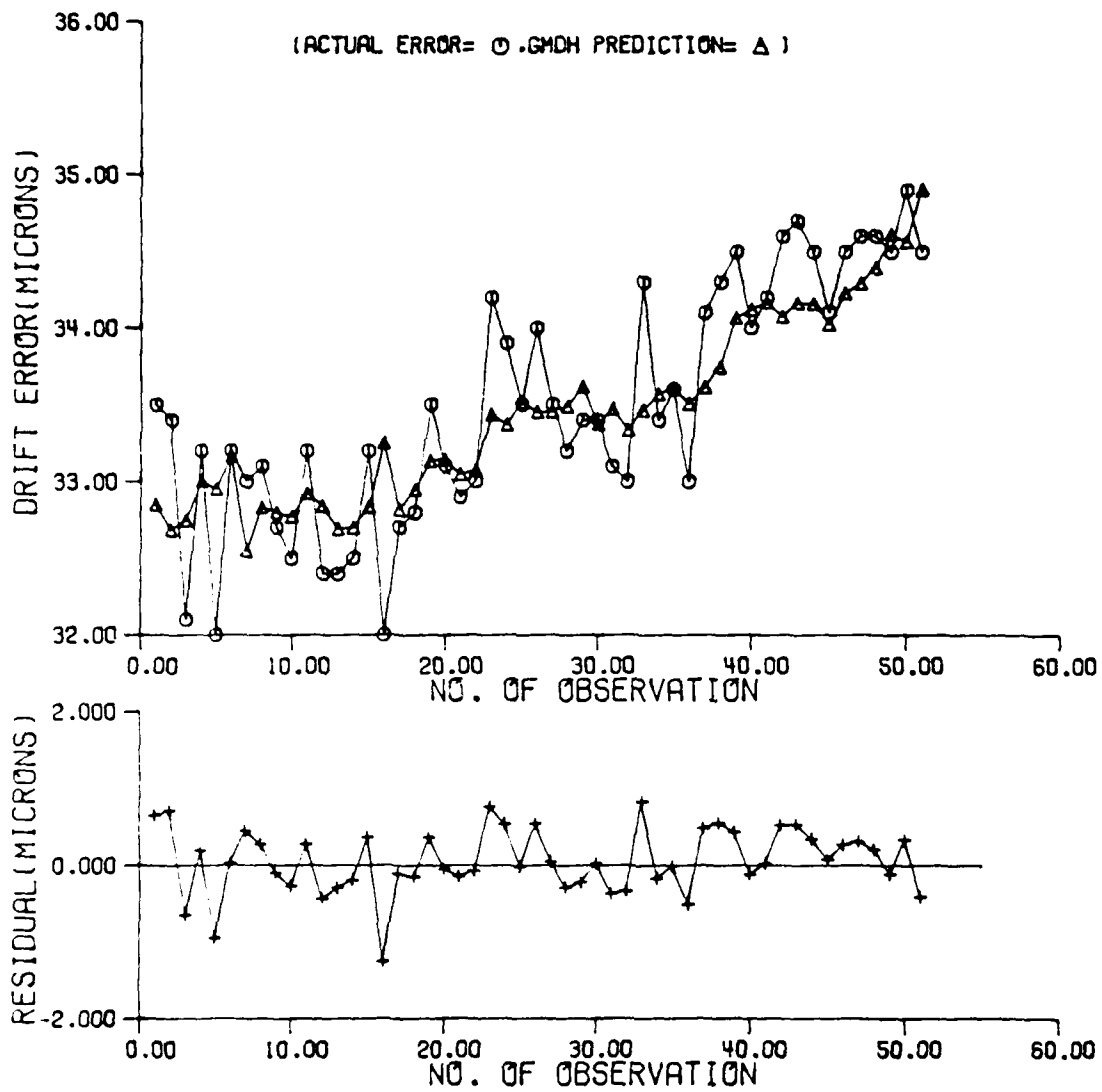


Figure 2.18 Drift error after a round trip of a short distance of 10 mm and its GMDH prediction for a bottom point.

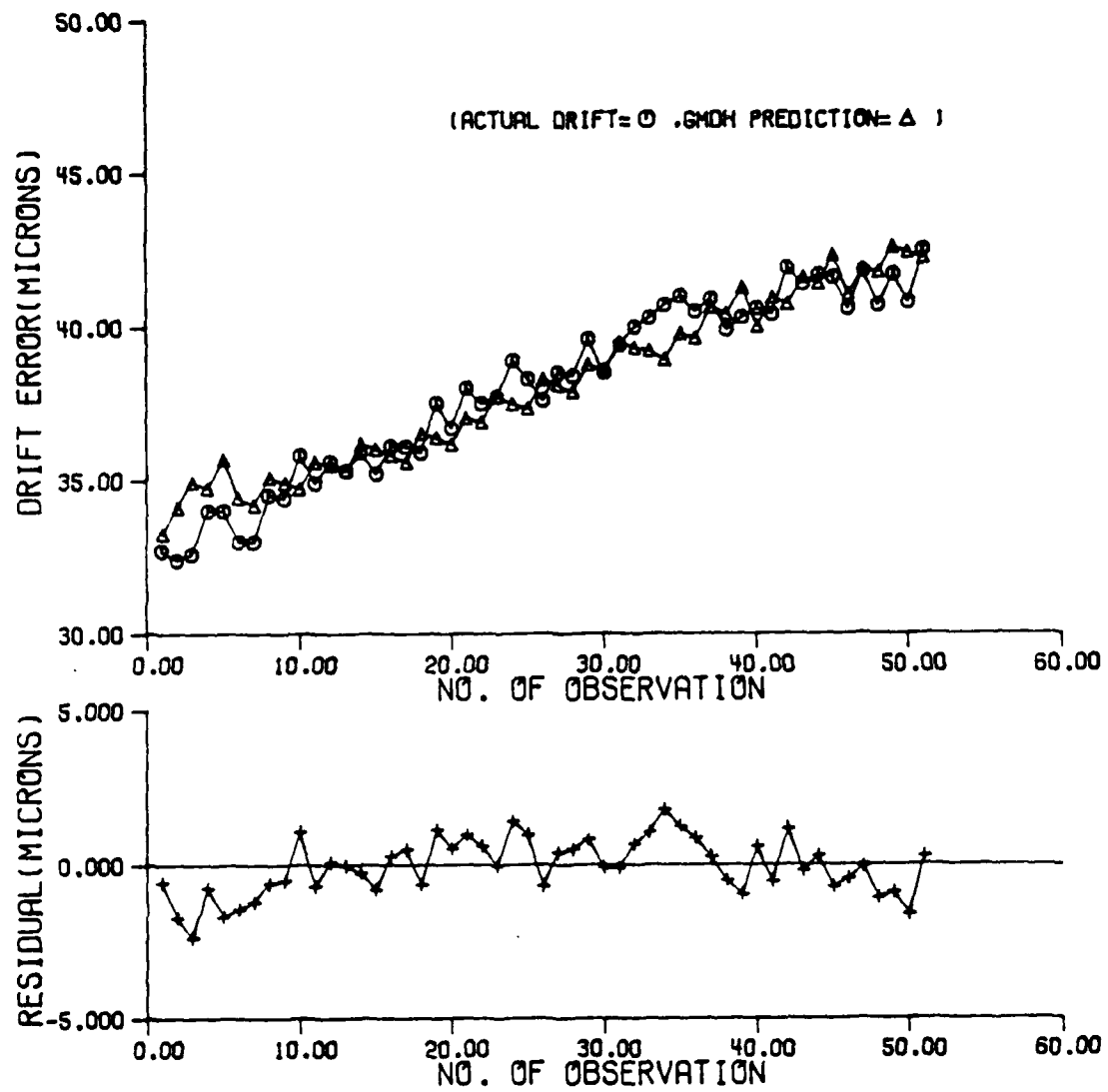


Figure 2.19 Drift error after a whole axis movement of 660 mm and its GMDH prediction for a bottom point.

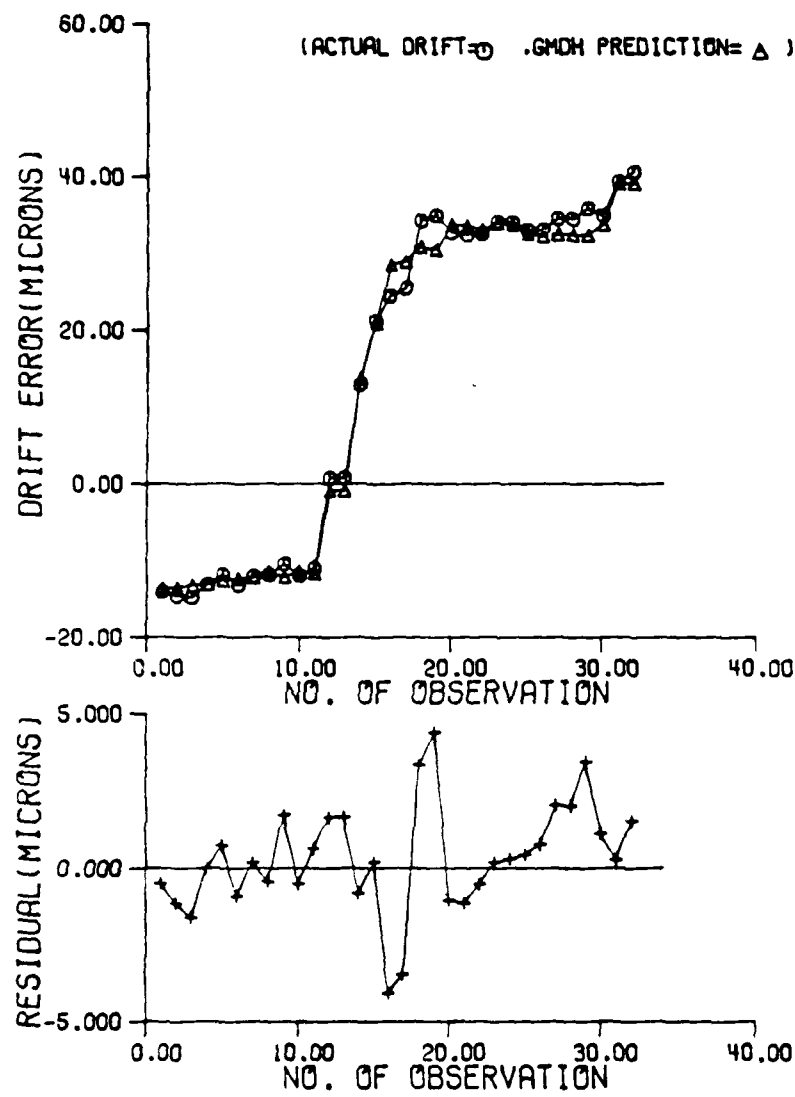


Figure 2.20 The GMDH prediction result on y axis drift error for a whole day experiment.

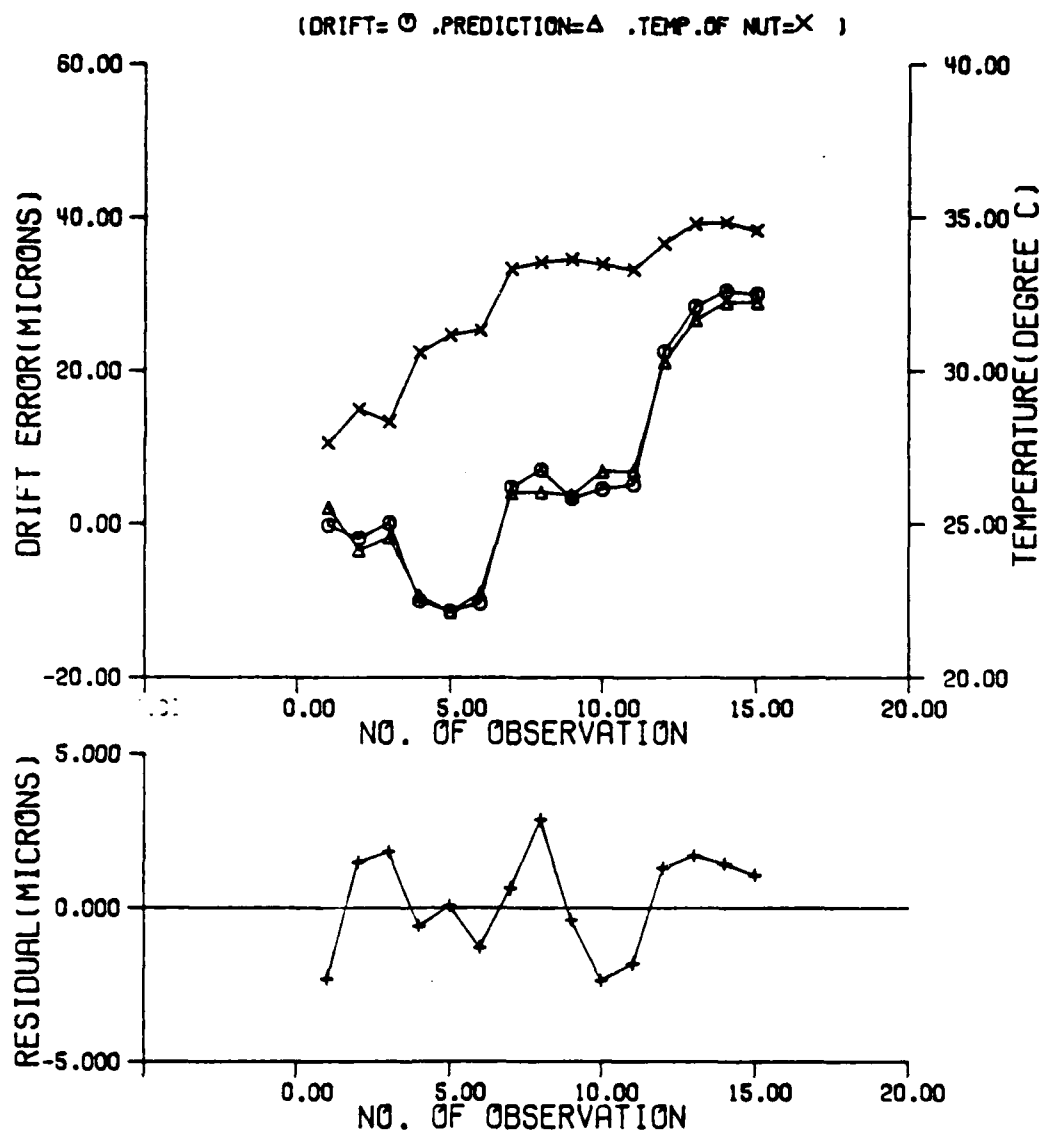


Figure 2.21 The GMDH prediction result on y axis drift error with different set of experiment data for a whole day.

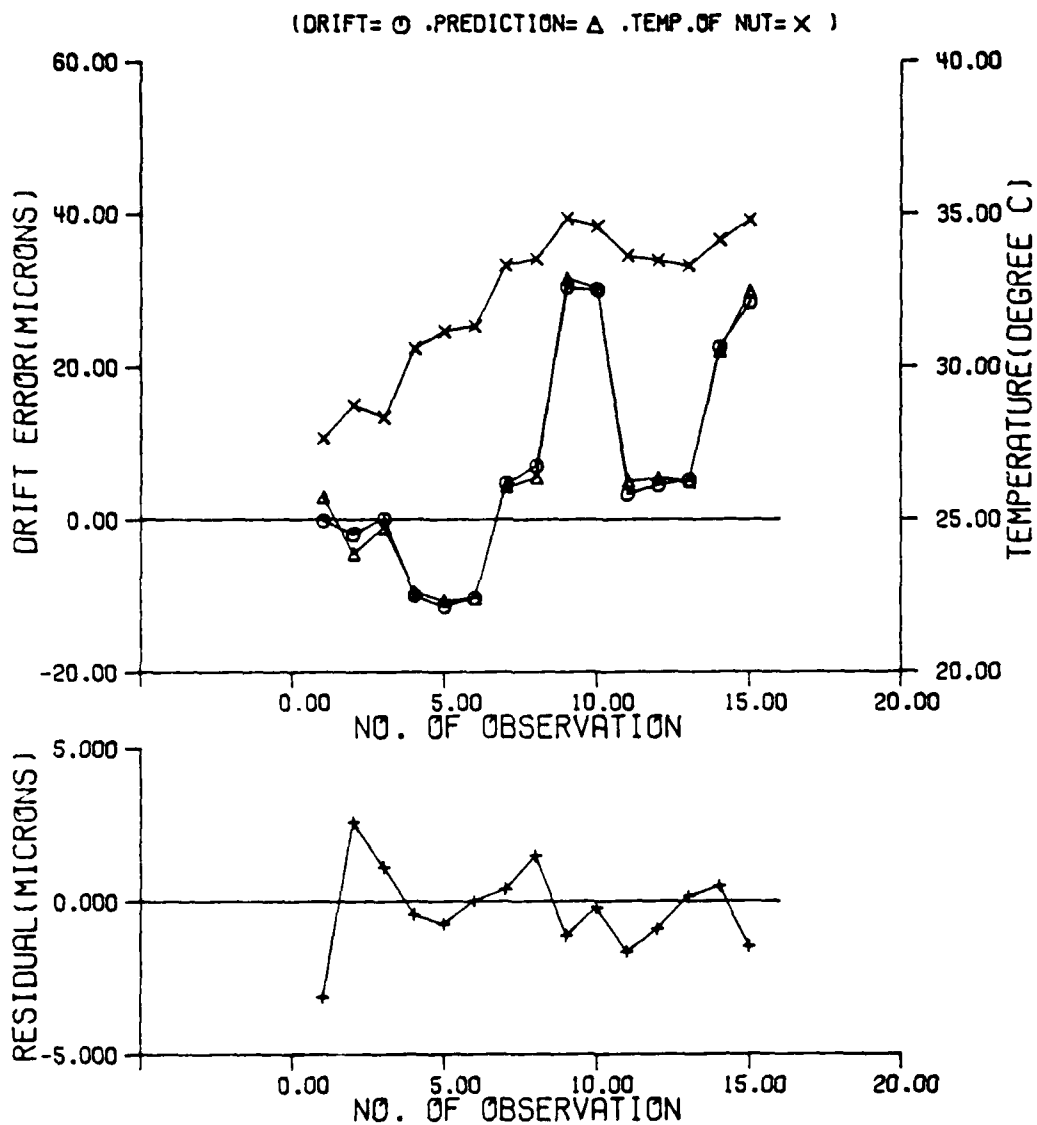


Figure 2.22 The GMDH prediction result on y axis drift error with different arrangement of input data.

Table 2.2 Repeatability of a machining center according to thermal conditions, feed rates, positions, moving directions (s^2 =variance, $3s$ =repeatability)

Position (z axis)	Feed rate (mm/min)	Direction	Thermal condition			
			cold		warmed-up	
			s^2	$3s$	s^2	$3s$
750 mm	3000	up	0.112	1.00	0.222	1.42
		down	0.256	1.52	1.053	3.08
	500	up	0.007	0.26	2.150	4.41
		down	0.027	0.49	1.180	3.26
690 mm	3000	up	0.087	0.89	0.120	1.04
		down	0.084	0.87	0.524	2.17
	500	up	0.529	2.18	0.192	1.32
		down	0.296	1.63	0.316	1.69
650 mm	3000	up	0.112	0.968	2.95	1.841
		down	0.668	2.45	2.473	4.72
	500	up	0.043	0.62	0.771	2.63
		down	0.034	0.55	0.425	1.95

Table 2.3 Mean of the backlash of a machining center according to thermal conditions, feed rates, positions

Position (z axis)	Feed rate (mm/min)	Thermal condi- tion	backlash
750	3000	cold	5.68
		warmed-up	5.76
mm	500	cold	5.62
		warmed-up	2.87
690	3000	cold	5.85
		warmed-up	1.97
mm	500	cold	5.43
		warmed-up	3.10
650	3000	cold	6.55
		warmed-up	2.81
mm	500	cold	3.89
		warmed-up	3.89

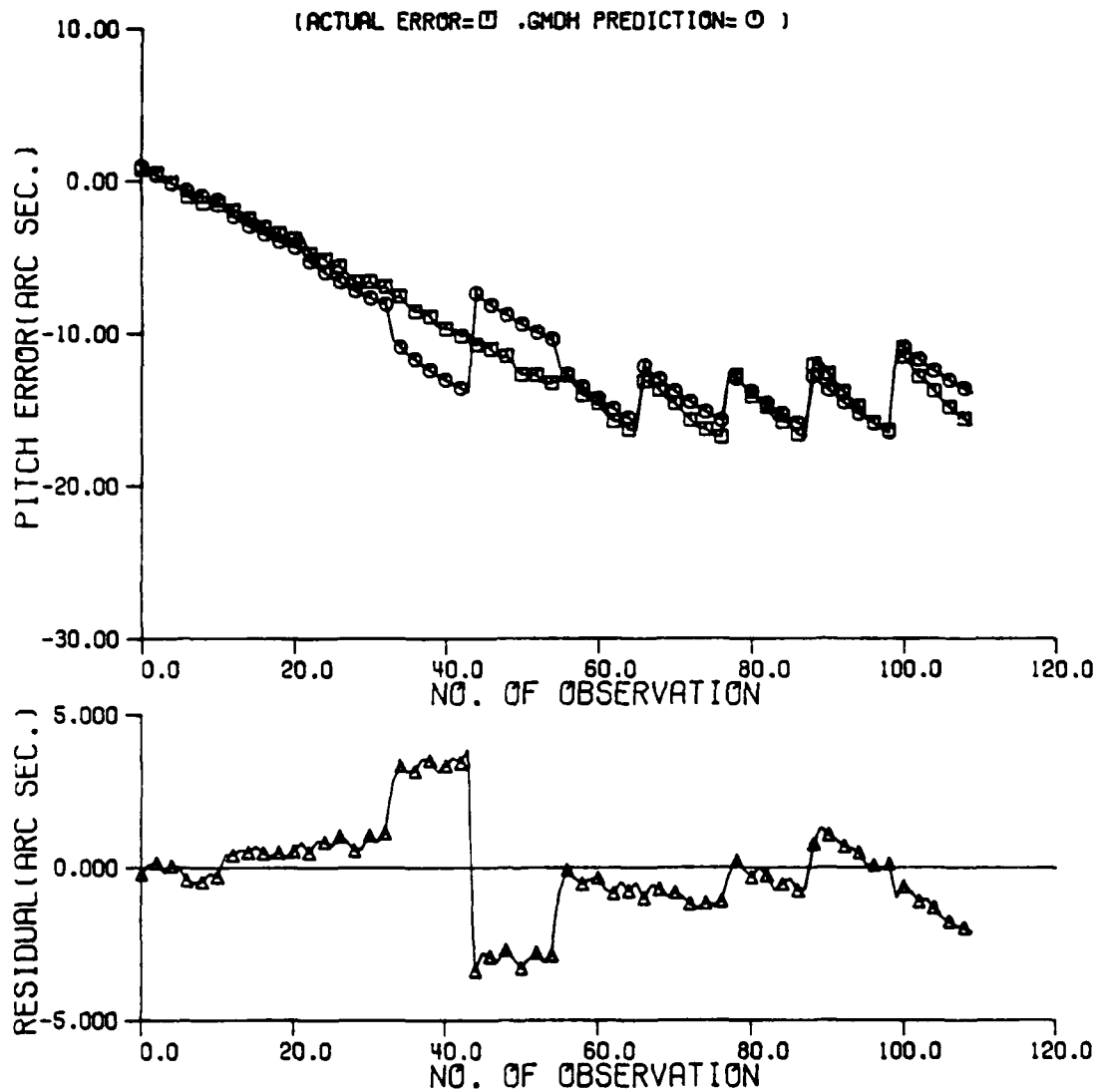


Figure 2.23 The result of the GMDH prediction on the x axis pitch error and its residual.

CHAPTER 3 - METHODOLOGY

3.1 Volumetric Error Assessment

When any of the three axes of a machining center moves, there appear several error components which affect the final position of the tool tip for each axis. Displacement errors such as the positioning error, the vertical straightness error, and the horizontal straightness error and some angular errors like pitch and yaw errors can be measured at the tool tip position with a commercial laser interferometer. The roll error can be measured with an electronic split level.

The vector $U_2(x_2, y_2, z_2)$ of the changed position of the commanded vector $U_1(x, y, z)$ for motion along one axis produced by rotational and displacement error components can be expressed using a homogeneous transformation of the space H as

$$U_2 = H \cdot U_1 \quad (3.1)$$

where H is a matrix which accounts for transformations of six error components for one axis, three rotational error transformations and three translational error transformations.

The general transformation for rotation of a vector about the axis of rotation $K(k_x, k_y, k_z)$ through an angle θ is given by:[18]

$$\text{Rot}(K, \theta) = \begin{pmatrix} k_x k_x \text{vers}\theta + \cos\theta & k_y k_x \text{vers}\theta - k_z \sin\theta & k_z k_x \text{vers}\theta + k_y \sin\theta & 0 \\ k_x k_y \text{vers}\theta + k_z \sin\theta & k_y k_y \text{vers}\theta + \cos\theta & k_z k_y \text{vers}\theta - k_x \sin\theta & 0 \\ k_x k_z \text{vers}\theta - k_y \sin\theta & k_y k_z \text{vers}\theta + k_x \sin\theta & k_z k_z \text{vers}\theta + \cos\theta & 0 \\ 0 & 0 & 0 & 1 \end{pmatrix} \quad (3.2)$$

where $\text{vers}\theta = 1 - \cos\theta$.

For movement along the y axis as in figure 3.1(b), the pitch error is due to a rotation transformation about the x axis by an angle e_x and can be expressed as

$$\text{Pitch error} = \text{Rot}(x, e_x) = \begin{pmatrix} 1 & 0 & 0 & 0 \\ 0 & \cos e_x & -\sin e_x & 0 \\ 0 & \sin e_x & \cos e_x & 0 \\ 0 & 0 & 0 & 1 \end{pmatrix} \quad (3.3)$$

When very small differential changes such as pitch error occur, $\sin e_x$ can be replaced by e_x and $\cos e_x$ by 1. Therefore Equation (2.3) becomes

$$\text{Pitch error} = \begin{pmatrix} 1 & 0 & 0 & 0 \\ 0 & 1 & -e_x & 0 \\ 0 & e_x & 1 & 0 \\ 0 & 0 & 0 & 1 \end{pmatrix} \quad (3.4)$$

In the same manner we obtain

$$\text{Roll error} = \text{Rot}(y, e_y) = \begin{bmatrix} 1 & 0 & e_y & 0 \\ 0 & 1 & 0 & 0 \\ -e_y & 0 & 1 & 0 \\ 0 & 0 & 0 & 1 \end{bmatrix} \quad (3.5)$$

and

$$\text{Yaw error} = \text{Rot}(z, e_z) = \begin{bmatrix} 1 & -e_z & 0 & 0 \\ e_z & 1 & 0 & 0 \\ 0 & 0 & 1 & 0 \\ 0 & 0 & 0 & 1 \end{bmatrix} \quad (3.6)$$

The positioning error d_y , the horizontal straightness error d_x , and the vertical straightness error d_z can be combined into the translation transformation given by

$$\text{Trans}(d_x, d_y, d_z) = \begin{bmatrix} 1 & 0 & 0 & d_x \\ 0 & 1 & 0 & d_y \\ 0 & 0 & 1 & d_z \\ 0 & 0 & 0 & 1 \end{bmatrix} \quad (3.7)$$

Therefore the homogeneous transformation of the space H is obtained by the matrix multiplication

$$H = \text{Rot}(x, e_x) \cdot \text{Rot}(y, e_y) \cdot \text{Rot}(z, e_z) \cdot \text{Trans}(d_x, d_y, d_z) \quad (3.8)$$

If we neglect second order terms, then

$$H = \begin{bmatrix} 1 & -e_z & e_y & d_x \\ e_z & 1 & -e_x & d_y \\ -e_y & e_x & 1 & d_z \\ 0 & 0 & 0 & 1 \end{bmatrix} \quad (3.9)$$

The machine tool movement is the combination of movements along three independent axes(i.e., x, y, and z axes). If

we measure the errors from a fixed measurement origin, we can use those data points to obtain the resultant errors within the work space. Figures 3.1(a), 3.1(b), and 3.1(c) show the error phenomenon of each axis and its notation. Using Eq. (3.9), if it is commanded to go to (x,y,z) from the measurement origin, we obtain the final position (x',y',z'):

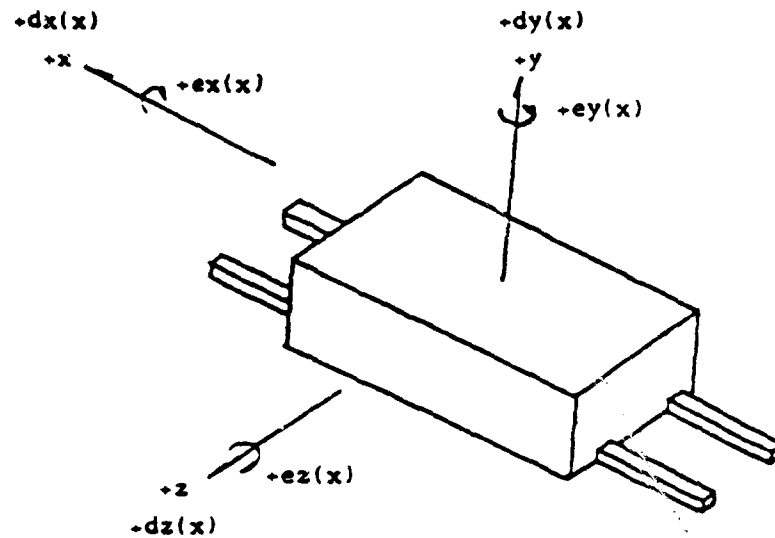
$$\begin{bmatrix} x' \\ y' \\ z' \\ 1 \end{bmatrix} = \begin{bmatrix} 1 & -ez(z) & ey(z) & dx(z) \\ ez(z) & 1 & -ex(z) & dy(z) \\ -ey(z) & ex(z) & 1 & dz(z) \\ 0 & 0 & 0 & 1 \end{bmatrix} \cdot \begin{bmatrix} 1 & -ez(y) & ey(y) & dx(y) \\ ez(y) & 1 & -ex(y) & dy(y) \\ -ey(y) & ex(y) & 1 & dz(y) \\ 0 & 0 & 0 & 1 \end{bmatrix} \cdot \begin{bmatrix} 1 & -ez(x) & ey(x) & dx(x) \\ ez(x) & 1 & -ex(x) & dy(x) \\ -ey(x) & ex(x) & 1 & dz(x) \\ 0 & 0 & 0 & 1 \end{bmatrix} \cdot \begin{bmatrix} x \\ y \\ z \\ 1 \end{bmatrix}$$

(if we neglect second order terms, then)

$$= \begin{bmatrix} 1 & -ez(x)-ez(y)-ez(z) \\ ez(x)+ez(y)+ez(z) & 1 \\ -ey(x)-ey(y)-ey(z) & ex(x)+ex(y)+ex(z) \\ 0 & 0 \\ ey(x)+ey(y)+ey(z) & dx(x)+dx(y)+dx(z) \\ -ex(x)-ex(y)-ex(z) & dy(x)+dy(y)+dy(z) \\ 1 & dz(x)+dz(y)+dz(z) \\ 0 & 1 \end{bmatrix} \cdot \begin{bmatrix} x \\ y \\ z \\ 1 \end{bmatrix} \quad (3.10)$$

Let $EX = ex(x)+ex(y)+ex(z)$

$EY = ey(x)+ey(y)+ey(z)$



($dx(x)$: positioning error
 $dy(x)$: vertical straightness error
 $dz(x)$: horizontal straightness error
 $ex(x)$: roll error
 $ey(x)$: yaw error
 $ez(x)$: pitch error)

Figure 3.1 The error components of x axis and their notations.

$$EZ = ez(x) + ez(y) + ez(z)$$

$$DX = dx(x) + dx(y) + dx(z)$$

$$DY = dy(x) + dy(y) + dy(z)$$

$$DZ = dz(x) + dz(y) + dz(z)$$

Then

$$\begin{bmatrix} x' \\ y' \\ z' \\ 1 \end{bmatrix} = \begin{bmatrix} x - y \cdot EZ + z \cdot EY + DX \\ y + x \cdot EZ - z \cdot EX + DY \\ z + y \cdot EX - x \cdot EY + DZ \\ 1 \end{bmatrix} \quad (3.11)$$

The resultant error vector is expressed as follows.

$$\text{Error} = \begin{bmatrix} \text{Error}_x \\ \text{Error}_y \\ \text{Error}_z \\ 1 \end{bmatrix} = \begin{bmatrix} x' - x \\ y' - y \\ z' - z \\ 1 \end{bmatrix} = \begin{bmatrix} -y \cdot EZ + z \cdot EY + DX \\ -z \cdot EX + x \cdot EZ + DY \\ -x \cdot EY + y \cdot EX + DZ \\ 1 \end{bmatrix} \quad (3.12)$$

The above equation (3.12) shows that the x component of the resultant error is the sum of the error resulting from rotation errors about y and z axis, ($z \cdot EY$ and $-y \cdot EZ$), and those from the displacement errors in the x direction, (DX).

In addition to the 18 errors of 3 moving axes, non-orthogonality errors are important to be considered. Figure 3.2 shows non-orthogonality errors of moving axes expressed with the assumption that the z moving axis coincides with the z reference axis.

The transformation matrix including non-orthogonality errors becomes:

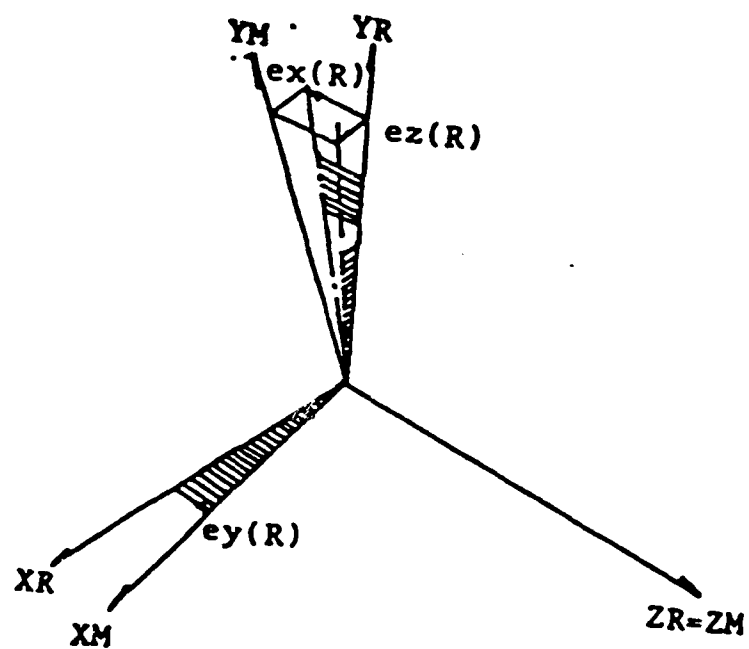


Figure 3.2 Non-orthogonality errors of moving axes with the assumption of the coincidence of the z moving axis with the z reference axis

$$H = \begin{bmatrix} 1 & -EZ & EY & DX \\ EZ & 1 & -EX & DY \\ -EY & EX & 1 & DZ \\ 0 & 0 & 0 & 1 \end{bmatrix} \cdot \begin{bmatrix} 1 & -ez(R) & ey(R) & 0 \\ ez(R) & 1 & -ex(R) & 0 \\ -ey(R) & ex(R) & 1 & 0 \\ 0 & 0 & 0 & 1 \end{bmatrix}$$

(if we neglect the second order terms, then)

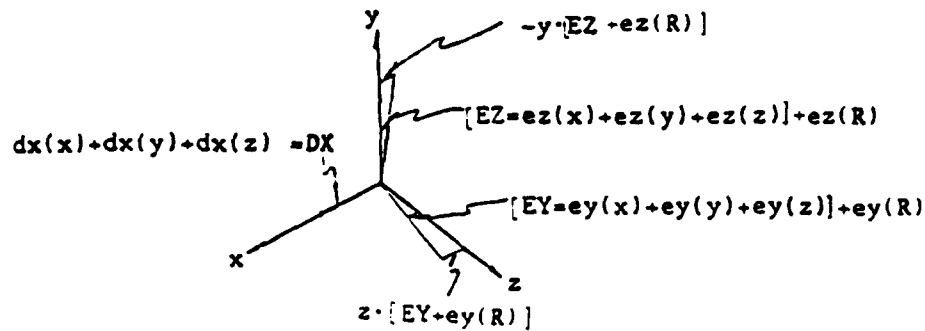
$$= \begin{bmatrix} 1 & -(EZ+ez(R)) & EY+ey(R) & DX \\ EZ+ez(R) & 1 & -(EX+ex(R)) & DY \\ -(EY+ey(R)) & EX+ex(R) & 1 & DZ \\ 0 & 0 & 0 & 1 \end{bmatrix} \quad (3.13)$$

The above equation (3.13) shows that the x component of the resultant error is the sum of the error resulting from rotation errors about y and z axis, ($z \cdot EY$ and $-y \cdot EZ$), and those from the displacement errors in the x direction, (DX). Non-angular errors are regarded as constant at certain thermal conditions. The error vector including non-orthogonality effects can be obtained by replacing angular errors of Equation (3.12). Figure 3.3 shows the effect of the individual errors on the resultant work space error vector.

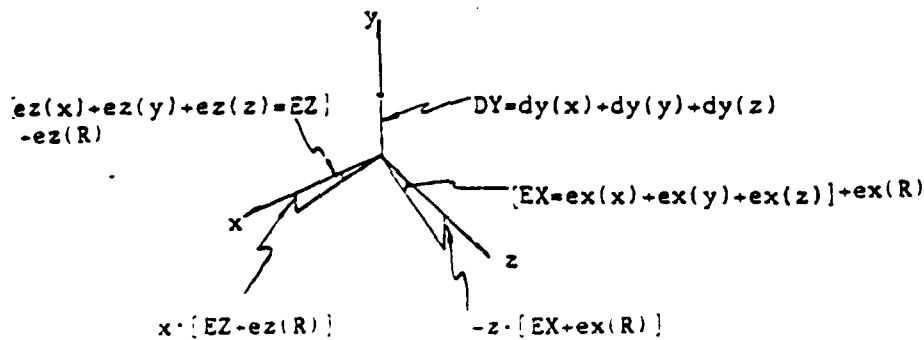
3.2 Mathematical Error Modeling for Touch Probe Application

Errors obtained by the probing metrology pallet can be used for compensation by two important mathematical modeling approaches. The first approach is using the regression analysis technique. Only coordinate data and calculated error values are used for regression analysis in a

$$(a) \text{ Error}_x = -y \cdot [EZ + ez(R)] + z \cdot [EY + ey(R)] + DX$$



$$(b) \text{ Error}_y = -z \cdot [EX + ex(R)] + x \cdot [EZ + ez(R)] + DY$$



$$(c) \text{ Error}_z = -x \cdot [EY + ey(R)] + y \cdot [EX + ex(R)] + DZ$$

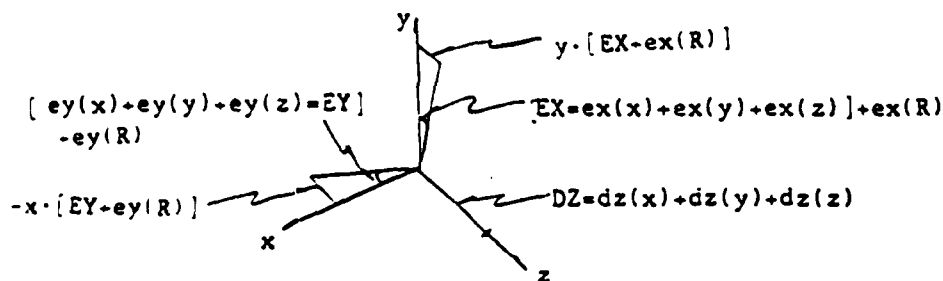


Figure 3.3 The effect of the error components on the resultant work space error vector

certain thermal condition. This technique is the simplest approach to be applied to a real production line, which needs only the feedback of touch probe coordinate sensing. The second approach is using the GMDH type approach. This technique needs the temperature feedback of several important spots on the machine tool in addition to the probe signal feedback. Several sets of measurement data should be used for modelling the error function. This causes some delay to be applied to the compensation purpose. After a certain stage of data acquisition, however, this approach enables the prediction of errors by the feedback of temperature information. This prediction capability can be used for the compensation of machining error and also for the determination of time for reentry of the metrology pallet.

3.2.1 Regression Analysis Approach For obtaining the regression function of the resultant error at the work space, the transformation of error components can be used. In addition to the 18 errors of 3 moving axes, non-orthogonality errors are considered to be important.

The transformation matrix including non-orthogonality errors, equation (3.12), shows that non-orthogonality errors add to the correspondent angular errors in certain amounts. Non-angular errors are regarded as the constant in a certain thermal condition. The error vector including

non-orthogonality effects can be obtained by replacing angular errors.

3.2.2 Expression of Resultant Errors using each Error Components From the measured values of machine tool errors[3], regression equations for each of the six error components of an axis can be obtained as a function of the position along each axis or as a constant, as follows:

$$\begin{aligned}
 ex(x) &= c_1 \\
 ey(x) &= c_2x + c_3 \\
 ez(x) &= c_4x + c_5 \\
 dx(x) &= c_6x^2 + c_7x + c_8 \\
 dy(x) &= c_9 \\
 dz(x) &= c_{10} \\
 ex(y) &= c_{11}y + c_{12} \\
 ey(y) &= c_{13} \\
 ez(y) &= c_{14}y + c_{15} \\
 dx(y) &= c_{16} \\
 dy(y) &= c_{17}y^2 + c_{18}y + c_{19} \\
 dz(y) &= c_{20} \\
 ex(z) &= c_{21}z + c_{22} \\
 ey(z) &= c_{23}z + c_{24} \\
 ez(z) &= c_{25}z + c_{26} \\
 dx(z) &= c_{27} \\
 dy(z) &= c_{28} \\
 dz(z) &= c_{29}z^2 + c_{30}z + c_{31}
 \end{aligned} \tag{3.14}$$

$$ex(R) = c_{32}$$

$$ey(R) = c_{33}$$

$$ez(R) = c_{34}$$

If Equation (3.14) is used in place of the equation (3.12), the x component of the error vector at (x,y,z) becomes

$$\begin{aligned} \text{Error}_x &= -y \cdot (EZ + ez(R)) + z \cdot (EY + ey(R)) + DX \\ &= -y \cdot \left| (c_4 x + c_5) + (c_{14} y + c_{16}) + (c_{25} z + c_{26}) + c_{34} \right| \\ &\quad + z \cdot \left| (c_2 x + c_3) + c_{13} + (c_{23} z + c_{24}) + c_{33} \right| \\ &\quad + \left| (c_6 x^2 + c_7 x + c_8) + c_{16} + c_{27} \right| \\ &= c_7 x - (c_5 + c_{16} + c_{26} + c_{34}) y + (c_3 + c_{13} + c_{24} + c_{33}) z \\ &\quad - c_{25} y z - c_4 x y + c_2 z x + c_6 x^2 - c_{14} y^2 + c_{23} z^2 \\ &\quad + (c_8 + c_{16} + c_{27}) \\ &= a_1 + a_2 x + a_3 y + a_4 z + a_5 xy + a_6 yz + a_7 zx \\ &\quad + a_8 x^2 + a_9 y^2 + a_{10} z^2 \end{aligned} \quad (3.15)$$

In the same manner, we obtain

$$\begin{aligned} \text{Error}_y &= -z \cdot (EX + ex(R)) + x \cdot (EZ + ez(R)) + DY \\ &= (c_5 - c_{15} - c_{26} - c_{34}) \cdot x + c_{18} \cdot y - (c_1 + c_{12} \\ &\quad + c_{22} + c_{32}) \cdot z + c_{14} xy - c_{11} yz - c_{25} zx + c_4 x^2 \\ &\quad + c_{17} y^2 - c_{21} z^2 + (c_9 + c_{19} + c_{28}) \\ &= a_{11} + a_{12} x + a_{13} y + a_{14} z + a_{15} xy + a_{16} yz \end{aligned}$$

$$+ a_{17}zx + a_{18}x^2 + a_{19}y^2 + a_{20}z^2 \quad (3.16)$$

and

$$\begin{aligned} \text{Error}_z &= -x'(EY+ey(R)) + y'(EX+ex(R)) + DZ \\ &= -(c_3+c_{13}+c_{24}+c_{33})'x + (c_1+c_{12}+c_{22}+c_{32})'y \\ &\quad + c_{30}z + c_{21}yz - c_{23}zx - c_2x^2 + c_{11}y^2 \\ &\quad + c_{29}z^2 + (c_{10}+c_{20}+c_{31}) \\ &= a_{21} + a_{22}x + a_{23}y + a_{24}z + a_{25}yz + a_{26}zx \\ &\quad + a_{27}x^2 + a_{28}y^2 + a_{29}z^2 \end{aligned} \quad (3.16)$$

3.2.3 Two approaches to obtain error regression functions by the touch probe

There are two feasible approaches for obtaining the error at a tool tip position within the work space by the touch probe. One is to have measurement points throughout the work space and a probe long enough to touch all the measurement points as shown in figure 3.4. The other is to have measurement points on a plane and two probes of different length, a long probe and a short one as shown in figure 3.5. The probe should be long enough to take care of the entire machining range of z axis. Each probe has a "dynamic" diameter value which takes care of "pretraveling" prior to triggering the signal to stop. Compensation for the pretraveling error can be found by measuring a block of known distance. For the two probe approach the metrology pallet should be positioned at two different z

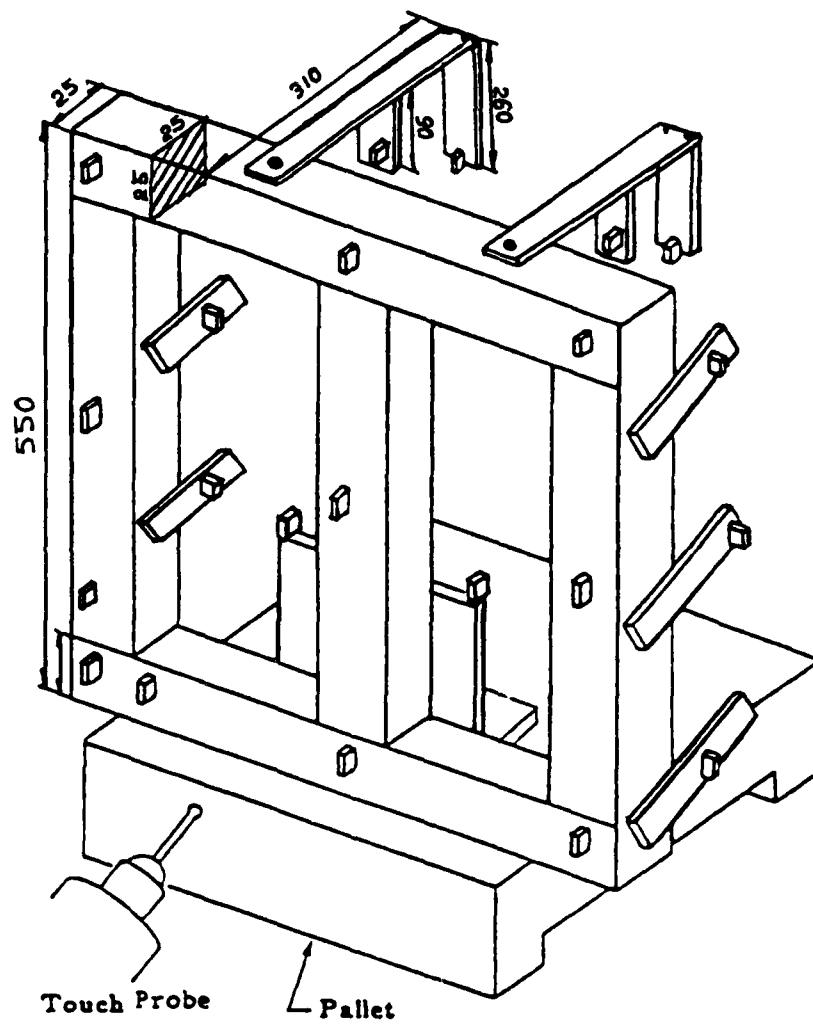


Figure 3.4 One probe approach to obtain errors in the work space

location to accomodate for variation of probe length. All measurement points are mounted on a metrology pallet.

Basically, two approaches should give the same results for obtaining the error values. The one probe approach has the disadvantage of a complex calibration structure while the two probe approach has the advantage of a simple calibration structure. The cost associated with a two probe approach is higher and it will occupy one more space at the tool chain.

For the two approaches, the formulation of the error model is the same. The general linear regression model for error components can be expressed as:

$$Y_i = \beta_0 + \beta_1 X_{i1} + \beta_2 X_{i2} + \dots + \beta_{p-1} X_{i,p-1} + \epsilon_i \quad (3.17)$$

and in matrix form:

$$Y = X\beta + \epsilon \quad (3.18)$$

In case of x axis, we have $y_i = \text{Error}x_i$, $X_{i1} = x_i$, $X_{i2} = y_i$, $X_{i3} = z_i$, $X_{i4} = x_i y_i$, $X_{i5} = y_i z_i$, $X_{i6} = z_i x_i$, $X_{i7} = y_i^2$, $X_{i8} = z_i^2$, and β 's are the coefficients. Equation (3.18) is the same as Equation (3.14) and Equation (3.18) represents the x component of the work space error.

The least squares normal equation for the general linear regression model(3.18) is:

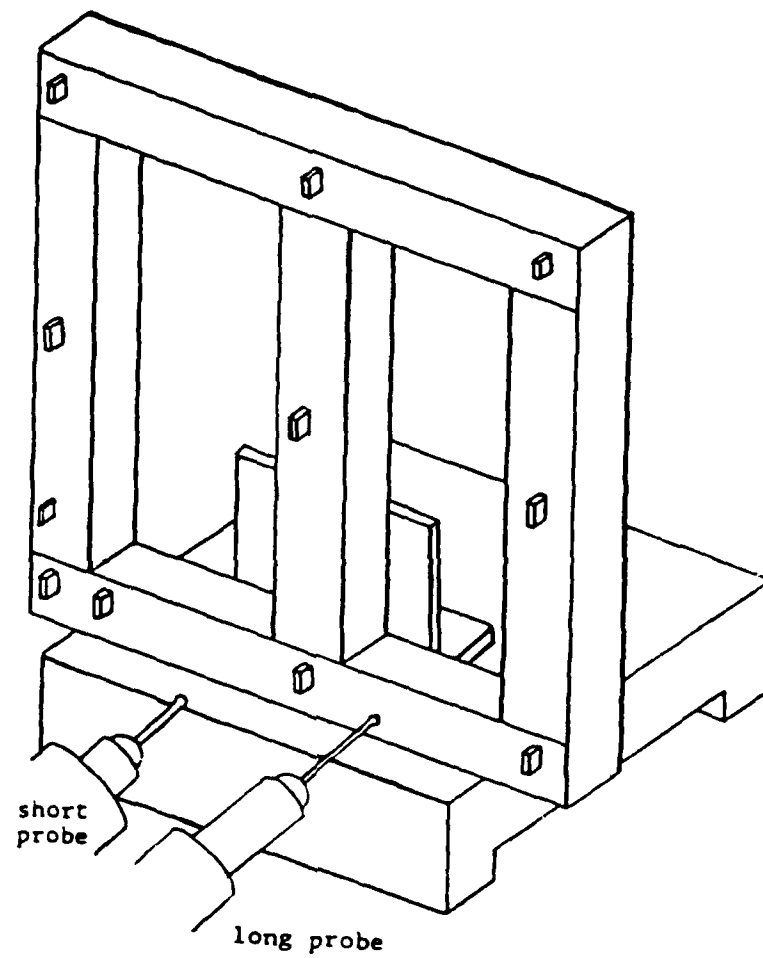


Figure 3.5 Two probe approach to obtain errors in the work space

$$(X^T X)b = X^T Y \quad (3.19)$$

and the least squares estimator is:

$$b = (X^T X)^{-1} X^T Y \quad (3.20)$$

which is an unbiased, minimum variance estimator.

3.3 Calculation of an Error

Error of the probe end at the machine tool with respect to the calibration values of the measurement points can be expressed as transform equation form as in figure 3.6. The transform equation for the probed point is

$$Pallet^{Pallet} Cal \cdot Error = Probe$$

The probed point is positioned with respect to base coordinate (the origin of machine absolute coordinate) by a transform Probe:

$$Probe = \begin{vmatrix} 1 & 0 & 0 & X_{abs} \\ 0 & 1 & 0 & Y_{abs} \\ 0 & 0 & 1 & Z_{abs} \\ 0 & 0 & 0 & 1 \end{vmatrix}$$

For our application, the absolute coordinate of the machine for the measurement points- X_{abs} , Y_{abs} , and Z_{abs} - are obtained directly from the machine controller sent to the host computer VAX 11/750 for the simulation of a Flexible Manufacturing System environment. The origin of the metrology pallet is positioned with respect to the base

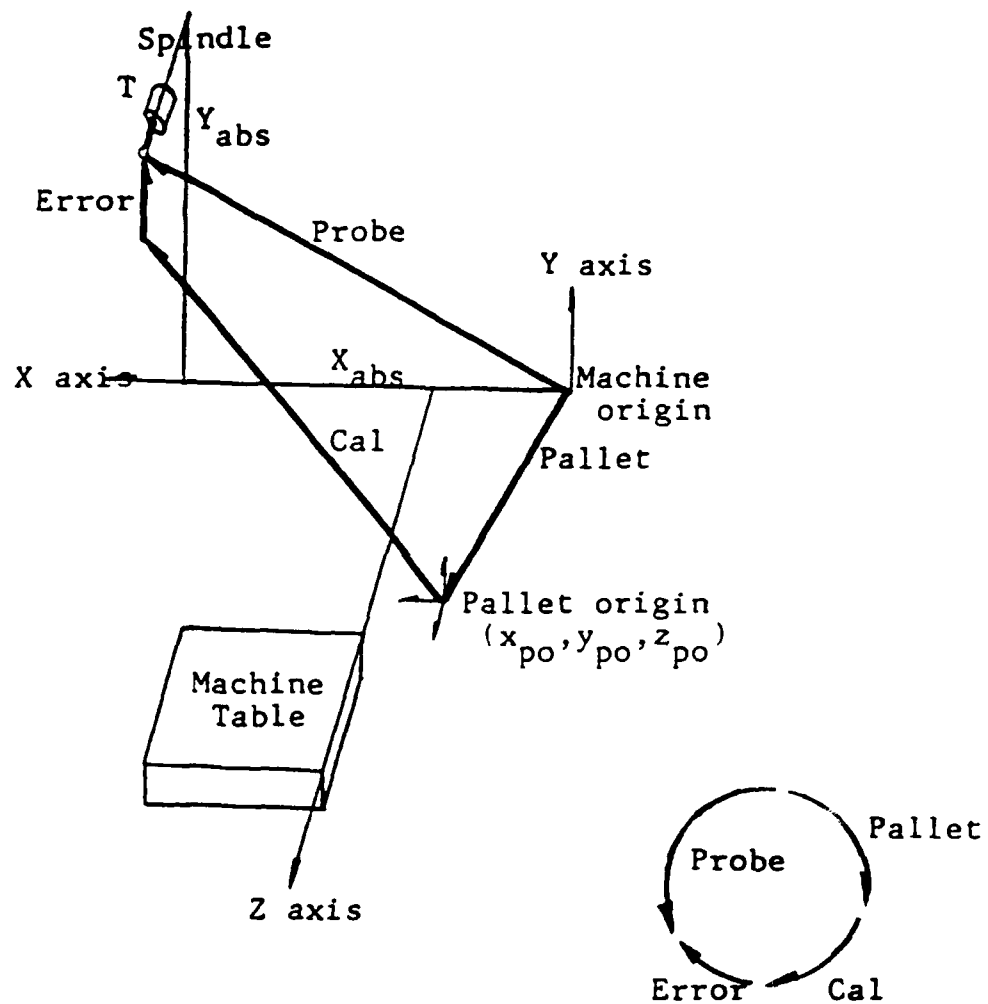


Figure 3.6 The transform equation for the error of the probe tip position

coordinates by a transform Pallet:

$$\text{Pallet} = \begin{bmatrix} 1 & 0 & 0 & X_{po} \\ 0 & 1 & 0 & Y_{po} \\ 0 & 0 & 1 & Z_{po} \\ 0 & 0 & 0 & 1 \end{bmatrix}$$

These values are obtained by probing the origin point of the metrology pallet, which contains error values for that point in the specific thermal condition of the machine tool.

The measurement point is positioned with respect to the pallet origin by a transformation Cal:

$$\text{Cal} = \begin{bmatrix} 1 & 0 & 0 & X_{cp} \\ 0 & 1 & 0 & Y_{cp} \\ 0 & 0 & 1 & Z_{cp} \\ 0 & 0 & 0 & 1 \end{bmatrix}$$

X_{cp} , Y_{cp} , and Z_{cp} are supposed to be the correct dimensions for a measurement point and are obtained by a transformation of measured values at CMM. Errors are calculated by

$$\text{Error} = (\text{Pallet} \cdot \text{Pallet}_{\text{Cal}})^{-1} \cdot \text{Probe}$$

$$\begin{aligned}
 & \begin{bmatrix} & & \text{Error}_x \\ 1 & 0 & 0 \\ & 0 & 1 & 0 & \text{Error}_y \\ & 0 & 0 & 1 & \text{Error}_z \\ 0 & 0 & 0 & & 1 \end{bmatrix} \\
 & = \begin{bmatrix} & & X_{po}+X_{cal} \\ 1 & 0 & 0 \\ & 0 & 1 & 0 & Y_{po}+Y_{cal} \\ & 0 & 0 & 1 & Z_{po}+Z_{cal} \\ 0 & 0 & 0 & & 1 \end{bmatrix}^{-1} \cdot \begin{bmatrix} & & X_{probe} \\ 1 & 0 & 0 \\ & 0 & 1 & 0 & Y_{probe} \\ & 0 & 0 & 1 & Z_{probe} \\ 0 & 0 & 0 & & 1 \end{bmatrix} \\
 & = \begin{bmatrix} & & -(X_{po}+X_{cal})+X_{probe} \\ 1 & 0 & 0 \\ & 0 & 1 & 0 & -(Y_{po}+Y_{cal})+Y_{probe} \\ & 0 & 0 & 1 & -(Z_{po}+Z_{cal})+Z_{probe} \\ 0 & 0 & 0 & & 1 \end{bmatrix} \quad (3.21)
 \end{aligned}$$

3.4 Calibration of the Metrology Pallet

If the whole metrology pallet is transferred to the machine tool automatically in a Flexible Manufacturing System which has a coordinate measuring machine, the measurement values of the metrology pallet at a CMM can be used as calibration values to calculate the errors in the working space. However, once the metrology pallet is detached from the table of a CMM and set up at the table of the machine tool, the measurement coordinate of the machine tool happens to be different from that of the CMM. That can be caused by set-up errors, clamping force effect, and surface waviness of base plate of the metrology pallet and machine tool table as figure 3.7. Inaccuracy of placing the metrology

AD-A174 974 THE SCIENCE OF AND ADVANCED TECHNOLOGY FOR
COST-EFFECTIVE MANUFACTURE OF (U) PURDUE UNIV
LAFAYETTE IN SCHOOL OF INDUSTRIAL ENGINEERING
UNCLASSIFIED S LEE ET AL NOV 86 N00014-83-K-0385 F/

THE SCIENCE OF AND ADVANCED TECHNOLOGY FOR
COST-EFFECTIVE MANUFACTURE OF (U) PURDUE UNIV
LAFAYETTE IN SCHOOL OF INDUSTRIAL ENGINEERING
S LEE ET AL NOV 86 N00014-83-K-0385 F/

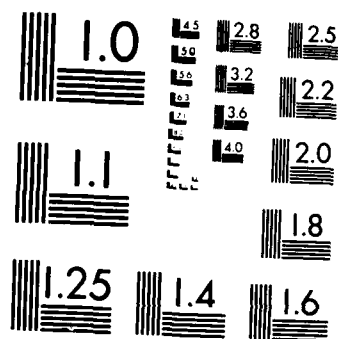
24

UNCLASSIFIED

S LEE ET AL NOV 86 N00014-83-K-0385

F/G 13/9

NL



MICROCOPY RESOLUTION TEST CHART
NATIONAL BUREAU OF STANDARDS 1963-A

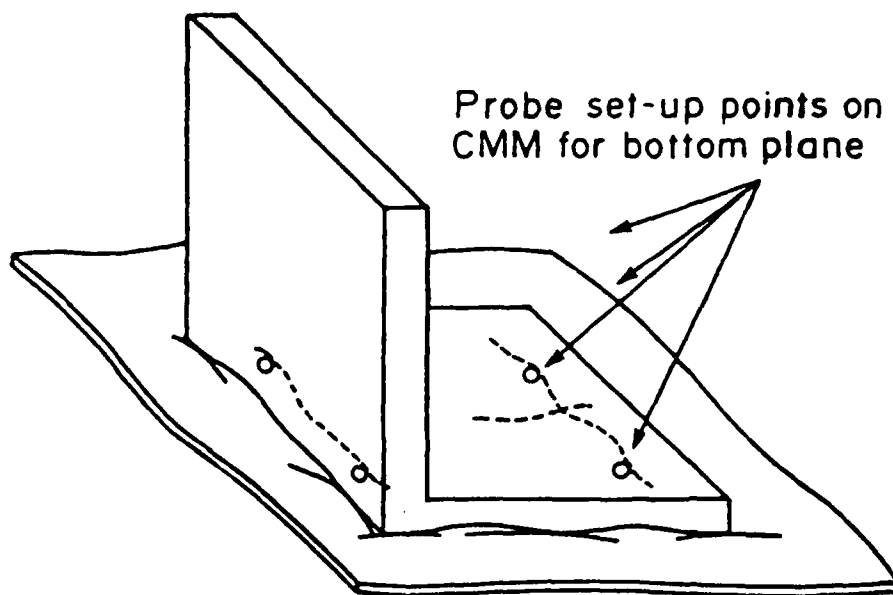


Figure 3.7 Variation of a coordinate system at the machine because of the waviness of the surfaces, clamping forces, and so on.

pallet on a machine tool table may also cause a different coordinate from that of the CMM at the Flexible Manufacturing System.

To obtain the same skewness of the metrology pallet at the machine tool as that of the metrology pallet at the CMM, the homogeneous transformation should be done to transform the CMM coordinate to the machine tool coordinate for the calibration values as:

$$X_m = T X_c \quad (3.22)$$

where X_m : transformed position vectors for calibration at the machine tool

T : homogeneous transformation matrix

X_c : position vectors of measured points at CMM

If the metrology pallet at the CMM has a differential change of rotation with respect to x, y, and z axes as shown in figure 3.8, the homogeneous transformation matrix can be expressed as;

$$T = \text{Rot}(x, \delta_x) \text{Rot}(y, \delta_y) \text{Rot}(z, \delta_z) \quad (3.23)$$

$$= \begin{bmatrix} 1 & -\delta_z & \delta_y & 0 \\ \delta_z & 1 & 1 & 0 \\ -\delta_y & \delta_x & \delta_x & 0 \\ 0 & 0 & 0 & 1 \end{bmatrix}$$

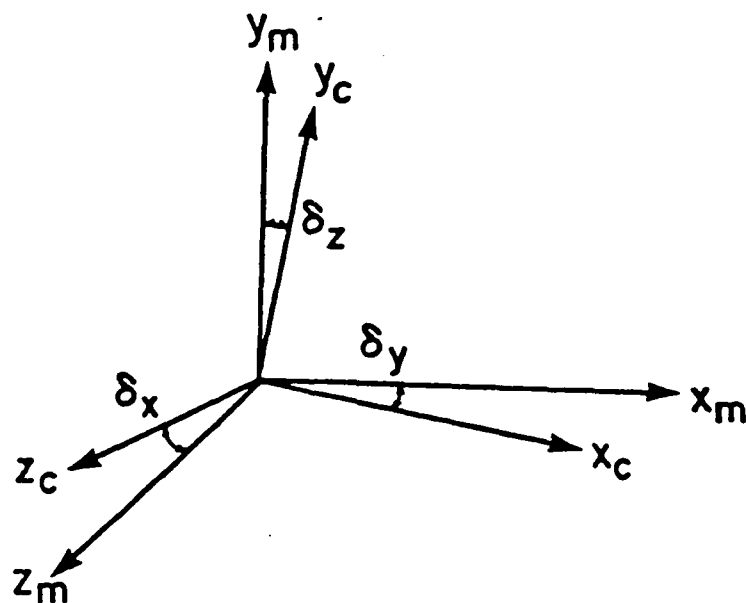


Figure 3.8 Differential change of a coordinate system with respect to x , y , and z axis at the machine.

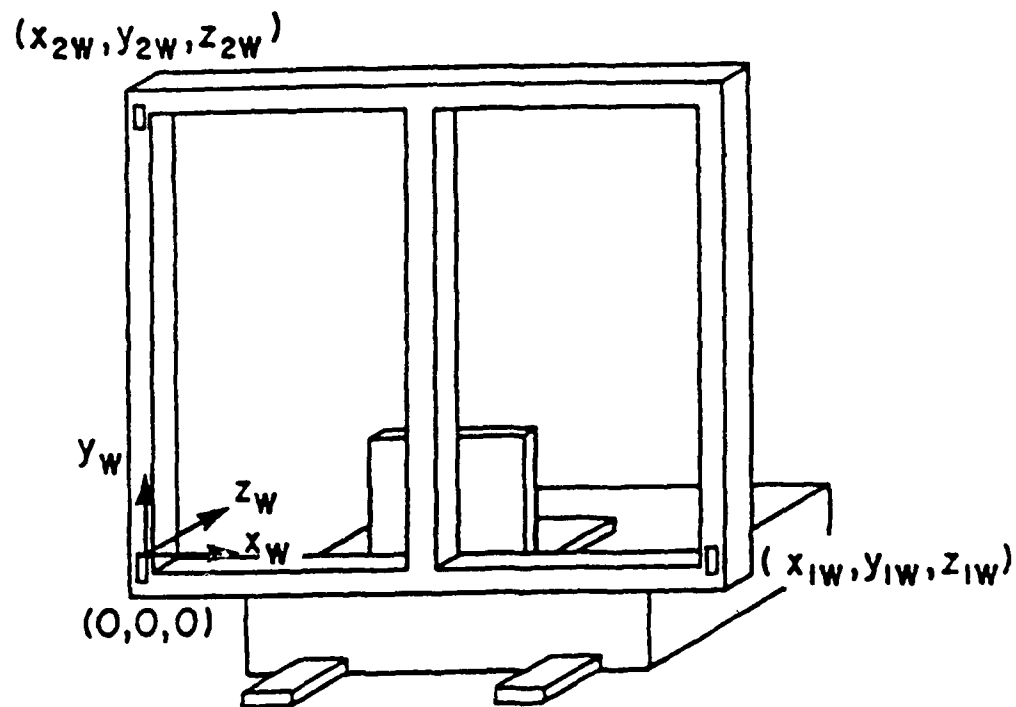
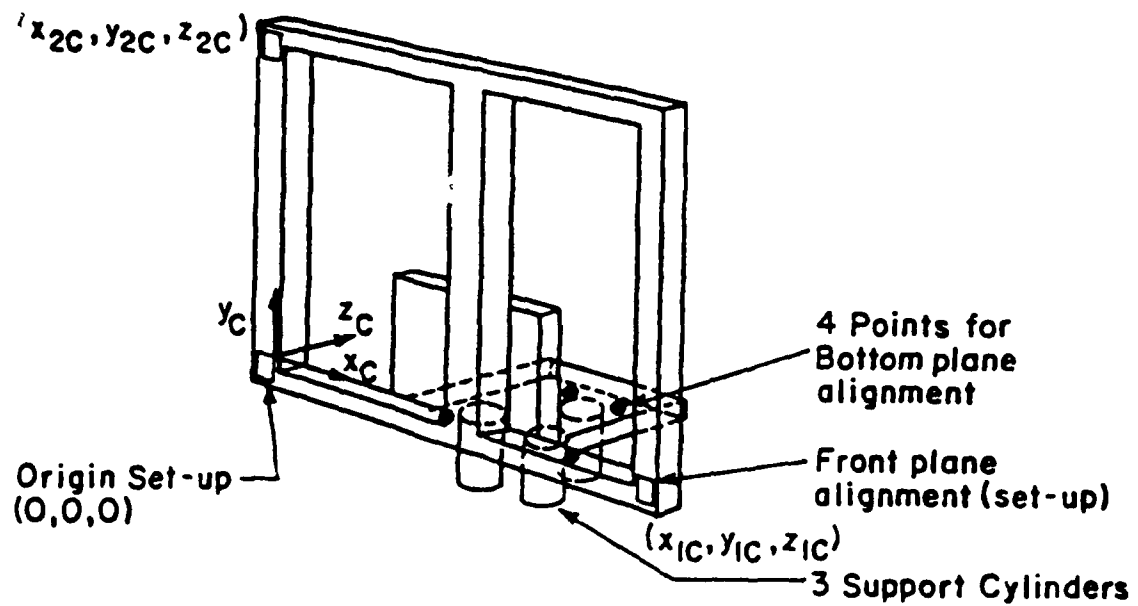


Figure 3.9 Four coordinate values from two extreme points used for calibration after homogeneous transformation

Four coordinate values from two extreme points of the metrology pallet at the machine tool, as shown in figure 3.9, are assumed to be the same as the calibration values after the homogeneous transformation; i.e., y_{1w} , z_{1w} , x_{2w} , and z_{2w} are the same as y_{1c} , z_{1c} , x_{2c} , and z_{2c} as figure 3.10.

From Equations (3.22) and (3.23), we have

$$\begin{aligned} y_{1w} &= x_{1c} \delta_z + y_{1c} - z_{1c} \delta_x \\ z_{1w} &= -x_{1c} \delta_y + y_{1c} \delta_x + z_{1c} \\ z_{2w} &= -x_{2c} \delta_y + y_{2c} \delta_x + z_{2c} \\ x_{2w} &= x_{2c} - y_{2c} \delta_z + z_{2c} \delta_y \end{aligned}$$

,which becomes

$$\begin{bmatrix} y_{1w} \\ z_{1w} \\ z_{2w} \\ x_{2w} \end{bmatrix} = \begin{bmatrix} -z_{1c} & 0 & x_{1c} & y_{1c} \\ y_{1c} & -x_{1c} & 0 & z_{1c} \\ y_{2c} & -x_{2c} & 0 & z_{2c} \\ 0 & z_{2c} & -y_{2c} & x_{2c} \end{bmatrix} \cdot \begin{bmatrix} \delta_x \\ \delta_y \\ \delta_z \\ 1 \end{bmatrix}$$

Therefore, we obtain

$$\begin{bmatrix} \delta_x \\ \delta_y \\ \delta_z \\ 1 \end{bmatrix} = \begin{bmatrix} -z_{1c} & 0 & x_{1c} & y_{1c} \\ y_{1c} & -x_{1c} & 0 & z_{1c} \\ y_{2c} & -x_{2c} & 0 & z_{2c} \\ 0 & z_{2c} & -y_{2c} & x_{2c} \end{bmatrix}^{-1} \begin{bmatrix} y_{1w} \\ z_{1w} \\ z_{2w} \\ x_{2w} \end{bmatrix} \quad (3.24)$$

Calibration values for the metrology pallet at the machine tool are calculated using Equations (3.21), (3.22), and (3.23).

$$\begin{bmatrix} x_{1m} & x_{2m} & . & . & . & x_{nm} \\ y_{1m} & . & . & . & . & . \\ z_{1m} & . & . & . & . & . \\ 1 & . & . & . & . & 1 \end{bmatrix} = |T| \cdot \begin{bmatrix} x_{1c} & x_{2c} & . & . & . & x_{nc} \\ y_{1c} & . & . & . & . & . \\ z_{1c} & . & . & . & . & . \\ 1 & . & . & . & . & 1 \end{bmatrix}$$

, i.e.,

$$X_m = T X_c$$

The modern machine tool, however, used to have some error compensation package in its controller so as not to have errors, specially positioning error, in cold condition. The actual measurement of error components in the cold condition for the machine tool used for experiment does not show significant amount of errors relative to that in the warmed-up condition. Calculation of errors with respect to coordinate values, which are obtained by probing the metrology pallet at the standard temperature environment, can be another alternative for the calibration of the metrology pallet from the application point of view. These calculated values reflect mainly thermal effects on machine tool errors.

3.5 Decomposition of the Resultant Error to Error Components

From equations (3.15), (3.16), and (3.17), the relationships between the resultant error components and the coefficients of error component equations can be obtained as follows:

$$\begin{aligned}
 \text{Error}_x &= zx \cdot c_2 + z \cdot c_3 - xy \cdot c_4 - y \cdot c_5 + x^2 \cdot c_6 + x \cdot c_7 + c_8 + z \cdot c_{13} \\
 &\quad - y^2 \cdot c_{14} - y \cdot c_{15} + c_{16} + z^2 \cdot c_{23} + z \cdot c_{24} - yz \cdot c_{25} \\
 &\quad - y \cdot c_{26} + c_{27} + z \cdot c_{33} - y \cdot c_{34} \\
 \text{Error}_y &= -z \cdot c_1 + x^2 \cdot c_4 + x \cdot c_5 + c_9 - yz \cdot c_{11} - z \cdot c_{12} + x \cdot c_{15} \\
 &\quad + y^2 \cdot c_{17} + y \cdot c_{18} + c_{19} - z^2 \cdot c_{21} - z \cdot c_{22} + zx \cdot c_{25} \\
 &\quad + x \cdot c_{26} + c_{28} - z \cdot c_{32} - x \cdot c_{34} \\
 \text{Error}_z &= y \cdot c_1 - x^2 \cdot c_2 - x \cdot c_3 + c_{10} + y^2 \cdot c_{11} + y \cdot c_{12} - x \cdot c_{13} + c_{20} \\
 &\quad + yz \cdot c_{21} + y \cdot c_{22} - zx \cdot c_{23} - x \cdot c_{24} + z^2 \cdot c_{29} + z \cdot c_{30} \\
 &\quad + c_{31} + y \cdot c_{32} + x \cdot c_{33}
 \end{aligned} \tag{3.26}$$

If n points are observed in the work space, then we have

$$\begin{bmatrix} \text{Error}_x_1 \\ \text{Error}_y_1 \\ \text{Error}_z_1 \\ . \\ . \\ . \\ \text{Error}_x_n \\ \text{Error}_y_n \\ \text{Error}_z_n \end{bmatrix} = \begin{bmatrix} 0 & z_1 x_1 & z_1 & . & . & -y_1 & c_1 \\ -z_1 & 0 & 0 & . & . & -x_1 & c_2 \\ y_1 & -x_1^2 & -x_1 & . & . & 0 & c_3 \\ . & . & . & . & . & . & . \\ . & . & . & . & . & . & . \\ . & . & . & . & . & . & . \\ 0 & z_n x_n & z_n & . & . & -y_n & c_{31} \\ -z_n & 0 & 0 & . & . & -x_n & c_{32} \\ y_n & -x_n^2 & -x_n & . & . & 0 & c_{33} \\ & & & & & & c_{34} \end{bmatrix} \tag{3.27}$$

which becomes

$$\text{Error} = A \cdot C \quad (3.28)$$

The coefficient matrix is obtained as

$$C = [A^T \cdot A]^{-1} \cdot A^T \cdot \text{Error} \quad (3.29)$$

These coefficients can be compared with those obtained from laser measurements in the same thermal condition. The absolute resultant errors probed need to be used for this method. Origin of the probing system, however, is not the same as the origin of the machine tool coordinate system. Relative errors to the probing origin at a certain thermal condition can be used for the decomposition to the error component of each axis. This error component is obtained relative to the probing origin. All the angular error components are calculated relative to the probing origin, which leads no constants at the error component equations. Positioning error equations do not contain constant terms, either. Only the relative effect of error component on the relative work space error are interested in that thermal condition. In other words, calculated coefficients represent the magnitude of each error component with respect to the probing origin in that specific thermal condition. Relative error of position (x_1, y_1, z_1) to the probing origin (x_0, y_0, z_0) is expressed as follows:

$$\begin{aligned}
RErrorx_1 &= Errorx_1 - Errorx_0 \\
&= (z_1x_1 - z_0x_0) \cdot c_2 - (x_1y_1 - x_0y_0) \cdot c_4 + (x_1^2 - x_0^2) \cdot c_6 \\
&\quad + (x_1 - x_0) \cdot c_7 - (y_1^2 - y_0^2) \cdot c_{14} + (z_1^2 - z_0^2) \cdot c_{23} \\
&\quad - (y_1z_1 - y_0z_0) \cdot c_{25} + (z_1 - z_0) \cdot c_{33} - (y_1 - y_0) \cdot c_{34} \\
RErrory_1 &= Errory_1 - Errory_0 \\
&= (x_1^2 - x_0^2) \cdot c_4 - (y_1z_1 - y_0z_0) \cdot c_{11} + (y_1^2 - y_0^2) \cdot c_{17} \\
&\quad + (y_1 - y_0) \cdot c_{18} - (z_1^2 - z_0^2) \cdot c_{21} + (z_1x_1 - z_0x_0) \cdot c_{25} \\
&\quad - (z_1 - z_0) \cdot c_{32} - (x_1 - x_0) \cdot c_{34} \\
RErrorz_1 &= Errorz_1 - Errorz_0 \\
&= -(x_1^2 - x_0^2) \cdot c_2 + (y_1^2 - y_0^2) \cdot c_{11} + (y_1z_1 - y_0z_0) \cdot c_{21} \\
&\quad - (z_1x_1 - z_0x_0) \cdot c_{23} + (z_1^2 - z_0^2) \cdot c_{29} + (z_1 - z_0) \cdot c_{30} \\
&\quad + (y_1 - y_0) \cdot c_{32} + (x_1 - x_0) \cdot c_{33}
\end{aligned} \tag{3.30}$$

If n points are observed in the work space, then we have

$$\begin{bmatrix} RErrorx_1 \\ RErrory_1 \\ RErrorz_1 \\ \cdot \\ \cdot \\ \cdot \\ RErrorx_n \\ RErrory_n \\ RErrorz_n \end{bmatrix} = \begin{bmatrix} (z_1x_1 - z_0x_0) & \cdot & \cdot & -(y_1 - y_0) & c_2 \\ 0 & \cdot & \cdot & -(x_1 - x_0) & c_4 \\ -(x_1^2 - x_0^2) & \cdot & \cdot & 0 & c_6 \\ \cdot & \cdot & \cdot & \cdot & \cdot \\ \cdot & \cdot & \cdot & \cdot & \cdot \\ \cdot & \cdot & \cdot & \cdot & \cdot \\ (z_nx_n - z_0x_0) & \cdot & \cdot & -(y_n - y_0) & c_{30} \\ 0 & \cdot & \cdot & -(x_n - x_0) & c_{32} \\ -(x_n^2 - x_0^2) & \cdot & \cdot & 0 & c_{33} \\ & & & & c_{34} \end{bmatrix} \tag{3.31}$$

which becomes

$$RError = A' \cdot C' \tag{3.32}$$

The coefficient matrix is obtained as

$$C' = [A'^T \cdot A']^{-1} \cdot A'^T \cdot R_{Error} \quad (3.33)$$

These results can be compared with those obtained from laser measurements in the same thermal condition.

In case of the two probe approach, a different calculation procedure is needed since only the z coordinate is different for the same point of the metrology pallet. Different probe length causes the different z coordinate for the same point. Each error value obtained by two probes is not the same by the effect of different z coordinate. These differences for x, y, and z axes can be used to decide the relative effect of error components on the relative resultant error at work space.

The difference of relative x error components for the same point with respect to short probe origin (x_0, y_0, z_0) from equation 3.15 becomes:

$$\begin{aligned} & \text{Error}_x(x_1, y_1, z_1) - \text{Error}_x(x_1, y_1, z_2) \\ &= -y_1'(EZ + ez(R)) + z_1'(EY + ey(R)) + DX \\ &\quad - (-y_1'(EZ + ez(R)) + z_2'(EY + ey(R)) + DX) \\ &= -y_1'(ez(z_1) - ez(z_2)) + z_1'ey(z_1) - z_2'ey(z_2) \\ &\quad + (z_1 - z_2)(ey(x_1) + ey(y_1) + ey(R)) + dx(z_1) - dx(z_2) \quad (3.34) \end{aligned}$$

If only the relative effect of angular errors is of interest with respect to the measurement origin, constant

terms of angular errors and positioning errors are not important any more. Equation (3.34) becomes:

$$\begin{aligned} & \text{Error}_x(x_1, y_1, z_1) - \text{Error}_x(x_1, y_1, z_2) \\ &= -(z_1 x_1 - z_2 x_1) c_2 + (z_1^2 - z_2^2) c_{23} \\ & \quad - (y_1 z_1 - y_1 z_2) c_{25} + (z_1 - z_2) c_{33} \end{aligned} \quad (3.35)$$

The difference of relative y error value becomes:

$$\begin{aligned} & \text{Error}_y(x_1, y_1, z_1) - \text{Error}_y(x_1, y_1, z_2) \\ &= -(y_1 z_1 - y_1 z_2) c_{11} - (z_1^2 - z_2^2) c_{21} \\ & \quad + (z_1 x_1 - z_2 x_1) c_{25} - (z_1 - z_2) c_{32} \end{aligned} \quad (3.36)$$

The difference of relative z error value becomes:

$$\begin{aligned} & \text{Error}_z(x_1, y_1, z_1) - \text{Error}_z(x_1, y_1, z_2) \\ &= (y_1 z_1 - y_1 z_2) c_{21} - (z_1 x_1 - z_2 x_1) c_{23} \\ & \quad + (z_1 - z_2) c_{30} \end{aligned} \quad (3.37)$$

3.6 Determination of Measurement points by a Touch Probe

While the location of measurement points on the pallet should be at the far end of the space within the physical limitation, the number of measurement points can be decided by having predetermined value for the confidence range of the regression prediction. The estimated mean response, \hat{y}_h , is

$$\hat{y}_h = \hat{x}_h' b \quad (3.38)$$

The estimated variance $S^2(\hat{y}_h)$ for the prediction is given by: [50]

$$s^2(\hat{y}_h) = \text{MSE}(1 + \mathbf{X}_h'(\mathbf{X}'\mathbf{X})^{-1}\mathbf{X}_h) \quad (3.39)$$

$$\text{where } \text{MSE} = \frac{\text{SSE}}{n-p} = \frac{\mathbf{e}'\mathbf{e}}{n-p} = \mathbf{Y}'\mathbf{Y} - \mathbf{b}'\mathbf{X}'\mathbf{Y}$$

The $1-\alpha$ confidence interval for $E(y_h)$ is:

$$\hat{y}_h - t(1-\frac{\alpha}{2}; n-p)s(\hat{y}_h) < E(y_h) < \hat{y}_h + t(1-\frac{\alpha}{2}; n-p)s(\hat{y}_h) \quad (3.40)$$

The experiment is to be designed to obtain

$$t(1-\frac{\alpha}{2}; n-p) \cdot s(\hat{y}_h) < s_a \quad (3.41)$$

However, MSE is not known unless the data is obtained and regression is done. To determine the number of measurement points, a trial and error method is used by increasing the number of measurements until the condition (3.41) is satisfied. The above procedure is followed for each of the three axes. Design of the three-dimensional experiment consists of following the above procedure for each of the three axes. The residual analysis by the regression helps the determination of measurement points. Frequent outlier outside two standard deviation value for a certain point shows some problems for that point, which needs to be excluded.

CHAPTER 4 - ONE DIMENSIONAL EXPERIMENT AND ANALYSIS

4.1 Experimental Setup

A commercially available machining center was tested for the applicability of the touch probe to be used for the error measurement. One-dimensional tests for the entire length of the machine tool axis were done using a steel bar with tungsten carbide inserts glued on, as shown in figure 4.1.

The dimensions of the workpiece vary with the ambient temperature. To obtain the correct dimension of the workpiece at the standard temperature of 20°C (68°F), the steel bar is used as a reference .

To prevent errors which can be caused by the surface roughness of the measurement points, lapped tungsten carbide inserts are used for the measurement points. Those are glued on the bar in random intervals, in order to obtain the trend of the systematic error.

The test bar is measured in the cold condition and the warm condition by the touch probe. A laser-null probe setup was used for the measurement of distances between the



Figure 4.1 The picture of the set-up for one dimensional experiment.

glued inserts in the cold and the warm condition.

4.2 Analysis and Results

Laser measurement is carried out just after probing the test bar. The linear regression of errors can be regarded as one of the best representations of systematic error trend. Statistical test on the probing results shows no significance on the quadratic assumption of errors because of the big scatter. Tests on the laser measurement values indicate the significance of assuming a quadratic approximation for the regression function. The method of obtaining the errors by laser, however, can have effects on the test of feasibility of quadratic approximation because of the big cyclic error component. Therefore both approximations, linear and quadratic, need to be compared for the compensation of errors.

Finding the incremental rate of the error(i.e., the slope of the regression line) is the main objective of the linear regression. Laser measurement offers one of the most accurate method for the measurement of errors, even though it requires much time and skill to set up. The error regression line obtained by using the touch probe can be compared with the one obtained from the laser measurement to see if the touch probe can be accurately used for compensation purposes in a real machining environment.

For the best estimate of parameters of the linear regression model, we have

$$\hat{y}_{ij} = b_{0j} + b_{1j}x_{ij}$$

(j=1 for the laser measurement of errors and
j=2 for the probe measurement of errors.)

When analyzing only two regression lines, a straightforward method of comparing the slopes of the regression functions is to construct an interval estimate. The confidence interval for the difference in the slopes, $\beta_{11} - \beta_{12}$, is:

$$(b_{11} - b_{12}) - t(1-\alpha/2; n_1+n_2-4)s(b_{11} - b_{12}) < \beta_{11} - \beta_{12} < \\ (b_{11} - b_{12}) + t(1-\alpha/2; n_1+n_2-4)s(b_{11} - b_{12})$$

Here, b_{11} and b_{12} are the slopes of the two separately fitted regression lines, and

$$s^2(b_{11} - b_{12}) = s^2(b_{11}) + s^2(b_{12}) \\ = n_1 \cdot (\text{std. error of } b_{11})^2 + n_2 \cdot (\text{std. error of } b_{12})^2$$

To construct 95 percent confidence limits for $\beta_{11} - \beta_{12}$ for the example in the cold condition, $b_{11} = 0.041$, $b_{12} = 0.036$, $s(b_{11} - b_{12}) = 0.0465$, $t(0.975; 18) = 2.101$, and $-0.103 < \beta_{11} - \beta_{12} < 0.093$ are obtained. These confidence limits suggest that the two slopes are the same or else do not differ much at a 5 percent level of significance.

In the warm condition, the regression line by the

laser measurement which is $\hat{y}_i = 0.1038x_i - 3.682$ and the regression line by the touch probe measurement which is $\hat{y}_i = 0.1044x_i - 9.428$ are obtained. Finally $t(0.975;18)=2.101$, $s(b_{11}-b_{12}) = 0.03$, and $-0.0636 < \beta_{11}-\beta_{12} < 0.0624$ are obtained.

This test using the above confidence interval, with a 5 percent level of significance, leads to the conclusion that the two slopes are the same since the confidence interval covers $\beta_{11}-\beta_{12}=0$.

From the above estimation, we can conclude that the linear regression line obtained by the touch probe has the same slope as that obtained by laser measurement in both cold and warm conditions.

Quadratic regression using probed results does not give as good a compensation of errors as does using laser measured results. Figure 4.2 shows the error without compensation, the error after compensation using the slope obtained by the laser measurement, and the error after compensation by probing in the cold condition with the linear and the quadratic approximation. Figure 4.3 shows the errors in the warm condition, in which the significant reduction of systematic error is shown. Table 4.1 shows the result for repeatability measured just before the experiment in the cold condition and just after the experiment in the warmed-up condition. It gives the same trend

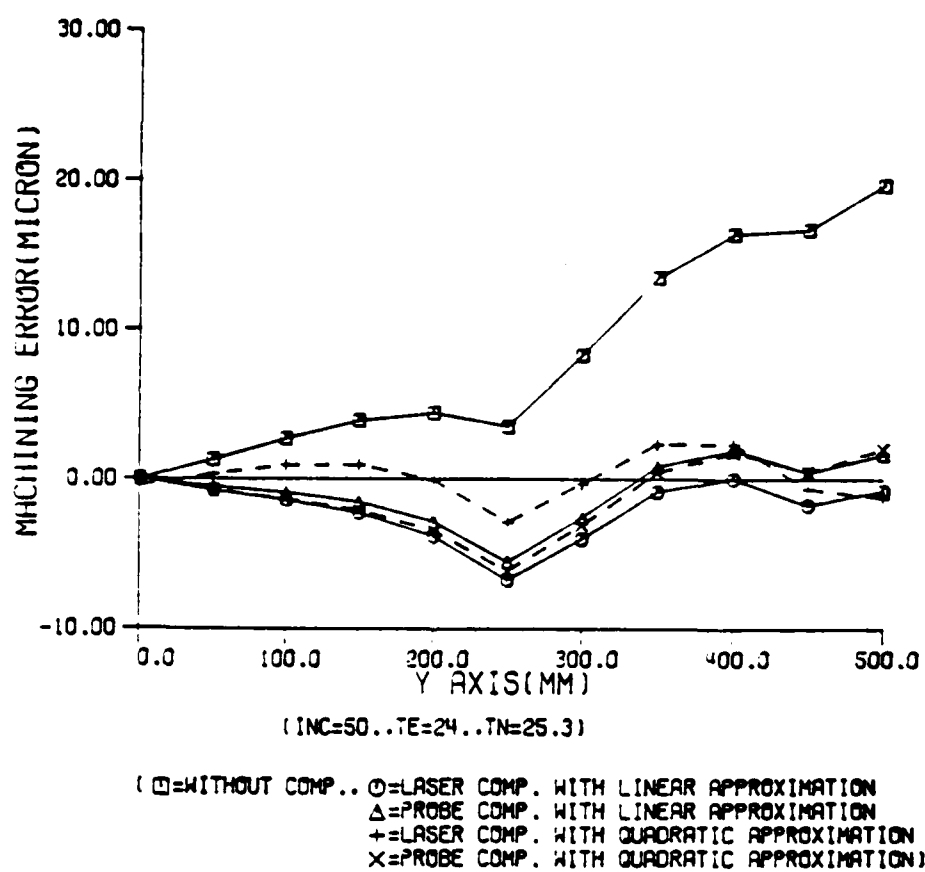


Figure 4.2 The error after compensation in the cold condition for one dimensional experiment

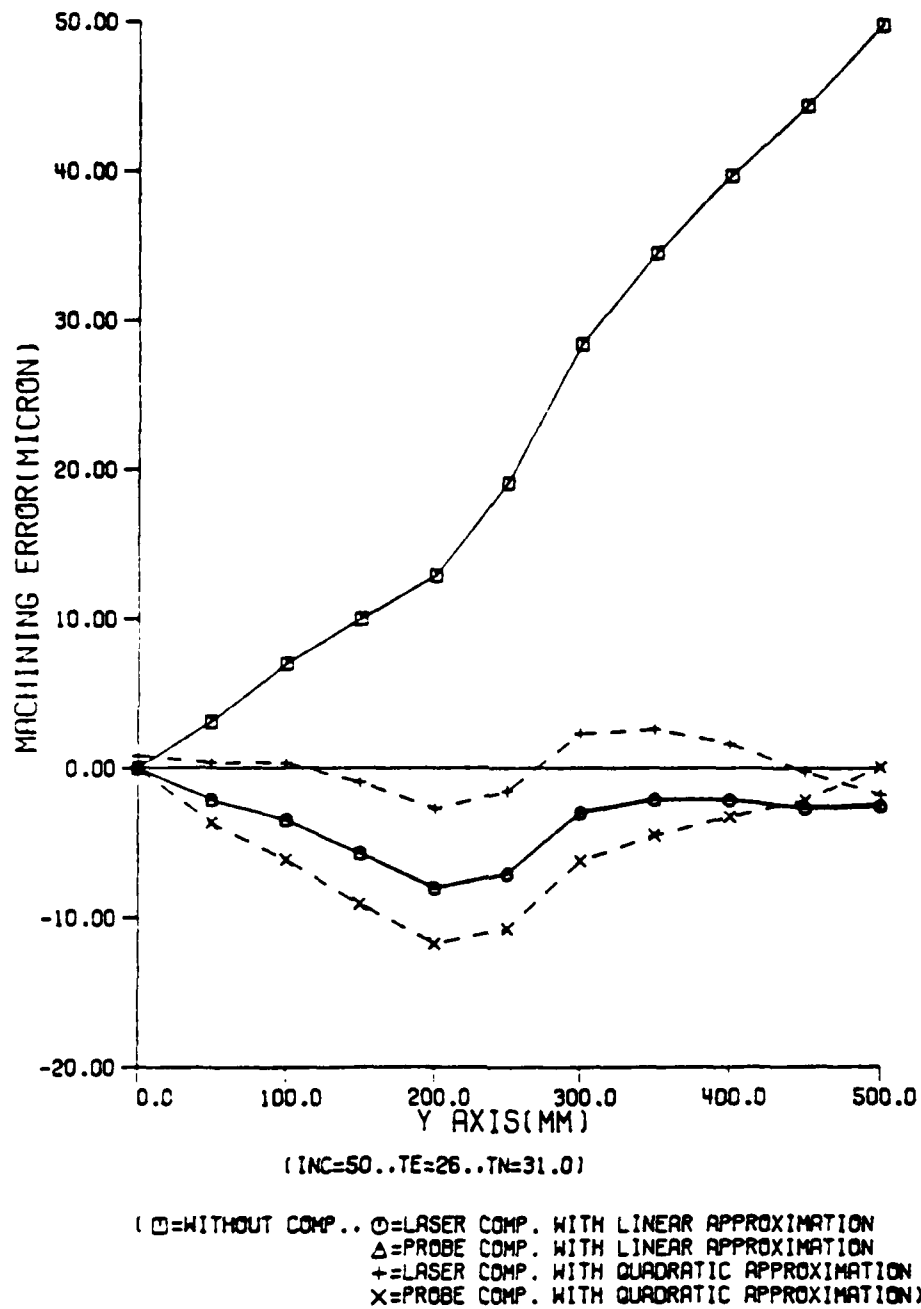


Figure 4.3 The error after compensation in the warm condition for one dimensional experiment

as the repeatability measurement and the analysis for chapter 2.1.2.

4.3 Conclusion for One Dimensional Analysis

The results of one-dimensional experiments and the resulting analysis show that probing the measurement points, which are precisely calibrated, is an appropriate technique for the compensation of machine tool errors in both cold and warm conditions representing a real machining environment. Using the probing technique presented, error compensation could be achieved with the same accuracy as the previously discussed laser measurement technique with the linear regression approach.

By the quadratic approximation of the errors, the probing technique does not give the same error reduction as the laser measurement technique, but it shows significant reduction of errors which is nearly five times the improvement of accuracy and within the repeatability range of the touch probe on the machine tool.

Table 4.1 Repeatability of a touch probe in the cold and the warmed-up condition when experimented for one dimensional analysis

	case	ther-	s ²	3s
			mal	
p r o b i n g	(1)with tool & pallet change	cold	8.4	8.7
		warm	14.9	11.6
	(2)without tool & pallet change	cold	6.4	7.6
		warm	5.2	6.8
(3)	laser for case(2)	cold	4.8	6.6
		warm	4.0	6.0
(4)	laser for machine	cold	0.3	1.5
		warm	0.9	2.9

CHAPTER 5 - THREE DIMENSIONAL PROBING EXPERIMENT

The thermal variations in the machine tool during the operation causes the change of all the error components. To obtain the resultant error at a certain thermal condition all the error components need at least one day of measurement using instruments which are difficult to set-up, like the laser interferometer. Twenty-one error components need too much time for measurement, and some error components require special skills for this measurement. This kind of approach has many difficulties when used on the actual production line. Modeling of the measured errors is one of the biggest problems to be solved.

The idea proposed here is to obtain resultant errors in the work space directly by touching measurement points on the metrology pallet. A touch probe acts as a very accurate microswitch. Triggering the probe stylus causes a single output signal to go to machine control through an interface circuit. A machine controller stores the positional information taken from each axis by the probe output signal from the interface. For the purpose of application to an unmanned manufacturing environment like an FMS, a software patch is added to the machine controller used for

the experiment. This software patch enables the controller to send the probed information to an outside computer. The VAX 11/750 minicomputer is used as a host computer to receive the probing information, analyze the data, correct the machining program, and dump the error corrected program into the machine controller to simulate the FMS environment. These "real time" probe readings reduce the possible uncertainty which may be caused by a long probing time.

Some errors, in the computer sampling times and the microcomputer interrupt driven probe measurement cycle, give a different repeatability of the probe feedback system from that of the machine tool itself. Repeatability of a touch probe system restricts the error compensation capability of this research. Repeatability is measured at various thermal conditions.

The basic idea of this approach is the calibration of the machine tool using accurately measured points on the metrology pallet. The measurement points are probed at a standard temperature in the standards room for calibration. Probing the metrology pallet while not on the machine represents the normal production situation and calculated error can compensate for combined effects of machine inaccuracies, thermal growth of the machine tool and also thermal growth of the workpiece itself.

For determining the errors by a touch probe on the machine tool, very accurate calibration of the metrology pallet on the machine tool is necessary. However, the actual situation of the machine tool, machining centers, or the FMS does not provide us with an easy and direct calibration method on the system. There are several possible ways of calibrating the metrology pallet. The best way is to calibrate it at the accurate coordinate measuring machine, which is directly connected to the CNC machine tool by an automatic material handling system, in the FMS environment. In this case, errors of the coordinate measuring machine are the limits of the inspection accuracy.

The other alternative is to measure the metrology pallet on an accurate stand-alone coordinate measuring machine. This measurement value can be used for the calculation of errors on the machine tool after the prescribed transformation procedure.

There is one more acceptable way of calibrating the metrology pallet. Because the machine tool does not have as much error for the positioning and other angular error components in the cold condition(i.e., not warmed-up condition), probed values of the measurement points in this condition of the machine tool can be used for the calibration. This approach cannot isolate the geometric error of the

machine tool in the cold condition. This method, however, does not have the error, which the calibration approach using a stand-alone coordinate measuring machine may induce while transforming. This transformation error arises because of the smallness of the difference values when compared with the coordinate values. For the experimental convenience and the purpose of investigating thermal errors, the last approach is taken-up for further experimentation. This method can give only the capability for compensating the changes in thermal errors from when the calibration is done.

Once a metrology pallet is calibrated, the differences between the calibrated measurements and the probed measurements can be used to compensate for thermal growth of the machine tool. Workpiece error, due to change in ambient temperature, can be compensated for because the metrology pallet made of steel will reflect this change.

5.1 Experimental Setup

The experiment is setup to observe the actual performance of a touch probe and metrology pallet system at various thermal conditions. The metrology pallet is constructed to cover the whole work space of the machine tool. The long touch probe is assembled using an extension housing and a long stylus to cover the maximum cutting range in

z axis. The short touch probe is also tested to see the adaptability to the whole work space. Temperatures of 54 important temperature points of the whole machine tool structure are observed during the experiment.

5.1.1 Design of the Metrology pallet

The metrology pallet is constructed to contain measurement points as shown in figure 5.1. It is made of steel to represent the workpiece material. All structures are bolted, pinned, and/or glued together to avoid distortions which may be caused by the residual stresses associated with other processes like welding. Commercially available cubic shaped tungsten carbide cutting inserts are used for providing lapped surfaces for measurement points. Measurement points are made to represent far ends of each coordinate axis, limited by the dimension of the probe. Intermittent points on each axis are added to obtain more measurement points. Figure A.4.1 of appendix 4 shows the sketch of the metrology pallet and the numbering system for the points. Probing has been done consistently to the same points on the cubic inserts at the coordinate measuring machine and at the machine tool.

Dimensional stability of the metrology pallet is one of the important conditions which helps to distinguish the thermal growth of the workpiece. If the thermal variation

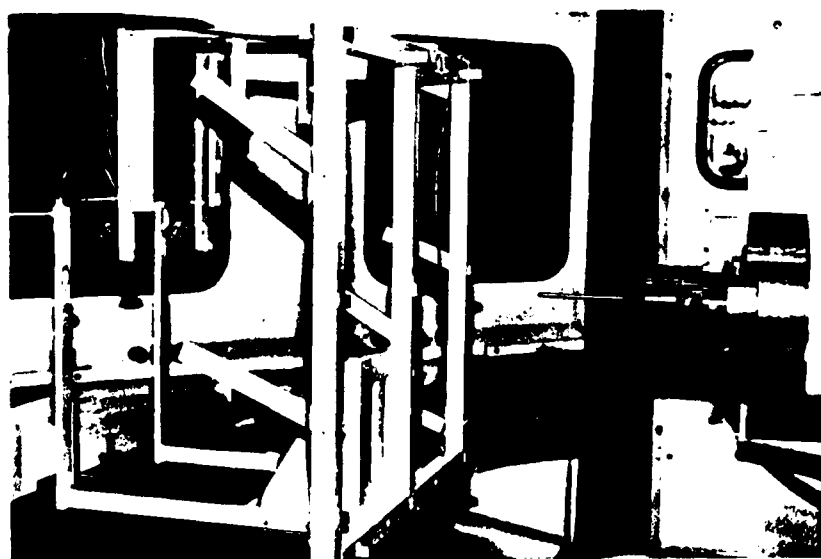


Figure 5.1 The picture of the metrology pallet constructed with 34 measurement points

of the metrology pallet represents the thermal variation of the workpiece, the touch probe information includes the errors not only from the machine tool but also from the workpiece. Distortion of the metrology pallet can be caused by non-uniform thermal variation as the temperature of the environment, including work space, varies. The uniform temperature variation of the metrology pallet shows the uniform variation of the metrology pallet dimensions. Figures 5.2 shows the temperature variation of several points on the metrology pallet during the the day without movement. Figures 5.3, 5.4, and 5.5 show those for the x axis, y axis, and z axis.

5.1.2 Construction of a Long Touch probe

A touch probe system made by Renishaw Electric company is installed on the experimental horizontal machining center made by Cincinnati Milacron company, model T10 with 10 hp spindle. The touch probe system consists of a probe head, a stylus, a housing, a shank, an inductance module, and an interface to the machine controller. The probe head is a very accurate micro switch which gives the electric signal when it makes contact. The electric signal goes to the controller interface through the inductance module on the spindle. The lengths of the stylus and the housing determine the probing range of the touch probe for the z axis. Two probes of different lengths are tested for the

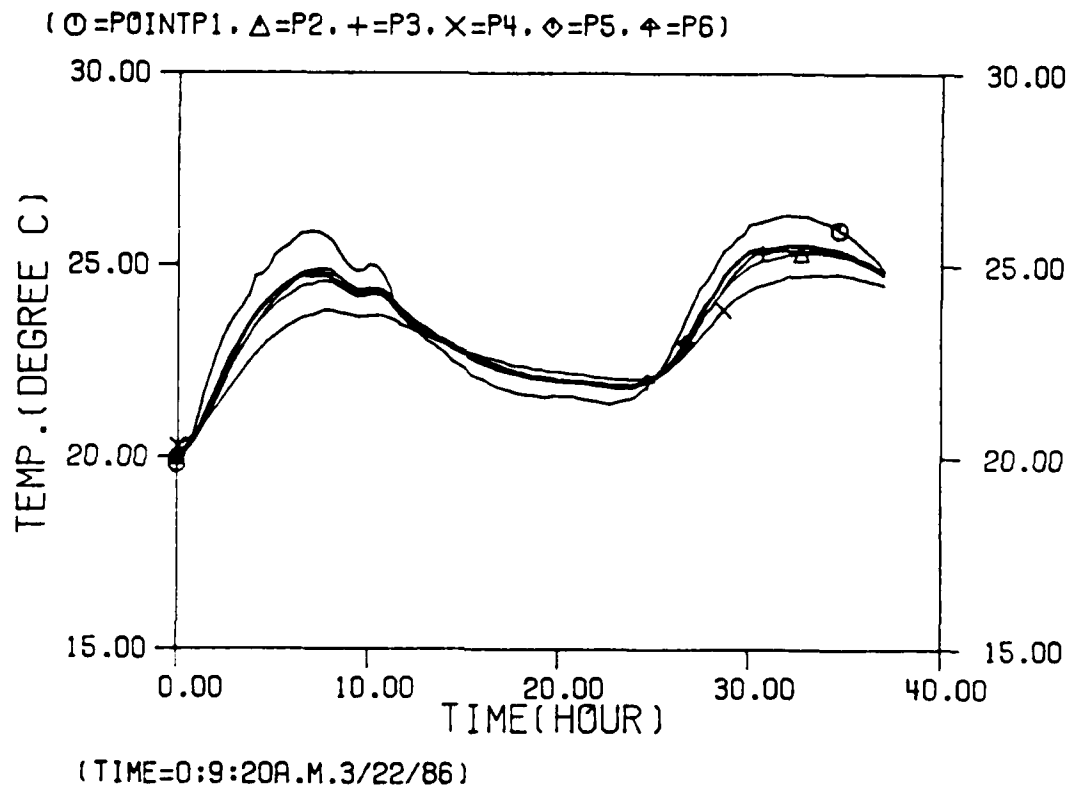


Figure 5.2 Temperature variation of metrology pallet without movement

experiment. One is a short probe with a regular housing and a 100 mm stylus and the other is a long probe with an extension housing and a 150 mm stylus. The length of the long probe nearly covers the maximum limit of the tool length which can be used for machining on T10. This can give the error information for the whole possible work space to be used for machining. Figure 5.6 shows the short probe and the long probe when constructed. After the assembly, each touch probe needs to be calibrated using the adjustment screw for the center of stylus ball to be on the center line of the spindle of the machine tool. There are several methods available for centering each type of probe. The specific one used for the experiment has the inductance module mounted on the machine and the probe. This does not allow the probe to rotate which is a disadvantage for the calibration purpose. The mechanical static adjustment is done first using two null probes for the x and y axis directions by rotating the probe body. Using the null probe on the spindle, the center of the spindle is set to the center of O-ring gauge, of known size and of tool room accuracy. A trial and error method is used to adjust the screw for the center of the probe to show nearly 0 offset from the center of the O-ring gauge.

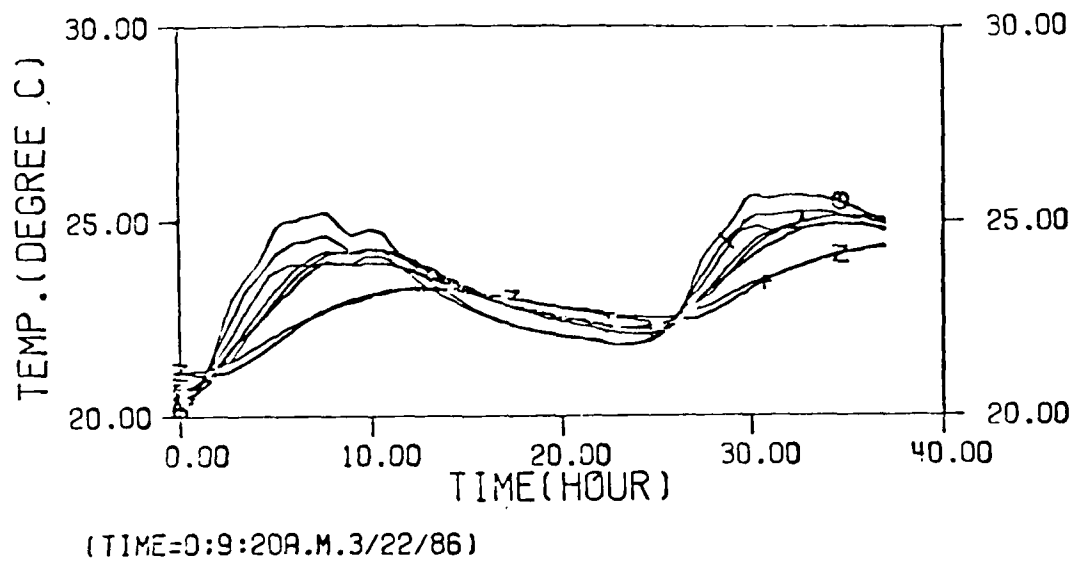


Figure 5.3 Temperature variation of machine x axis without movement

5.2 Experimental Procedure

To observe the effects of the thermal changes on the errors, the machine is moved continuously in three axes for about an hour. Then the metrology pallet is probed with a short and a long probe. For calibration, probing is first done when the machine is cold. Table 5.1 shows the temperature values of the machine tool when the first probing is done for the calibration.

Table 5.1 Temperatures when the calibration probing is done.

point	:	temperature in °C
x1	:	18.9580658786
x2	:	26.7030771526
x3	:	19.9273800996
x4	:	19.7299070129
x5	:	19.8311607721
x6	:	20.3271050919
x7	:	19.5333603232
x8	:	19.8321637991
y8	:	19.6594719236
y1	:	19.2044650699
y2	:	19.2809863438
y3	:	19.678212942
y4	:	20.1247198214
y5	:	19.7764686885
y6	:	20.0037347263
y7	:	19.4081617763
z1	:	19.0415593551
z2	:	18.8397214018
z3	:	19.0157064911
z4	:	19.0415593551

Table 5.1 Continued.

point : temperature in °C	
z5	: 19.117102318
z6	: 19.3674928228
z7	: 19.6415757172
z8	: 19.0207267324
p1	: 19.6822824926
p2	: 19.0604790171
p3	: 19.0117262948
p4	: 18.6865686091
p5	: 18.8218937573
p6	: 18.9948727937

For the experiment 20 sets of probing information are obtained for 3 working days. Eleven sets of information are obtained for 14 hours of the first day representing 2 shift work. Four sets and 6 sets of information are obtained for the second and the third working day representing 1 shift work each.

5.2.1 Acquisition of Data

Probing information and temperature information are automatically recorded by each data acquisition system.

5.2.1.1 Acquisition of Probe Information Data

Probing data is obtained automatically through the automatic data acquisition system for probing. It consisted of the machine tool controller, the VAX 11/750

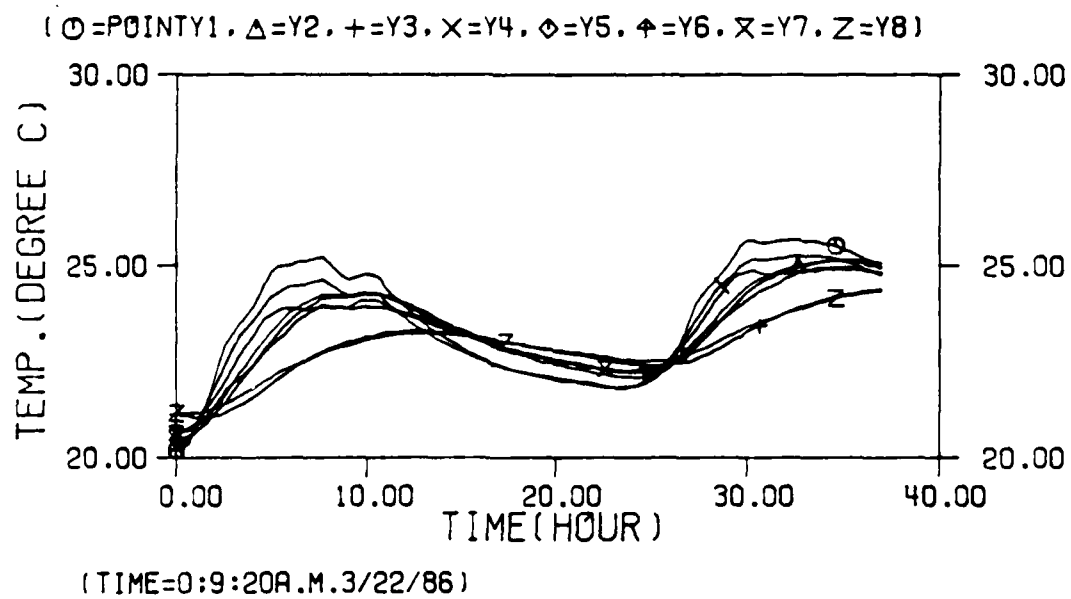


Figure 5.4 Temperature variation of machine y axis without movement

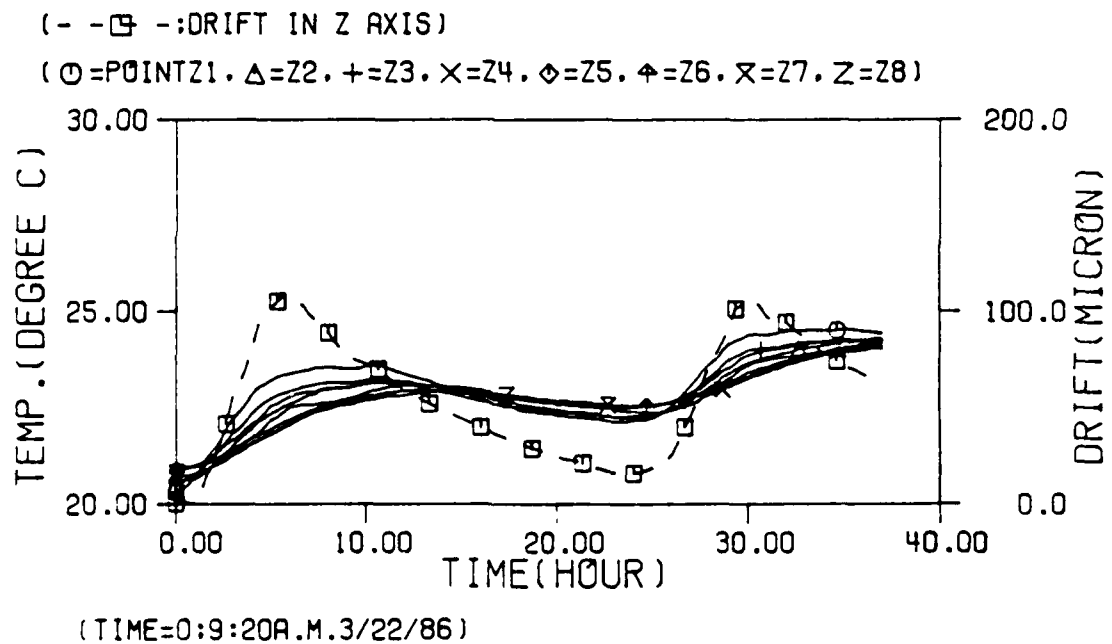


Figure 5.5 Temperature variation of machine z axis without movement

minicomputer, and the connecting cord through RS 232C serial port. A special software patch is written for the machine controller to send the coordinate information to the serial interface RS 232C port. The information given to the serial interface port of the host computer is recorded by the software program written in C language for the VAX 11/750 minicomputer. Figure 5.7 is the picture of the equipment used for the probe information acquisition.

5.2.1.2 Acquisition of Temperature Data

Temperature data is recorded automatically using thermocouples and the Hewlett Packard data acquisition system. Twentyfour temperature points are continuously observed at all times while the machine is operating for three working days. Results are shown in figures 5.8, 5.9, 5.10, and 5.11 for the pallet, the x axis, the y axis, and the z axis respectively. Temperature information is observed at 20 minute intervals during the experiment.

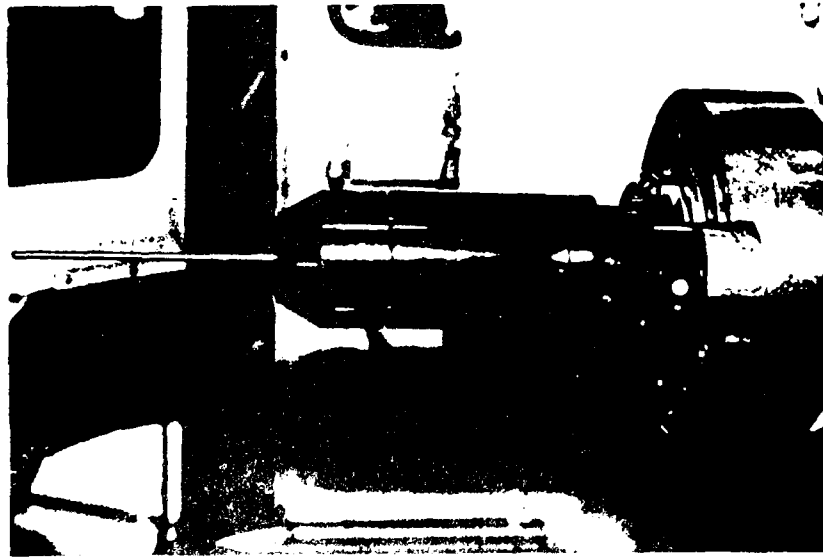
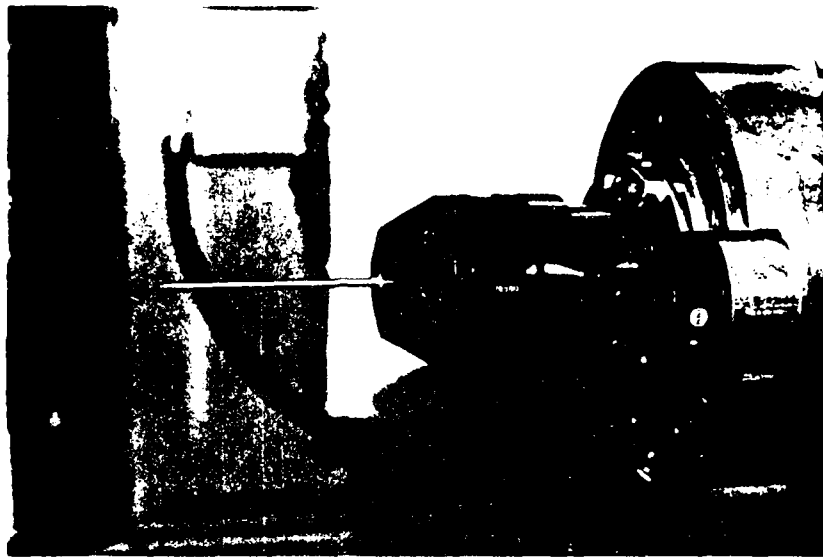


Figure 5.3 The short probe and the long probe



Figure 5.4 The picture of the information acquisition system for probing

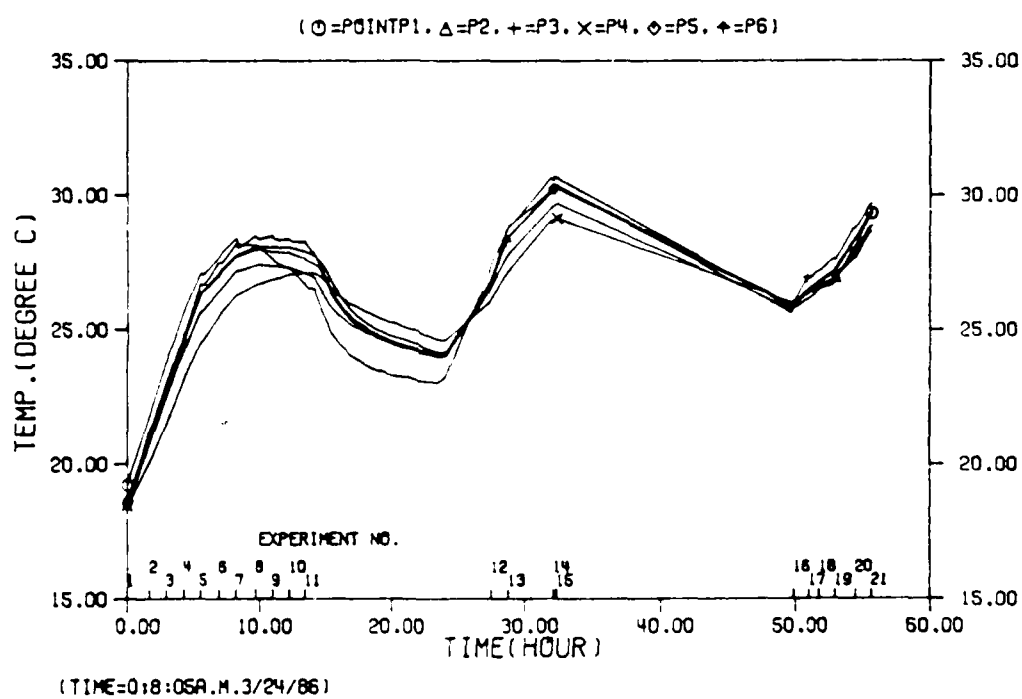


Figure 5.8 Temperature variation of metrology pallet with movement

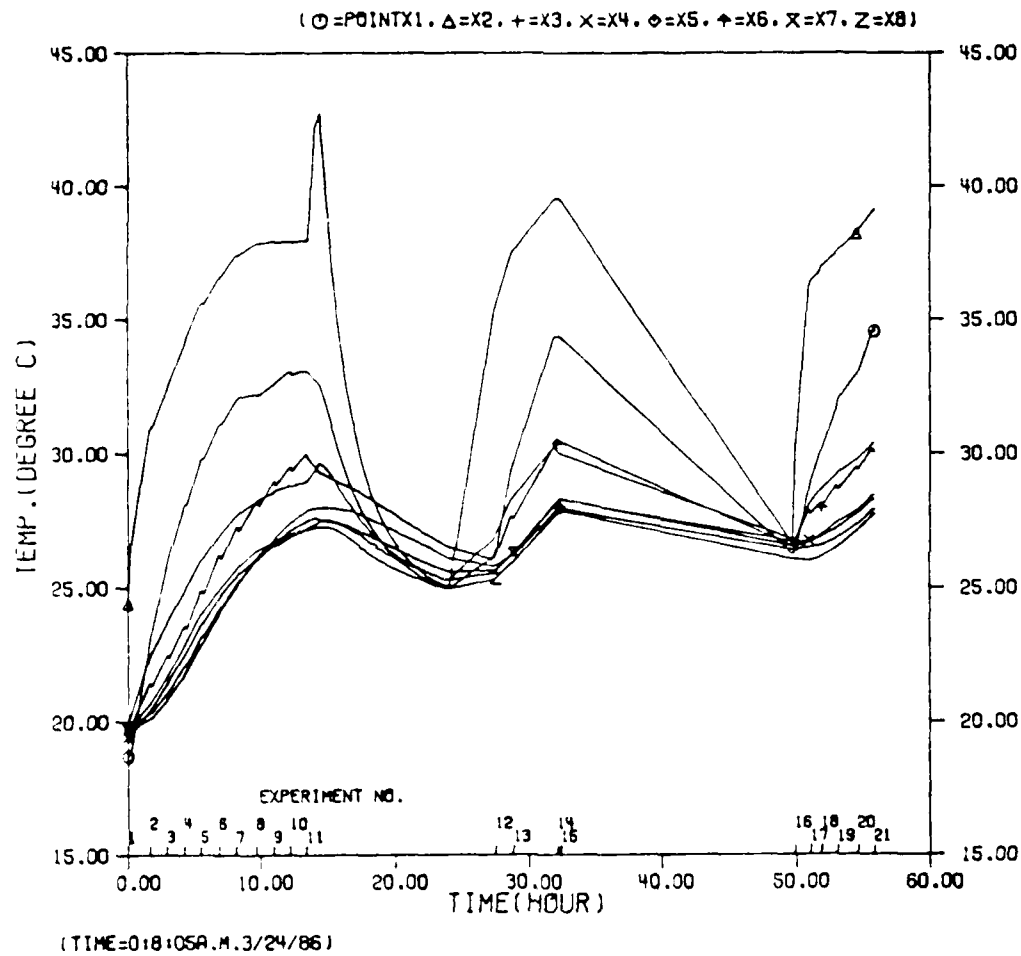


Figure 5.9 Temperature variation of machine x axis with movement

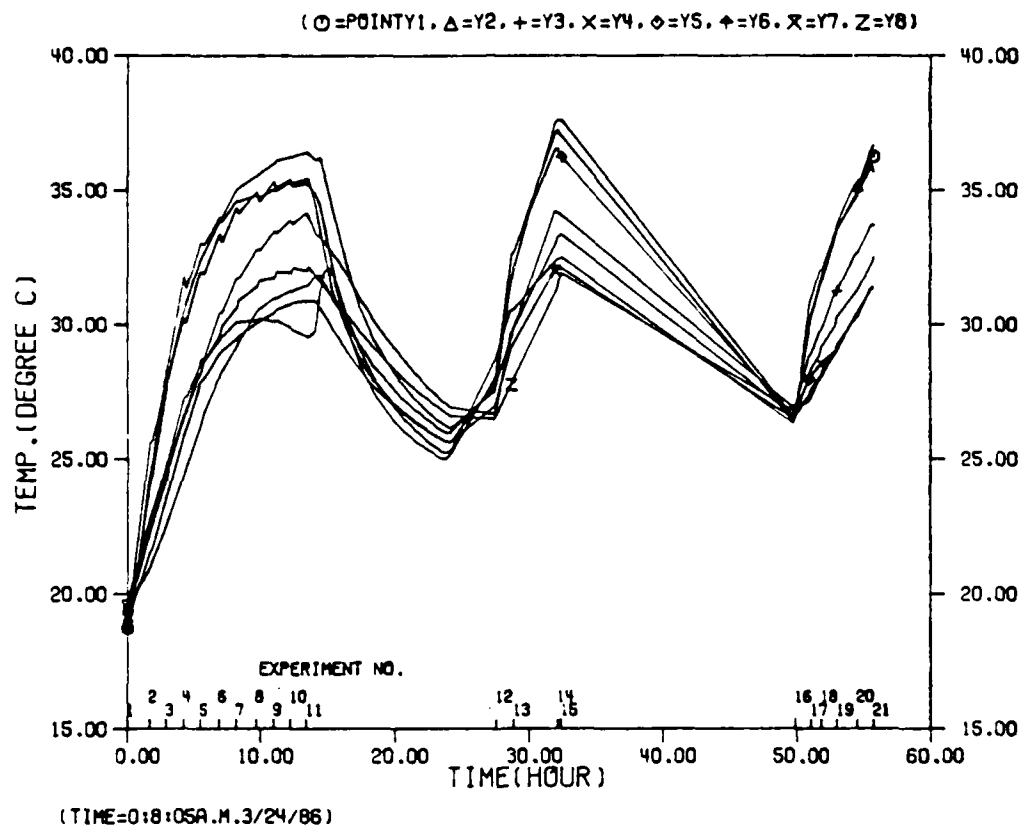


Figure 5.10 Temperature variation of machine y axis with movement

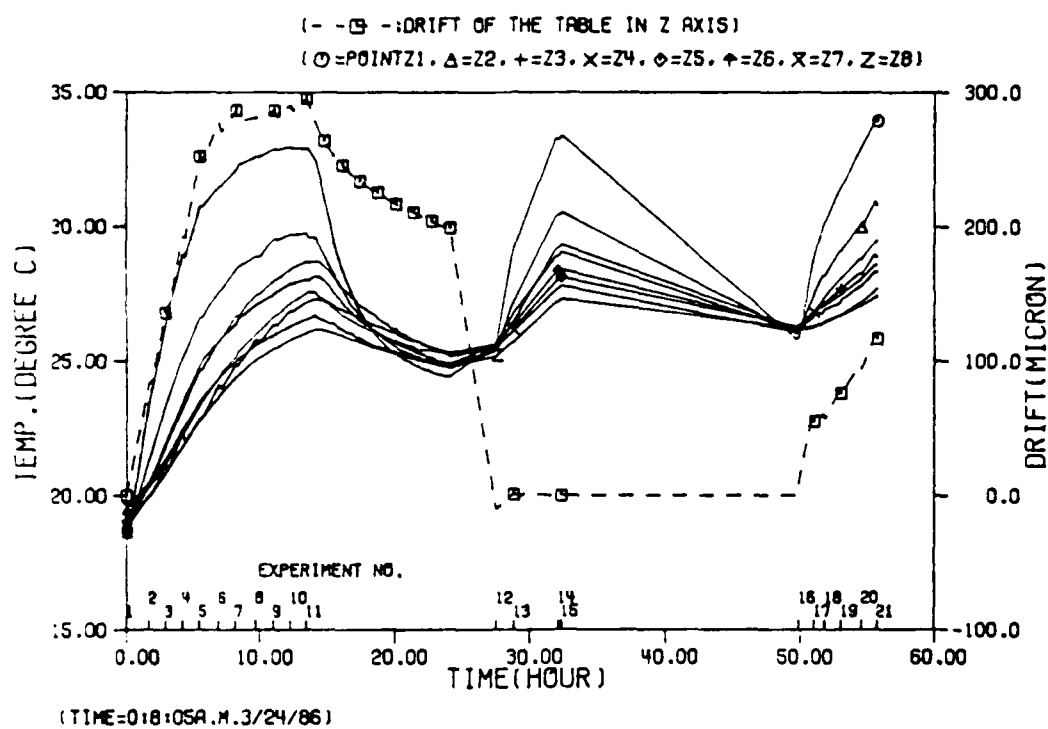


Figure 5.11 Temperature variation of machine z axis with movement

CHAPTER 6 - ANALYSIS OF THREE DIMENSIONAL PROBING EXPERIMENT

6.1 Repeatability of a Touch probe

Repeatability of a touch probe is one of the important factors restricting the compensation capability of the metrology pallet system. Machining accuracy cannot be improved better than the repeatability of a touch probe which is the basic sensing tool for measuring the metrology pallet on the machine tool. Ten measurements are done continuously to have the same operating condition for each case except for the condition that is varied. For a short probe the result of the repeatability measurement is shown in table 6.1. For a long probe which is assembled with an extension housing, repeatabilities for several cases are measured as shown in tables 6.2 and 6.3.

The laser reading taken when the machine probes the position is the actual movement of the machine. It includes the repeatability factor of the machine axis itself in addition to the repeatability of the probe sensing system. The variance of laser readings is not much different from that of probing, which means good repeatability of the machine axis as shown in table 6.1. This

Table 6.1 Repeatability of a touch probe at the machine tool in the cold and the warmed-up condition for the short probe (s.d.=standard deviation, in micro meter)

case		axis	ther- mal	var.	s.d.	range
s h o r t p r o b e	(1)with tool & pallet change	x	cold	17.80	4.22	13.
			warm	14.89	3.86	13.
		y	cold	12.04	3.47	11.
			warm	15.56	3.94	12.
		z	cold	8.40	2.90	10.
			warm	14.90	3.86	11.
p r o b e	(2)without tool & pallet change (first posi- tion)	x	cold	11.16	3.34	10.
			warm	19.78	4.45	16.
		y	cold	8.06	2.84	10.
			warm	18.89	4.35	12.
		z	cold	6.40	2.53	6.
			warm	5.21	2.28	8.
(3)	laser for case(2)	z	cold	4.84	2.2	6.6
			warm	3.95	1.99	5.9
(4)	laser for machine	z	cold	0.30	0.50	
			warm	4.00	2.00	

shows us that the uncertainty of the probing cycle is mainly from the uncertainty of the probe sensing system. There are two exceptional variance values. One is the variance of the x axis when both the probe and the pallet are again loaded on to the spindle and the table respectively in the warmed-up condition, the scatter range of which is

Table 6.2 Repeatability of the long probe in the cold condition(a:axis,var.:variance,s:stand.dev.,r:range,in micro meter)

	case	axis	var.	s	r
l o n g	(1)with tool & pallet change	x	9.38	3.06	10.
		y	25.8	5.8	13.
		z	11.5	3.4	7.
	(2)without tool & pallet change (first)	x	10.93	3.31	8.
		y	8.06	2.84	10.
		z	4.62	2.15	5.
p r o b e	(3)without tool & pallet change (second)	x	22.1	4.70	15.
		y	2.23	1.49	5.
		z	15.33	3.92	8.
	(4)without tool & pallet change (third)	x	85.96	9.27	26.
		y	2..68	1.64	5.
		z	12.5	3.54	13
(5)	laser meas- urement for case(2)	z	7.72	2.78	8.8
(6)	laser meas- urement for case(3)	z	14.8	3.85	11.6
(7)	laser meas- urement for case(4)	z	13.25	3.64	12.8
(8)	laser meas- urement for machine		0.3	0.5	

too high, at 30 μm . The other is the variance of the x axis when the probe and the pallet are not loaded on again

Table 6.3 Repeatability of the long probe in the warm condition(a:axis,var.:variance,s:stand.dev.,r:range,in micro meter)

case		a	var.	s	r
l o n g	(1)with tool & pallet change	x	106.54	10.32	30.
		y	20.	4.47	13.
		z	25.07	5.01	15.
	(2)without tool & pallet change (first)	x	18.67	4.32	10.
		y	14.04	3.75	12.
		z	14.04	3.75	12.
p r o b e	(3)without tool & pallet change (second)	x	12.01	3.47	12.
		y	32.22	5.68	18.
		z	13.38	3.66	10.
	(4)without tool & pallet change (third)	x	9.73	3.12	11.
		y	29.88	5.47	15.
		z	16.01	4.00	12.
(5)	laser meas- urement for case(2)	z	19.05	4.36	12.3
(6)	laser meas- urement for case(3)	z	14.43	3.80	11.3
(7)	laser meas- urement for case(4)	z	18.86	4.34	12.5
(8)	laser meas- urement for machine		4.0	2.0	

for a third measurement point in the cold condition. The scatter range is also very high, at 26 μ m. It will be

interesting to know if the variance of each case is the same. If the sample sizes n_j are all equal, a simple test to decide the equality of all the variances is due to Hartley.[50] It is based solely on the largest sample variance, denoted by $\max(s_j^2)$, and the smallest sample variance, denoted by $\min(s_j^2)$. The test statistic is:

$$H = \max(s_j^2) / \min(s_j^2)$$

If the H value is less than or equal to $H(1-\alpha; r, n)$, the equality of the variances hold where $H(1-\alpha; r, n)$ is the $(1-\alpha)100$ percentile of the distribution of H for r factor levels and sample sizes of n . For the case of short probe in table 6.1, variances for probing each axis in two thermal conditions are shown. H statistics for 12 factor levels and 10 sample size is 10.7 from the table of percentiles of the H statistic distribution. Calculation of H gives 3.8 which leads to the equality of variances for the short probe when we have different thermal conditions, different axes, and different conditions of the pallet and probe. For the case of the long probe in table 6.2 and 6.3, variances of three axes in two thermal conditions are shown. If the exceptional values described above is included, it cannot be said that all the variances for all the cases are equal. Exceptional values, however, can be disregarded in both ways, good or bad, if we have many observations. Calculation of H without two extreme values in both ways gives

32.22/4. = 7.0 which leads to the equality of variances for the long probe when we have different thermal conditions, different axes, different positions, and different condition of the pallet and the probe. Most individual tests for each operating condition also support the above conclusion. Most tests for axis variation give the conclusion of equal variances if the extreme values are excluded. Tests for the effect of the thermal condition on the variance also give the conclusion of equal variances with the extreme values excluded. Tests on the effect of changing the position, the pallet and the probe also give the same result. The mean of variances without two extreme values in both ways is 16.27, which gives the standard deviation of 4.0 μ m. The total mean of the scattering range of probing without two extreme values in both ways is 11.5 μ m which is nearly the same as 11.0 μ m of the short probe case.

6.2 Regression Prediction of Errors at Work Space

Using the information from the probing cycle with the short probe and the long probe, three methods of obtaining the error regression function are tested. The use of one probe, the short probe or the long probe, can give the complete information for obtaining the error regression function for each axis. A long probe approach can have more complete information for the whole work space but the use

of a larger metrology pallet may cause some difficulty in maintaining structural consistency of the pallet for the thermal variation. Using the length difference between a long and short probe, the error regression function can be obtained with the simple structure of a metrology pallet. Only the front surface of the metrology pallet is used for the two probe approach. If the actual part machined can give enough information to obtain the error regression function, the actual machined part can be used with ease on the metrology pallet instead of constructing an additional structure for the two probe approach. For the three day experiment, a complete regression analysis is done for the x, y, and z error components in the case of the short probe approach, the long probe approach, and the two probe approach. Figures 6.1 and 6.2 show the results of the regression analysis for x and y error components corresponding to the measurement origin when using the short probe. From figure A.6.2 to figure A.6.10, the results of the regression analysis of the measurement origin is shown for the short probe, the long probe, and the two probe approach. Regression prediction and its residuals are shown. Residuals are within 5 micro meters in most cases which means good predictability by regression analysis. The first 11 experiments were done the first day for 14 hours and the second 4 experiments were done the second day for 6 hours. Experiment numbers 16 to 21 were

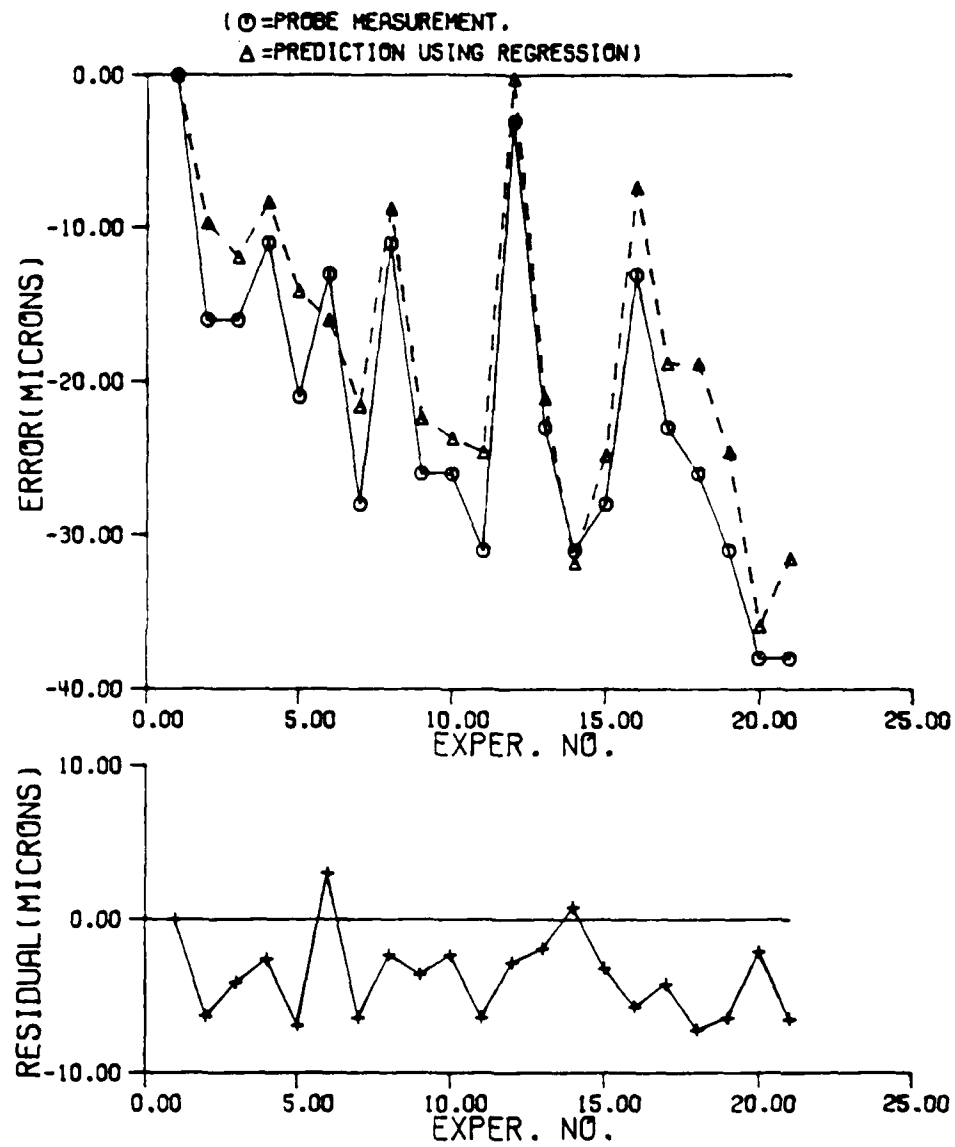


Figure 6.1 The prediction result of x errors and residuals for the measurement origin by regression.

done the third day for 8 hours. For each experiment, regression analysis is done for errors of each axis. Figure 6.3 shows the relative z error variation for the point number 11 which is the right side upper corner point on the front plane of the metrology pallet.

Table 6.4 Repeatability result of test no. 11 for three positions for a short and a long probes (s.d.=standard deviation,in micron)

Posi- tion	Axis	short probe		long probe	
		s.d.	range	s.d.	range
no. 1	x	3.5	12.0	11.1	33.0
	y	5.0	18.0	4.4	15.0
	z	1.6	3.1	2.0	8.0
no. 11	x	4.1	12.0	7.0	25.0
	y	3.9	13.0	3.5	12.0
	z	3.7	13.0	2.9	7.0
no. 18	x	3.1	10.0	10.3	35.0
	y	3.0	8.0	6.9	23.0
	z	3.4	12.0	4.2	13.0

Figure 6.4 shows the relative y error variation for point number 22, which is the center point on the front plane of the metrology pallet. Figures A.6.13 to A.6.22 show the

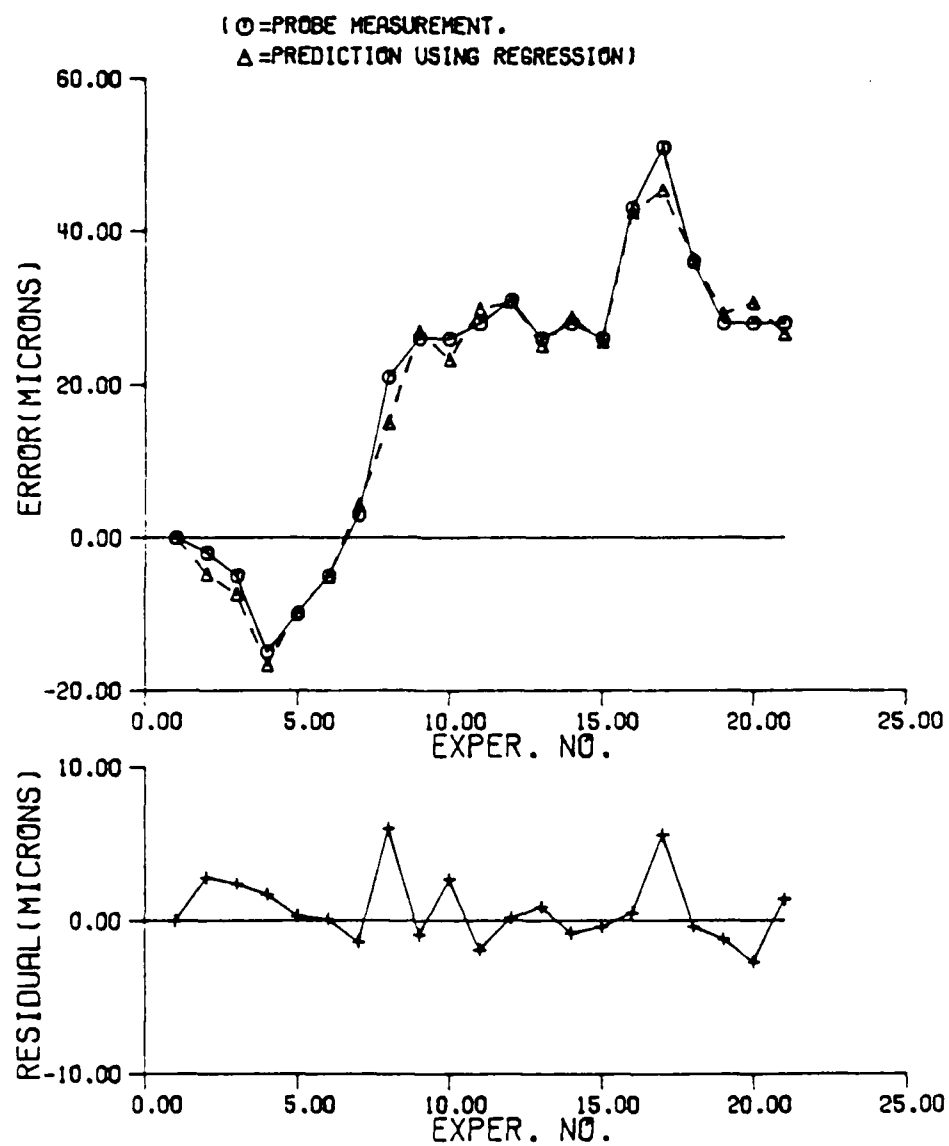


Figure 6.2 The prediction result of y errors and residuals for the measurement origin by regression.

regression prediction and the residual for each case of three axes for point number 11.

Table 6.4 contains the repeatability test results at three different positions for the long and the short probe in the warmed-up condition of test number 11. Appendix 4 contains all the error data for each experiment, error regression coefficients for x, y, and z axes, and the temperature information.

6.3 Determination of Probing Interval using GMDH

Even though the regression analysis gives good predictability of errors for the whole work space for a certain thermal condition, it cannot predict the changes in errors between the measurement cycles. Thermal errors, however, are not subject to dramatic changes during the machine operation. Error changes at a certain point can be predicted by modeling the error probed with the temperature information, using the GMDH technique. Once it is modeled with the temperature information, the amount of error change is determined by the temperature change information. The GMDH algorithm determines the most important temperature variables which are relevant for predicting the error changes. The results of applying the GMDH technique to the x axis error of the origin of measurement, for the 21 test data points with the temperature information is shown in

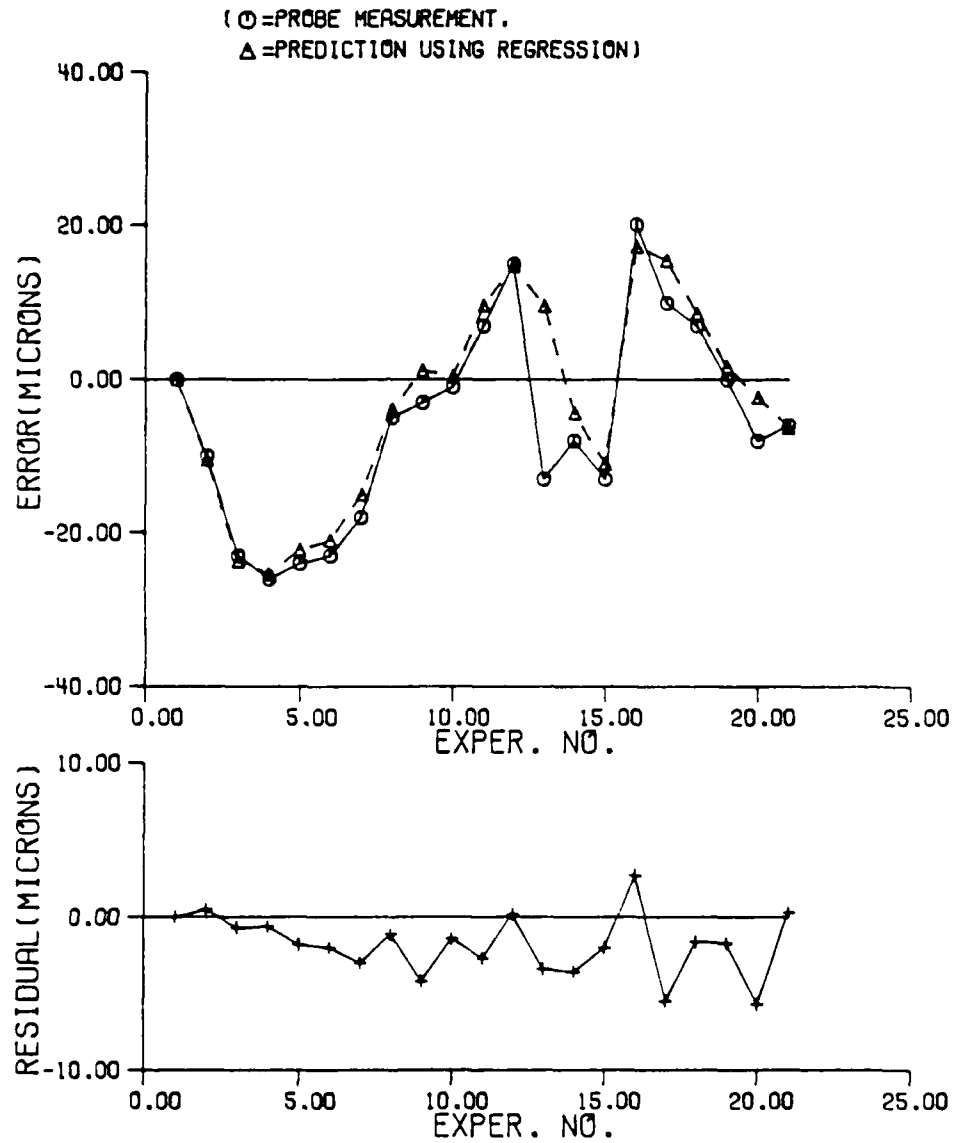


Figure 6.3 The prediction result of relative z errors and residuals for the point no. 11 by regression.

figure 6.5. The last three data points are used for a checking data set and the first eighteen data points are used for a training data set. Even though the prediction by the GMDH technique is not exactly the same as the actual data, the prediction trend is following the change in the errors. The residual analysis also shows acceptable residual ranges and directions. When the GMDH prediction is applied without the last data, the result of predicting the last error is a 3 micro meter residual from the actual error as shown at figure 6.7.

Using the first eighteen data points, the GMDH prediction on the next three observations is done as shown in figure 6.7. Fifteen data points are used for training and next the three data points are used for checking. Computation is stopped after the first generation of computation. Prediction residuals for the last three points are 1, -1.5, and 3.5 micro meters, which shows a very good predictability. Selected variables are different from those of figure 6.5 and figure 6.6. In the case of the twenty-one data points, temperature points x3 and x4 on the ball screw nut and the spindle motor of the x-axis respectively are selected as important. In the case of the 20 data points, temperature points x3 and z6 on the ball screw nut of the x axis and the middle point near the z axis guideway respectively are selected as important. In the case of the 18 data points, however, temperature points x3 and y2 on the

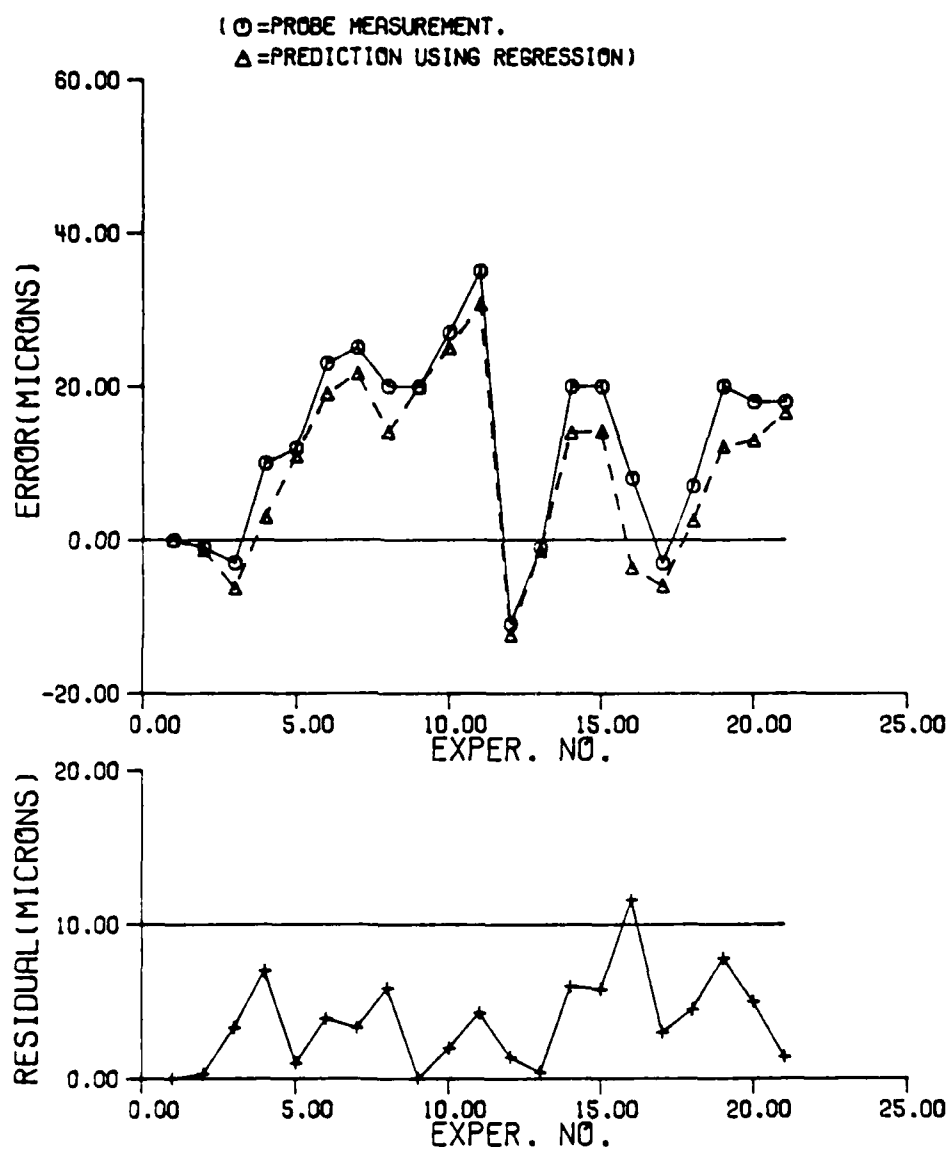


Figure 6.4 The prediction result of relative y errors and residuals for the point number 22 by regression.

ball screw nut of x axis and the screw end bearing of the y axis are selected as important. This shows that the GMDH variables can be changed according to the future data obtained. The GMDH technique on the thermal drift is very sensitive to the data input. This effect can be made to be less sensitive and hence improved, by having less temperature variables. Figure 6.8 shows the prediction result when only 11 data points of the first day's observations are used for the prediction of next 10 data points for the second day's and the third day's operation. Computation is stopped after the first generation with temperature variables of x1 and y4 on the x screw motor and the top point near the y axis guideway respectively. The result shows a good trend of prediction, but the magnitude of the residual is very large-between 10 and 20 micro meters. This shows that sufficient data from several days is required to predict the next several data points using GMDH modeling.

This prediction capability of the GMDH modeling can be used for the determination of the time for the probing cycle. Drift errors or relative errors of certain points are chosen to be monitored by GMDH model. Temperature data points are obtained in a certain time interval to calculate the predicted error value. Larger change than the predetermined value(for example 5 micro meters) from the former probed error initiates the probing cycle to update the error regression function for better compensation.

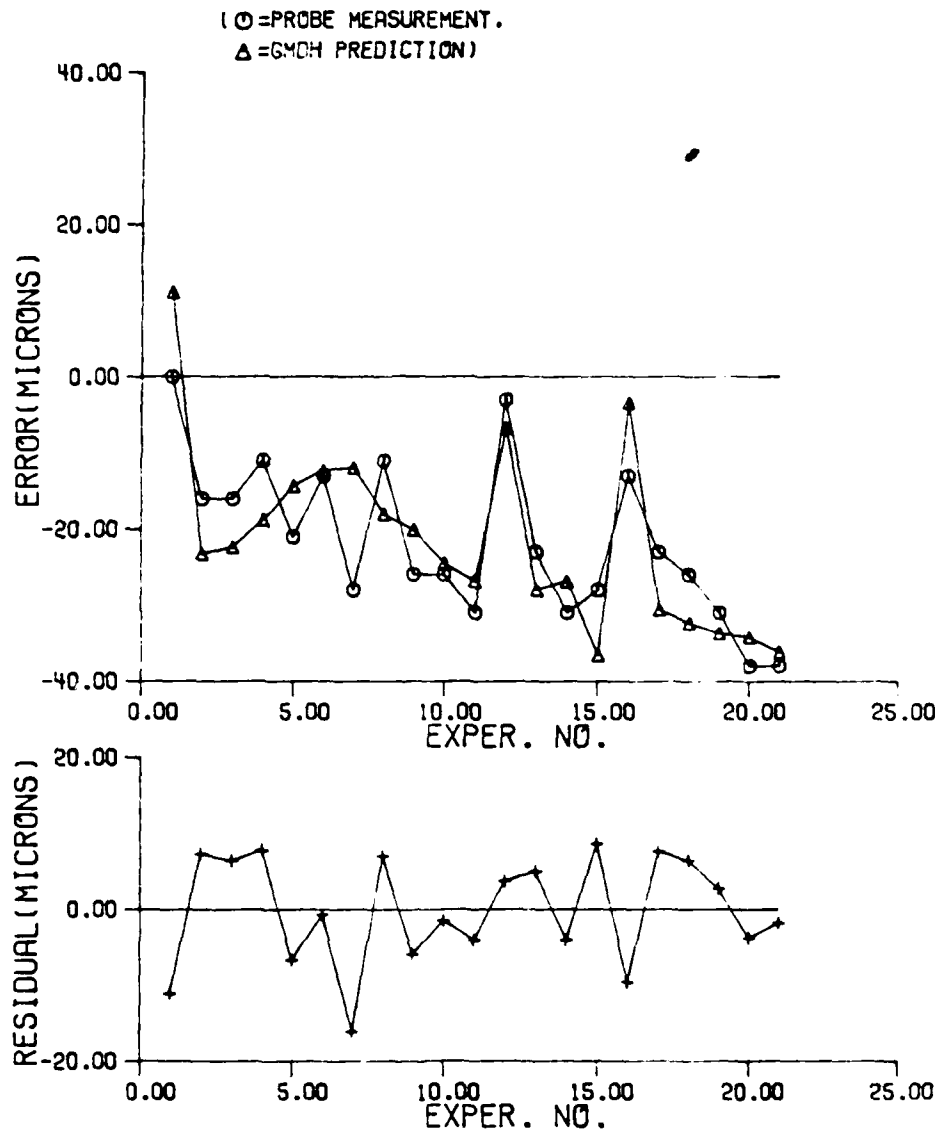


Figure 6.5 GMDH prediction on x drift error of measurement origin using 21 set of data.

Figure 6.9 shows the prediction result of the y drift error for the origin of measurement. Twenty data points are used to predict the last data points. Sixteen data points are used for training and 4 data points are used for checking. Computation is stopped after the first generation. Temperature variables x3 and y8 on the surface of the ball screw nut of the x axis and the bottom point near the column guideway respectively are determined to be important. The residual of the predicted error is -0.2 micro meters, which is a near perfect prediction. If the difference of 5 micro meters of error from the former error data is preset to be monitored, the prediction of figure 6.9 for the y drift error of the origin shows that a less than one hour period is required for probing cycle for nearly 6 hours of operation. Between 6 and 8 hours of operation, around one hour interval is recommended. Beyond 8 hours updating the error function is not required at all. Each observation is done around every hour.

Several other errors and other points can be selected for monitoring. Relative errors are good alternatives. If the biggest possible error is important, the far end of the metrology pallet can be monitored as shown in figure 6.10. The GMDH prediction result is shown in figure 6.10 for the relative error of point 11 on the z axis. Twenty data points are used to predict the last data points. Seventeen data points are used for training and 3 data points are

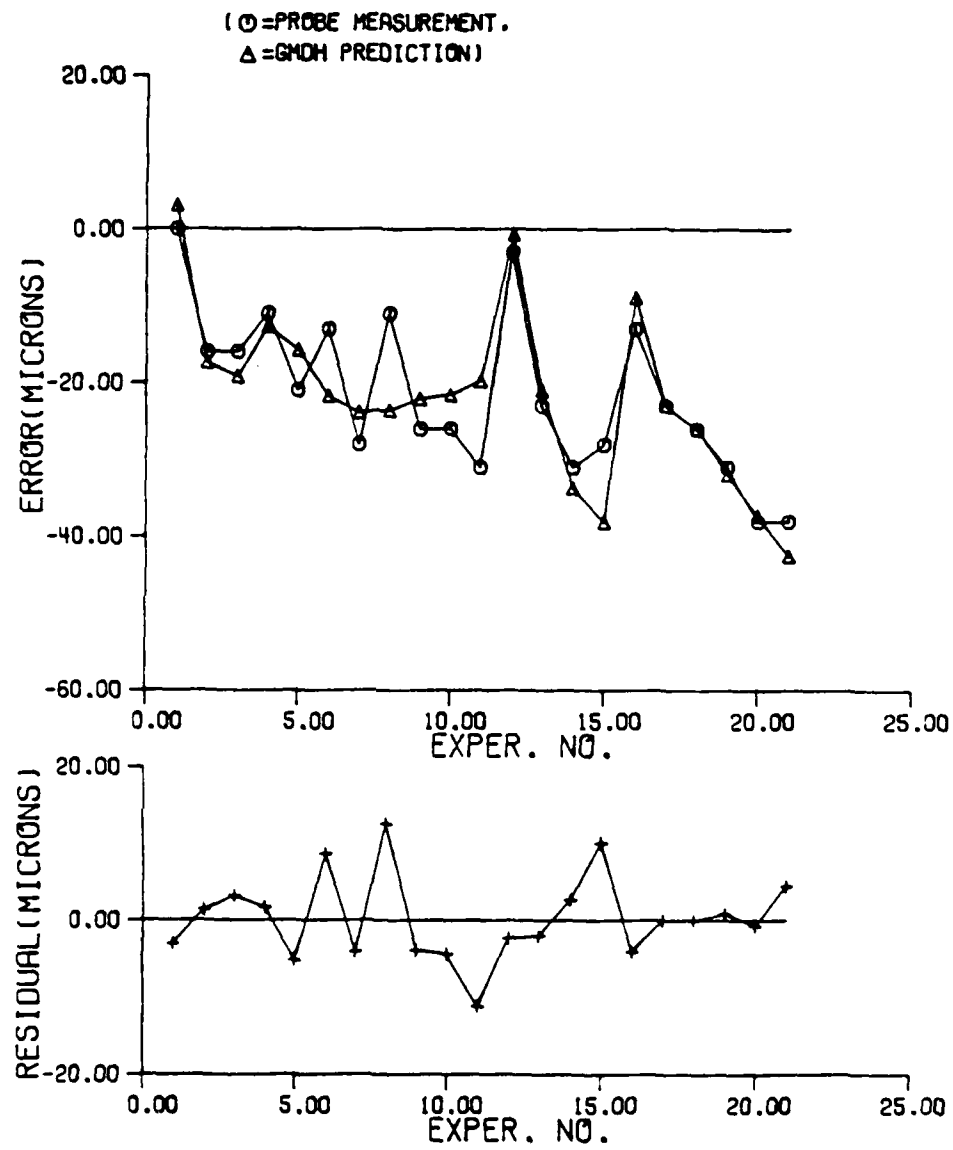


Figure 6.6 GMDH prediction on x drift error of measurement origin using 20 set of data.

used for checking. Computation is stopped after the first generation. Temperature variables x_3 and y_8 on the surface of the ball screw nut of the x axis and the bottom point near the column guideway respectively, are determined to be important. The residual of the predicted error for the last data point is 0. micro meters, which is the perfect prediction.

If the errors of the middle range of the work space are important, the center point can be selected for monitoring. Figure 6.11 shows the GMDH prediction result of y -axis relative error of point 22. Twenty-one data points are used to predict the last data point. Eighteen data points are used for training and 3 data points are used for checking. Computation is stopped after the first generation. Temperature variables x_4 and x_7 on the left corner near the x -axis guideway and the right end corner near the x -axis guideway respectively are determined to be important. The residual of the predicted error for the last data point is -0.3 micro meter.

6.4 Decomposition of Resultant Error into Error Components

Decomposition analysis of probed relative errors into relative error components has been done by the regression technique as described in chapter 3.5. Here the word "relative" needs to be explained. A probed relative error

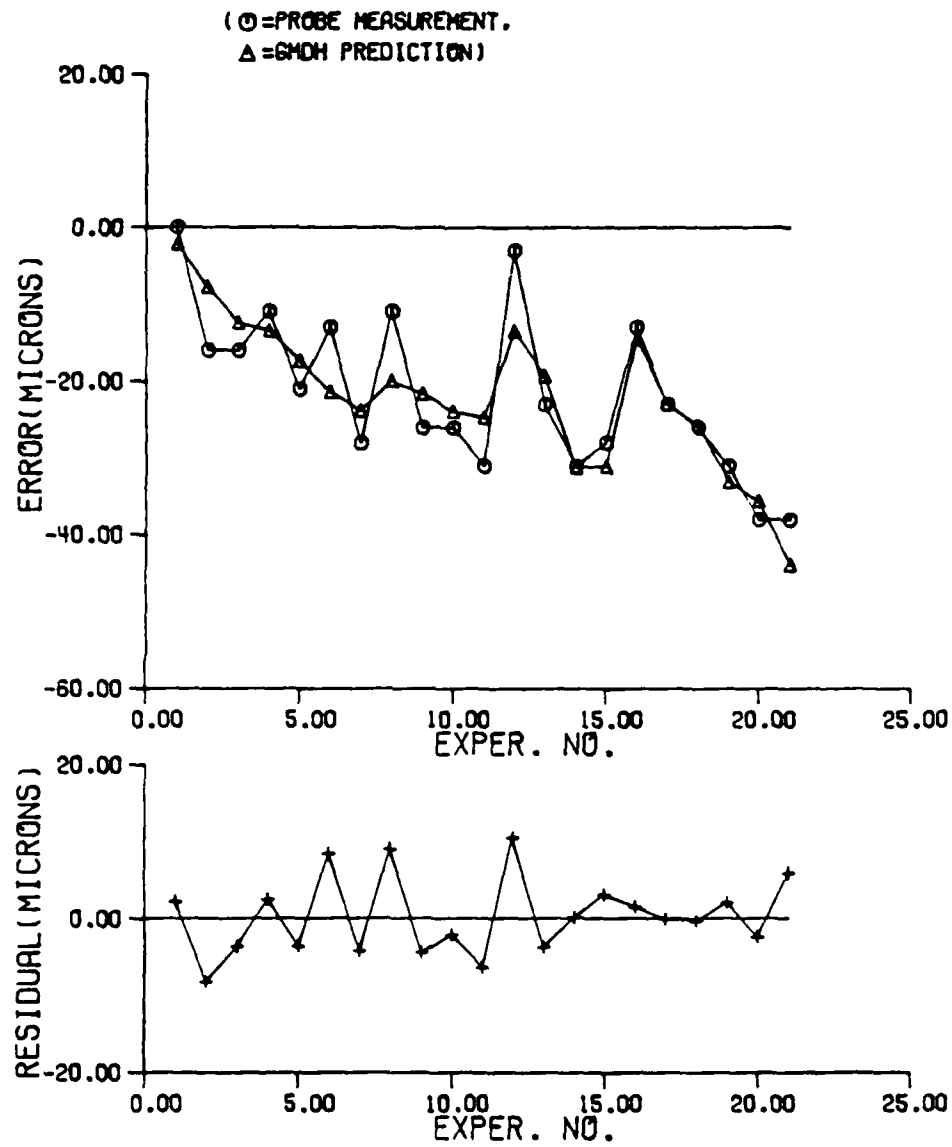


Figure 6.7 GMDH prediction on x drift error of measurement origin using 18 set of data.

with respect to the pallet's origin of measurement represents thermal changes in the error from the time when the pallet is calibrated for the experiment. Since the drift of the origin includes error values of all the error components of that position in that specific thermal condition, final decomposed error component values represent the relative values to those of the origin. Decomposed error values are compared with the predicted value for the same thermal condition by using a GMDH technique after correcting the drift. Because of the calibration method used for the experiment, predicted error component values for the thermal condition, when the calibration is done, need to be subtracted from the predicted error component values obtained by a GMDH technique. The final calculated error values show the relative effect of the error component on the resultant relative error in the work space. For examples of this decomposition procedure, actual experiment data of test number 11 are used for the short probe approach, the long probe approach and the two probe approach. The linear assumption and the quadratic assumption of positioning errors are compared.

Table 6.5 shows the result of the decomposition procedure when the short probe is used for test number 11. Linear positioning errors are used for calculation. Since relative errors are used for calculation, several important coefficients of error equations are obtained for error

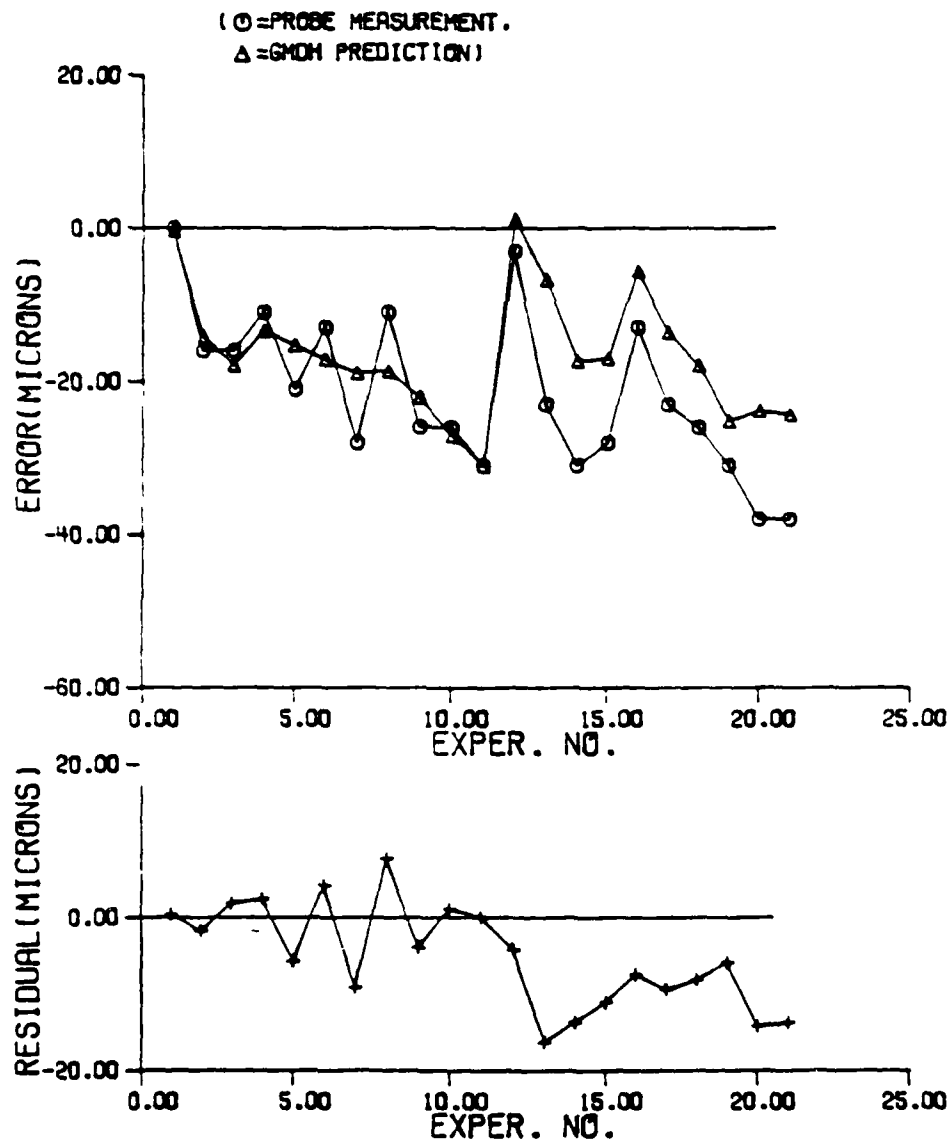


Figure 6.8 GMDH prediction on x drift error of measurement origin using 11 set of data.

components. Calculated coefficients correspond to those in equation (3.15). Recalculation of the resultant error follows using the obtained coefficients. Table A.6.1 of appendix 6 shows the result of decomposition procedure for test number 11 with the assumption of the quadratic positioning error when the short probe is used. Table A.6.2 of appendix 6 shows the result of the decomposition procedure for test number 11 when the long probe is used. Quadratic positioning errors are used for the calculation. Table A.6.3 of appendix 6 shows the decomposition result for test number 11 when the linear positioning errors are assumed for a long probe. Table A.6.4 of appendix 6 shows the decomposition result when using two probes. A sample FORTRAN program for calculating decomposed coefficients is shown in table A.6.5 of appendix 6.

Since the relative error to be decomposed is calculated with respect to the origin, the drift error of the error component at a certain thermal condition is subtracted. As described earlier in chapter 3, if the calibration is done at a coordinate measuring machine on the FMS line, error values include geometric error components, and the decomposed values represent the predicted values after the drift is corrected. Since the calculated relative error represents only thermal variation from the cold condition, when the calibration probing is done, the corresponding error component in the cold condition needs

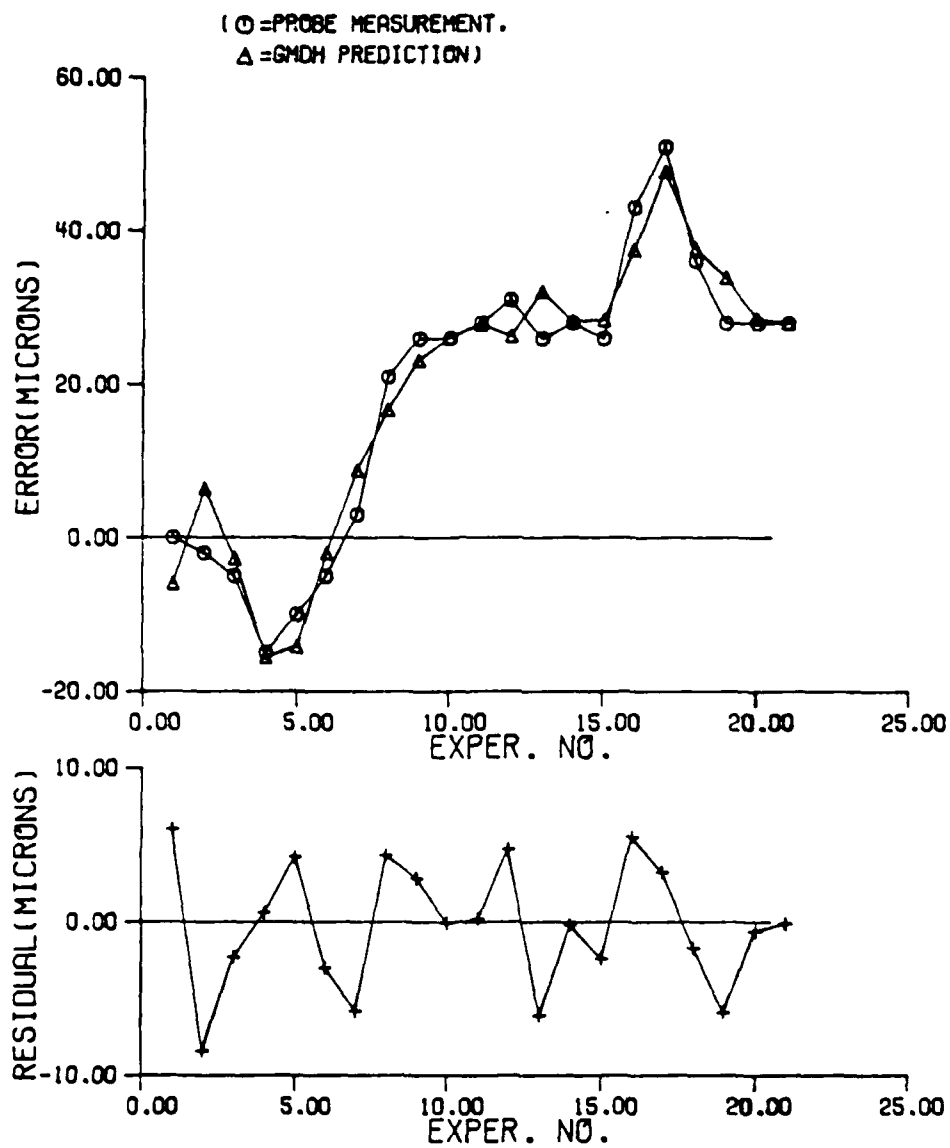


Figure 6.9 GMDH prediction on y drift error of measurement origin using 20 set of data.

to be subtracted from the predicted value at a certain thermal condition. This decomposition procedure only shows the relative effect of a varied error component on the resultant relative work space error.

There are three approaches to obtaining decomposition results. The short probe approach and the long probe approach have two kinds of assumptions regarding the positioning error. There are linear assumption and quadratic assumption of the positioning error. In general linear assumption gives better results if the errors are recalculated using decomposed coefficients.

Coefficients of the positioning error components are larger than angular error components by a factor of 10 or 20 and coefficients of squareness error are larger than the angular error components significantly. This shows that positioning errors and squareness errors are important to formulating final resultant error in the work space.

The difference between the two predictions is the value, which is to be compared with the decomposed positioning error after the drift is corrected. Only the short probe approach and the long probe approach give the decomposition for the y positioning error. Decomposition results are not so different from each other. Most of them show around 30 micro meters for 0.5 m movement. These values are reasonable compared to the actual measurements.

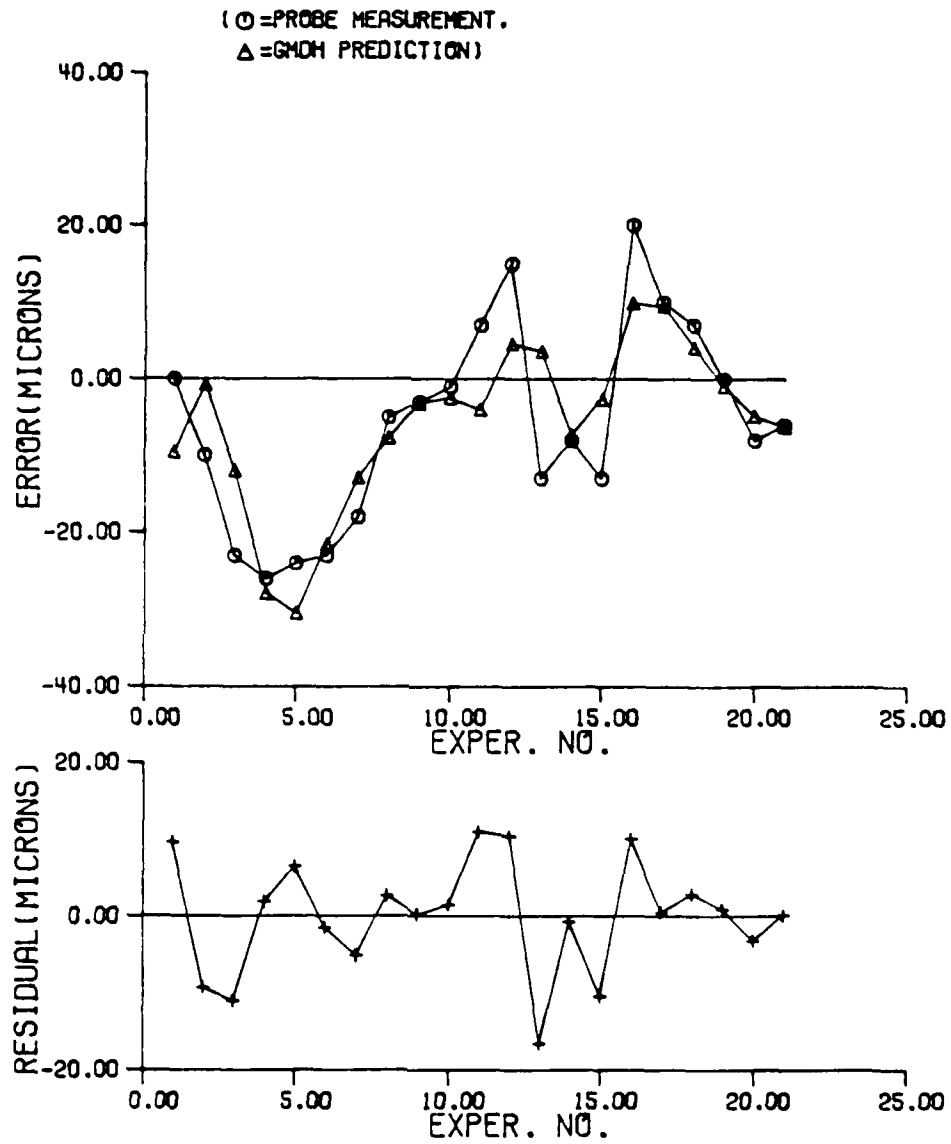


Figure 6.10 GMDH prediction on z relative error of point 11 using 20 set of data.

Calculated coefficients for angular errors are not significant except $c(14)$ for the y yaw error. Actual measurement shows only significant drift phenomenon for the whole range of axis. Once the error in the calibration is subtracted, the decomposed value should be negligible. Except for this error component, those decomposed coefficients for other angular errors are acceptable. Using the GMDH modeling of x pitch error, the decomposed coefficient $c(4)$ for the x pitch error can be compared. Results of GMDH prediction on the x pitch error for the thermal conditions when the calibration is done and test number 11 are shown in figure 6.12. Comparison between the GMDH prediction and the decomposed results are shown in figure 6.13.

Effect of the z pitch error, z yaw error, and z roll error on the resultant relative error is negligible since the coefficients $c(21)$, $c(23)$, and $c(25)$ are less than 0.2×10^{-5} for all 5 cases. This means that there is less than 1 micro meter variation for 0.5 m movement. This is verified by the actual measurement. Even though the magnitude of yaw error changes, the curve drifts only as thermal changes occur. The final variation with respect to the cold calibrated condition, therefore, is not significant once the drift is subtracted at a certain thermal condition.

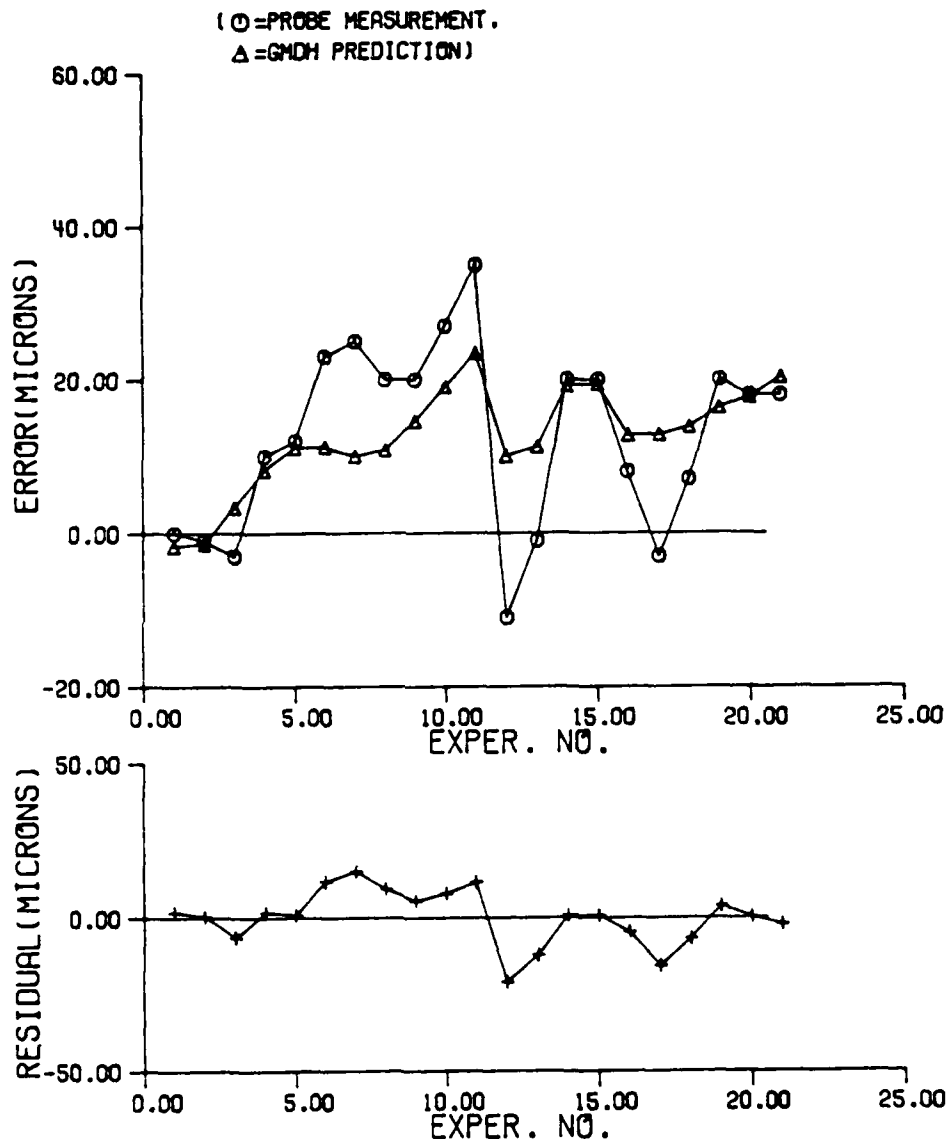


Figure 6.11 GMDH prediction on y relative error of point 22 using 21 set of data.

6.5 Determination of Measurement Points

While the required minimum number of measurement points is 10 for 10 coefficients of the error regression function, as many measurement points as possible are made within the physical limitation of the metrology pallet for the analysis. Cubic tungsten carbide inserts are glued on the steel structure so that the far ends of the work space can be covered. The locations of the center of each edge of the front plane and the center of the front plane are selected for the x and y information of the front surface. Some additional points are selected to get the information at different z depth. Within the physical limitation of the probe and the metrology pallet, 23 points are made for the short probe application and 34 points are for the long probe application.

For the determination of measurement points, the residual analysis is applied first, after the regression of error values. If the residual analysis shows an error value as an outlier outside 95 % confidence interval (i.e., $\pm 2\sigma$), it means that value does not fit into the regression function very well. It can show if any point has a problem. Error regression functions are obtained for a three day experiment. Outliers are recorded for each test to see if any specific point becomes the outlier frequently. Table 6.6 shows the point numbers of outliers after the residual

Table 6.5 Result of decomposition with the assumption of linear positioning error for test no. 11 using a short probe

*** Coefficients of error equations.***						
c(2)=	-0.21517e-05					
c(4)=	0.47349e-05					
c(7)=	0.73452e-05					
c(11)=	-0.27213e-05					
c(14)=	-0.38044e-04					
c(18)=	0.97870e-04					
c(21)=	0.39965e-08					
c(23)=	0.25063e-06					
c(25)=	-0.69498e-06					
c(30)=	0.28924e-05					
c(32)=	0.42331e-04					
c(33)=	-0.25479e-04					
c(34)=	0.18195e-04					

Calculation of relative errors using calculated coefficients						
no.	rerrorx	cal.ern	rerrory	cal.ery	rerrorz	cal.ern
2	13.0	1.6	5.0	21.4	-2.0	-10.2
3	1.0	0.3	5.0	28.0	5.0	-6.1
4	8.0	1.7	26.0	41.4	3.0	-2.9
5	3.0	-0.6	36.0	49.7	5.0	3.0
6	-2.0	2.9	48.0	66.9	2.0	7.7
7	-7.0	3.1	61.0	75.7	21.0	13.4
8	-15.0	6.3	66.0	72.9	-5.0	6.5
9	-9.0	4.1	58.0	71.1	18.0	6.7
10	1.0	7.2	58.0	69.8	-3.0	1.6
11	5.0	5.0	55.0	67.2	7.0	0.2
12	6.0	7.1	63.0	69.4	-5.0	-1.0
13	8.0	2.1	33.0	40.4	-7.0	-10.6
14	-2.0	4.8	38.0	47.5	-12.0	-10.1
15	6.0	6.3	20.0	24.1	-18.0	-19.9
16	8.0	5.6	7.0	21.6	-17.0	-20.3
17	6.0	5.0	17.0	18.8	-20.0	-20.9
18	-2.0	4.5	10.0	14.3	-15.0	-21.5
19	10.0	2.8	5.0	18.1	-18.0	-15.1
20	6.0	2.6	23.0	37.8	-10.0	-9.9
21	3.0	2.7	32.0	42.4	-5.0	-7.0
22	5.0	0.7	35.0	43.9	-5.0	-4.3
23	11.0	1.1	15.0	41.2	-5.0	-4.1

analysis for 34 measurement points of a long probe system. There are several points which become an outlier more than 5 times for 3 day tests. Points 12, 17, 18, 19, and 20

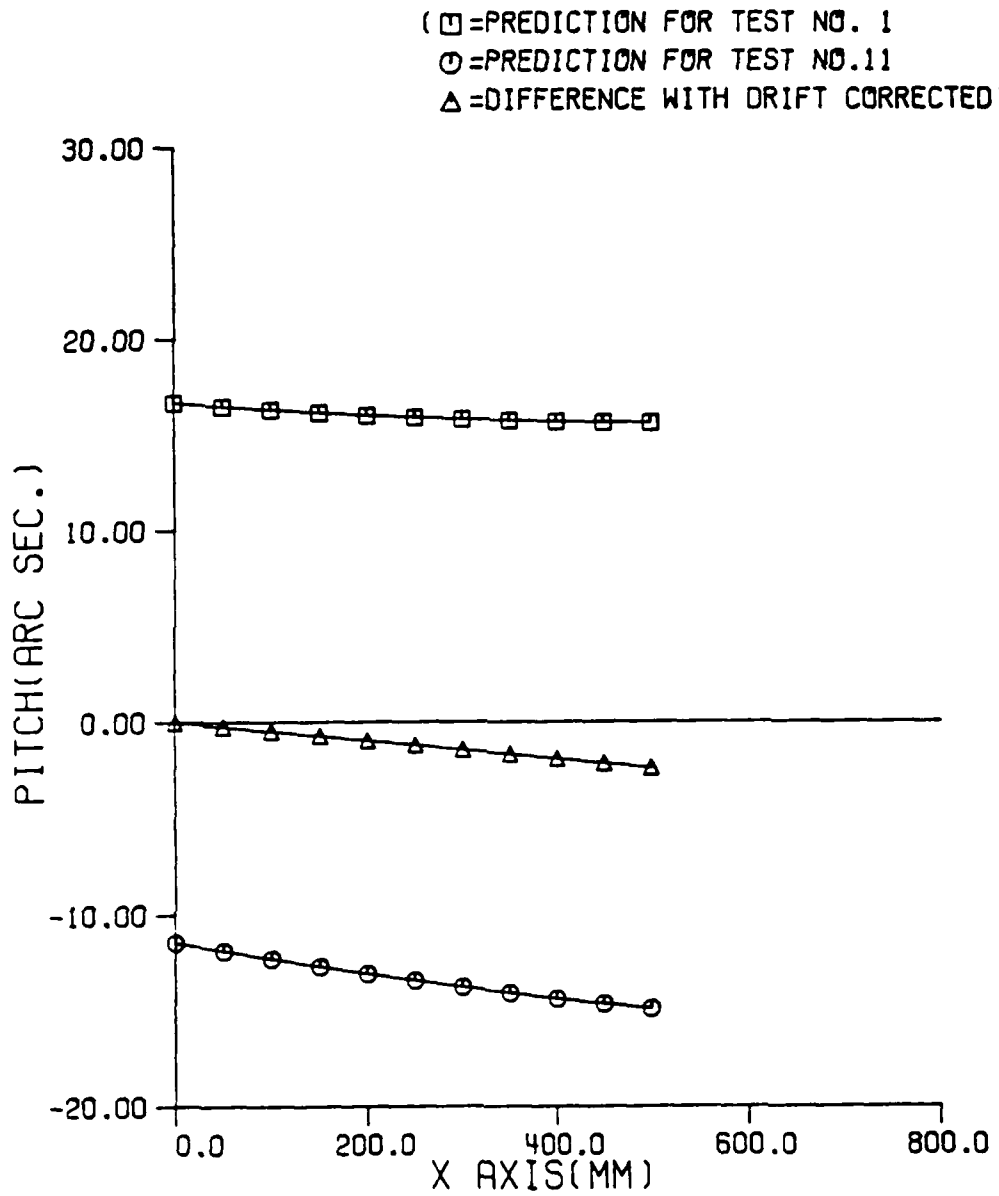


Figure 6.12 Results of GMDH prediction on x pitch error when calibration is done and test no. 11.

become outliers more than 5 times. Points 17, 18, and 19 are on the same branch of the pallet, screwed and glued to the main frame. Frequent outliers from z and y error values of those points show some instability of the branch resulting in a wide range of the scatter. Points 12 and 20 are on the long thin bar screwed to the main frame, which also shows some scatter. These points should not be included for further analysis. The residual analysis for the short probe system does not show many outliers. Only 5 points have outliers once or twice for 3 day tests. All 23 points are used for the short probe system. Figure A.4.1 of appendix 4 shows the numbering system for the short and the long probe system before the residual analysis. Figure A.4.2 of appendix 4 shows the numbering system for the short and the long probe system after the residual analysis. Twenty-nine points are used for the long probe system. For the remaining 23 and 29 points, the regression analysis is done again to obtain the Mean Error Sum of Square(MSE) for each test in the 20 different thermal conditions. The root of the MSE can be described as the standard deviation of the regression function. Table 6.7 shows the variation of the root of MSE values for the short and the long probe system. Standard deviation values do not vary dramatically as the thermal condition changes. Test number 11 is selected in the warmed-up condition for further analysis. Table 6.8 shows the variation of MSE

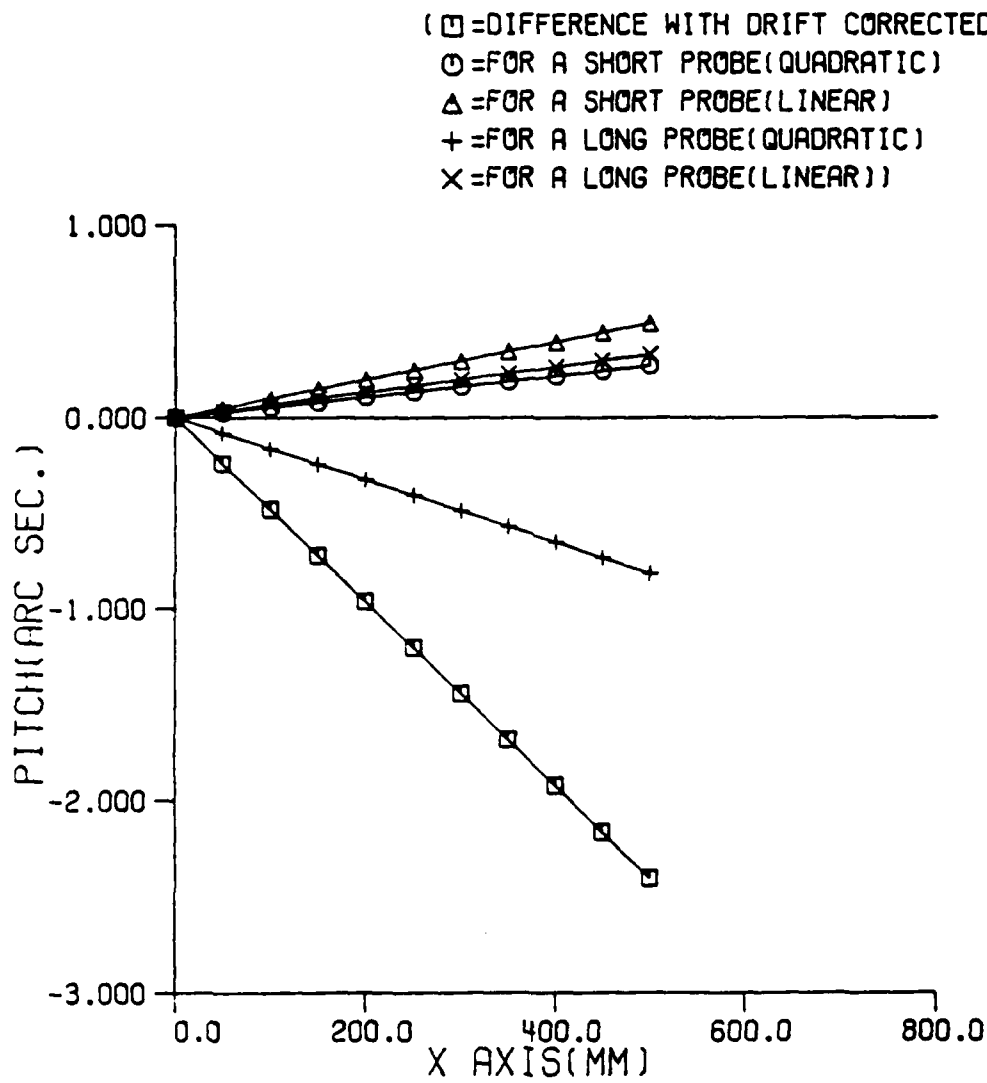


Figure 6.13 Comparison between the GMDH prediction and the decomposed results for x pitch error

values according to the number of points for test no. 11 of the short probe system. The far end point is selected for the X_h matrix of the equation (3.39) to be the maximum. If the confidence interval for the far end point of no. 11 satisfies the condition of equation (3.41), then those for other points satisfy the condition. To examine the optimal number of measurement points, MSE and the confidence interval are calculated. Ten measurement points are selected as the starting structure of the metrology pallet. Those are numbers 1, 4, 7, 8, 10, 11, 12, 15, 18, and 22 of the short probe system of figure A.4.2. These basic points cover the far end points in the work space. One measurement point is added to the previous structure to be analyzed. One example of the possible combination is shown in table 6.8. The sequence of the addition of the measurement point is numbers 9, 13, 19, 5, 14, 6, 16, 20, 23, 21, 17, 3, and 2. The number in parenthesis in table 6.8 shows the number added to the previous structure. The x axis MSE and confidence interval are the biggest, and one needs to take care of these. As the number of points increases, the confidence interval becomes narrower. From the 18 points the confidence interval becomes stable. There can be several criteria for the determination of the preset value of equation (3.41). A reasonable criterion is the repeatability of the probe. The repeatability of the probe is the limitation of the system performance. The repeatability of the

Table 6.6 Point numbers of outliers after the residual analysis for a long probe system.

Test no.	Point Number		
	x	y	z
2	12	19	12,17,18
3	8	20	13,17
4	*	19,20	17
5	*	*	17,19
6	18	*	18,19
7	*	13	19
8	20	19,20	*
9	10	11	13
10	13	*	12,18
11	*	*	12
12	*	19	17
13	32	20	*
14	18	13	*
15	20,18	24	12
16	20	19	17,18,19
17	*	19,20	14,17
18	18	12	12
19	18,20	*	12
20	*	*	*
21	*	12	18

short probe for the point number 11 of test 11 is 12.3 micro meter from table 6.4. From the eighteen points the structure satisfies the criterion of probe repeatability. Other calculations for the different point or the different tests show a similar result. For the machining experiment all twenty-three points are used for modeling to have better confidence interval and to provide experimental convenience. The probing cycle time mainly depends on the time of travel. Each probing for one point needs nine

Table 6.7 Variation of standard deviation of error regression function for a long and a short probes(in micro meter) (stand.dev. = square root of MSE)

Test no.	short probe			long probe		
	x	y	z	x	y	z
2	6.30	5.64	3.73	6.95	8.16	7.78
3	6.16	4.55	4.08	9.76	7.01	8.17
4	4.35	6.01	3.16	10.31	7.90	5.99
5	6.30	5.64	3.73	9.45	5.90	8.13
6	5.41	3.34	5.17	11.76	7.59	5.34
7	4.44	4.82	4.01	13.32	10.74	5.53
8	5.09	4.58	4.08	9.43	7.46	5.42
9	5.53	3.78	4.70	9.78	9.60	6.51
10	6.03	4.17	2.79	10.11	6.19	6.01
11	5.58	4.84	3.74	8.95	9.36	7.08
12	4.74	5.08	3.17	8.07	8.55	5.89
13	5.02	4.27	4.45	9.56	10.38	5.35
14	5.27	4.55	3.18	9.12	11.81	6.94
15	4.56	3.52	5.10	10.59	11.79	6.42
16	6.76	5.99	3.63	9.90	7.51	5.79
17	5.91	5.64	5.88	8.27	8.11	7.11
18	6.12	4.18	3.73	9.53	7.69	5.94
19	5.78	4.21	3.55	7.35	11.03	7.42
20	5.38	4.43	5.35	11.67	12.29	8.07
21	5.74	5.28	4.05	10.70	10.33	7.28

seconds. Therefore the time needed for probing five additional points is only 45 seconds.

Table 6.8 Variation of MSE and confidence interval according to the number of points for test no.11 of a short probe system (s.d.= standard deviation in micro meter)(c.i.= confidence interval).

no. of points	x		y		z	
	MSE	c.i.	MSE	c.i.	MSE	c.i.
10	*	*	*	*	*	*
11(+9)	58.0	89.5	15.5	46.3	45.1	78.8
12(+13)	35.4	23.7	9.6	12.3	34.9	23.6
13(+19)	55.2	22.0	6.5	7.6	42.5	19.3
14(+5)	41.4	16.8	33.1	15.0	33.1	15.1
15(+14)	47.3	16.7	8.5	7.1	26.7	12.6
16(+6)	47.3	16.0	14.7	8.9	23.1	11.2
17(+16)	41.9	14.6	20.7	10.2	19.8	10.0
18(+20)	37.1	12.4	19.5	9.7	20.7	10.0
19(+23)	34.8	12.7	25.7	10.9	15.7	8.5
20(+21)	33.6	12.3	26.1	10.8	15.4	8.3
21(+17)	30.8	11.6	26.1	10.7	14.1	7.8
22(+3)	29.3	11.3	29.3	11.3	24.5	10.4
23(+2)	31.1	11.6	14.0	7.8	14.0	7.8

CHAPTER 7 - MACHINING EXPERIMENT

The positioning capability is important for every operations of a machining center, such as drilling, reaming, tapping, endmilling, face milling, boring and so on. The endmilling operation is selected for the machining experiment for the x and y axis accuracy test. It can give flat surfaces for the measurement setup and also some corners for the coordinate measurement.

The compensation is achieved in two steps of a computer program. The first step of the computer program formulates the error regression function using the automatically fed probed data. The second step reads the original NC program and writes the corrected NC program using the error regression function. This program is sent to the machine controller, automatically downloaded by the host computer. A coordinate measuring machine measures the dimensions of the machined workpieces.

7.1 Experimental Setup

To reduce the thermal variation of errors during the machining experiment, one workpiece is machined for each

thermal condition. The specification of the tool holder, the insert, and the workpiece used is as follows;

Tool holder: Endmill with two cutting inserts

(made by Erickson tool co.)

(Outside diameter = 1 1/4" with no lead angle)

Cutting Insert: TPGN160304 P20 by BAILDONIT Tool co.

(Radius of insert = 0.4mm)

Workpiece: Low carbon steel plate (AISI 1020)

7.1.1 Design of the Workpiece

Three workpieces are flame cut from the big steel plate to have the same material and properties. Four sides of each workpiece are face milled to the same dimension. Then both faces of each workpiece are ground, which is necessary for measurement at a coordinate measuring machine. Rough machining is done to have four rectangular shapes at each corner of the plate on both sides. For each side of each rectangle, 5 mm deep grooves are machined to leave only 12 mm of unmachined side at each corner. This is so as to have a small portion of the workpiece to be finish machined. This reduces the effect of the tool wear and the cutting force on the final machined dimension. The picture of the workpiece ready to be finish machined for the experiment at the machine table is shown in figure 7.1.

For the workpiece preparation for the finishing cut as

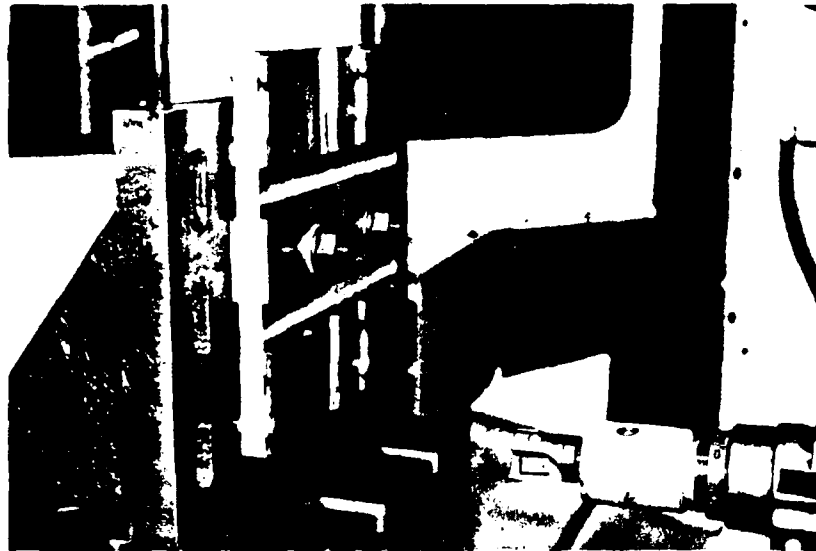
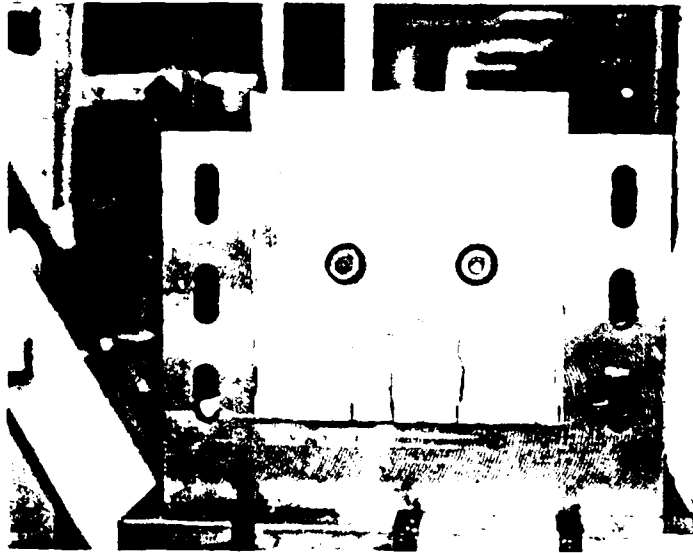


Figure 7.1 Workpiece prepared for machining experiment and the cutting tool

shown in figure A.7.1, all the corners of the four rectangular projection are machined. The machining conditions for the experimental finishing cut are the cutting speed of 130 m/min, feed rate of 80 mm/min, width of 3 mm, and 0.4 mm depth of cut. Complete machining of one workpiece needs around 11 minutes. The feed rate selected is very low to have a smooth surface for a CMM measurement. The depth of cut selected is very small so as not to have large cutting forces and tool deflection. A calibration cut is carried out on one of its slots before the finishing cut on the corners. this is for measuring the effective tool diameter due to tool deflection under the same cutting conditions.

7.1.2 Experimental Procedure

For the machining experiment, four corners of the right upper rectangle are machined for the error measurement and the three other corners of the whole workpiece for the setup of the measurement coordinate. It reduces the machining time and the effect of the tool wear. Tool deflection is taken into account by measuring the width of the slot for tool diameter calculation. Machined surfaces are represented as thick lines in figure 7.1. Machining experiments are done in the cold condition and after 10 hours of operation. Twelve minutes of probing with 48 minutes of continuous movement is repeated for 10 hours. This represents continuous working during the day. The

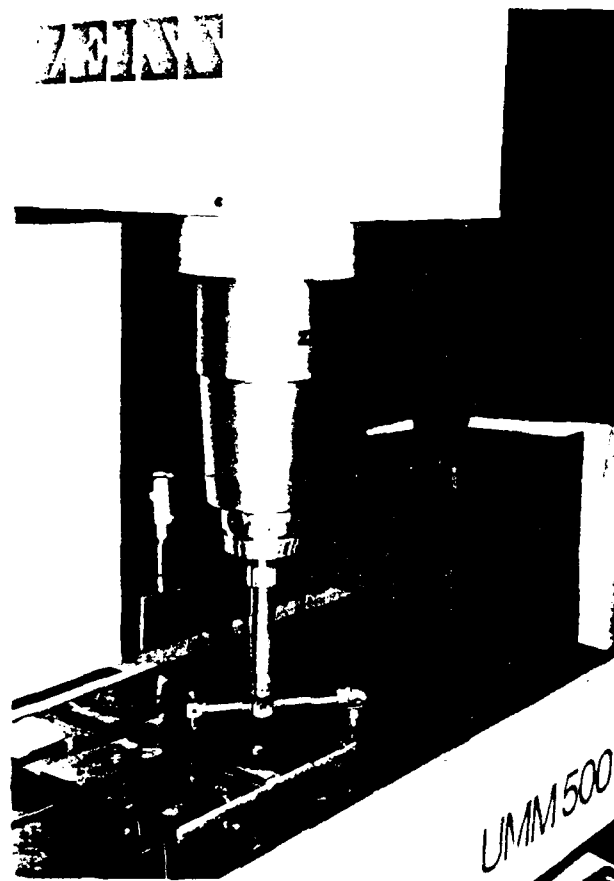


Figure 7.2 Workpiece being measured at the Zeiss coordinate measuring machine

values obtained by probing the metrology pallet for the first time, at the start of the day, are used for calibration. The calculated errors at a certain thermal condition represent the thermal variation of the machining center from the calibrated condition. If the FMS environment has the coordinate measuring machine on the line, this metrology pallet can be calibrated at the CMM.

7.1.3 Machining Program Preparation

The machining program is written by the FORTRAN program and downloaded to the machine controller automatically through the downloading procedure. Under the FMS environment the host computer takes care of downloading and uploading of machining programs when a compensated program is ready. Periodically probed values for the metrology pallet are sent to the host computer via a serial or parallel port to be used for updating the error regression function for the error compensation. As a host computer, the VAX 11/750 minicomputer is connected to the T10 ACRAMATIC controller through a RS232C serial port for uploading and downloading the programs. This host computer should have the required subroutine for calculating the inverse matrix for computing the error regression function. The compensated machining program is written after the error regression functions are updated. This is sent to be downloaded to the machine controller through the serial port while the

previous operation is being carried out. The pictures of the machine controller and the VAX 11/750 minicomputer are shown in figure 7.3.

7.2 Analysis

For each workpiece a short slot is machined using the same machining condition to decide the tool diameter for that workpiece as mentioned in 7.1.1. Machining is done with a non-compensation program in the cold and the fully warmed-up conditions. Each cycle needs around 11 minutes of machining time. The variation of the tool radius is shown in table 7.1 for a certain set of machining experiments. The same cutting inserts are used for the continuous machining of workpieces. Machining 110 mm caused around a 7 micro meter change in the tool radius dimension for each workpiece. The tool radius is varied almost by 30 micro meters for machining four workpieces. This shows the importance of tool wear in obtaining the correct dimension of the machined workpiece.

For an actual machining experiment, the first probing follows the non-compensation machining in the cold condition after 40 minutes of a warm-up period. Since this probing is used for calibration, this assumes that there is no error in the cold condition. After 10 hours of operation, another non-compensation machining is done. Probing

cycles using the short and the long probe follow to calculate errors for the compensation. Using the obtained error regression functions obtained, errors are calculated for machined coordinates as shown in table 7.2. The actual measurement results for a cold machining and a warm machining are also shown.

Calibration of the metrology pallet at an accurate CMM makes it possible to measure the resultant errors in the cold condition. The probing procedure assumes no error in the cold condition. The error obtained by cold machining can be assumed to represent the geometric and the thermal errors combined in that thermal condition. The addition of cold machining errors to the probed errors can simulate the actual FMS environment with an accurate coordinate measuring machine.

Errors obtained by short probe, long probe, and two probe approaches are shown as cases 3, 4, and 5 respectively in table 7.2. Cold machining errors are added to those of cases 3, 4, and 5 to become cases 6, 7, and 8 respectively. The resultant error after compensation for each case is shown in table 7.3. Those are drawn in figures 7.4 and 7.5. To compare the result, the magnitude of the error is calculated for each case using x and y error components as shown in table 7.4. Errors with other compensation methods are compared for each machined point.

From the calculation of the mean error, the long probe system shows the best compensation result, which is around 45 % of the non-compensation error in magnitude. This shows that a 50 micro meter error for 238 mm by 258 mm dimension of point 15 can be reduced to a 23 micro meter error. The fact that the dimension of the workpiece is relatively small gives a more promising future for the compensation.

The short probe system shows around 50 percent error, which means 200 percent improvement after compensation. The two probe system shows around 75 percent error. Addition of cold machining errors to probed errors does not improve the compensation capability. This shows that the calibration of the metrology pallet on the machine tool in the cold condition is an acceptable way for application in a real machining environment such as an FMS.



Figure 7.3 The pictures of the machine controller and the VAX 11/750 minicomputer used for machining program preparation

Table 7.1 Variation of a tool diameter after each completion of machining 110 mm for 11 minutes.

work- piece	1st machining		2nd machining	
	radius in mm	variation in μm	radius in mm	variation in μm
no. 1	16.0667	0.	16.0774	0.
no. 2	16.0617	5.	16.0616	15.8
no. 3	16.0506	16.1	16.0513	26.1
no. 4	16.0406	26.1	16.0493	28.1

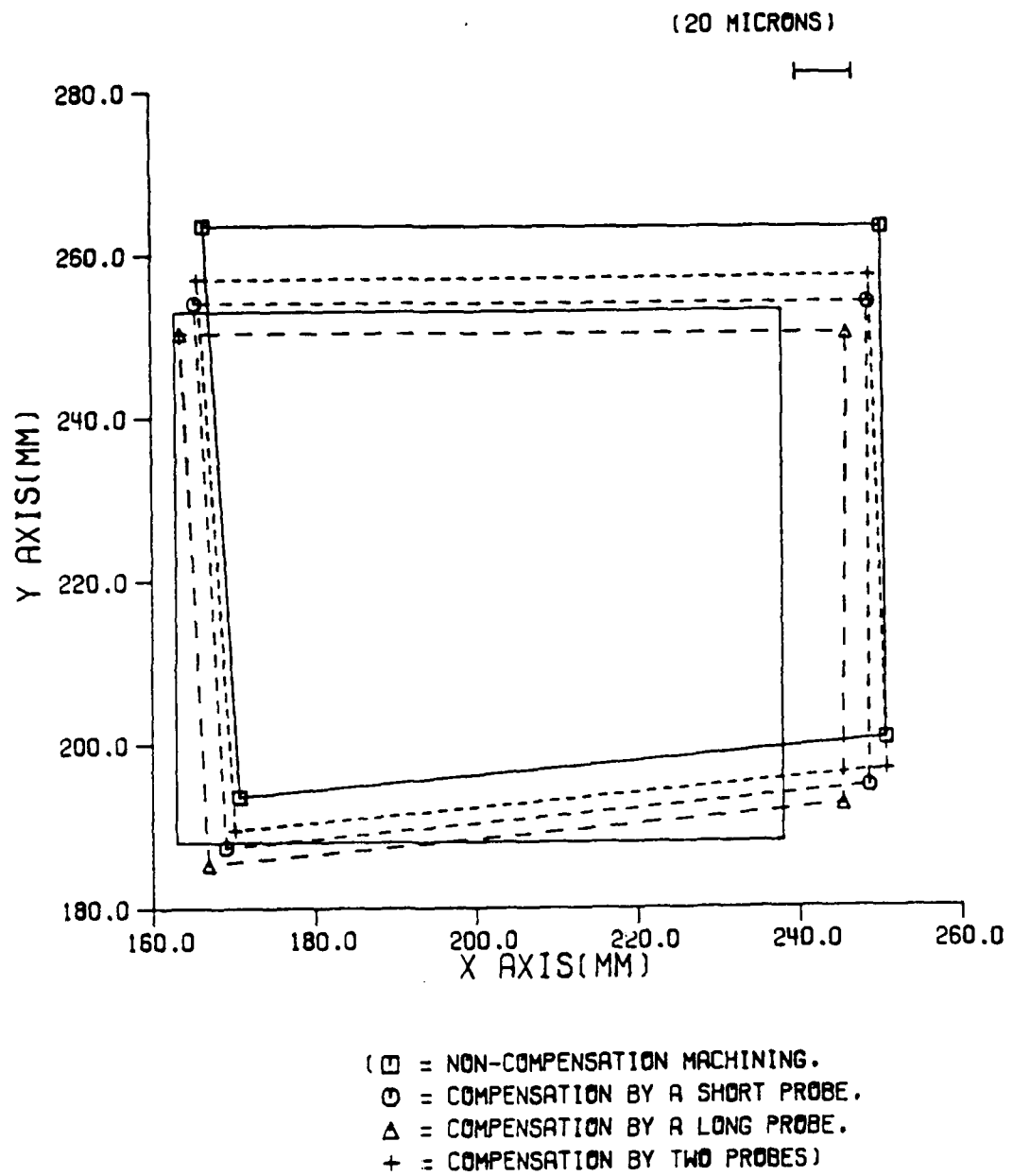


Figure 7.4 Error after the non-compensation machining and the compensation without cold machining errors

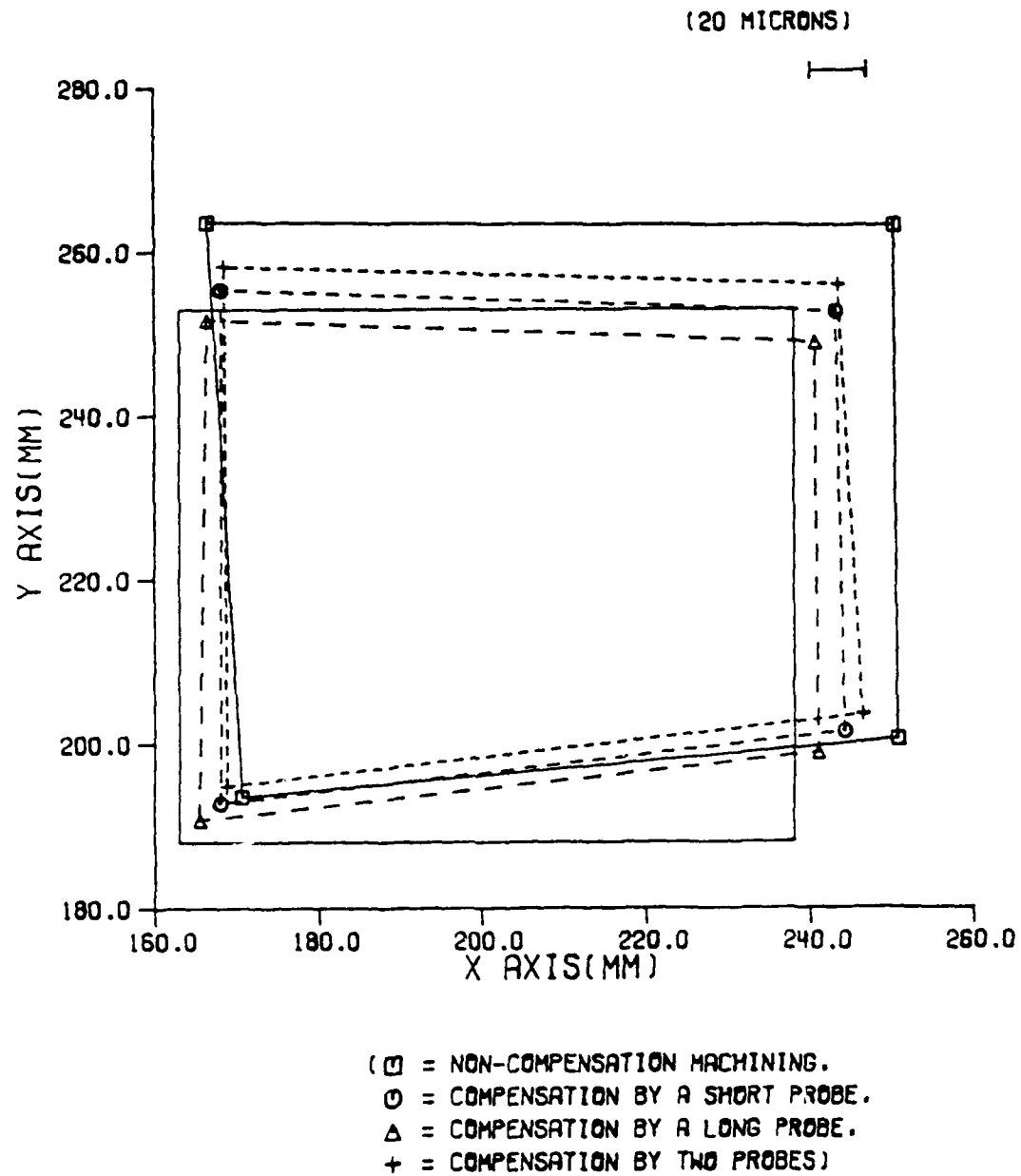


Figure 7.5 Error after the non-compensation machining and the compensation with cold machining errors

Table 7.2 Machining error and its calculation using a pallet system.

(case no. 1: machining error in the cold condition
 case no. 2: machining error in the warm condition
 case no. 3: calculated error by a short probe system,
 case no. 4: calculated error by a long probe system,
 case no. 5: calculated error by two probe system,
 case no. 6: case 3 with case 1 taken into account,
 case no. 7: case 4 with case 1 taken into account,
 case no. 8: case 5 with case 1 taken into account)
 (in micro meter)

point		13		14	
case		x	y	x	y
no. (1)		3.7	-15.4	-8.0	-3.7
no. (2)		21.8	15.7	9.9	30.2
no. (3)		3.8	17.5	3.2	27.2
no. (4)		11.1	23.4	8.2	37.7
no. (5)		1.6	11.5	2.2	19.0
no. (6)		7.5	2.1	-4.8	23.5
no. (7)		14.8	8.0	0.2	34.0
no. (8)		5.3	-3.9	-5.8	15.3

point		15		16	
case		x	y	x	y
no. (1)		15.4	3.5	12.6	-19.4
no. (2)		35.3	28.8	36.4	35.8
no. (3)		5.0	26.4	6.0	16.7
no. (4)		12.5	37.1	15.3	23.1
no. (5)		4.2	17.0	-0.3	10.8
no. (6)		20.4	29.9	18.6	-2.7
no. (7)		27.9	40.6	27.9	3.7
no. (8)		19.6	20.5	12.3	-8.6

Table 7.3 Error after compensation by a pallet system
with cold machining error taken into account.

(case 2: machining error in the warm condition
case 3: simulated machining error by a short probe system,
case 4: simulated machining error by a long probe system,
case 5: simulated machining error by two probe system,
case 6: case 3 with case 1 taken into account,
case 7: case 4 with case 1 taken into account,
case 8: case 5 with case 1 taken into account,
case 1: machining error in the cold condition)
(in micro meter)

point		13		14	
case		x	y	x	y
no. (2)		21.8	15.7	9.9	30.2
no. (3)		18.0	-1.8	6.7	3.0
no. (4)		10.7	-7.7	1.7	-7.5
no. (5)		20.2	4.2	7.7	11.2
no. (6)		14.3	13.6	14.7	6.7
no. (7)		7.0	7.7	9.7	-3.8
no. (8)		16.5	19.6	15.7	14.9
point		15		16	
case		x	y	x	y
no. (2)		35.3	28.8	36.4	35.8
no. (3)		30.3	2.4	30.4	19.1
no. (4)		22.8	-8.3	21.1	12.7
no. (5)		31.1	11.8	36.7	25.0
no. (6)		14.9	-1.1	17.8	38.5
no. (7)		7.4	-11.8	8.5	31.1
no. (8)		15.7	8.3	24.1	44.4

Table 7.4 Percentage error after compensation by a pallet system with and without the cold machining error taken into account.

(case 2: machining error in the warm condition
 case 3: simulated machining error by a short probe system,
 case 4: simulated machining error by a long probe system,
 case 5: simulated machining error by two probe system,
 case 6: case 3 with case 1 taken into account,
 case 7: case 4 with case 1 taken into account,
 case 8: case 5 with case 1 taken into account,
 case 1: machining error in the cold condition)
 (per.=percent, errors are in micro meter)

point	13		14	
case	error	per.	error	per.
no. (2)	26.9	100.0	31.8	100.0
no. (3)	18.0	67.3	7.3	23.1
no. (4)	13.2	49.1	7.7	24.2
no. (5)	20.6	76.8	13.6	42.8
no. (6)	19.7	73.5	16.2	50.8
no. (7)	10.4	38.7	10.4	32.8
no. (8)	25.6	95.4	21.6	68.1

point	15		16		mean	
case	error	per.	error	per.	error	per.
no. (2)	45.6	100.0	51.1	100.0	38.8	100.0
no. (3)	30.4	66.7	35.9	70.3	22.9	59.0
no. (4)	24.3	53.3	24.6	48.2	17.4	44.9
no. (5)	33.3	73.0	44.4	87.0	28.0	72.1
no. (6)	14.9	32.8	42.4	83.1	23.3	60.1
no. (7)	13.9	30.6	32.2	63.1	16.7	43.1
no. (8)	17.8	39.0	50.5	99.0	28.9	74.4

CHAPTER 8 - CONCLUSIONS

For the one dimensional error analysis, the GMDH technique made it possible to predict positioning errors and angular errors very accurately based on the temperature information. The positioning error is predicted to within 7 micro meter residual errors for a magnitude of 120 micro meter errors in the warmed-up condition. The pitch error, which is the typical angular error, is predicted within 3 arc second residual errors for a magnitude of 17 arc second errors in the warmed-up condition.

Error components predicted by the GMDH technique are used for comparison with those from the decomposition procedure of the work space resultant errors, obtained by probing the metrology pallet. The decomposition procedure for each axis is also set-up, establishing the relative contribution of each error component to the change in the resultant errors using regression analysis. The decomposed result shows that the positioning errors and squareness errors give more contribution than angular errors to the work space error, which coincides with the actual measured result. Comparison of the x pitch error and the y positioning error shows acceptable magnitudes of decomposed

AD-A174 974

THE SCIENCE OF AND ADVANCED TECHNOLOGY FOR
COST-EFFECTIVE MANUFACTURE OF (U) PURDUE UNIV
LAFAYETTE IN SCHOOL OF INDUSTRIAL ENGINEERING

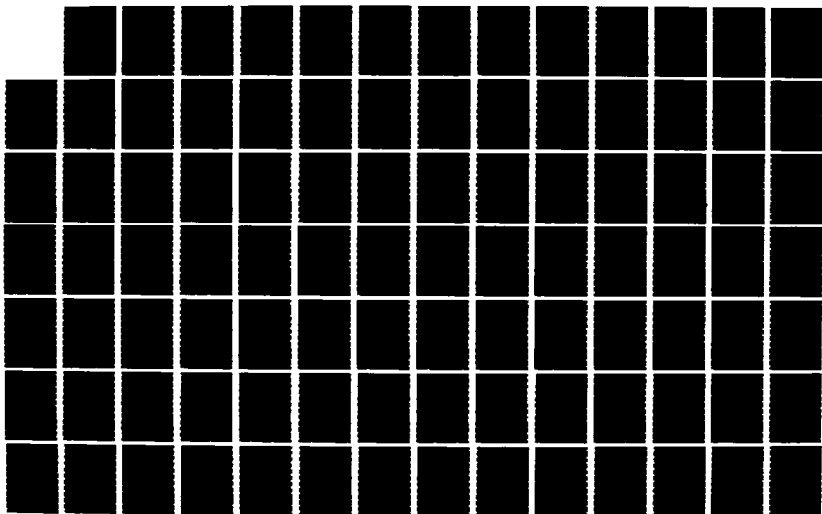
3/4

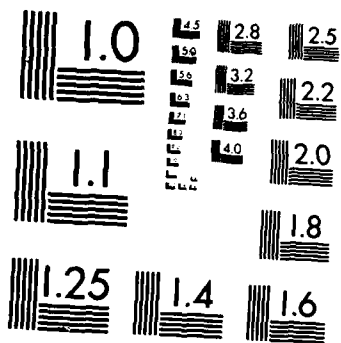
UNCLASSIFIED

S LEE ET AL NOV 86 N00014-83-K-0385

F/G 13/9

NL





MICROCOPY RESOLUTION TEST CHART
NATIONAL BUREAU OF STANDARDS-1963-A

errors.

The "Dynamic" method of compensating the backlash error is proposed following the ANOVA(Analysis of Variance) analysis to determine the important factors affecting the backlash. The thermal variation is determined to be important and is to be monitored for GMDH modeling and compensation.

The thermal drift phenomenon is also investigated by the GMDH technique with the temperature information. The thermal drift error is predicted within 3 micro meter residual errors for all the cases. The determination of probing intervals for the metrology pallet is done dynamically in accordance with the thermal changes of the machine-tool using the drift error model obtained by the GMDH(General Method of Data Handling) technique of Ivakhnenko.

To determine tool tip position errors with a touch probe on a machine tool, a metrology pallet has been constructed. The error model for touch probe application has been constructed from the actual error measurements in the working space of a machine tool

The error calculation procedure including the calibration of a metrology pallet on a machine tool is formulated. Three approaches to obtaining error regression functions at the tool tip position within the work space have been

formulated using one or two touch probes and the metrology pallet. A short probe system has the advantage of a more stable simple structure for the metrology pallet. A long probe system has the advantage of covering more work space. The two probe system with two different length probes needs smaller number of measurement points than the above two approaches. Even an accurately measured workpiece can be used for the two probe approach. Workpiece dimensional variation due to the thermal changes is compensated for because the metrology pallet reflects this change.

The quadratic error regression model is able to predict the work space error within 5 micro meter residual errors for a magnitude of 50 micro meter errors. GMDH modeling on the drift error or the relative error with the temperature information makes the system determine the probing interval. It updates the error regression functions if the predicted error change exceeds a predetermined value. It predicts the drift error within 7 micro meter residual errors for 40 to 70 errors of most cases.

A machining experiment is conducted to show the actual error compensation capability of the metrology pallet system. Two cases of application to the FMS environment are simulated. The one is an FMS which has a coordinate measuring machine for the calibration of the metrology pallet. The other is an FMS without a coordinate measuring

machine, for which the probing values in the cold condition are used for the calibration. Final average performance for the above two cases does not differ very much, which indicates the strong possibility of using pallet system in a FMS line without a coordinate measuring machine. Errors of a certain corner out of four corners are reduced to 24 % or 35 %, which is a 410 % or 300 % improvement. From the calculation of the mean error, the long probe system shows the best compensation result, which is around 45 % of the non-compensation error in the magnitude. This shows that a 50 micro meter error for a 238 mm by 258 mm dimension is reduced to a 23 micro meter error. The short probe system shows around 50 percent error, which means 200 percent improvement after the compensation. Two probe system shows around 75 percent error. The fact that the dimension of the workpiece is relatively small gives a more promising future for the compensation.

CHAPTER 9 - RECOMMENDATIONS

(1) For the application of the GMDH technique to the positioning error compensation, several points need to be given careful consideration.

First, the range of temperature data used for the GMDH modeling restricts the application range in which the GMDH prediction is feasible. Data on temperature variation of the environment is necessary if the GMDH model needs to be used throughout the year. If the facility to simulate the temperature variation of the environment is not available, the change of the model coefficient according to the temperature range of the environment may be required.

Second, the error model for the other direction may not be necessary if the backlash error model is used combined with the error model for the one direction. The backlash error is determined by GMDH modeling with the temperature information.

Third, the modeler needs to investigate if the data sequence for the GMDH input affects the final results. If the results are affected, the same sequence or trend of data input for the prediction is needed as data input for

the modeling.

The same consideration needs to be applied to other cases including the angular error prediction using the GMDH technique, the drift error prediction, and the probing interval determination.

For the probing interval determination, the change of the relative error of the far end point with respect to the origin of measurement is the best criterion to monitor if the touch probe resets the workpiece coordinate whenever the machining is done. Otherwise, the change of the drift error of any point may be a good criterion to monitor.

(2) For the construction of the metrology pallet, a shape, similar to the most frequent workpiece may be preferable, to represent the same thermal variation and distortion of the workpiece. If the workpiece and the clamping fixture cover almost the whole work space, attaching the measurement points to the workpiece structure is a good idea. Granite structure may be feasible for the thermally stable structure, but needs compensation for the thermal variation of the workpiece. Instead of cubic inserts for the measurement points, superfinished ball bearing may work excellently.

(3) Even though the author could not be successful in applying the GMDH technique to modeling the probed work

space errors with 3 coordinate informations and temperature information at 24 points, it is still challenging to tackle the problem. Once it is successful, very frequent probing cycles are not necessary after a certain period of data acquisition. Less scatter of the probed error may be helpful, which can be achieved by better design of the probe and the interface.

(4) Even though the criterion which the author used for the determination of measurement points works fine, other approaches could also be recommended. The statistical analysis on the variance of a specific point can be used for the apriori determination without the actual measurement data.

(5) For the machining experiment, the boring operation may give better result because of the better coordinate setup by using bored holes. The surface waviness due to the endmill operation results in larger uncertainties in measurement in addition to the machine tool error itself.

(6) Relationship between the tool wear and the dimensional change of the tool diameter needs to be investigated. This is one of the most important factor to affect the accuracy of the machined workpiece. It is recommended to include the above relationship for compensation.

LIST OF REFERENCES

LIST OF REFERENCES

1. Technology of Machine Tools, M.T.T.F., vol.5; "Machine Tool Accuracy", Lawrence Livermore Laboratory, Univ. of Cal., Livermore, Ca, UCRL-529660-5, 1980.
2. Bryan, J.B., "International status of thermal error research", Annals of C.I.R.P., vol.XVI, pp203-215, 1968.
3. Schultschik, R., "The components of the volumetric accuracy", Annals of C.I.R.P., vol 26, pp223-228, 1977.
4. Sata, T., Takeuchi, Y., Sakamoto, M., Weck, M., "Improvement of Working Accuracy on NC Lathe by Compensation for Thermal Expansion of Tool", the annals of C.I.R.P. vol.30, 1981 p445.
5. Okushima, K., Kakino, Y., Higashimoto, A., "Compensation of Thermal Displacement by Coordinate System Correction", Ibid, vol.24/1/1975, p327.
6. Love, W.J., and Scarr, A.J., "The determination of the volumetric accuracy of multi axis machines", Proc. of MTDR, vol.17, pp.307-315, 1973.
7. Hocken, R., et al, "Three dimensional metrology", Ibid, vol. 26, pp403-408, 1977.
8. Sata, T., et al, "Analysis of thermal deformation of machine tool structure and its application", Proc. of MTDR, vol.17, pp275, 1973.
9. Spur, G., and DeHaas, P., "Thermal behavior of NC machine tools", Ibid, vol.14, pp267-273, 1973.

10. Weck, M., and Zangs, L., "Computing the thermal behavior of machine tools using the Finite Element Method-Possibilities and Limitations", Ibid, vol. 16, pp185-193, 1975.
11. McClure, E. R., "Thermally induced errors", Technology of Machine Tools, M.T.T.F., vol. 5:1980.
12. Okushima, K., et al, "Compensation of thermal displacement by coordinate system correction", Annals of C.I.R.P., vol. 24, pp327-331, 1975.
13. Sata, T., Takeuchi, Y., and Okubo, N., "Improvement of working accuracy of a machining center by computer control compensation", Proc. of MTDR, vol. 27, pp93-99, 1977.
14. Pfeifer, T., and Furst, A., "Advantages and conditions for a direct measurement of the workpiece-geometry on NC-machine tools", Information control problems in manufacturing technology, pp165-172, 1977.
15. Pfeifer, T., and Furst, A., "Workpiece measurements on NC (CNC) machine tools: Machine configurations/application examples", Ibid, pp279-290, 1979.
16. Schaffer, G., "Sensors: the eyes and ears of CIM", American Machinist, Special Report 756, pp109-124, July 1983.
17. Mason, G., "Probing for that touch of quality", Machinery and production engineering, 16 Aug. 1978, pp. 31-32.
18. Kellock, B., "Machine Tool Probes-an Export Success", Machinery and production engineering, 13 May, 1981, pp. 47-48.
19. Roe, J., "In-Cycle Gauging as a Production Tool.", Pub. of Renishaw Elec. Ltd., 1981, England.
20. Roe, J., "Datuming of Machine Tool Probes", Pub. of Renishaw Elect. Ltd., Oct, 1981, England.

21. Programming Manual for T-10", Cincinnati Milacron Co.,
Pub.no.6-MC-8108,1981,Cincinnati,Ohio.
22. Vitullo, E.R., "Application of In-Process Gauging on
Machining Centers", Tech. Report of SME MS84-237, 1984.
23. NA, "No Need to Touch with Latest Probe", Machinery and
production engineering, 18 Nov., 1981, pp47-49.
24. Schultschik, R., "Possibilities and Limits of Error Feed-
back in Automatic Machining", the annals of C.I.R.P.,
vol. 30, 1981, pp467-471.
25. Peters, J., "Metrology in Design and Manufacturing-Facts
and Trends", Ibid, 1977.
26. Sweet, A., Noller, D., and Lee, S., "Statistical design for
the location of planes and circles when using a probe",
Precision Engineering, Vol. 5, no. 3, Nov., 1985.
27. "Watching as axes heat up and grow", American Machinist,
pp146, Nov., 1984
28. Barash, M.M., and Liu, C.R., "Proposal for research on the
science of an advanced technology for cost-effective
manufacture of high precision engineering products",
Purdue University, W.Laf., Indiana, Oct., 1982.
29. Barash, M.M., and Lee, S., "Accuracy improvement of a CNC
Machining Center by a touch probe", ONR Report, Purdue
University, W.Laf., Indiana, Feb., 1984.
30. McKeown, P.A., "Some Aspects of the design of High Preci-
sion Measuring Machines", the annals of C.I.R.P., 1982.
31. Tlusty, J., "Techniques for Testing Accuracy of NC Mach-
Tools", MTDR, vol. 12, 1971, pp.333-340.
32. Anderson, "Machine Tool Testing-A Practical Approach",
MTDR, vol. 13, 1972, pp.325-331.

33. Saxena, U., and Spanier, P., "On the Positioning Capability of Numerically Controlled Machines", ASME pub. 79-WA/Prod-20, 1979.
34. Golder, A., "A Statistical Approach to Machine Tool Testing", MTDR, vol. 16, 1975, pp. 331-336.
35. Tlustý, J., "Testing of Accuracy of NC Machine Tools", UCRL-52960 Supp., Supplement 1 of Technology of Machine Tools, Lawrence Livermore Laboratory, University of Cal. Livermore, Cal., 1982.
36. Hemingray, C.P., Cowley, A., and Burdekin, M., "Positioning Accuracy of Numerically Controlled Machine Tools", MTDR, vol. 14, 1973, pp. 281-284.
37. Hemingray, C.P., "Some Aspects of the Accuracy Evaluation of Machine Tools", MTDR, vol. 14, 1973, pp. 281-284.
38. Vanberck, P., Bagiasha, K., and Peters, J., "Continuous Measurement of Linear Motion Errors in Single Tool Cutting", MTDR, vol. 19, 1978, pp. 375-381.
39. Kamyshev, A.I., "Comparative Analysis of Methods for Testing the Positioning Accuracy of NC Machine Tools", Soviet Engineering Research, vol. 1, no. 3, 1981, pp. 71-73.
40. CIRP STC <<Me>> Working Party on 3 DU, "A Proposal for Defining and specifying the dimensional uncertainty of Multi-Axis Measuring Machines", the annals of C.I.R.P., vol. 27, 1978, pp. 623-630.
41. Knapp, K., "Test of the Three-Dimensional Uncertainty of Machine Tools and Measuring Machines and its Relation to the Machine Errors", Ibid, vol. 32/1/1983, pp. 459-464.
42. Venugopal, R., "Thermal Effects on the Accuracy of Numerically Controlled Machine Tools", Ph.D. Thesis of Purdue University, W.Laf., Indiana, May 1986.

43. Liu, C.R., and Ferreira P.M., "Adaptive modeling of Machining Error", CIDMAC ANNUAL Report, 1984-1985, CIDMAC, Purdue University, W.Lafayette, IN, 47907.
44. Ivakhnenko, A.G., "The Group Method of Data Handling in Prediction Problems", Sov. Autom. Control, vol. 9, no. 6, 1976, pp. 21-30.
45. Farlow, S.J., "Self-Organizing Methods in Modeling: GMDH Type Algorithms", Marcel Dekker, inc., New York & Basel, 1984.
46. Donmez, A.M., "A General Methodology for Machine Tool Accuracy enhancement. Theory, Application, and Implementation", Ph.D. Thesis, Purdue Univ., W. Lafayette, IN, August, 1985.
47. Ferreira, P.M., and Liu, C.R., "An Analytical Quadratic Model for the Geometric Error of a Machine Tool", J. of Manufacturing System, vol. 5, no. 1, 1986, pp. 51-63.
48. Paul, Richard P., "Robot manipulators: Mathematics, Programming, and Control", The MIT Press, Cambridge, MA, chap. 4, 1981.
49. NMTBA, "Definition and evaluation of accuracy and repeatability for numerically controlled machine tools", 2nd ed., Aug., 1972, NMTBA.
50. Neter, J., and Wasserman, W., "Applied linear statistical models", Richard D. Irwin, Inc., Homewood, Ill, Chap 3, 1974.

APPENDICES

Appendix 1 - GMDH Modeling Technique

In the real world, there are often some systems which seem to be too complex to model as a function.^[45] Modelers are forced to make wild guesses at function variables, which is easy to put their prejudices into models. Many types of mathematical models require the modeler to know things about the system that are generally hard to find. There has been a distinguishable trend away from the restrictive assumptions of parametric analysis and toward a more computer oriented area of what is generally known as nonparametric data analysis. Only the data decides the model, nothing else can. One of the heuristic approaches to see the data for model determination is the General Method of Data Handling(GMDH) technique, which was introduced in 1969 and has been developed by the Russian cyberneticist and engineer, A.G. Ivakhnenko.^[44,45]

GMDH technique starts with a basic primeval form of equation which is a quadratic equation of each two variables. A new generation of more complex offsprings is constructed and a survival-of-the-fittest principle is applied to determine which new equations live and which equations die. Surviving new generation equations may represent a

real world better than the original. If all the surviving equations are combined, another generation of more complex equations is obtained. Continuing this process for many generations may cause overspecialization of the real world. Stopping the process before overspecialization of the real world gives the optimal complexity of a model-not too simple and not too complex. The modeler needs to provide input/output data from observations and the computer does all the rest to determine the important variables and self-organizes the model.

1.1 General Method of Data Handling-Overview

The GMDH algorithm allows one to model complex systems without having specific knowledge of the system or massive amounts of data. The modeler need only to collect a relatively small number of input/output observation and the computer does the rest. The philosophy is to let the computer do more work in deciding the optimal model for a certain environment.

For each pair of input variables x_i and x_j and the output y , the quadratic regression equations

$$y = A + Bx_i + Cx_j + Dx_i^2 + Ex_j^2 + Fx_ix_j \quad (A.1)$$

are computed as figure A.1.1.

In figure A.1.1, the first generation variables are

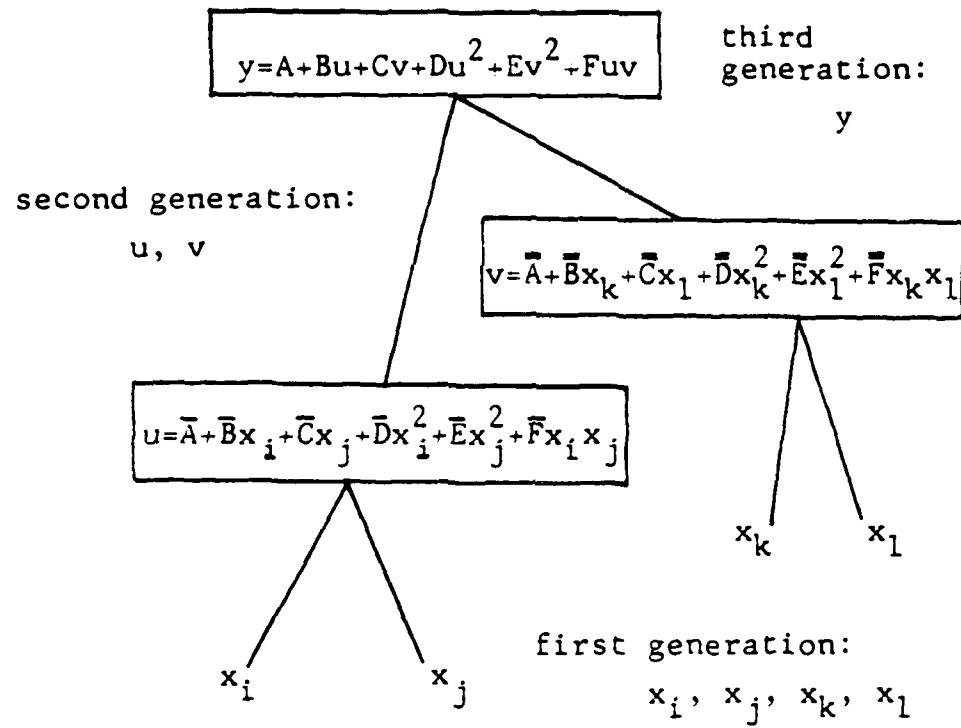


Figure A.i.1 Basic scheme of propagation of variables.

the original inputs x_1, x_j, x_k, x_l . The second generation variables like u and v are the quadratics in x_1, x_j, x_k, x_l . The third generation variables like y are quadratics in variables of the previous generation. $M(M-1)/2$ higher order variables for predicting the output y are obtained in place of the original m variables x_1, x_2, \dots, x_m .

After the saving procedure which determines the best prediction of y , a certain number of equations (say m_1) are saved and used for generating new independent observations. From these new independent variables they are combined exactly as done before. A new collection of $m_1(m_1 - 1)/2$ regression equations predict y from the new variables. This process is continued until the regression equations begin to have a poorer predictability power than did the previous ones. After stopping, the best of the quadratic polynomials in that generation is obtained, which is an estimate of y as a quadratic of two variables, which are themselves quadratics of two more variables, which are themselves quadratics of two more variables, ... , which are quadratics in the original variables. In other words, if we were to make the necessary algebraic substitutions, we would arrive at a very complicated polynomial of the form:

$$y = a + \sum_{i=1}^m c_i x_i + \sum_{i=1}^m \sum_{j=1}^m c_{ij} x_i x_j + \sum_{i=1}^m \sum_{j=1}^m \sum_{k=1}^m d_{ijk} x_i x_j x_k + \dots \quad (A.2)$$

which is known as the Ivakhnenko polynomial.

1.2 Algorithm of the GMDH technique-Details

The real advantage of the GMDH algorithm comes about when the modeler works with large, complex systems. The computation procedure is started by collecting regression type data like n observations of the form shown in figure A.1.2.

Y		X			
		x_1	x_2		x_m
y_1	training observation	x_{11}	x_{12}	.	x_{1m}
y_2		x_{21}	x_{22}	.	x_{2m}
.	
.	
y_{nt}	checking observation	$x_{nt,1}$	$x_{nt,2}$.	$x_{nt,m}$
.	
.	
y_n		x_{n1}	x_{n2}	.	x_{nm}

Fig. A.1.2 Input to the GMDH algorithm.

There are three steps in the GMDH computation procedure.

Step 1 (constructing new variables $z_1, z_2, \dots, z_{m(m-1)/2}$): The first step is to take all of the independent variables (columns of X) two at a time and construct the regression polynomial

$$y = A + Bu + Cv + Du^2 + Ev^2 + Fuv$$

that best fits the dependent observations y_i in the training set. For each of these regression surfaces, evaluate the polynomial at all n data points and store these n new observations (new generation of variables) in the first column of a new array Z as figure A.1.3. The resulting columns of z are computed in a similar manner.

Step 2 (screening out the least effective variables): This step computes the root mean square (also called the regularity criterion) r_j for each column j of Z to determine independent variables to be survived which best estimate the dependent variable y . The regularity criterion can be varied as the user's preference, one of which is very basic form r_j

$$r_j^2 = \frac{\sum_{i=nt+1}^n (y_i - z_{ij})^2}{\sum_{i=nt+1}^n y_i^2} \quad j=1, 2, \dots, m(m-1)/2.$$

Columns of Z are ordered according to increasing r_j . A predetermined number of columns, like m_1 , can be selected or those columns which satisfy $r_j < K$ (K : some prescribed

number chosen in advance as figure A.1.3).

y_1	z_{11}	z_{12}	z_{1a_1}
y_2	z_{21}	z_{22}	z_{2a_1}
.	.	.	.
.	.	.	.
.	.	.	.
y_{nt}	$z_{nt,1}$	$z_{nt,2}$	z_{nt,a_1}
.	.	.	.
.	.	.	.
.	.	.	.
y_n	z_{n1}	z_{n2}	z_{na_1}

Fig. A.1.3 Construction of the new array Z to compute next generation of variables.

Step 3 (test for optimality): From step 2 we find the smallest of the r_j 's and call it RMIN. We then plot it on a graph.

If the value of RMIN is less than the value of RMIN from the previous generation, we go back and repeat steps 1 and 2. If the value of RMIN is greater than the preceding value, we assume that the "RMIN curve" has reached its minimum and stop the process (and use the results from the preceding generation). Once all the quadratic regression coefficients at each generation are scored in the computer, it is fast to compute the prediction \bar{y} of the output y from these quadratics.

APPENDIX 2 - Data for One Dimensional Error Analysis

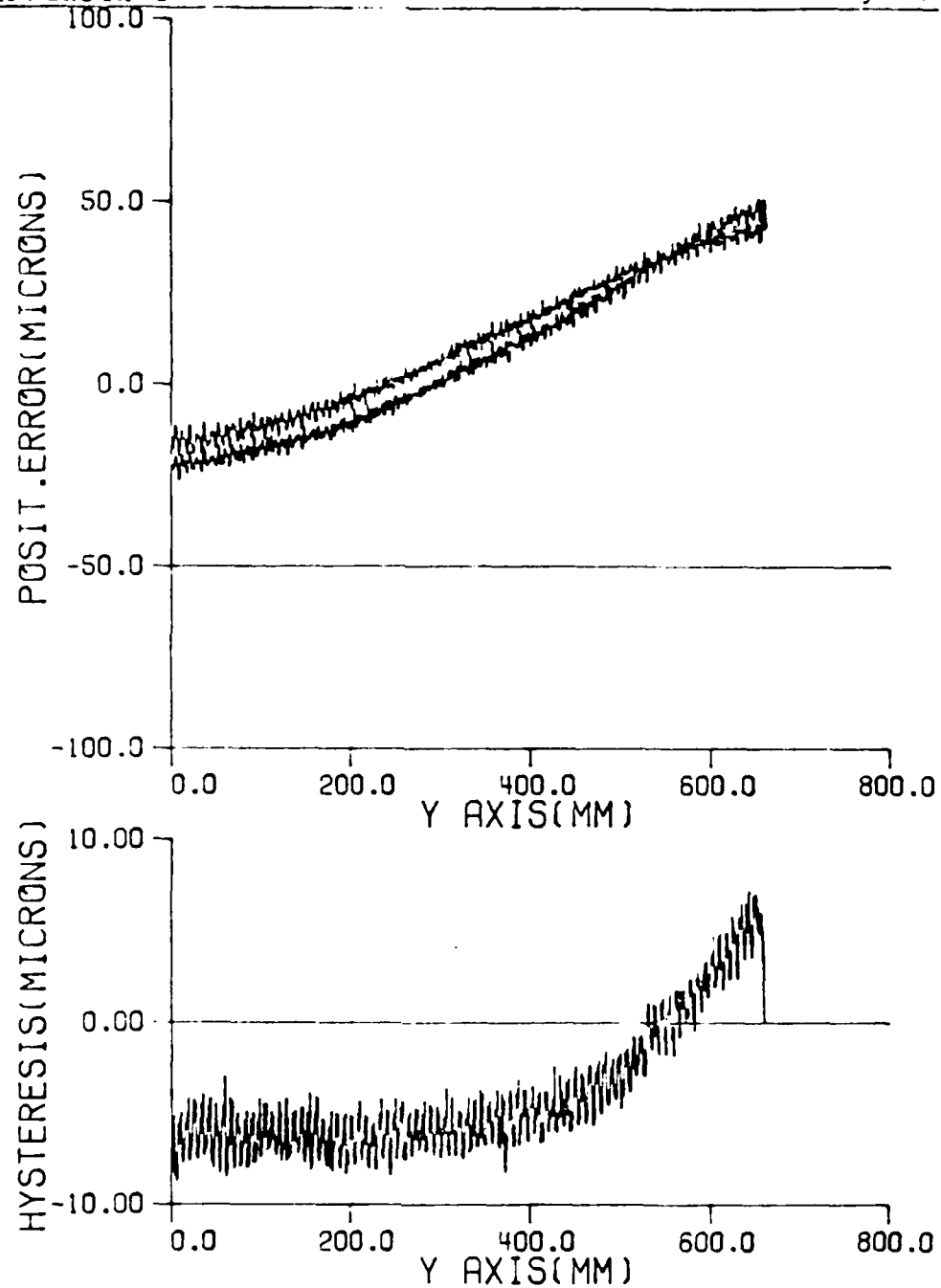


Figure A.2.1 Positioning error and its hysteresis for a whole y axis movement after 360 minutes with 1 mm increment.

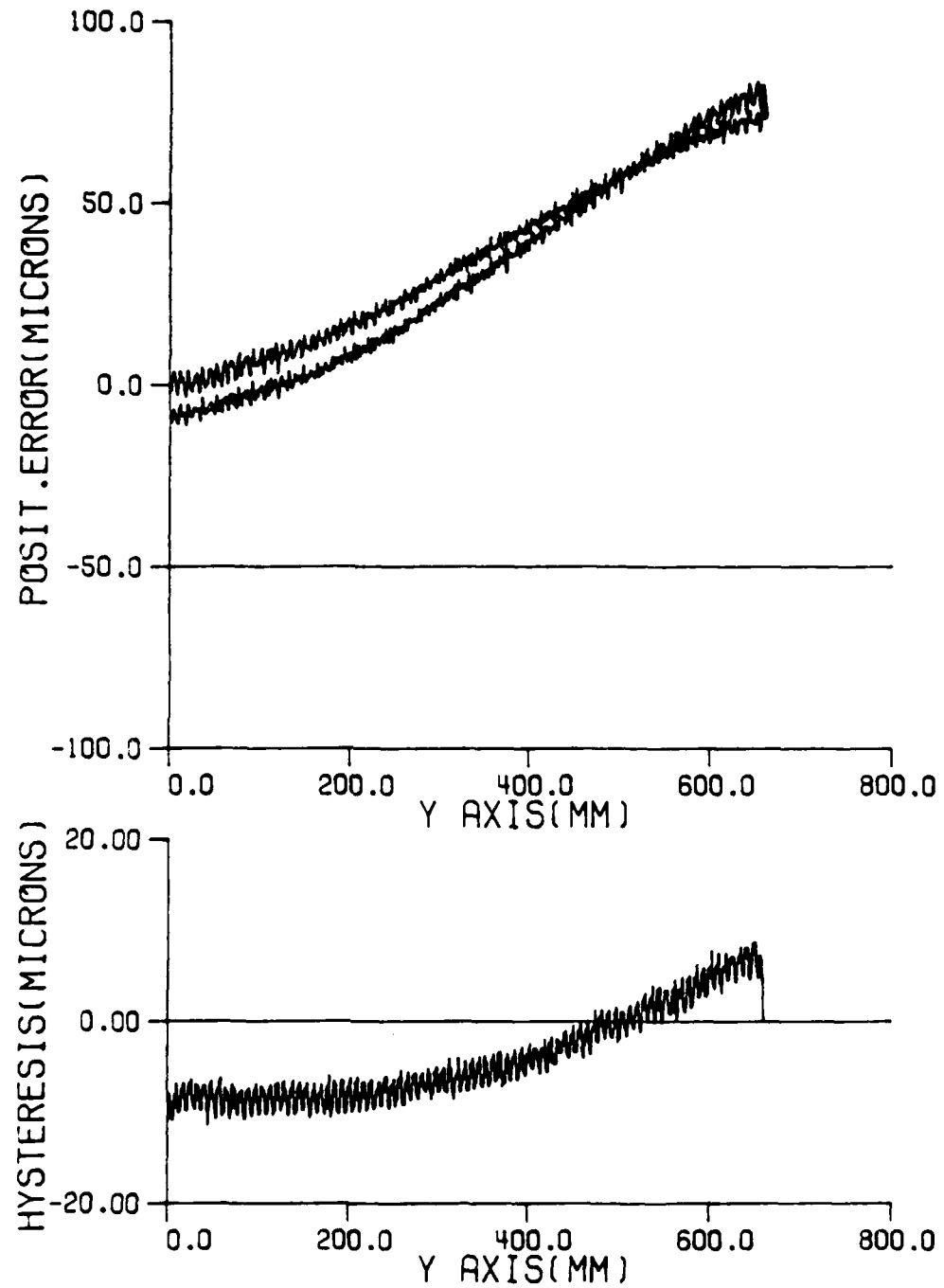


Figure A.2.2 Positioning error and its hysteresis for a whole y axis movement after 490 minutes with 1 mm increment.

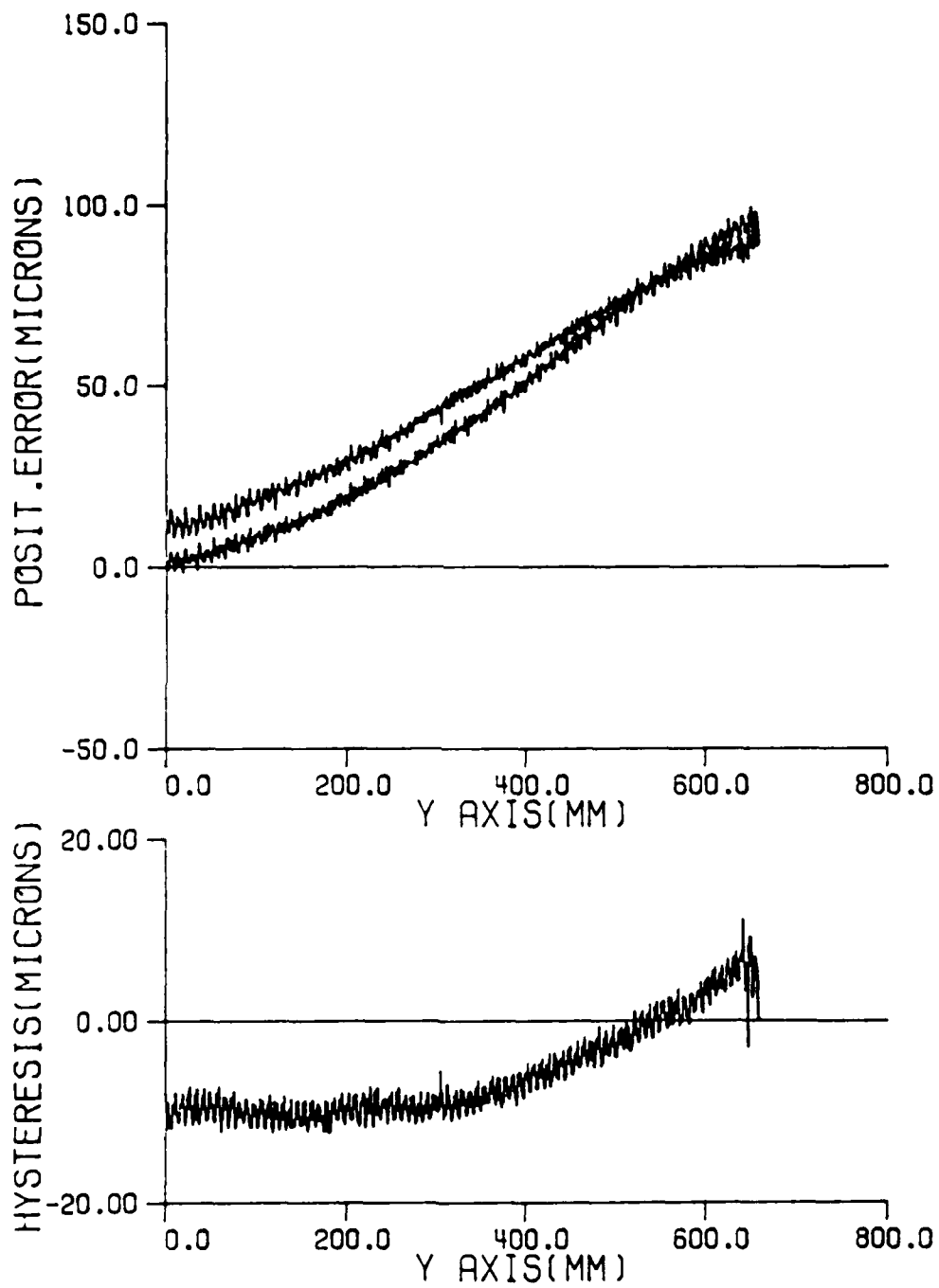


Figure A.2.3 Positioning error and its hysteresis for a whole y axis movement after 610 minutes with 1 mm increment.

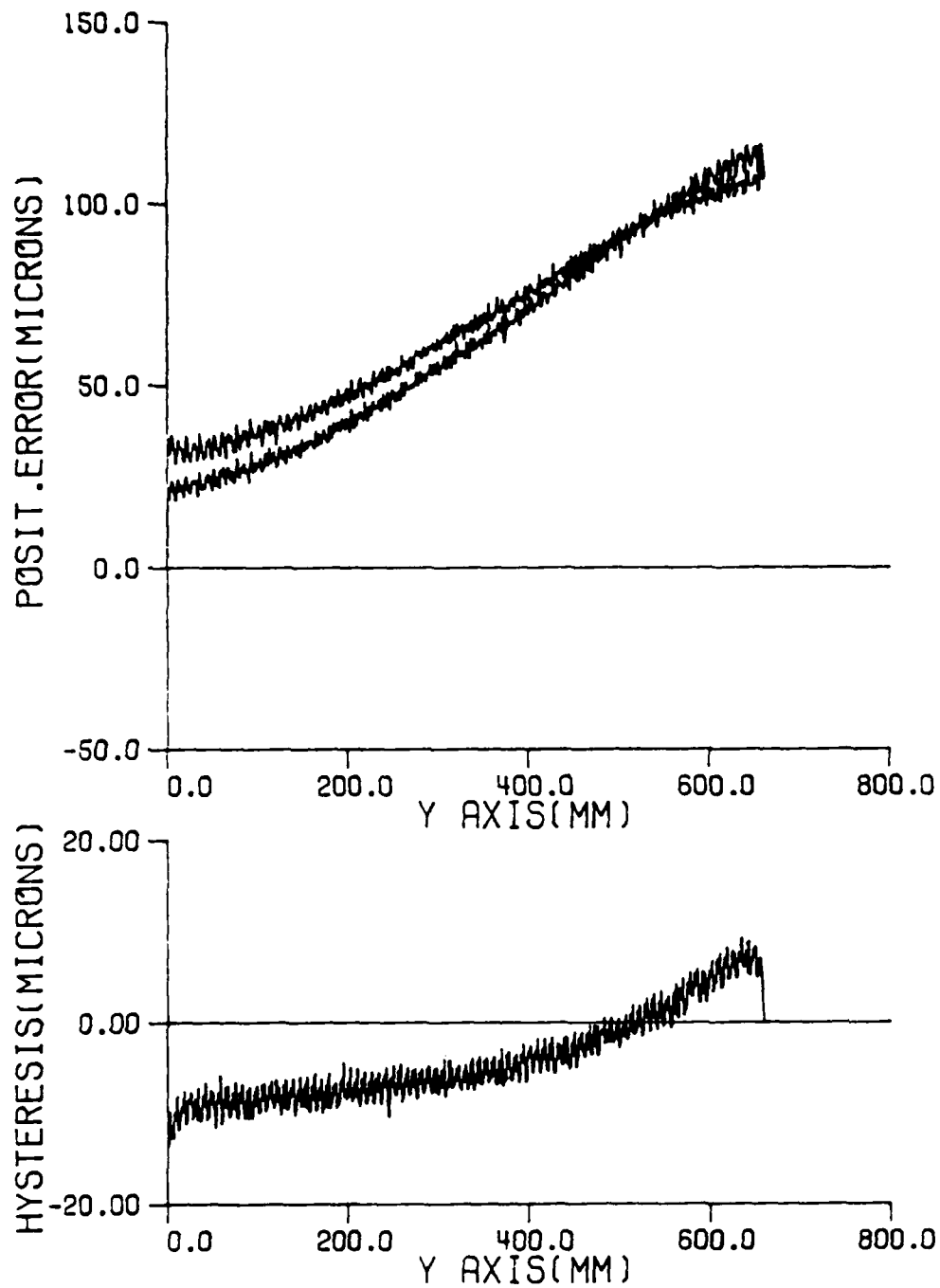


Figure A.2.4 Positioning error and its hysteresis for a whole y axis movement after 740 minutes with 1 mm increment.

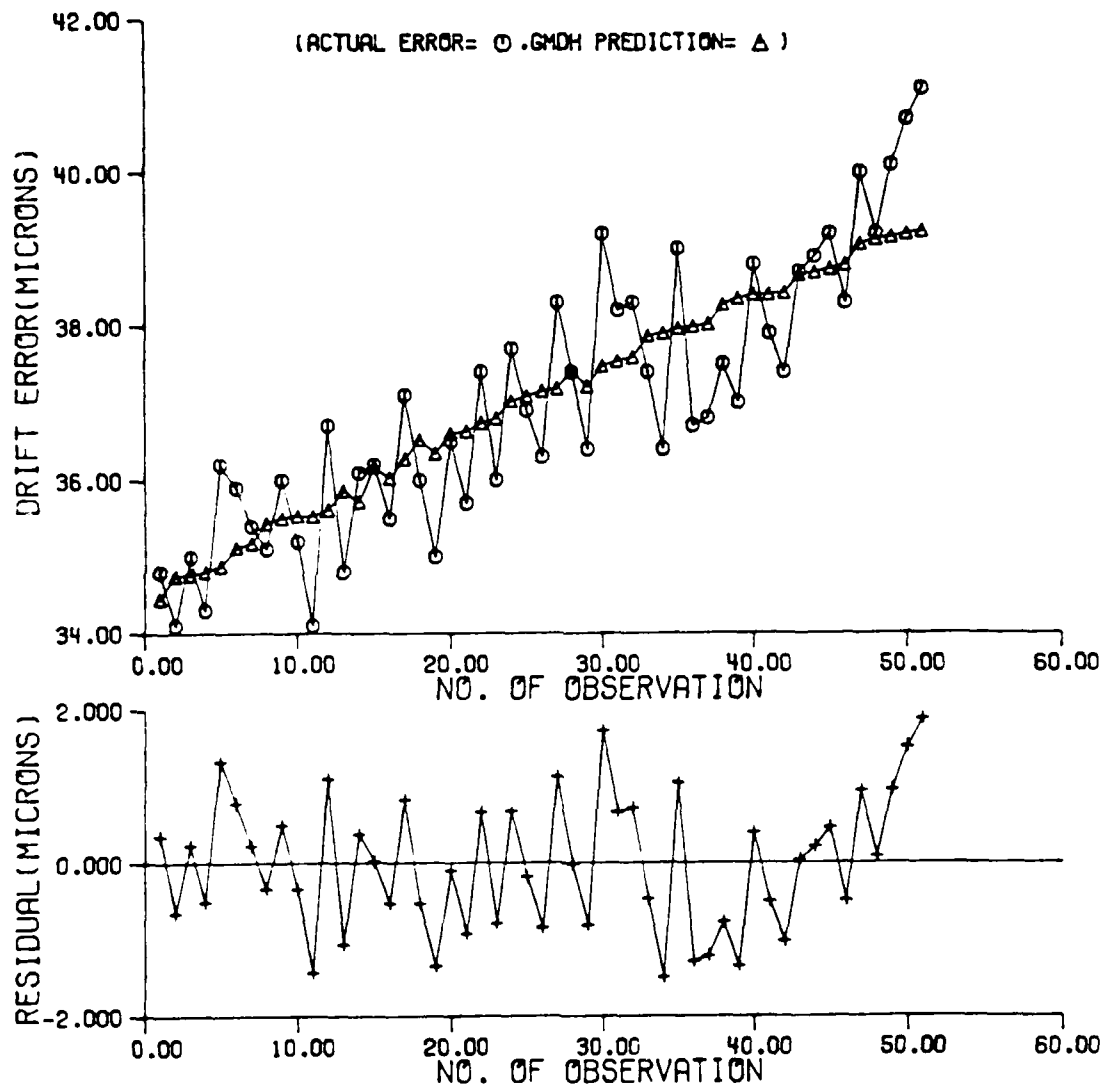


Figure A.2.5 GMDH prediction on the drift error after each trip of 20 mm at 0 mm.

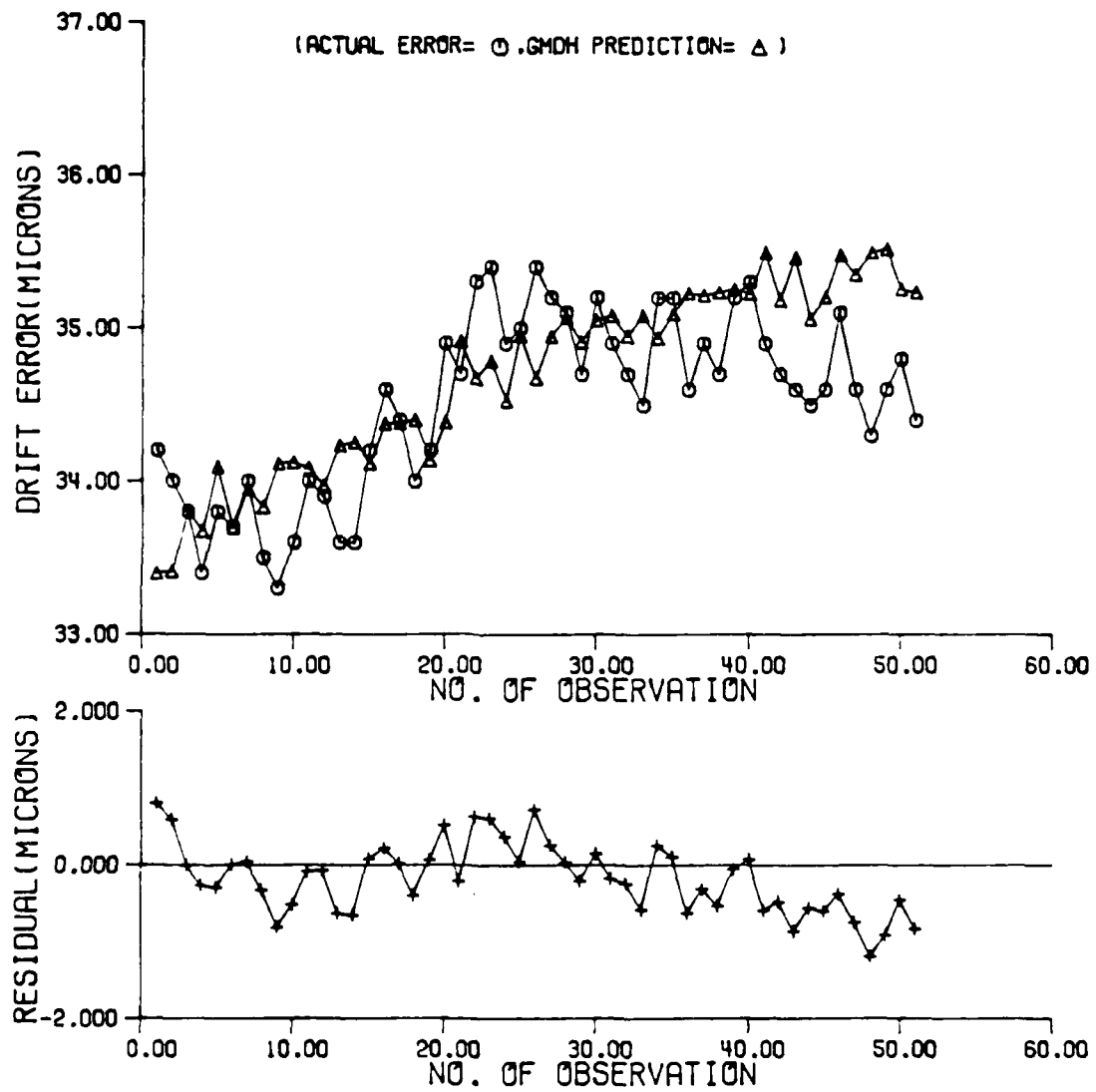


Figure A.2.6 GMDH prediction on the drift error after each trip of 20 mm at 5 mm(down).

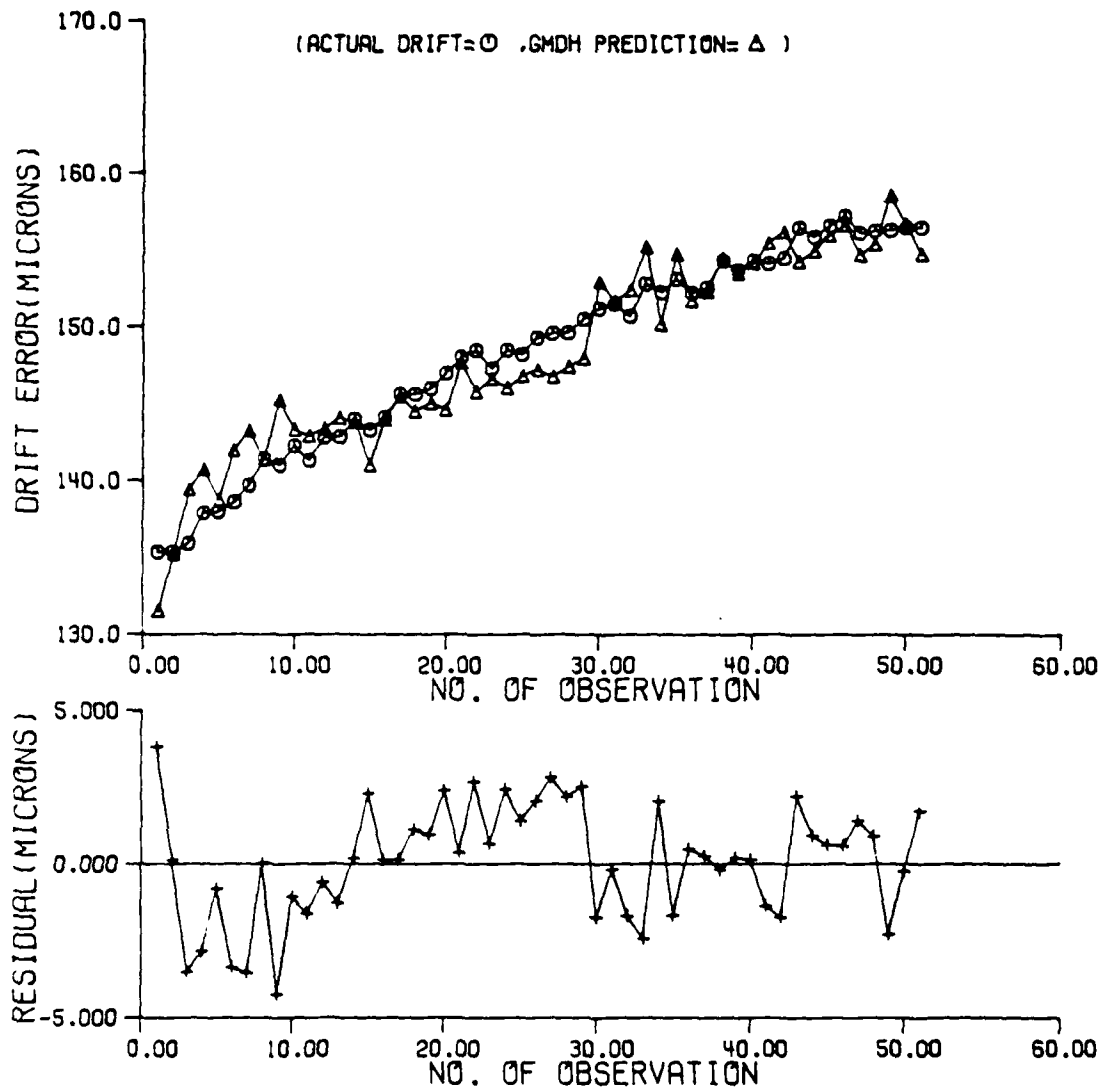


Figure A.2.8 GMDH prediction on the drift error after each trip of 1320 mm at 660 mm.

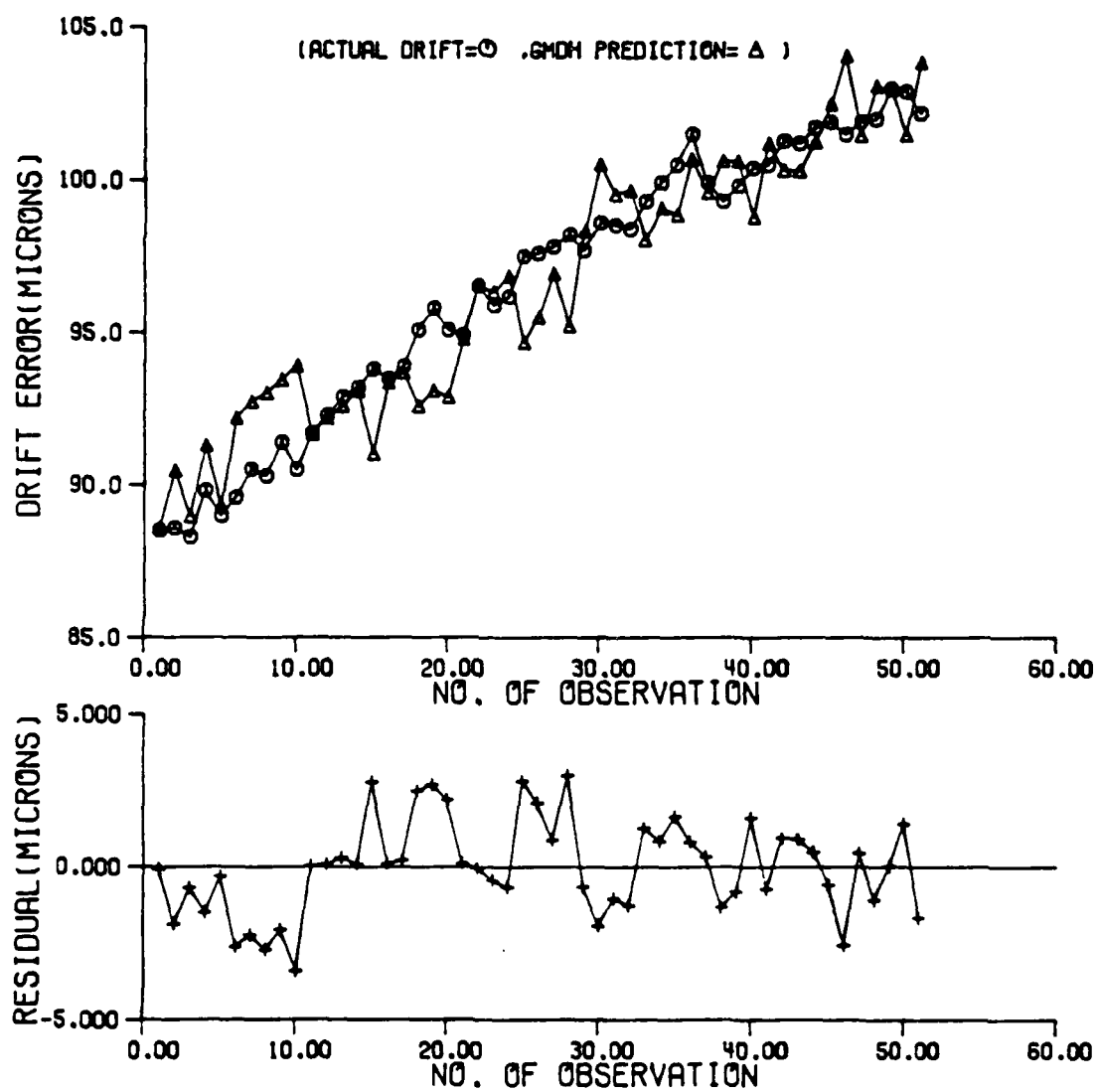


Figure A.2.9 GMDH prediction on the drift error after each trip of 1320 mm at 330 mm.

Table A.2.1 Part of output of 4-way anova analysis program for backlash

```

run name      a four-way anova
variable list  thermal position feed direction backlash
n of cases    240
var labels    thermal      thermal condition of machine/
                position    position of the machine/
                feed        feed rate/
                direction   direction of the movement/
                backlash    backlash at the certain condition/
value labels   thermal      (1) cold (2) warmed-up/
                position    (1) z=750mm (2) z=690mm (3) z=650mm/
                feed        (1) f=500mm:min (2) f=3000mm:min/
                direction   (1) backward (2) forward/
anova         backlash by thermal(1,2) position(1,3) feed(1,2)
                direction(1,2)/

-----
total population
-----
      4.61
(    240)
-----

thermal
      1          2
-----
      5.82      3.39
(    120) (    120)
-----

position
      1          2          3
-----
      4.96      4.10      4.75
(    80) (    80) (    80)
-----

feed
      1          2
-----
      4.44      4.78
(    120) (    120)
-----

directio
      1          2
-----
      4.60      4.61
(    120) (    120)
-----

                position
                        1          2          3
thermal 1 -----
      1          5.66      5.62      6.19

```

Table A.2.1 Continued.

	(40)	(40)	(40)		
2	4.27	2.59	3.31		
	(40)	(40)	(40)		

feed					
	1	2			
thermal	-----				
1	5.64	6.00			
	(60)	(60)			
2	3.23	3.55			
	(60)	(60)			

direction					
	1	2			
thermal	-----				
1	5.81	5.83			
	(60)	(60)			
2	3.39	3.39			
	(60)	(60)			

source of var.	sum of squares	df	mean square	f	signif of f

main effects	393.725	5	78.745	156.257	.001
thermal	354.780	1	354.780	704.007	.001
position	31.992	2	15.996	31.742	.001
feed	6.936	1	6.936	13.763	.001
directio	.017	1	.017	.033	.856

2-way interact.	75.814	9	8.424	16.716	.001
thermal pos.	32.792	2	16.396	32.536	.001
thermal feed	.024	1	.024	.048	.827
thermal dir.	.006	1	.006	.012	.913
position feed	42.777	2	21.389	42.442	.001
position dir.	.110	2	.055	.109	.896
feed dir.	.104	1	.104	.207	.650

3-way interact.	62.304	7	8.901	17.662	.001
thermal pos. feed	61.783	2	30.891	61.299	.001
thermal pos. dir.	.133	2	.067	.132	.876
thermal feed dir.	.253	1	.253	.503	.479
position feed dir.	.134	2	.067	.133	.875

4-way interactions	.217	2	.109	.215	.806
thermal pos. feed	.217	2	.109	.215	.806
direction					

explai ed	532.060	23	23.133	45.904	.001
residual	108.852	216	.504		
total	640.912	239	2.682		

Appendix 3 - Location of Temperature Points

Table A.3.1. Location of temperature points for x axis

Axis	Thermocouple	Placement
	number	point
x	1	Lead screw motor
	2	Lubricant motor
	3	Nut of ball screw
	4	Near ball screw motor
	5 - 11	On guideways
	12 - 14	On side plates
	15	On oil tank

Table A.3.2 Location of temperature points for y axis

Axis	Thermocouple number	Placement point
y	1	Lead screw motor
	2	Near ball screw motor
	3	Nut of ball screw
	4	Spindle motor
	5 - 11	On guideways, spindle side
	12 - 16	On back side
	17	Spindle blower
	18	On the spindle

Table A.3.3 Location of temperature points for z axis

Axis	Thermocouple	Placement
	number	point
z	1	On ball screw motor
	2	Near ball screw motor
	3	Nut of ball screw
	4	B axis motor
	5 - 12	On guideways
	13 - 15	On front plate
	16 - 17	On side plates
	18	On the spindle

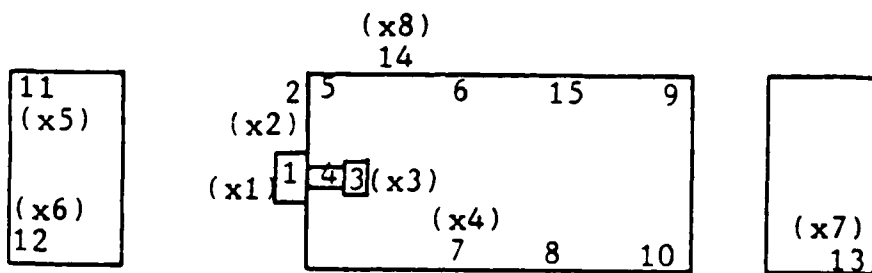


Figure A.3.1 Location of temperature points of x axis

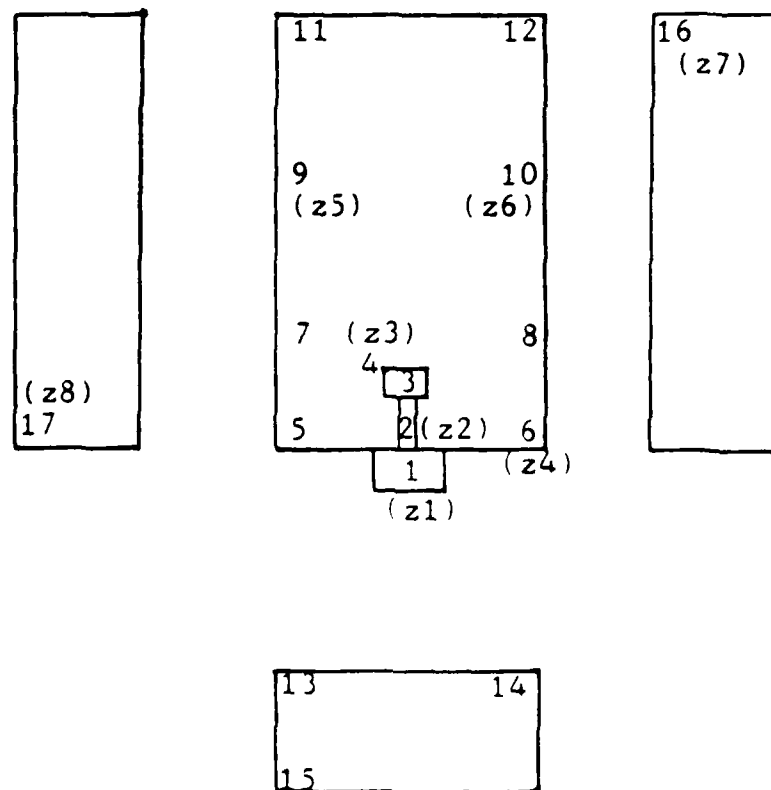


Figure A.3.2 Location of temperature points of y axis

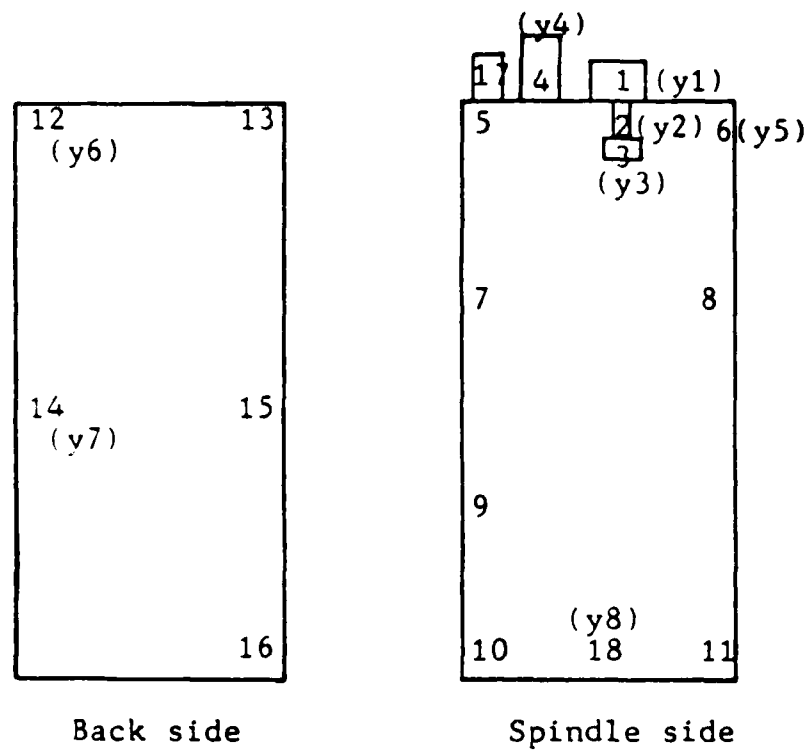
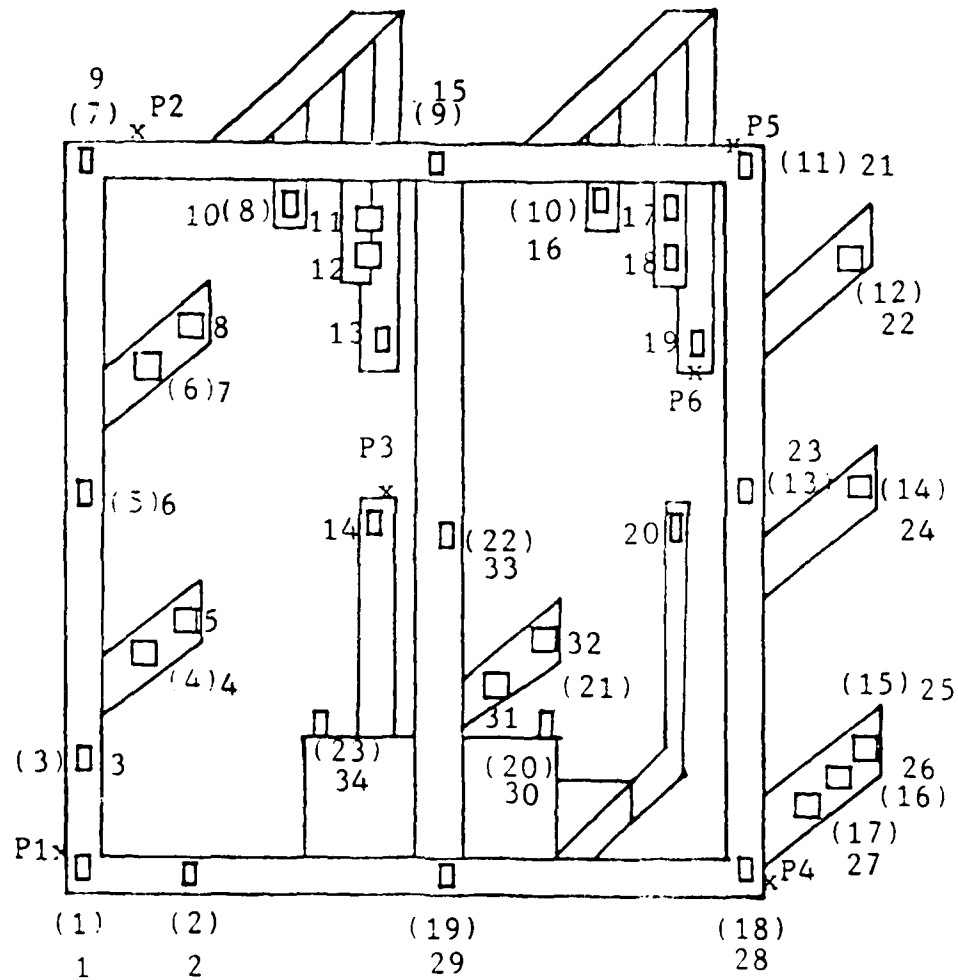


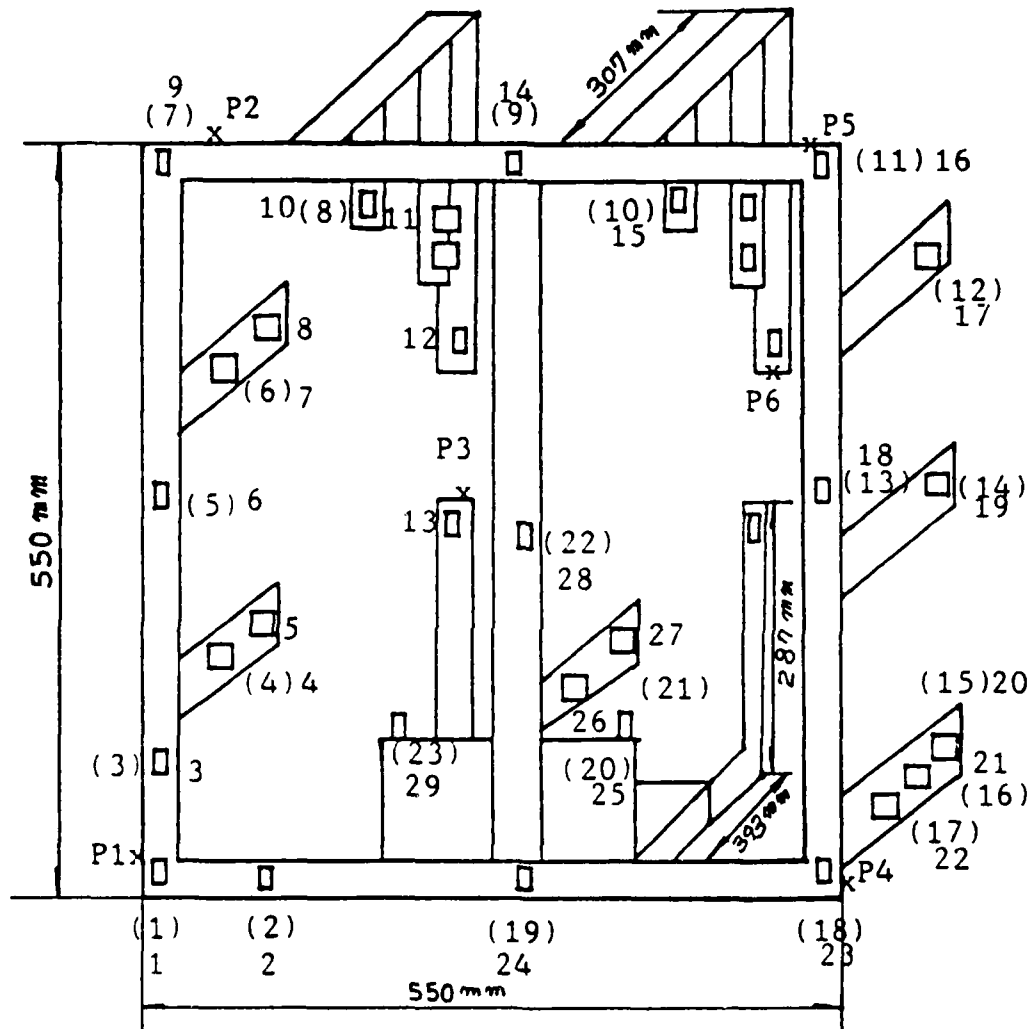
Figure A.3.3 Location of temperature points of z axis

Appendix 4 - Data For Probing Experiment



Number with parenthesis: for a short probe system
 Number without parenthesis: for a long probe system
 (before residual analysis)

Fig. A.4.1 Numbering system for a pallet before residual analysis.



Number with parenthesis: for a short probe system
 Number without parenthesis: for a long probe system
 (after residual analysis)

Figure A.4.2 Numbering system for a pallet after residual analysis.

Table A.4.1 contains all the error data for each experiment, and the temperature information used for chapter 6. Absolute errors for each point are presented for a short probe system and a long probe system with the temperature information. Temperature information is presented for two different thermal conditions-the first when the probing cycle is initiated and the second when the cycle ends. The sequence of each axis temperature reading follows that of figures A.3.1 to A.3.3.

Figures A.4.3 to A.4.8 shows the regression results for test 11 for a short and a long probe system. From figures A.4.9 to A.4.15, the result of regression analysis for the measurement origin is shown for a long probe and two probe approach. Regression prediction and its residual are shown. Residuals are within 5 micron in most cases which means good predictability by regression analysis. Figures A.4.16 to A.4.24 show the regression prediction and the residual after prediction for the point number 11. These graphic representation of the regression result give better idea on the capability of the regression analysis.

Table A.4.1 Error data for three dimensional probing experiments with temperature information.
(error in micron)

Coordinates used for probing experiments

a short probe system				a long probe system		
number	x	y	z	x	y	z
1	59.668	18.541	498.894	59.602	18.465	649.151
2	131.238	18.586	498.805	131.170	18.513	649.054
3	61.043	72.892	499.023	60.977	72.821	649.270
4	98.218	179.130	415.178	98.137	179.043	565.425
5	59.275	291.393	499.049	97.972	203.265	511.854
6	97.875	439.022	421.703	59.204	291.317	649.301
7	60.207	553.175	498.447	97.802	438.946	571.958
8	202.894	480.717	331.396	97.921	483.567	512.712
9	331.144	552.032	498.119	60.123	553.091	648.686
10	407.684	481.646	332.732	202.828	480.641	481.645
11	604.234	551.163	497.583	216.392	423.094	347.782
12	630.902	542.677	415.691	200.814	317.387	342.336
13	604.112	281.357	497.868	201.500	287.448	256.136
14	630.937	315.411	400.891	331.068	551.959	648.371
15	631.039	77.504	397.761	407.618	481.570	482.979
16	631.054	66.191	430.238	604.156	551.100	647.825
17	631.072	51.799	462.120	630.821	542.601	565.938
18	601.707	17.796	497.972	604.034	281.291	648.122
19	331.979	18.774	498.744	630.871	315.345	551.132
20	452.632	215.061	452.623	630.968	77.441	548.008
21	363.033	236.838	424.850	630.986	66.130	580.487
22	329.472	278.314	498.609	630.996	51.728	612.372
23	212.678	215.012	458.937	601.638	17.733	648.224
24				331.908	18.706	648.993
25				452.561	214.987	602.877
26				362.955	236.765	575.092
27				362.480	270.661	533.535
28				329.386	278.241	648.866
29				212.610	214.939	609.184

TEST # = 2

A short probe system				A long probe system		
number	x	y	z	x	y	z
1	-16.000	-2.000	20.000	17.000	11.000	28.000
2	-8.000	-8.000	25.000	26.000	13.000	18.000
3	-12.000	0.	22.000	21.000	18.000	30.000
4	-5.000	-5.000	18.000	8.000	5.000	17.900
5	-5.000	3.000	15.000	18.000	18.000	21.000
6	-15.000	5.000	10.000	13.000	18.000	16.000
7	-10.000	5.000	20.000	18.000	22.000	11.000
8	-15.000	0.	15.000	13.000	18.000	30.000
9	-20.000	7.000	12.000	0.	27.000	10.000
10	-13.000	0.	5.000	15.000	18.000	10.000
11	-23.000	-8.000	10.000	11.000	38.000	38.000
12	-23.000	0.	2.000	5.000	18.000	0.
13	-13.000	0.	8.000	-7.000	10.000	5.000
14	-28.000	-5.000	16.000	3.000	33.000	20.000
15	-25.000	-3.000	15.000	10.000	23.000	15.000
16	-8.000	-13.000	13.000	16.000	33.000	5.000
17	-15.000	7.000	10.000	-7.000	2.000	3.000
18	-15.000	-11.000	10.000	13.000	0.	15.000
19	2.000	-13.000	15.000	2.000	13.000	13.000
20	-12.000	-5.000	10.000	13.000	5.000	10.000
21	-10.000	-6.000	12.000	13.000	0.	13.000
22	-16.000	-3.000	7.000	5.000	7.000	13.000
23	-3.000	-8.000	18.000	10.000	15.000	18.000
24				23.000	5.000	12.000
25				5.000	3.000	13.000
26				3.000	5.000	10.000
27				8.000	5.000	15.000
28				0.	11.000	18.000
29				21.000	8.000	18.000
TEMPX	23.10	30.88	21.43	21.13	20.91	20.86
TEMPX	20.11	20.51	20.16	20.44	20.31	22.42
TEMPX	20.41	20.66	35.65			
TEMPY	24.42	23.95	22.60	22.77	22.03	22.28
TEMPY	21.04	20.79	20.65	20.32	20.25	25.60
TEMPY	22.16	21.54	21.12	20.77	35.10	20.96
TEMPZ	23.48	21.28*****		20.51	20.07	20.34
TEMPZ	19.85	19.89	19.97	20.29	19.94	20.09
TEMPZ	19.99	20.36	20.19	20.47	19.95	
TEMPX	23.40	30.98	21.33	21.13	21.10	20.96
TEMPX	20.16	20.61	20.21	20.56	20.36	22.59
TEMPX	20.54	20.79	36.20			
TEMPY	24.81	24.34	22.70	23.02	22.28	22.55
TEMPY	21.26	21.02	20.82	20.45	20.32	25.67
TEMPY	22.43	21.69	21.34	20.92	35.17	21.18
TEMPZ	23.83	21.51*****		20.72	20.18	20.52
TEMPZ	19.93	19.95	20.03	20.40	20.05	20.18
TEMPZ	20.15	20.57	20.33	20.57	20.05	

TEST # = 3

A short probe system				A long probe system		
number	x	y	z	x	y	z
1	-16.000	-5.000	20.000	7.000	0.	28.000
2	-10.000	-8.000	23.000	13.000	0.	20.000
3	-17.000	-2.000	22.000	18.000	18.000	18.000
4	-8.000	-12.000	15.000	13.000	-3.000	21.000
5	-5.000	-10.000	8.000	18.000	8.000	18.000
6	-20.000	2.000	5.000	23.000	3.000	18.000
7	-10.000	0.	5.000	6.000	17.000	13.000
8	-23.000	0.	5.000	38.000	11.000	0.
9	-22.000	-8.000	0.	7.000	12.000	0.
10	-25.000	-5.000	-10.000	3.000	21.000	0.
11	-36.000	-11.000	-3.000	5.000	30.000	0.
12	-33.000	-3.000	-10.000	5.000	20.000	-31.000
13	-28.000	-3.000	-5.000	18.000	13.000	-8.000
14	-46.000	-5.000	3.000	-2.000	21.000	0.
15	-28.000	-10.000	5.000	8.000	7.000	-5.000
16	-23.000	-15.000	13.000	-5.000	8.100	-25.000
17	-15.000	-8.000	5.000	-22.000	5.000	-7.000
18	-18.000	-11.000	8.000	-10.000	7.000	-3.000
19	-8.000	-21.000	8.000	-16.000	8.000	0.
20	-23.000	-15.000	5.000	3.000	5.000	5.000
21	-18.000	-8.000	0.	0.	0.	8.000
22	-10.000	-8.000	0.	-2.000	0.	13.000
23	-10.000	-15.000	10.000	-6.000	5.000	16.000
24				12.000	5.000	15.000
25				8.000	-8.000	10.000
26				-7.000	5.000	-2.000
27				3.000	0.	8.000
28				0.	-5.000	12.000
29				28.000	0.	8.000
TEMPX	25.86	32.34	22.49	22.86	22.49	21.75
TEMPX	20.76	21.56	20.81	21.48	21.03	23.63
TEMPX	21.38	21.63	38.07			
TEMPY	28.37	27.54	24.70	24.85	24.18	24.26
TEMPY	23.47	22.68	22.29	21.50	21.27	28.01
TEMPY	24.58	23.59	23.00	22.07	36.84	22.54
TEMPZ	26.43	23.36*****		21.97	21.09	21.78
TEMPZ	20.74	20.86	21.16	21.19	20.92	20.97
TEMPZ	21.14	21.85	21.21	21.36	20.82	
TEMPX	26.14	32.57	22.38	22.82	22.53	22.16
TEMPX	20.90	21.57	20.85	21.59	21.12	23.81
TEMPX	21.52	21.76	38.35			
TEMPY	28.62	27.96	24.81	25.08	24.61	24.71
TEMPY	23.33	22.91	22.57	21.78	21.38	28.14
TEMPY	24.79	23.83	23.16	22.20	37.02	22.78
TEMPZ	26.71	23.52*****		22.17	21.20	21.97
TEMPZ	20.81	20.98	20.93	21.30	20.95	21.11
TEMPZ	21.31	22.05	21.35	21.48	20.94	

TEST # = 4

A short probe system				A long probe system		
number	x	y	z	x	y	z
1	-11.000	-15.000	8.000	17.000	5.000	18.000
2	-8.000	-13.000	8.000	13.000	5.000	2.000
3	-12.000	-15.000	2.000	21.000	8.000	2.000
4	-3.000	-15.000	5.000	13.000	-11.000	3.000
5	-10.000	-15.000	-8.000	28.000	5.000	-5.000
6	-13.000	-8.000	-11.000	23.000	-2.000	-5.000
7	-7.000	-13.000	-8.000	28.000	2.000	0.
8	-18.000	-2.000	-15.000	23.000	5.000	-10.000
9	-35.000	-5.000	-15.000	15.000	5.000	-23.000
10	-36.000	-8.000	-23.000	13.000	26.000	-16.000
11	-48.000	-11.000	-18.000	18.000	18.000	-10.000
12	-48.000	-5.000	-26.000	36.000	13.000	-3.000
13	-33.000	-8.000	-15.000	8.000	-5.000	12.000
14	-43.000	-7.000	-12.000	0.	0.	-5.000
15	-33.000	-10.000	-3.000	0.	2.000	-25.000
16	-28.000	-20.000	-5.000	-20.000	8.100	-23.000
17	-22.900	2.000	-7.000	-25.000	2.000	-25.000
18	-33.000	-11.000	3.000	-12.000	2.000	-10.000
19	-13.000	-21.000	0.	-13.000	8.000	-23.000
20	-25.000	-15.000	-7.000	-18.000	10.000	-13.000
21	-26.000	-11.000	-11.000	-7.000	-5.000	-8.000
22	-21.000	-5.000	-13.000	-13.000	0.	-5.000
23	-15.000	-21.000	-8.000	17.000	-3.000	0.
24				23.000	-10.000	2.000
25				23.000	-10.000	-10.000
26				-5.000	-2.000	-15.000
27				3.000	-5.000	-3.000
28				-8.000	3.000	-8.000
29				28.000	5.000	-7.000
TEMPX	28.10	34.02	23.59	24.33	24.01	23.00
TEMPX	21.69	22.78	21.77	22.80	22.06	24.85
TEMPX	22.48	22.83	39.85			
TEMPY	31.79	30.55	26.65	27.29	26.68	26.60
TEMPY	25.82	24.74	24.27	23.02	22.60	30.21
TEMPY	27.00	25.92	25.06	23.54	38.96	24.43
TEMPZ	28.98	25.16*****		23.52	22.26	23.25
TEMPZ	21.64	21.92	22.34	22.24	21.97	22.07
TEMPZ	22.41	23.45	22.36	22.49	21.82	
TEMPX	28.11	34.34	23.48	24.36	23.99	23.50
TEMPX	21.87	22.81	21.80	22.91	22.15	25.03
TEMPX	22.62	22.99	39.96			
TEMPY	31.34	30.78	26.74	27.30	27.15	26.88
TEMPY	25.68	25.05	24.65	23.47	22.73	30.06
TEMPY	27.30	26.13	25.19	23.74	39.17	24.71
TEMPZ	28.86	25.32*****		23.72	22.41	23.45
TEMPZ	21.75	22.04	21.97	22.39	22.04	22.32
TEMPZ	22.56	23.63	22.49	22.61	21.92	

TEST # = 5

A short probe system				A long probe system		
number	x	y	z	x	y	z
1	-21.000	-10.000	3.000	10.000	3.000	5.000
2	-5.000	-6.000	2.000	16.000	10.000	0.
3	-20.000	-5.000	7.000	23.000	5.000	-5.000
4	-15.000	0.	0.	13.000	0.	-10.000
5	-10.000	0.	-10.000	8.000	0.	-5.000
6	-10.000	0.	-16.000	36.000	8.000	-2.000
7	-13.000	5.000	-8.000	26.000	7.000	-15.000
8	-23.000	11.000	-15.000	23.000	13.000	-20.000
9	-33.000	7.000	-13.000	0.	7.000	-25.000
10	-43.000	5.000	-21.000	33.000	13.000	-26.000
11	-46.000	-6.000	-21.000	8.000	23.000	-13.000
12	-48.000	5.000	-31.000	3.000	23.000	-39.000
13	-43.000	5.000	-18.000	5.000	0.	2.000
14	-54.000	-2.000	-20.000	-7.000	16.000	-20.000
15	-46.000	-8.000	-10.000	-3.000	10.000	-28.000
16	-33.000	-10.000	-10.000	-22.000	10.000	-38.000
17	-30.000	0.	-15.000	-25.000	7.000	-25.000
18	-33.000	-11.000	-2.000	-20.000	2.000	-18.000
19	-15.000	-16.000	-13.000	-22.900	13.000	-31.000
20	-28.000	-2.000	-12.000	-18.000	10.000	-23.000
21	-28.000	2.000	-13.000	-5.000	0.	-18.000
22	-21.000	2.000	-18.000	10.000	10.000	-20.000
23	-15.000	-3.000	-8.000	-6.000	7.000	-10.000
24				10.000	5.000	-18.000
25				3.000	3.000	-23.000
26				0.	13.000	-30.000
27				-10.000	7.000	-20.000
28				0.	8.000	-13.000
29				18.000	0.	-15.000
TEMPX	29.77	35.60	24.88	25.94	25.20	24.66
TEMPX	22.82	23.90	22.69	24.02	23.11	25.99
TEMPX	23.58	23.97	41.13			
TEMPY	33.03	32.41	28.67	28.52	28.62	28.18
TEMPY	27.59	26.62	26.30	24.78	23.94	31.97
TEMPY	29.03	27.82	26.71	24.98	40.31	26.23
TEMPZ	30.72	26.58	27.32	24.82	23.46	24.62
TEMPZ	22.87	23.12	22.85	23.32	22.97	23.39
TEMPZ	23.59	24.72	23.32	23.52	22.75	
TEMPX	29.84	35.62	24.78	25.84	25.47	24.85
TEMPX	22.98	24.07	22.89	24.22	23.23	26.13
TEMPX	23.73	24.12	41.08			
TEMPY	32.97	32.65	28.74	28.62	28.94	28.60
TEMPY	27.55	26.91	26.57	25.05	24.14	31.88
TEMPY	29.23	27.97	26.96	25.18	40.36	26.70
TEMPZ	30.77	26.67*****		25.10	23.60	24.71
TEMPZ	22.86	23.21	22.96	23.53	23.14	23.63
TEMPZ	23.75	24.91	23.55	23.68	22.91	

TEST # = 6

A short probe system				A long probe system		
number	x	y	z	x	y	z
1	-13.000	-5.000	5.000	-21.000	-2.000	13.000
2	-18.000	-3.000	10.000	-27.000	10.000	7.000
3	-22.000	-2.000	7.000	-17.000	11.000	-3.000
4	-13.000	0.	5.000	-30.000	20.000	0.
5	-20.000	8.000	-5.000	-25.000	23.000	3.000
6	-15.000	15.000	-5.000	-20.000	13.000	-5.000
7	-10.000	20.000	-2.000	-25.000	22.000	-17.000
8	-23.000	21.000	-21.000	-8.000	36.000	-8.000
9	-38.000	25.000	-5.000	-23.000	30.000	-13.000
10	-41.000	25.000	-18.000	-13.000	54.000	-21.000
11	-46.000	22.000	-18.000	-38.000	58.000	-5.000
12	-48.000	25.000	-18.000	-23.000	41.000	-6.000
13	-38.000	15.000	-20.000	-22.000	18.000	5.000
14	-54.000	10.000	-12.000	-50.000	38.000	-10.000
15	-43.000	2.000	-16.000	-23.000	30.000	-23.000
16	-36.000	-8.000	-20.000	-58.000	38.000	-23.000
17	-41.000	5.000	-7.000	-76.000	30.000	-28.000
18	-41.000	2.000	-2.000	-38.000	18.000	-13.000
19	-21.000	2.000	-5.000	-59.000	23.000	-28.000
20	-30.000	6.000	-12.000	-61.000	8.000	-18.000
21	-33.000	10.000	-11.000	-30.000	15.000	-13.000
22	-23.000	18.000	-8.000	-58.000	15.000	-17.000
23	-13.000	2.000	-5.000	-36.000	15.000	-7.000
24				-33.000	18.000	-8.000
25				-33.000	5.000	-13.000
26				-45.000	15.000	-22.900
27				-15.000	25.000	-8.000
28				-38.000	23.000	-8.000
29				-10.000	16.000	-13.000
TEMPX	31.06	36.54	26.24	27.29	26.56	25.62
TEMPX	23.98	25.33	23.91	25.28	24.18	26.92
TEMPX	24.59	24.91	41.94			
TEMPY	34.01	33.84	30.42	29.40	29.91	29.57
TEMPY	29.09	28.26	27.72	26.01	25.32	33.35
TEMPY	30.25	28.91	28.28	26.37	41.15	28.05
TEMPZ	31.47	27.57*****		25.74	24.48	25.79
TEMPZ	23.94	24.29	24.12	24.34	24.07	24.29
TEMPZ	24.46	25.69	24.19	24.36	23.65	
TEMPX	31.14	36.64	26.09	27.12	26.55	26.06
TEMPX	24.20	25.40	24.03	25.43	24.30	27.07
TEMPX	24.79	25.04	42.08			
TEMPY	33.84	34.00	30.45	29.52	30.20	29.94
TEMPY	29.01	28.57	27.89	26.25	25.49	33.07
TEMPY	30.35	29.01	28.35	26.52	41.38	28.29
TEMPZ	31.53	27.67*****		25.88	24.58	25.86
TEMPZ	23.94	24.36	23.99	24.55	24.19	24.46
TEMPZ	24.58	25.83	24.33	24.48	23.79	

TEST # = 7

A short probe system				A long probe system		
number	x	y	z	x	y	z
1	-28.000	3.000	10.000	2.000	18.000	18.000
2	-20.000	10.000	13.000	6.000	28.000	7.000
3	-20.000	11.000	12.000	31.000	33.000	8.000
4	-23.000	13.000	5.000	33.000	17.000	3.000
5	-23.000	23.000	3.000	13.000	33.000	6.000
6	-20.000	25.000	-3.000	28.000	36.000	3.000
7	-15.000	40.000	8.000	8.000	40.000	0.
8	-25.000	36.000	-8.000	25.000	56.000	-10.000
9	-35.000	43.000	7.000	0.	58.000	-8.000
10	-36.000	33.000	-8.000	28.000	59.000	-18.000
11	-43.000	38.000	-8.000	8.000	73.000	-5.000
12	-48.000	38.000	-13.000	8.000	74.000	10.000
13	-38.000	25.000	-10.000	16.000	25.000	0.
14	-49.000	26.000	-7.000	13.000	64.000	-5.000
15	-38.000	15.000	-5.000	18.000	61.000	-13.000
16	-33.000	13.000	-12.000	3.000	61.000	3.000
17	-38.000	17.000	-13.000	-27.000	43.000	-15.000
18	-30.000	15.000	-8.000	-5.000	40.000	-15.000
19	-13.000	-3.000	-3.000	-18.000	31.000	-20.000
20	-30.000	16.000	-7.000	-28.000	23.000	-8.000
21	-31.000	27.000	-5.000	-7.000	28.000	-15.000
22	-26.000	28.000	-11.000	-15.000	22.000	-12.000
23	-18.000	18.000	2.000	5.000	33.000	-7.000
24				25.000	18.000	0.
25				0.	36.000	-3.000
26				-7.000	28.000	-17.900
27				3.000	28.000	-10.000
28				-15.000	41.000	-8.000
29				28.000	31.000	-5.000
TEMPX	31.99	37.39	27.27	28.34	27.47	26.71
TEMPX	24.99	26.34	24.89	26.27	25.09	27.69
TEMPX	25.39	25.65	42.75			
TEMPY	34.58	35.02	31.73	30.08	30.79	30.62
TEMPY	29.91	29.50	28.62	26.96	26.47	34.35
TEMPY	30.86	29.48	29.28	27.36	42.00	29.15
TEMPZ	32.11	28.39*****		26.39	25.26	26.68
TEMPZ	24.87	25.26	24.84	25.16	24.94	25.01
TEMPZ	25.14	26.41	24.84	24.99	24.38	
TEMPX	32.08	37.40	27.11	28.09	27.48	27.04
TEMPX	25.15	26.43	25.00	26.38	25.20	27.77
TEMPX	25.50	25.77	42.74			
TEMPY	34.58	35.08	31.72	30.10	30.97	30.90
TEMPY	29.93	29.76	28.73	27.07	26.56	34.14
TEMPY	30.97	29.56	29.30	27.47	42.06	29.36
TEMPZ	32.29	28.50*****		26.57	25.34	26.69
TEMPZ	24.80	25.27	24.83	25.34	25.02	25.15
TEMPZ	25.22	26.52	24.93	25.07	24.46	

TEST # = 8

A short probe system				A long probe system		
number	x	y	z	x	y	z
1	-11.000	21.000	10.000	7.000	26.000	18.000
2	-15.000	15.000	15.000	8.000	28.000	7.000
3	-10.000	16.000	12.000	11.000	51.000	8.000
4	-10.000	21.000	8.000	10.000	27.000	9.900
5	-15.000	31.000	8.000	33.000	41.000	11.000
6	-18.000	38.000	2.000	18.000	49.000	6.000
7	-18.000	46.000	13.000	18.000	63.000	11.000
8	-23.000	56.000	2.000	10.000	72.000	-5.000
9	-33.000	53.000	15.000	2.000	63.000	0.
10	-33.000	51.000	0.	8.000	79.000	-8.000
11	-38.000	58.000	5.000	13.000	84.000	-15.000
12	-30.000	53.000	-5.000	3.000	71.000	-6.000
13	-31.000	33.000	-7.000	23.000	51.000	7.000
14	-46.000	33.000	-5.000	-5.000	77.000	13.000
15	-33.000	23.000	-8.000	5.000	71.000	-10.000
16	-23.000	15.000	-7.000	-10.000	71.000	-5.000
17	-22.900	25.000	-5.000	-25.000	71.000	-5.000
18	-28.000	15.000	-2.000	-12.000	48.000	-10.000
19	-13.000	15.000	2.000	-18.000	56.000	-13.000
20	-25.000	31.000	-2.000	-13.000	31.000	-13.000
21	-31.000	35.000	0.	3.000	28.000	-13.000
22	-21.000	41.000	-8.000	0.	43.000	-15.000
23	-18.000	23.000	-3.000	-3.000	35.000	-7.000
24				28.000	36.000	-3.000
25				3.000	38.000	-8.000
26				8.000	41.000	-8.000
27				3.000	45.000	-13.000
28				23.000	61.000	0.
29				36.000	43.000	-5.000
TEMPX	32.19	37.85	28.23	29.09	28.33	27.72
TEMPX	26.06	27.45	25.96	27.28	26.03	28.23
TEMPX	26.06	26.35	43.28			
TEMPY	34.81	35.53	32.80	30.16	31.33	31.40
TEMPY	30.74	30.57	29.53	27.85	27.55	34.93
TEMPY	31.28	30.04	30.06	28.31	42.32	30.47
TEMPZ	32.59	28.90*****		27.07	25.99	27.46
TEMPZ	25.70	26.19	25.82	26.02	25.82	25.87
TEMPZ	25.70	27.00	25.38	25.60	25.04	
TEMPX	32.18	37.86	28.07	28.83	28.29	27.97
TEMPX	26.19	27.49	26.04	27.31	26.09	28.31
TEMPX	26.16	26.41	43.22			
TEMPY	34.69	35.63	32.76	30.22	31.53	31.62
TEMPY	30.68	30.82	29.66	28.00	27.63	34.57
TEMPY	31.33	30.12	30.10	28.41	42.27	30.58
TEMPZ	32.59	28.85*****		27.14	26.02	27.49
TEMPZ	25.70	26.22	25.70	26.12	25.85	25.95
TEMPZ	25.75	27.02	25.41	25.68	25.11	

TEST # = 9

A short probe system				A long probe system		
number	x	y	z	x	y	z
1	-26.000	26.000	20.000	-13.000	31.000	28.000
2	-20.000	28.000	25.000	-7.000	28.000	25.000
3	-25.000	33.000	22.000	-33.000	44.000	28.000
4	-18.000	31.000	23.000	-18.000	27.000	30.900
5	-20.000	49.000	20.000	-15.000	51.000	21.000
6	-23.000	53.000	12.000	-35.000	56.000	23.000
7	-20.000	61.000	36.000	-15.000	76.000	28.000
8	-28.000	77.000	13.000	-10.000	77.000	25.000
9	-40.000	63.000	30.000	-31.000	76.000	28.000
10	-28.000	73.000	10.000	-43.000	87.000	5.000
11	-33.000	66.000	17.000	-25.000	122.000	7.000
12	-28.000	71.000	10.000	-18.000	81.000	35.000
13	-28.000	43.000	10.000	-48.000	58.000	22.000
14	-41.000	59.000	11.000	-35.000	89.000	23.000
15	-30.000	28.000	2.000	-28.000	84.000	18.000
16	-25.000	23.000	5.000	-58.000	86.000	13.000
17	-22.900	33.000	5.000	-61.000	81.000	13.000
18	-30.000	27.000	5.000	-58.000	58.000	15.000
19	-26.000	22.000	10.000	-43.900	64.000	2.000
20	-20.000	41.000	10.000	-38.000	46.000	3.000
21	-26.000	43.000	7.000	-15.000	40.000	3.000
22	-28.000	46.000	7.000	-51.000	38.000	8.000
23	-20.000	38.000	15.000	-36.000	48.000	13.000
24				-23.000	41.000	10.000
25				-38.000	51.000	15.000
26				-23.000	51.000	8.000
27				-30.000	58.000	10.000
28				-41.000	64.000	18.000
29				-27.000	46.000	18.000
TEMPX	32.58	37.94	28.98	29.62	28.84	28.42
TEMPX	26.79	28.11	26.67	27.86	26.64	28.55
TEMPX	26.54	26.71	43.09			
TEMPY	35.02	36.00	33.47	30.08	31.78	31.73
TEMPY	31.20	31.17	30.18	28.52	28.18	35.33
TEMPY	31.71	30.42	30.54	28.89	42.21	30.98
TEMPZ	32.85	29.53*****		27.48	26.48	27.97
TEMPZ	26.28	26.89	26.35	26.65	26.35	26.40
TEMPZ	26.03	27.28	25.64	25.96	25.44	
TEMPX	32.64	37.88	28.83	29.34	28.85	28.58
TEMPX	26.90	28.17	26.75	27.92	26.68	28.63
TEMPX	26.55	26.77	43.29			
TEMPY	34.95	36.11	33.39	30.14	31.93	31.96
TEMPY	31.21	31.43	30.28	28.55	28.21	35.07
TEMPY	31.79	30.53	30.45	28.94	42.24	30.97
TEMPZ	32.84	29.51*****		27.56	26.51	28.03
TEMPZ	26.29	26.90	26.31	26.71	26.41	26.46
TEMPZ	26.09	27.34	25.68	26.02	25.48	

TEST # =10

A short probe system				A long probe system		
number	x	y	z	x	y	z
1	-26.000	26.000	31.000	7.000	33.000	35.900
2	-20.000	25.000	30.000	36.000	41.000	28.000
3	-27.000	28.000	35.000	28.000	41.000	30.000
4	-18.000	38.000	30.000	3.000	45.000	30.900
5	-23.000	51.000	28.000	0.	69.000	23.000
6	-25.000	68.000	28.000	0.	77.000	33.000
7	-28.000	76.000	48.000	8.000	86.000	36.000
8	-41.000	74.000	23.000	3.000	94.000	28.000
9	-38.000	79.000	38.000	-8.000	94.000	36.000
10	-25.000	68.000	20.000	0.	92.000	17.000
11	-28.000	76.000	30.000	-5.000	106.000	12.000
12	-30.000	81.000	23.000	28.000	91.000	22.000
13	-28.000	46.000	13.000	5.000	71.000	27.000
14	-31.000	56.000	16.000	-12.000	97.000	41.000
15	-35.000	33.000	17.000	5.000	99.000	23.000
16	-18.000	30.000	15.000	0.	99.000	18.000
17	-20.000	40.000	10.000	13.000	99.000	22.900
18	-20.000	33.000	13.000	0.	79.000	18.000
19	-15.000	25.000	15.000	-3.000	84.000	8.000
20	-15.000	54.000	18.000	0.	59.000	5.000
21	-13.000	53.000	15.000	11.000	53.000	3.000
22	-18.000	53.000	20.000	-5.000	55.000	16.000
23	-15.000	40.000	25.000	2.000	56.000	13.000
24				18.000	53.000	10.000
25				5.000	64.000	15.000
26				-5.000	71.000	8.000
27				5.000	68.000	15.000
28				0.	69.000	23.000
29				18.000	64.000	18.000
TEMPX	33.06	37.94	29.52	29.91	29.25	28.98
TEMPX	27.40	28.62	27.23	28.35	27.13	28.81
TEMPX	26.88	26.98	43.14			
TEMPY	35.28	36.22	33.86	29.86	31.88	31.93
TEMPY	31.54	31.56	30.79	29.06	28.65	35.40
TEMPY	31.85	30.74	30.79	29.28	41.91	31.24
TEMPZ	32.96	29.71*****		27.88	26.85	28.42
TEMPZ	26.76	27.42	26.88	27.14	26.83	26.88
TEMPZ	26.31	27.54	25.87	26.29	25.80	
TEMPX	32.92	37.88	29.36	29.70	29.24	29.09
TEMPX	27.46	28.70	27.33	28.36	27.16	28.82
TEMPX	26.92	27.02	43.43			
TEMPY	35.12	36.28	33.75	29.80	31.96	32.13
TEMPY	31.55	31.82	30.77	29.07	28.73	35.27
TEMPY	31.96	30.82	30.75	29.34	41.91	31.28
TEMPZ	32.92	29.72*****		27.89	26.91	28.47
TEMPZ	26.76	27.45	26.84	27.20	26.86	26.96
TEMPZ	26.35	27.57	25.91	26.35	25.83	

TEST # = 11

A short probe system				A long probe system		
number	x	y	z	x	y	z
1	-31.000	28.000	38.000	-41.000	44.000	54.000
2	-18.000	33.000	36.000	-15.000	46.000	43.000
3	-30.000	33.000	43.000	-15.000	46.000	41.000
4	-23.000	54.000	41.000	-25.000	53.000	46.000
5	-28.000	64.000	43.000	-20.000	66.000	41.000
6	-33.000	76.000	40.000	-35.000	77.000	54.000
7	-38.000	89.000	59.000	-25.000	91.000	49.000
8	-46.000	94.000	33.000	-33.000	99.000	48.000
9	-40.000	86.000	56.000	-54.000	106.000	46.000
10	-30.000	86.000	35.000	-30.000	107.000	38.000
11	-26.000	83.000	45.000	-40.000	137.000	25.000
12	-25.000	91.000	33.000	-30.000	99.000	43.000
13	-23.000	61.000	31.000	-48.000	79.000	35.000
14	-33.000	66.000	26.000	-58.000	107.000	56.000
15	-25.000	48.000	20.000	-41.000	107.000	41.000
16	-23.000	35.000	21.000	-48.000	107.100	41.000
17	-25.000	45.000	18.000	-43.000	109.000	41.000
18	-33.000	38.000	23.000	-61.000	84.000	41.000
19	-21.000	33.000	20.000	-49.000	79.000	28.000
20	-25.000	51.000	28.000	-38.000	66.000	25.000
21	-28.000	60.000	33.000	-20.000	61.000	20.000
22	-26.000	63.000	33.000	-51.000	78.000	23.000
23	-20.000	43.000	33.000	-39.000	48.000	31.000
24				-26.000	46.000	23.000
25				-33.000	74.000	33.000
26				-33.000	64.000	20.000
27				-23.000	78.000	25.000
28				-36.000	82.000	45.000
29				-30.000	59.000	36.000
TEMPX	33.09	37.97	29.98	30.30	29.52	29.40
TEMPX	27.86	29.03	27.69	28.64	27.47	28.96
TEMPX	27.18	27.15	43.00			
TEMPY	35.24	36.42	34.15	29.55	31.83	32.00
TEMPY	31.71	31.81	31.01	29.38	28.99	35.43
TEMPY	31.93	30.89	30.98	29.57	41.81	31.46
TEMPZ	32.91	29.75*****		28.05	27.09	28.71
TEMPZ	27.10	27.88	27.17	27.53	27.17	27.24
TEMPZ	26.46	27.70	26.07	26.56	26.04	
TEMPX	33.05	37.95	29.85	30.02	29.55	29.43
TEMPX	27.92	29.04	27.75	28.63	27.50	29.02
TEMPX	27.23	27.16	43.17			
TEMPY	35.20	36.37	34.04	29.51	31.89	32.15
TEMPY	31.74	32.01	31.06	29.41	29.04	35.46
TEMPY	31.93	30.89	30.94	29.60	41.75	31.47
TEMPZ	32.88	29.61*****		28.00	27.14	28.70
TEMPZ	27.14	27.90	27.22	27.58	27.19	27.26
TEMPZ	26.48	27.73	26.07	26.58	26.09	

TEST # =12

A short probe system				A long probe system		
number	x	y	z	x	y	z
1	-3.000	31.000	20.000	22.000	44.000	26.000
2	3.000	28.000	15.000	44.000	41.000	18.000
3	-5.000	31.000	22.000	21.000	49.000	13.000
4	0.	33.000	35.000	18.000	27.000	30.900
5	-2.000	28.000	33.000	21.000	46.000	28.000
6	-8.000	17.000	43.000	18.000	44.000	28.000
7	-10.000	25.000	56.000	28.000	38.000	39.000
8	-23.000	36.000	40.000	18.000	44.000	38.000
9	-17.000	18.000	40.000	25.000	35.000	36.000
10	-23.000	25.000	33.000	10.000	56.000	25.000
11	-21.000	15.000	35.000	11.000	66.000	38.000
12	-25.000	17.000	35.000	23.000	71.000	45.000
13	-23.000	13.000	15.000	8.000	41.000	50.000
14	-26.000	20.000	23.000	8.000	33.000	43.000
15	-20.000	23.000	15.000	13.000	38.000	23.000
16	-3.000	15.000	13.000	-2.000	38.000	23.000
17	-5.000	30.000	5.000	0.	28.000	26.000
18	-10.000	17.000	10.000	3.000	30.000	15.000
19	-3.000	17.000	10.000	5.000	38.000	8.000
20	-5.000	21.000	18.000	8.000	38.000	3.000
21	-8.000	25.000	30.000	11.000	38.000	0.
22	-13.000	20.000	17.000	10.000	45.000	0.
23	-8.000	18.000	25.000	15.000	43.000	8.000
24				25.000	33.000	0.
25				3.000	28.000	15.000
26				0.	41.000	8.000
27				21.000	40.000	20.000
28				0.	38.000	18.000
29				31.000	36.000	13.000
TEMPX	26.10	34.99	26.05	25.73	26.17	26.07
TEMPX	25.78	25.85	25.68	25.68	25.63	26.79
TEMPX	25.51	25.29	37.08			
TEMPY	27.92	27.49	26.65	28.61	27.78	27.61
TEMPY	27.17	26.53	26.43	26.14	26.02	27.73
TEMPY	27.34	26.92	26.46	26.17	40.47	26.47
TEMPZ	25.61	25.36*****		25.58	25.44	25.44
TEMPZ	25.34	25.36	25.63	25.58	25.68	25.61
TEMPZ	25.34	25.27	25.26	25.41	25.17	
TEMPX	26.30	35.52	26.12	25.83	26.25	26.15
TEMPX	25.81	25.88	25.71	25.73	25.63	27.01
TEMPX	25.59	25.32	37.80			
TEMPY	28.22	27.78	26.90	28.88	28.05	27.88
TEMPY	27.24	26.60	26.55	26.21	26.02	28.32
TEMPY	27.53	27.17	26.63	26.24	40.82	26.61
TEMPZ	25.82	25.45*****		25.70	25.50	25.48
TEMPZ	25.40	25.40	25.63	25.63	25.72	25.70
TEMPZ	25.43	25.33	25.36	25.50	25.21	

TEST # =13

A short probe system				A long probe system		
number	x	y	z	x	y	z
1	-23.000	26.000	43.000	-8.000	38.000	35.900
2	-20.000	25.000	36.000	13.000	41.000	30.000
3	-25.000	23.000	38.000	-10.000	54.000	35.000
4	-20.000	31.000	41.000	-13.000	35.000	38.000
5	-25.000	39.000	36.000	-2.000	51.000	36.000
6	-38.000	33.000	40.000	-10.000	51.000	49.000
7	-25.000	38.000	56.000	-2.000	45.000	46.000
8	-38.000	44.000	38.000	0.	54.000	43.000
9	-35.000	30.000	48.000	-15.000	45.000	43.000
10	-38.000	28.000	33.000	-15.000	67.000	33.000
11	-38.000	25.000	30.000	8.000	84.000	30.000
12	-48.000	28.000	23.000	-12.000	81.000	15.000
13	-38.000	25.000	18.000	-28.000	46.000	17.000
14	-46.000	26.000	28.000	-27.000	51.000	31.000
15	-38.000	20.000	23.000	-13.000	48.000	26.000
16	-25.000	18.000	21.000	-28.000	58.000	28.000
17	-25.000	22.000	10.000	-40.000	43.000	30.900
18	-30.000	20.000	15.000	-15.000	35.000	15.000
19	-15.000	17.000	18.000	-33.000	56.000	10.000
20	-28.000	18.000	21.000	-15.000	46.000	10.000
21	-26.000	30.000	25.000	-10.000	43.000	10.000
22	-21.000	25.000	20.000	-20.000	35.000	11.000
23	-18.000	18.000	30.000	2.000	38.000	18.000
24				7.000	38.000	18.000
25				-10.000	43.000	28.000
26				-10.000	43.000	10.000
27				16.000	40.000	25.000
28				-13.000	41.000	28.000
29				6.000	38.000	28.000
TEMPX	29.35	37.30	27.65	27.62	27.45	26.82
TEMPX	26.16	26.52	26.11	26.30	26.11	28.21
TEMPX	26.18	25.84	41.58			
TEMPY	32.54	31.57	29.68	30.53	29.73	29.48
TEMPY	29.04	27.92	27.95	26.94	26.58	32.61
TEMPY	29.87	29.09	28.19	27.22	42.15	27.75
TEMPZ	28.89	27.03*****		26.66	26.13	26.37
TEMPZ	25.95	26.00	26.35	26.30	26.22	26.25
TEMPZ	26.08	26.20	25.91	26.05	25.69	
TEMPX	29.65	37.54	27.55	27.58	27.50	27.16
TEMPX	26.23	26.58	26.13	26.43	26.16	28.36
TEMPX	26.28	25.91	41.84			
TEMPY	32.71	32.08	29.85	30.55	30.09	29.85
TEMPY	28.90	28.17	28.24	27.24	26.68	32.71
TEMPY	30.14	29.29	28.37	27.32	42.32	27.99
TEMPZ	29.28	27.23*****		26.84	26.23	26.52
TEMPZ	26.01	26.06	26.25	26.40	26.30	26.40
TEMPZ	26.18	26.33	26.01	26.16	25.74	

TEST # =14

A short probe system				A long probe system		
number	x	y	z	x	y	z
1	-31.000	28.000	38.000	-13.000	38.000	38.000
2	-30.000	28.000	33.000	-7.000	33.000	43.000
3	-38.000	36.000	38.000	-10.000	46.000	35.000
4	-23.000	44.000	41.000	-18.000	40.000	41.000
5	-38.000	41.000	41.000	-12.000	69.000	36.000
6	-38.000	53.000	45.000	-12.000	61.000	44.000
7	-41.000	63.000	53.000	-20.000	76.000	39.000
8	-48.000	69.000	33.000	-10.000	72.000	38.000
9	-50.000	61.000	48.000	-28.000	68.000	38.000
10	-51.000	63.000	28.000	-15.000	87.000	25.000
11	-56.000	58.000	30.000	-2.000	101.000	23.000
12	-58.000	61.000	25.000	-12.000	104.000	27.000
13	-36.000	41.000	21.000	-35.000	51.000	30.000
14	-56.000	41.000	16.000	-22.000	74.000	43.000
15	-48.000	33.000	15.000	-5.000	66.000	31.000
16	-36.000	23.000	13.000	-35.000	74.000	18.000
17	-43.000	35.000	10.000	-40.000	71.000	13.000
18	-38.000	25.000	15.000	-10.000	56.000	23.000
19	-26.000	22.000	23.000	-35.900	66.000	2.000
20	-35.000	36.000	18.000	-28.000	48.000	5.000
21	-43.000	45.000	25.000	-25.000	40.000	3.000
22	-31.000	48.000	22.000	-22.900	45.000	6.000
23	-33.000	35.000	30.000	-21.000	43.000	8.000
24				-5.000	46.000	10.000
25				-13.000	48.000	18.000
26				-30.000	56.000	10.000
27				3.000	51.000	15.000
28				-28.000	59.000	23.000
29				-2.000	38.000	26.000
TEMPX	34.32	39.50	30.25	30.98	30.16	29.58
TEMPX	28.04	28.89	27.82	28.63	27.79	30.28
TEMPX	28.16	27.65	44.56			
TEMPY	37.11	37.52	34.23	32.34	33.12	32.95
TEMPY	32.39	31.96	31.28	29.80	29.19	36.52
TEMPY	33.31	31.98	31.62	29.97	43.97	31.13
TEMPZ	33.27	30.36*****		28.85	27.98	29.12
TEMPZ	27.83	28.32	27.93	28.27	28.03	28.02
TEMPZ	27.71	28.54	27.39	27.61	27.17	
TEMPX	34.35	39.56	30.12	30.82	30.24	29.68
TEMPX	28.14	28.97	27.90	28.70	27.85	30.36
TEMPX	28.24	27.73	44.64			
TEMPY	37.24	37.62	34.16	32.42	33.37	33.25
TEMPY	32.38	32.08	31.41	29.88	29.24	36.57
TEMPY	33.37	32.04	31.70	30.07	44.08	31.33
TEMPZ	33.26	30.45*****		28.92	28.07	29.23
TEMPZ	27.87	28.36	28.04	28.36	28.09	28.11
TEMPZ	27.77	28.63	27.45	27.70	27.21	

TEST # =15

A short probe system				A long probe system		
number	x	y	z	x	y	z
1	-28.000	26.000	28.000	-41.000	36.000	38.000
2	-23.000	25.000	25.000	-40.000	38.000	25.000
3	-27.000	31.000	30.000	-22.000	41.000	28.000
4	-20.000	31.000	28.000	-20.000	27.000	33.000
5	-30.000	39.000	31.000	-20.000	48.000	23.000
6	-31.000	43.000	25.000	-51.000	46.000	28.000
7	-35.000	51.000	41.000	-50.000	63.000	31.000
8	-38.000	64.000	15.000	-41.000	61.000	28.000
9	-38.000	53.000	30.000	-41.000	60.000	31.000
10	-46.000	53.000	25.000	-48.000	69.000	12.000
11	-54.000	53.000	15.000	-45.000	91.000	23.000
12	-50.000	45.000	13.000	-38.000	84.000	27.000
13	-38.000	33.000	5.000	-71.000	43.000	12.000
14	-59.000	36.000	3.000	-71.000	66.000	31.000
15	-43.000	25.000	-5.000	-36.000	68.000	15.000
16	-33.000	20.000	5.000	-68.000	71.000	13.000
17	-33.000	25.000	0.	-61.000	56.000	9.900
18	-33.000	27.000	5.000	-51.000	38.000	13.000
19	-21.000	25.000	10.000	-43.900	81.000	-3.000
20	-30.000	31.000	5.000	-68.000	36.000	-5.000
21	-38.000	38.000	10.000	-50.000	33.000	0.
22	-31.000	46.000	7.000	-35.000	33.000	-2.000
23	-30.000	30.000	18.000	-49.000	41.000	5.000
24				-49.000	41.000	5.000
25				-51.000	53.000	8.000
26				-61.000	48.000	-2.000
27				-40.000	48.000	5.000
28				-53.000	46.000	18.000
29				-43.000	38.000	13.000
TEMPX	34.36	39.52	30.05	30.75	30.27	29.73
TEMPX	28.17	29.05	27.95	28.74	27.91	30.41
TEMPX	28.30	27.76	44.58			
TEMPY	37.10	37.58	34.15	32.43	33.40	33.28
TEMPY	32.48	32.19	31.44	29.96	29.32	36.38
TEMPY	33.42	32.04	31.75	30.08	44.01	31.56
TEMPZ	33.24	30.41*****		28.93	28.05	29.24
TEMPZ	27.93	28.44	28.03	28.37	28.15	28.12
TEMPZ	27.83	28.68	27.49	27.73	27.24	
TEMPX	34.34	39.50	29.98	30.73	30.34	29.86
TEMPX	28.28	29.13	28.03	28.86	27.96	30.44
TEMPX	28.32	27.86	44.58			
TEMPY	37.01	37.61	34.08	32.51	33.54	33.35
TEMPY	32.48	32.31	31.46	30.01	29.43	36.22
TEMPY	33.45	32.10	31.83	30.20	44.06	31.90
TEMPZ	33.39	30.53*****		29.08	28.13	29.34
TEMPZ	27.96	28.49	28.13	28.42	28.23	28.20
TEMPZ	27.86	28.78	27.54	27.81	27.32	

TEST # =16

A short probe system				A long probe system		
number	x	y	z	x	y	z
1	-13.000	43.000	38.000	15.000	56.000	26.000
2	3.000	45.000	33.000	21.000	51.000	25.000
3	-12.000	41.000	38.000	11.000	61.000	25.000
4	-5.000	46.000	46.000	10.000	48.000	38.000
5	-15.000	44.000	53.000	23.000	61.000	33.000
6	-13.000	45.000	61.000	3.000	61.000	39.000
7	-20.000	53.000	74.000	16.000	68.000	49.000
8	-28.000	61.000	48.000	10.000	72.000	46.000
9	-25.000	43.000	63.000	-8.000	63.000	46.000
10	-18.000	46.000	56.000	20.000	69.000	35.000
11	-8.000	38.000	58.000	11.000	89.000	40.000
12	-7.000	45.000	51.000	21.000	84.000	38.000
13	-8.000	36.000	33.000	-5.000	51.000	50.000
14	-18.000	38.000	46.000	0.	59.000	53.000
15	-15.000	30.000	25.000	20.000	58.000	41.000
16	-8.000	35.000	28.000	11.000	61.000	33.000
17	-2.000	45.000	23.000	-2.000	61.000	46.000
18	-13.000	40.000	23.000	10.000	56.000	23.000
19	-3.000	33.000	25.000	15.000	58.000	20.000
20	-2.000	34.000	38.000	-2.000	56.000	13.000
21	-8.000	40.000	40.000	33.000	51.000	8.000
22	5.000	51.000	40.000	0.	55.000	11.000
23	-8.000	30.000	46.000	15.000	61.000	13.000
24				28.000	53.000	5.000
25				18.000	51.000	23.000
26				5.000	56.000	20.000
27				36.000	63.000	30.000
28				2.000	56.000	33.000
29				23.000	46.000	33.000
TEMPX	26.23	26.62	26.79	26.42	26.62	26.70
TEMPX	26.70	26.65	26.60	26.40	26.38	26.53
TEMPX	26.53	26.04	26.82			
TEMPY	26.41	26.60	26.92	26.31	26.60	26.63
TEMPY	26.75	26.73	26.75	26.66	26.56	26.56
TEMPY	26.63	26.51	26.49	26.54	29.27	26.80
TEMPZ	25.80	26.02*****		26.12	26.19	26.21
TEMPZ	26.39	26.39	26.29	26.26	26.36	26.27
TEMPZ	26.05	25.95	26.07	26.07	26.22	
TEMPX	26.26	30.02	26.77	26.48	26.63	26.73
TEMPX	26.68	26.66	26.60	26.38	26.38	26.70
TEMPX	26.51	26.04	29.80			
TEMPY	26.51	26.76	26.95	26.59	26.81	26.81
TEMPY	26.78	26.71	26.76	26.66	26.56	26.79
TEMPY	26.69	26.59	26.57	26.52	34.85	26.83
TEMPZ	25.88	26.08*****		26.18	26.23	26.20
TEMPZ	26.35	26.37	26.38	26.33	26.40	26.31
TEMPZ	26.08	25.96	26.09	26.14	26.23	

TEST # =17

A short probe system				A long probe system		
number	x	y	z	x	y	z
1	-23.000	51.000	58.000	-3.000	69.000	69.000
2	-15.000	43.000	58.000	16.000	61.000	58.000
3	-20.000	41.000	63.000	-7.000	77.000	58.000
4	-15.000	51.000	71.000	0.	66.000	71.000
5	-35.000	54.000	66.000	-10.000	74.000	66.000
6	-36.000	53.000	68.000	-12.000	72.000	77.000
7	-33.000	63.000	94.000	-2.000	88.000	84.000
8	-35.000	74.000	63.000	-15.000	92.000	79.000
9	-40.000	61.000	81.000	-33.000	94.000	89.000
10	-30.000	63.000	56.000	-15.000	110.000	66.000
11	-26.000	53.000	68.000	11.000	119.000	61.000
12	-30.000	53.000	63.000	0.	99.000	43.000
13	-23.000	46.000	61.000	-12.000	84.000	81.000
14	-31.000	46.000	59.000	-10.000	79.000	76.000
15	-28.000	40.000	40.000	0.	76.000	54.000
16	-10.000	30.000	41.000	-10.000	79.000	61.000
17	-13.000	43.000	33.000	-15.000	78.000	66.000
18	-20.000	27.000	43.000	0.	68.000	58.000
19	-15.000	38.000	48.000	-3.000	71.000	48.000
20	-20.000	41.000	51.000	-10.000	59.000	41.000
21	-21.000	40.000	61.000	8.000	58.000	46.000
22	-18.000	48.000	55.000	-9.900	55.000	46.000
23	-23.000	33.000	63.000	-3.000	56.000	46.000
24				5.000	58.000	40.000
25				3.000	51.000	51.000
26				-12.000	71.000	46.000
27				-2.000	66.000	51.000
28				-10.000	77.000	61.000
29				6.000	64.000	56.000
TEMPX	28.72	36.17	27.89	27.77	27.15	26.98
TEMPX	26.74	26.74	26.67	26.50	26.47	28.04
TEMPX	26.67	25.98	39.22			
TEMPY	29.87	29.61	28.78	27.98	27.76	27.95
TEMPY	27.63	27.17	27.32	26.83	26.68	30.65
TEMPY	27.90	27.37	27.22	26.90	40.04	27.13
TEMPZ	28.62	27.33*****		26.60	26.47	26.69
TEMPZ	26.57	26.62	26.57	26.79	26.52	26.50
TEMPZ	26.21	26.26	26.21	26.23	26.28	
TEMPX	29.00	36.43	27.73	27.54	27.25	27.22
TEMPX	26.73	26.83	26.68	26.51	26.49	28.18
TEMPX	26.69	26.00	40.23			
TEMPY	30.25	30.23	28.87	28.09	28.16	28.33
TEMPY	27.55	27.36	27.43	26.92	26.72	30.94
TEMPY	28.09	27.58	27.36	26.99	40.22	27.27
TEMPZ	28.95	27.48*****		26.73	26.53	26.80
TEMPZ	26.58	26.65	26.70	26.85	26.58	26.53
TEMPZ	26.26	26.34	26.21	26.26	26.31	

TEST # =18

A short probe system				A long probe system		
number	x	y	z	x	y	z
1	-26.000	36.000	51.000	7.000	54.000	64.000
2	-15.000	30.000	53.000	11.000	59.000	43.000
3	-12.000	38.000	55.000	8.000	64.000	58.000
4	-18.000	49.000	63.000	-2.000	50.000	64.000
5	-33.000	49.000	69.000	23.000	64.000	59.000
6	-36.000	53.000	71.000	5.000	61.000	69.000
7	-25.000	56.000	86.000	-2.000	68.000	69.000
8	-33.000	69.000	58.000	-13.000	72.000	69.000
9	-30.000	53.000	76.000	-21.000	68.000	76.000
10	-38.000	53.000	45.000	-18.000	87.000	50.000
11	-31.000	53.000	58.000	-2.000	99.000	51.000
12	-35.000	53.000	48.000	-5.000	91.000	50.000
13	-23.000	38.000	41.000	-10.000	66.000	58.000
14	-41.000	38.000	46.000	-10.000	74.000	76.000
15	-28.000	30.000	43.000	15.000	68.000	46.000
16	-15.000	30.000	36.000	8.000	61.000	59.000
17	-20.000	35.000	33.000	-10.000	66.000	51.000
18	-20.000	30.000	38.000	-17.000	51.000	48.000
19	-18.000	35.000	41.000	-8.000	64.000	33.000
20	-20.000	34.000	46.000	0.	53.000	31.000
21	-26.000	38.000	43.000	3.000	53.000	33.000
22	-16.000	43.000	48.000	-9.900	60.000	28.000
23	-18.000	30.000	56.000	-8.000	61.000	35.900
24				15.000	53.000	38.000
25				3.000	48.000	48.000
26				-5.000	61.000	31.000
27				-10.000	53.000	43.000
28				-10.000	51.000	51.000
29				3.000	51.000	43.000
TEMPX	30.00	36.74	28.11	28.23	27.74	27.42
TEMPX	26.86	27.01	26.74	26.69	26.54	28.59
TEMPX	26.91	26.10	40.88			
TEMPY	31.42	31.30	29.69	28.43	28.48	28.84
TEMPY	28.36	27.91	27.74	27.18	26.94	32.00
TEMPY	28.89	28.04	27.89	27.33	40.43	27.96
TEMPZ	30.04	28.19*****		27.14	26.75	27.31
TEMPZ	26.77	26.94	26.80	27.04	26.72	26.72
TEMPZ	26.43	26.70	26.35	26.40	26.43	
TEMPX	30.12	36.95	27.97	28.09	27.83	27.65
TEMPX	26.90	27.07	26.77	26.72	26.56	28.68
TEMPX	26.97	26.14	41.51			
TEMPY	31.53	31.74	29.78	28.53	28.88	29.14
TEMPY	28.22	28.14	27.83	27.24	26.95	32.06
TEMPY	29.02	28.19	27.98	27.41	40.56	28.07
TEMPZ	30.19	28.19*****		27.19	26.77	27.41
TEMPZ	26.80	26.99	26.92	27.09	26.75	26.75
TEMPZ	26.48	26.80	26.38	26.46	26.48	

TEST # =19

number	A short probe system			A long probe system		
	x	y	z	x	y	z
1	-31.000	28.000	58.000	10.000	38.000	61.000
2	-15.000	28.000	51.000	23.000	43.000	56.000
3	-27.000	36.000	60.000	16.000	64.000	71.000
4	-18.000	38.000	63.000	-5.000	50.000	69.000
5	-38.000	41.000	61.000	-10.000	56.000	59.000
6	-38.000	53.000	68.000	-17.000	64.000	66.000
7	-33.000	58.000	79.000	-10.000	78.000	72.000
8	-46.000	66.000	51.000	-8.000	84.000	66.000
9	-40.000	51.000	71.000	-8.000	83.000	71.000
10	-38.000	56.000	51.000	10.000	87.000	71.000
11	-38.000	48.000	58.000	-7.000	104.000	53.000
12	-38.000	56.000	51.000	-10.000	91.000	43.000
13	-26.000	41.000	38.000	-22.000	56.000	68.000
14	-43.000	43.000	39.000	-7.000	89.000	74.000
15	-28.000	28.000	38.000	-5.000	68.000	51.000
16	-23.000	25.000	33.000	-28.000	74.000	48.000
17	-18.000	30.000	28.000	-15.000	63.000	46.000
18	-20.000	25.000	36.000	-17.000	58.000	48.000
19	-18.000	28.000	41.000	-13.000	56.000	33.000
20	-23.000	34.000	41.000	-10.000	48.000	31.000
21	-18.000	38.000	43.000	-2.000	45.000	33.000
22	-26.000	48.000	43.000	-7.000	45.000	34.000
23	-23.000	28.000	51.000	-8.000	53.000	35.900
24				28.000	46.000	38.000
25				-2.000	43.000	46.000
26				16.000	51.000	38.000
27				-5.000	78.000	48.000
28				-15.000	51.000	53.000
29				8.000	43.000	46.000
TEMPX	31.60	37.43	28.78	29.19	28.51	28.09
TEMPX	27.17	27.53	27.02	27.19	26.80	29.17
TEMPX	27.39	26.46	42.20			
TEMPY	33.27	33.44	31.21	29.02	29.63	29.92
TEMPY	29.34	29.05	28.58	27.73	27.36	33.44
TEMPY	30.02	28.95	28.83	27.93	40.96	28.88
TEMPZ	31.38	29.07*****		27.63	27.14	28.02
TEMPZ	27.19	27.53	27.14	27.46	27.04	27.01
TEMPZ	26.75	27.26	26.60	26.67	26.70	
TEMPX	31.97	37.58	28.64	29.03	28.59	28.32
TEMPX	27.22	27.64	27.08	27.25	26.86	29.27
TEMPX	27.44	26.51	42.82			
TEMPY	33.51	33.75	31.24	29.24	30.02	30.27
TEMPY	29.29	29.29	28.76	27.83	27.46	33.56
TEMPY	30.17	29.12	28.90	28.05	41.30	29.01
TEMPZ	31.49	29.11*****		27.70	27.18	28.09
TEMPZ	27.21	27.58	27.28	27.50	27.11	27.09
TEMPZ	26.79	27.36	26.65	26.72	26.72	

TEST # =20

A short probe system				A long probe system		
number	x	y	z	x	y	z
1	-38.000	28.000	46.000	10.000	46.000	49.000
2	-33.000	30.000	48.000	3.000	53.000	43.000
3	-40.000	38.000	48.000	-15.000	51.000	48.000
4	-33.000	44.000	53.000	-20.000	45.000	51.000
5	-43.000	46.000	51.000	-30.000	64.000	49.000
6	-36.000	58.000	50.000	-23.000	59.000	54.000
7	-38.000	66.000	69.000	-7.000	78.000	61.000
8	-51.000	72.000	35.000	-28.000	79.000	51.000
9	-61.000	58.000	61.000	-18.000	83.000	48.000
10	-53.000	61.000	35.000	-36.000	87.000	40.000
11	-56.000	66.000	38.000	-33.000	114.000	28.000
12	-43.000	56.000	38.000	-23.000	107.000	33.000
13	-43.000	41.000	28.000	-12.000	56.000	58.000
14	-51.000	48.000	33.000	-40.000	74.000	56.000
15	-43.000	33.000	25.000	-41.000	79.000	38.000
16	-31.000	30.000	23.000	-20.000	81.100	28.000
17	-35.000	38.000	18.000	-53.000	94.000	33.000
18	-30.000	25.000	31.000	-43.000	81.000	41.000
19	-28.000	25.000	30.000	-35.900	66.000	20.000
20	-30.000	39.000	28.000	-30.000	51.000	28.000
21	-38.000	40.000	33.000	-12.000	43.000	20.000
22	-36.000	46.000	35.000	-5.000	45.000	18.000
23	-33.000	30.000	38.000	-26.000	41.000	26.000
24				0.	48.000	25.000
25				-5.000	46.000	28.000
26				-33.000	64.000	25.000
27				-25.000	61.000	30.000
28				-31.000	59.000	40.000
29				-12.000	38.000	36.000
TEMPX	32.90	38.19	29.45	30.11	29.36	28.97
TEMPX	27.72	28.43	27.53	28.04	27.33	29.75
TEMPX	27.85	27.09	42.91			
TEMPY	34.76	35.26	32.63	30.18	31.13	31.15
TEMPY	30.57	30.40	29.72	28.60	28.24	34.66
TEMPY	31.35	30.21	30.04	28.90	42.10	30.33
TEMPZ	32.86	30.07*****		28.27	27.66	28.80
TEMPZ	27.65	28.19	27.75	28.00	27.61	27.61
TEMPZ	27.22	27.97	26.97	27.17	27.05	
TEMPX	33.02	38.31	29.41	29.96	29.45	28.99
TEMPX	27.77	28.46	27.55	28.09	27.36	29.80
TEMPX	27.89	27.14	43.00			
TEMPY	34.87	35.16	32.68	30.25	31.10	31.27
TEMPY	30.84	30.52	29.86	28.67	28.33	34.80
TEMPY	31.49	30.33	30.08	29.01	42.17	30.43
TEMPZ	33.00	29.99	31.95	28.24	27.62	28.82
TEMPZ	27.70	28.24	27.80	23.07	27.65	27.65
TEMPZ	27.26	28.04	27.02	27.21	27.07	

TEST # =21

A short probe system				A long probe system		
number	x	y	z	x	y	z
1	-38.000	28.000	46.000	-23.000	41.000	51.000
2	-23.000	30.000	43.000	-20.000	38.000	43.000
3	-33.000	31.000	50.000	-22.000	54.000	41.000
4	-28.000	38.000	46.000	-13.000	53.000	51.000
5	-45.000	49.000	48.000	-35.000	56.000	49.000
6	-46.000	55.000	45.000	-25.000	56.000	51.000
7	-43.000	71.000	64.000	-22.000	68.000	61.000
8	-48.000	79.000	30.000	-33.000	102.000	46.000
9	-55.000	61.000	48.000	-43.000	78.000	46.000
10	-58.000	63.000	33.000	-30.000	94.000	33.000
11	-56.000	53.000	40.000	-28.000	117.000	25.000
12	-56.000	63.000	28.000	-40.000	99.000	43.000
13	-43.000	48.000	23.000	-53.000	61.000	50.000
14	-59.000	51.000	31.000	-38.000	77.000	51.000
15	-38.000	33.000	17.000	-31.000	81.000	31.000
16	-41.000	33.000	21.000	-43.000	76.000	28.000
17	-33.000	33.000	20.000	-45.000	71.000	30.900
18	-35.000	33.000	20.000	-40.000	63.000	28.000
19	-28.000	22.000	25.000	-35.900	84.000	23.000
20	-28.000	49.000	23.000	-30.000	51.000	10.000
21	-38.000	40.000	30.000	-23.000	38.000	13.000
22	-36.000	46.000	33.000	-22.900	43.000	13.000
23	-28.000	30.000	33.000	-34.000	48.000	18.000
24				-21.000	36.000	18.000
25				-30.000	46.000	23.000
26				-43.000	56.000	18.000
27				-2.000	63.000	18.000
28				-43.000	61.000	35.000
29				-2.000	46.000	33.000
TEMPX	34.52	39.03	30.16	30.84	30.09	29.58
TEMPX	28.26	29.12	28.04	28.70	27.87	30.33
TEMPX	28.41	27.65	43.83			
TEMPY	36.32	36.54	33.70	31.32	32.34	32.25
TEMPY	31.76	31.38	30.87	29.48	28.97	35.94
TEMPY	32.54	31.33	31.04	29.77	43.17	31.28
TEMPZ	33.94	30.94*****		28.97	28.14	29.44
TEMPZ	28.12	28.70	28.32	28.58	28.17	28.14
TEMPZ	27.73	28.58	27.39	27.61	27.39	
TEMPX	34.53	39.13	30.02	30.71	30.15	29.71
TEMPX	28.30	29.13	28.10	28.78	27.91	30.39
TEMPX	28.44	27.74	44.08			
TEMPY	36.24	36.67	33.69	31.39	32.50	32.50
TEMPY	31.73	31.58	30.95	29.56	29.05	35.68
TEMPY	32.57	31.36	31.07	29.81	43.27	31.36
TEMPZ	33.93	30.76*****		28.89	28.18	29.50
TEMPZ	28.16	28.74	28.33	28.60	28.21	28.21
TEMPZ	27.79	28.62	27.45	27.70	27.43	

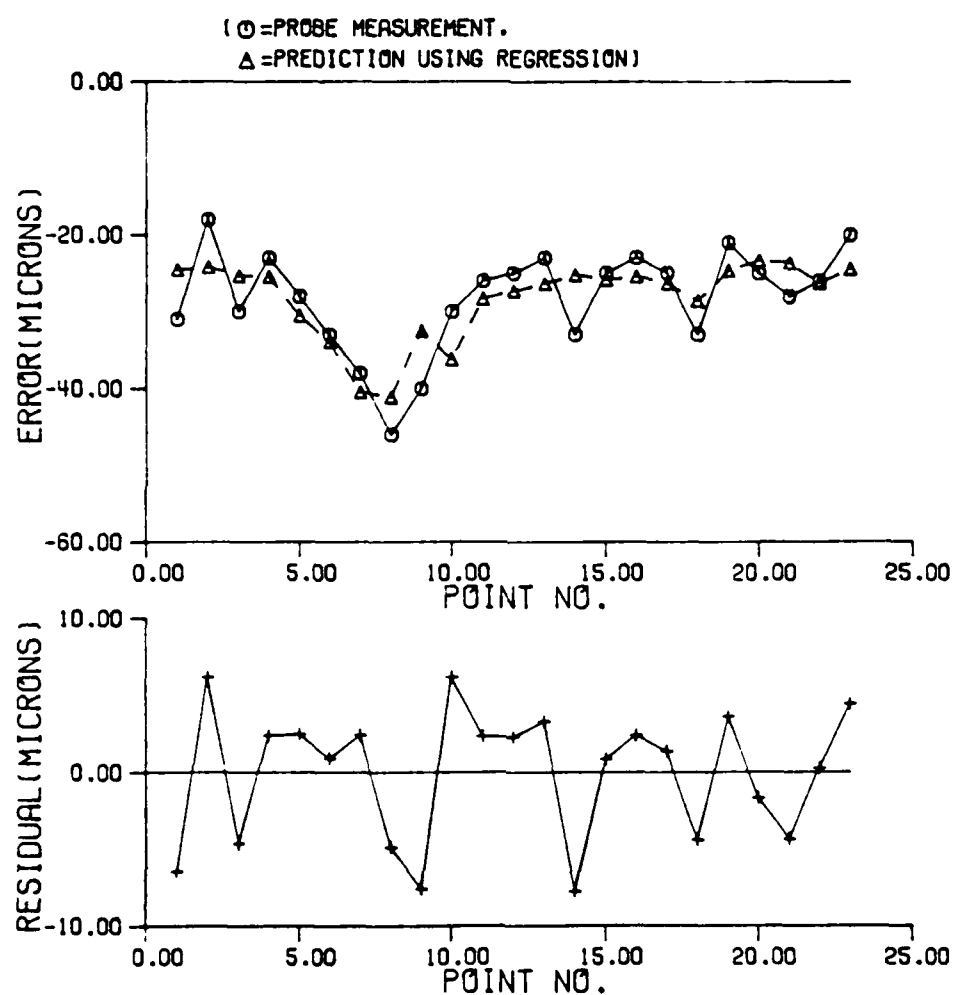


Figure A.4.3 The regression result of x absolute errors of test 11 and residual for short probe.

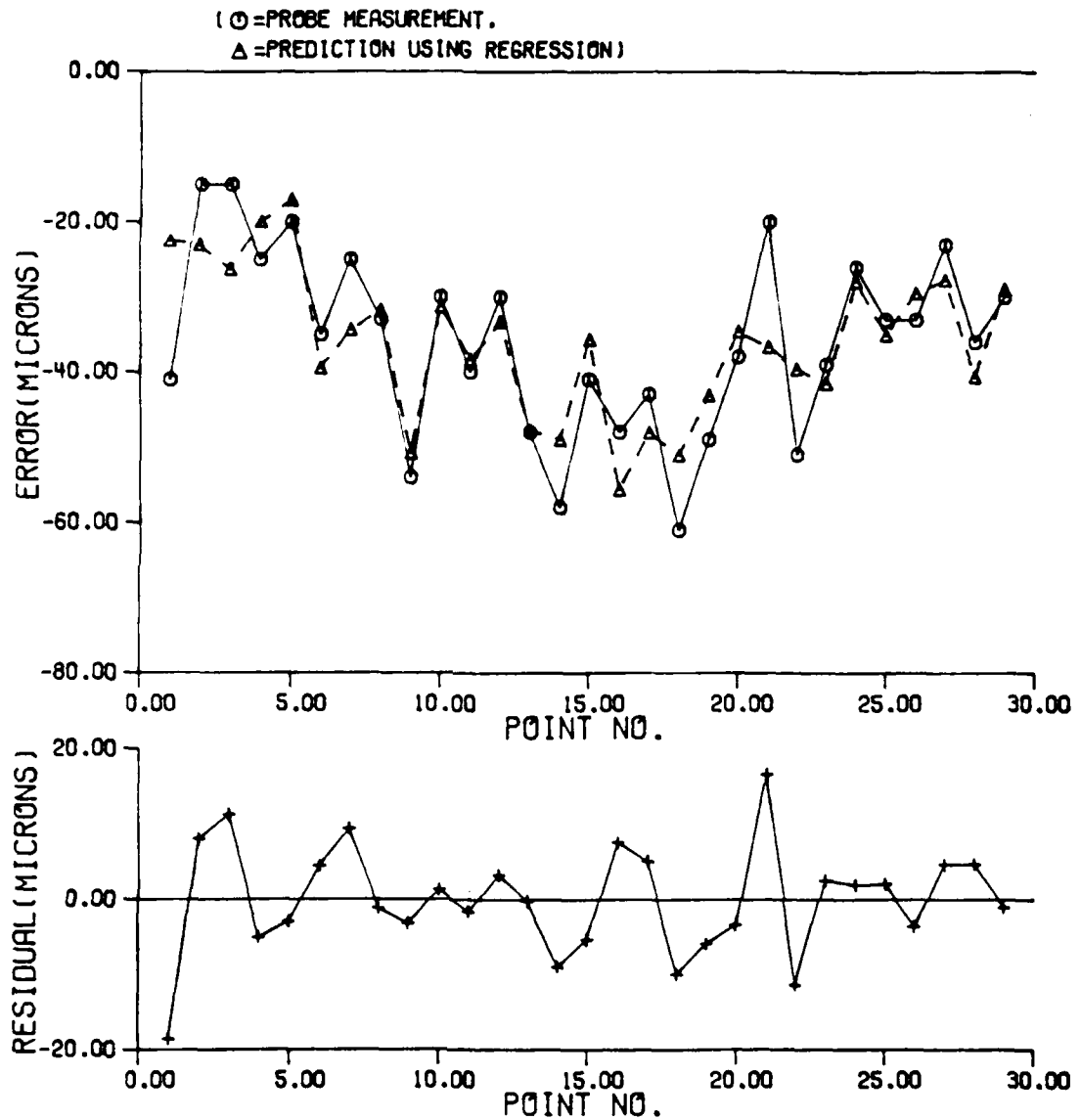


Figure A.4.4 The regression result of x absolute errors of test 11 and residual for long probe.

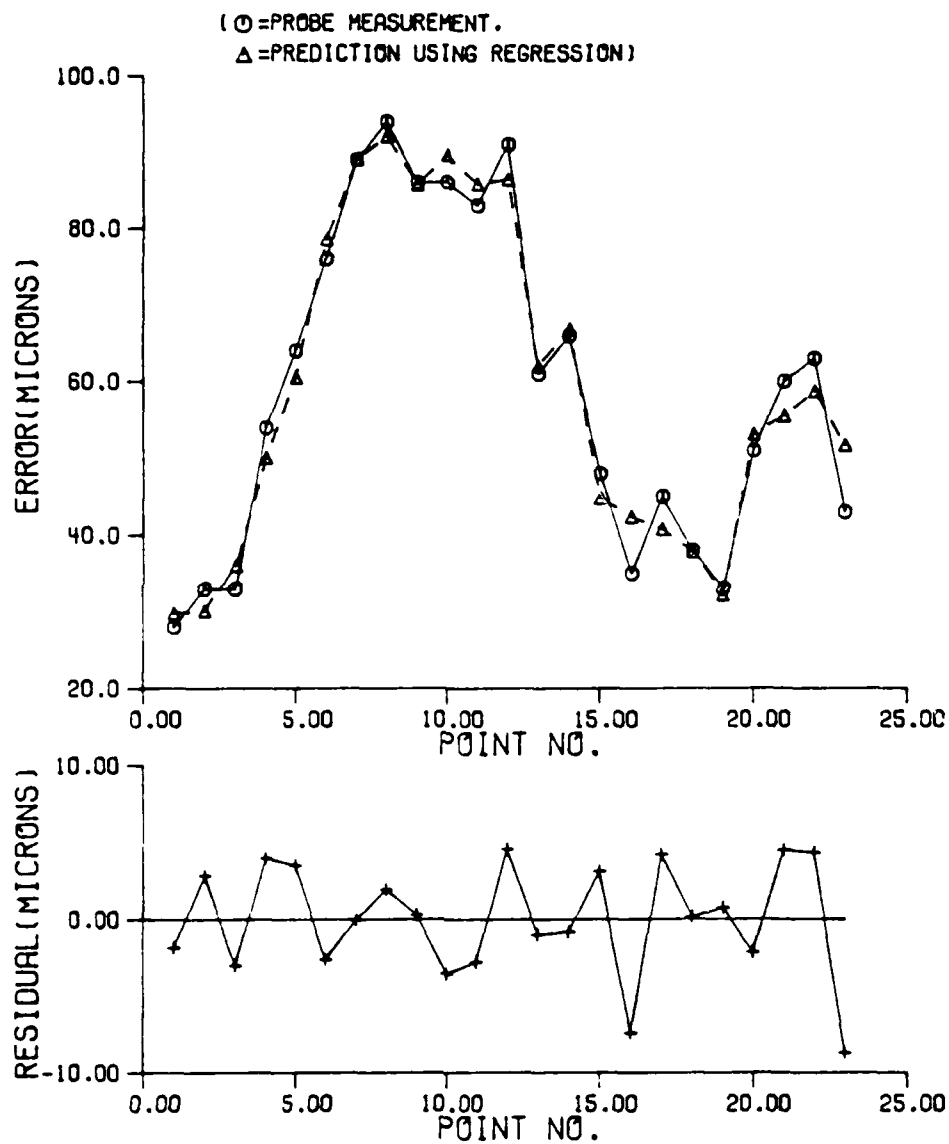


Figure A.4.5 The regression result of y absolute errors of test 11 and residual for short probe.

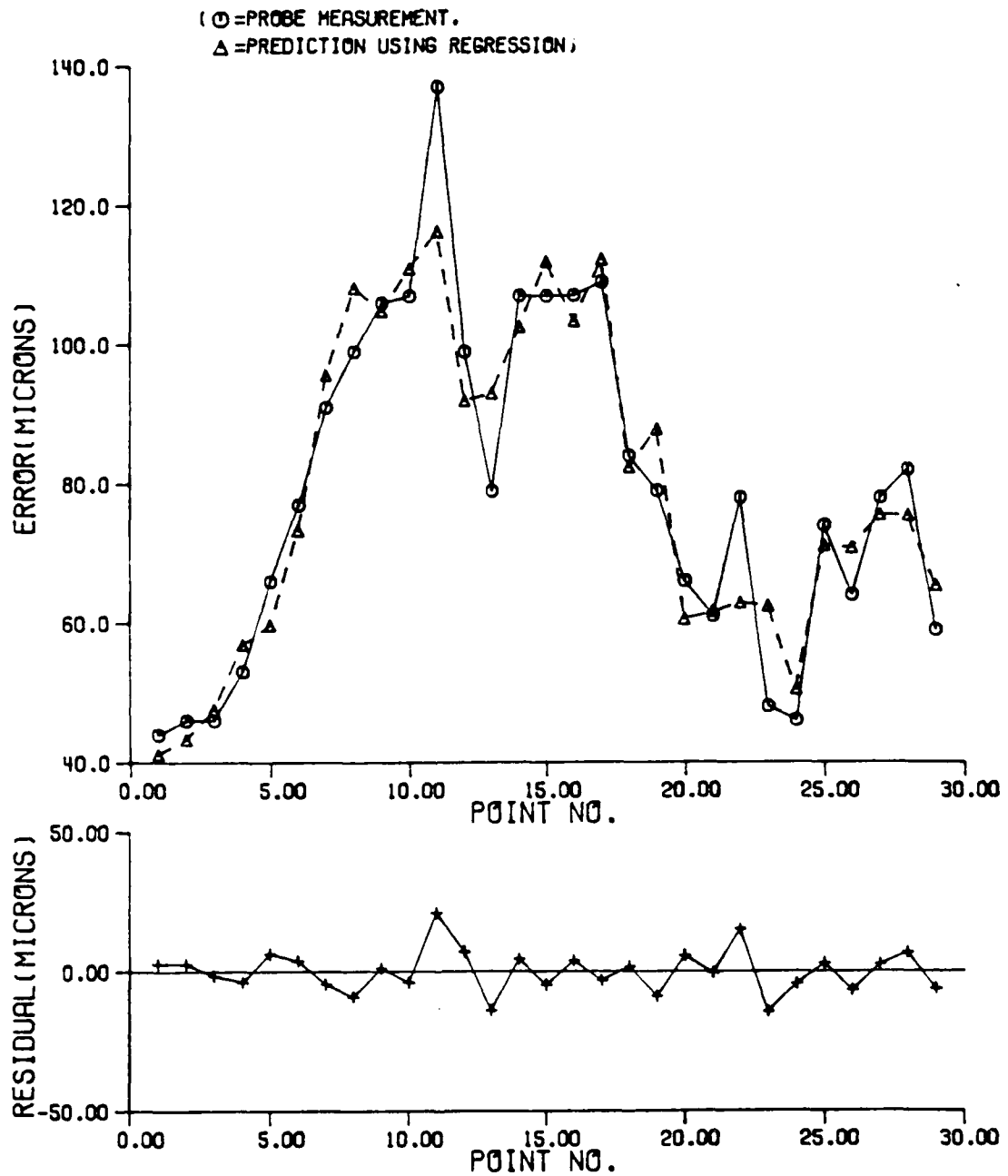


Figure A.4.0 The regression result of y absolute errors of test 11 and residual for long probe.

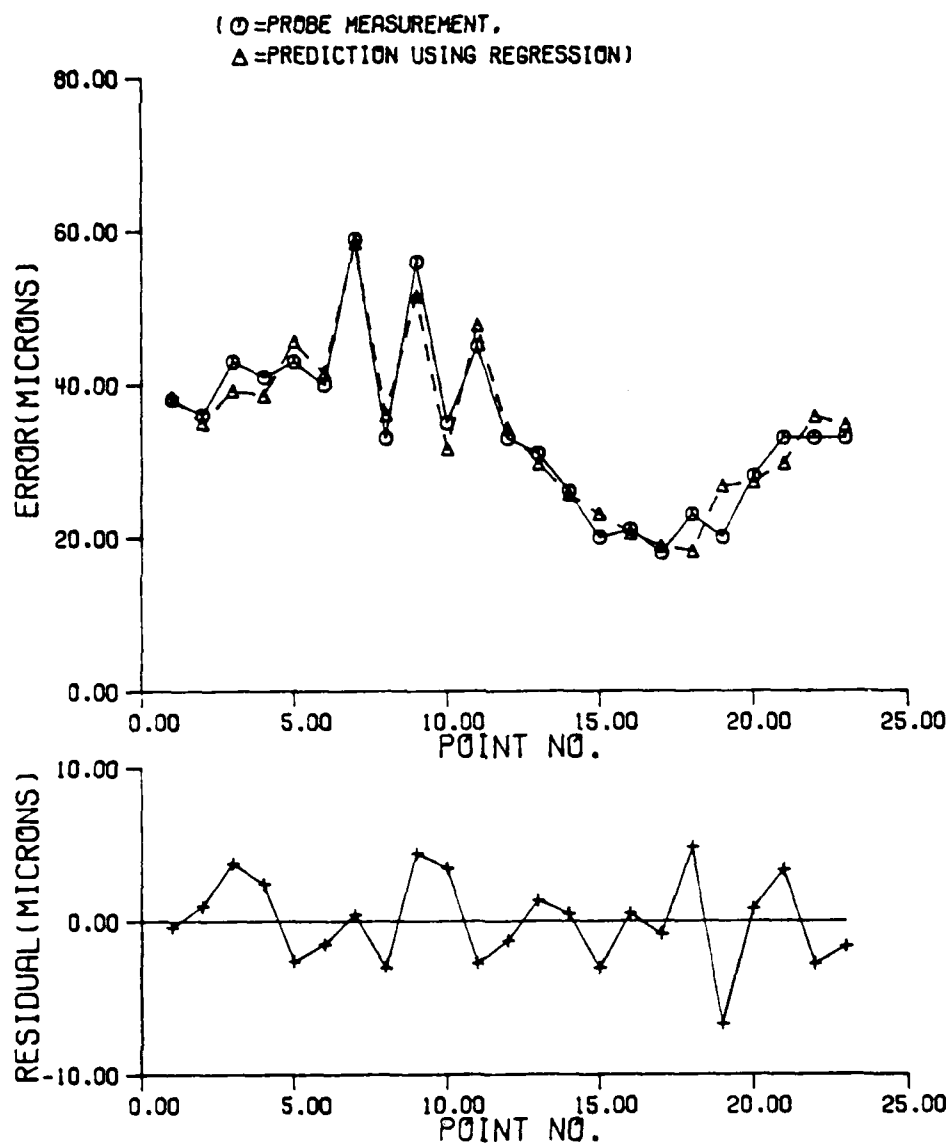


Figure A.4.7 The regression result of z absolute errors of test 11 and residual for short probe.

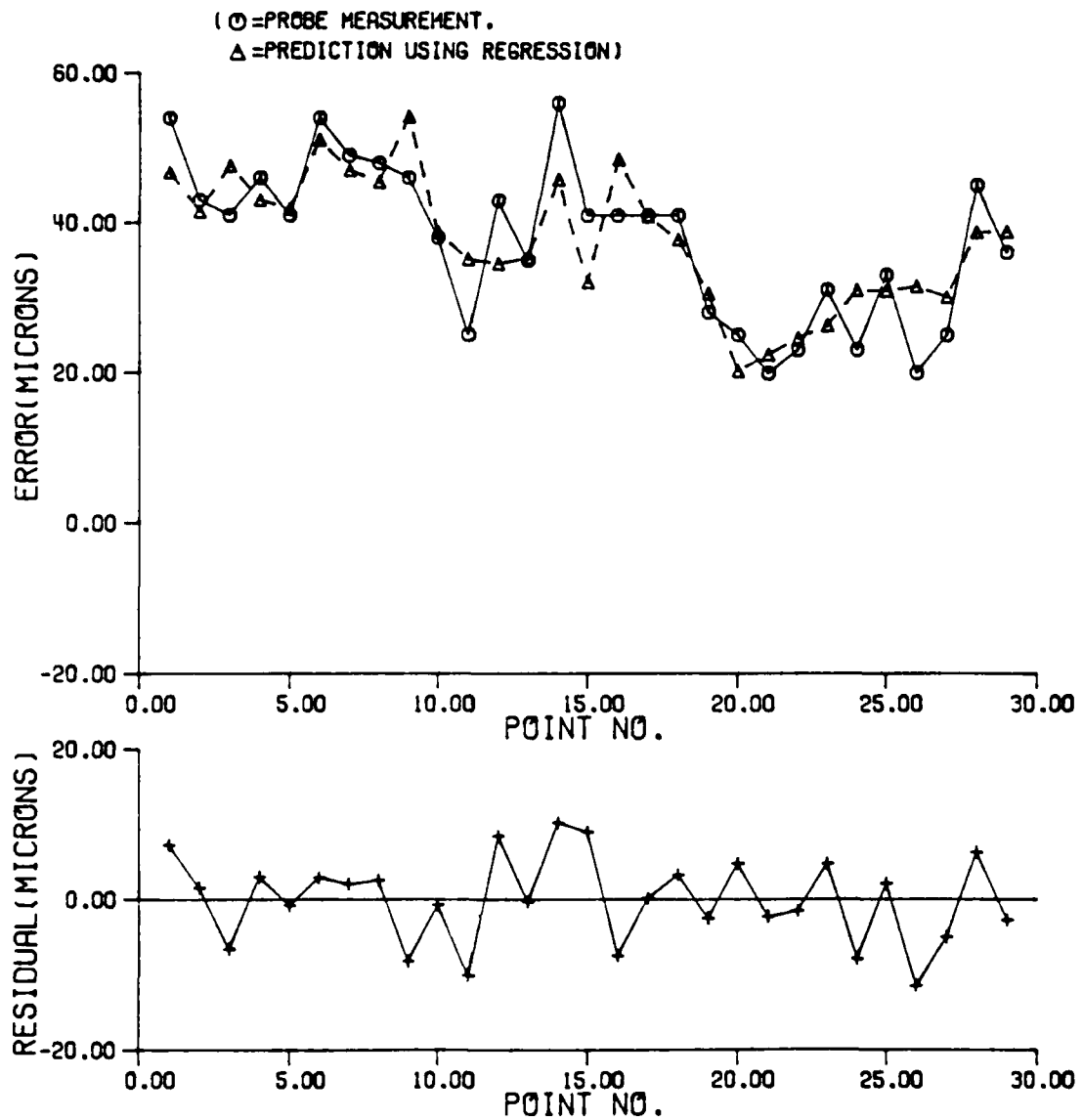


Figure A.4.8 The regression result of z absolute errors or test 11 and residual for long probe.

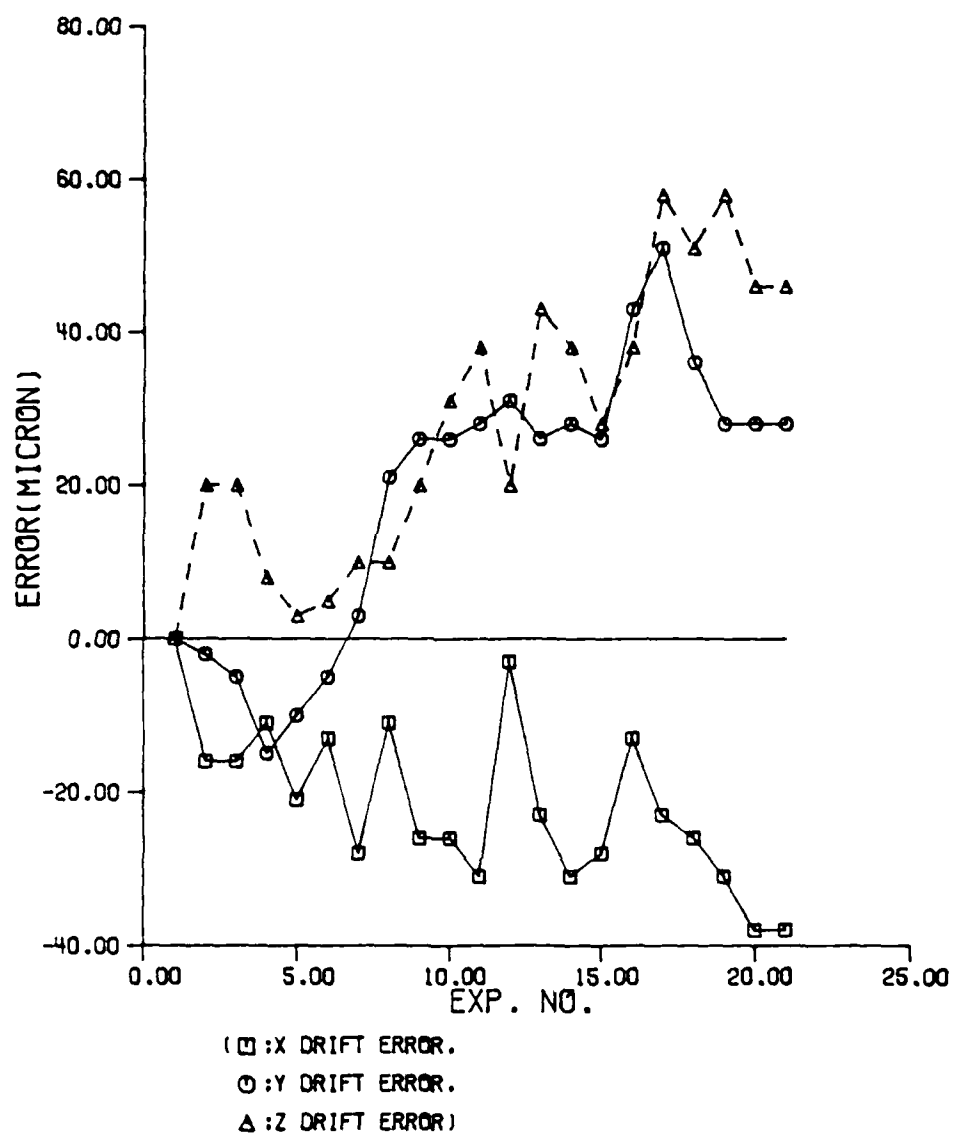


Figure A.4.9 The variation of x, y, and z errors for the measurement origin during three day experiment.

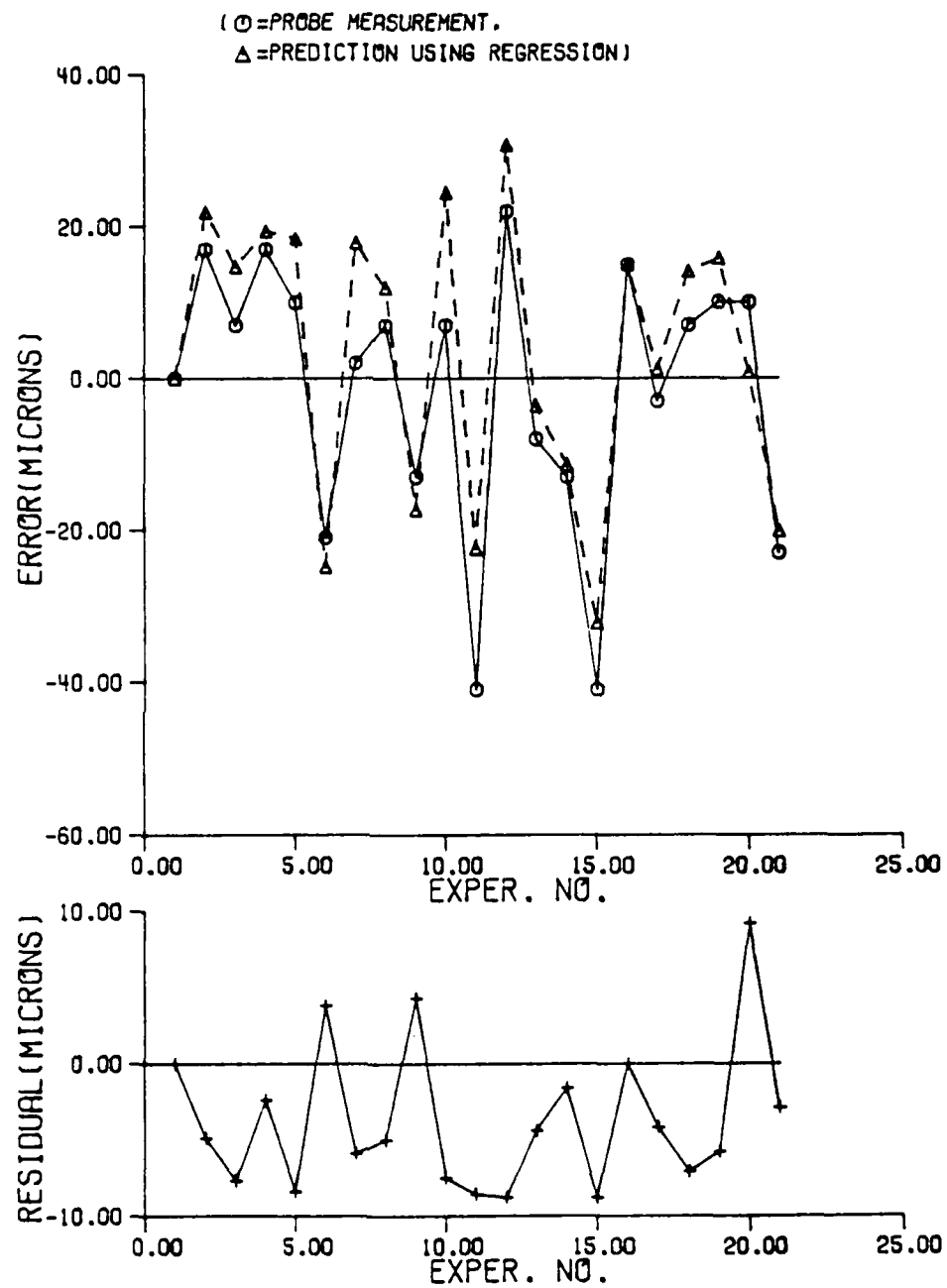


Figure A.4.10 The regression result of x absolute errors of point 1 and residual for long probe.

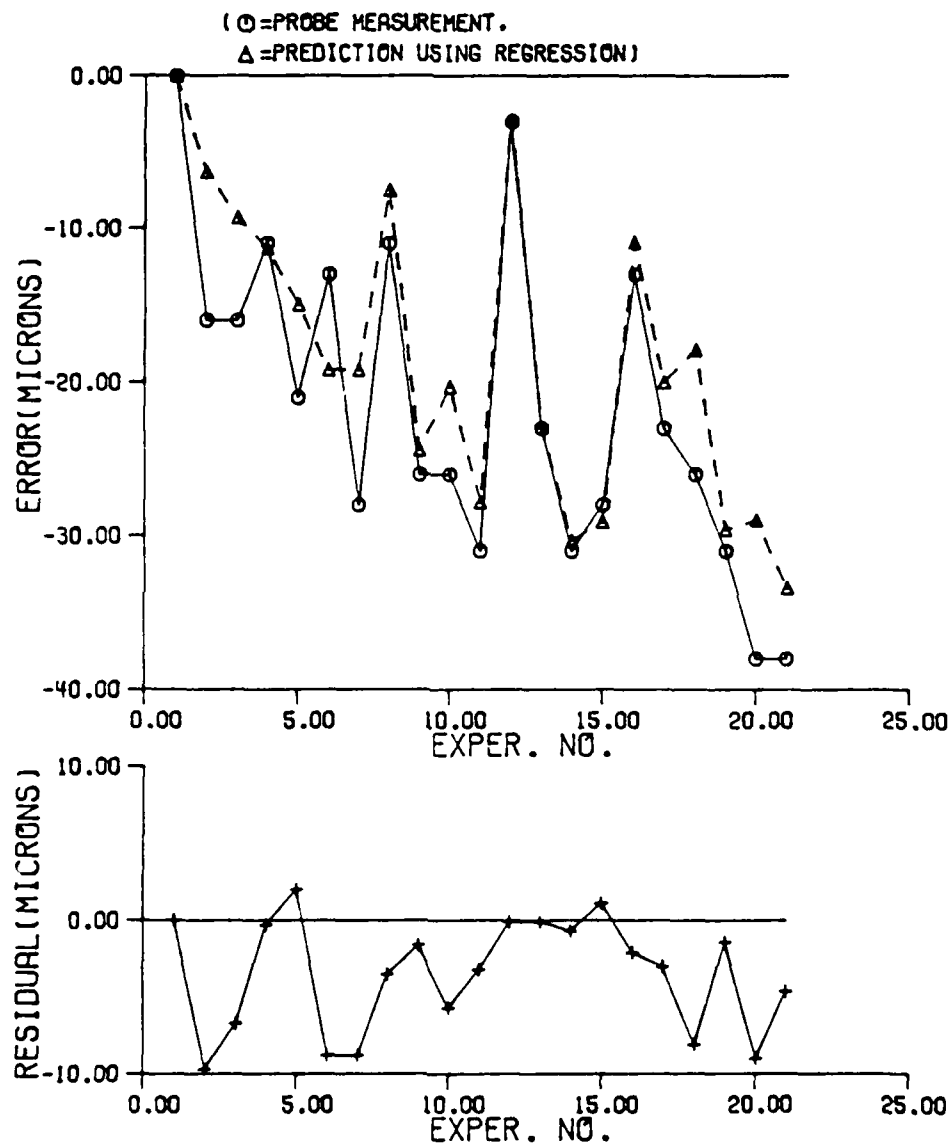


Figure A.4.11 The regression result of x absolute errors of point 1 and residual for two probe.

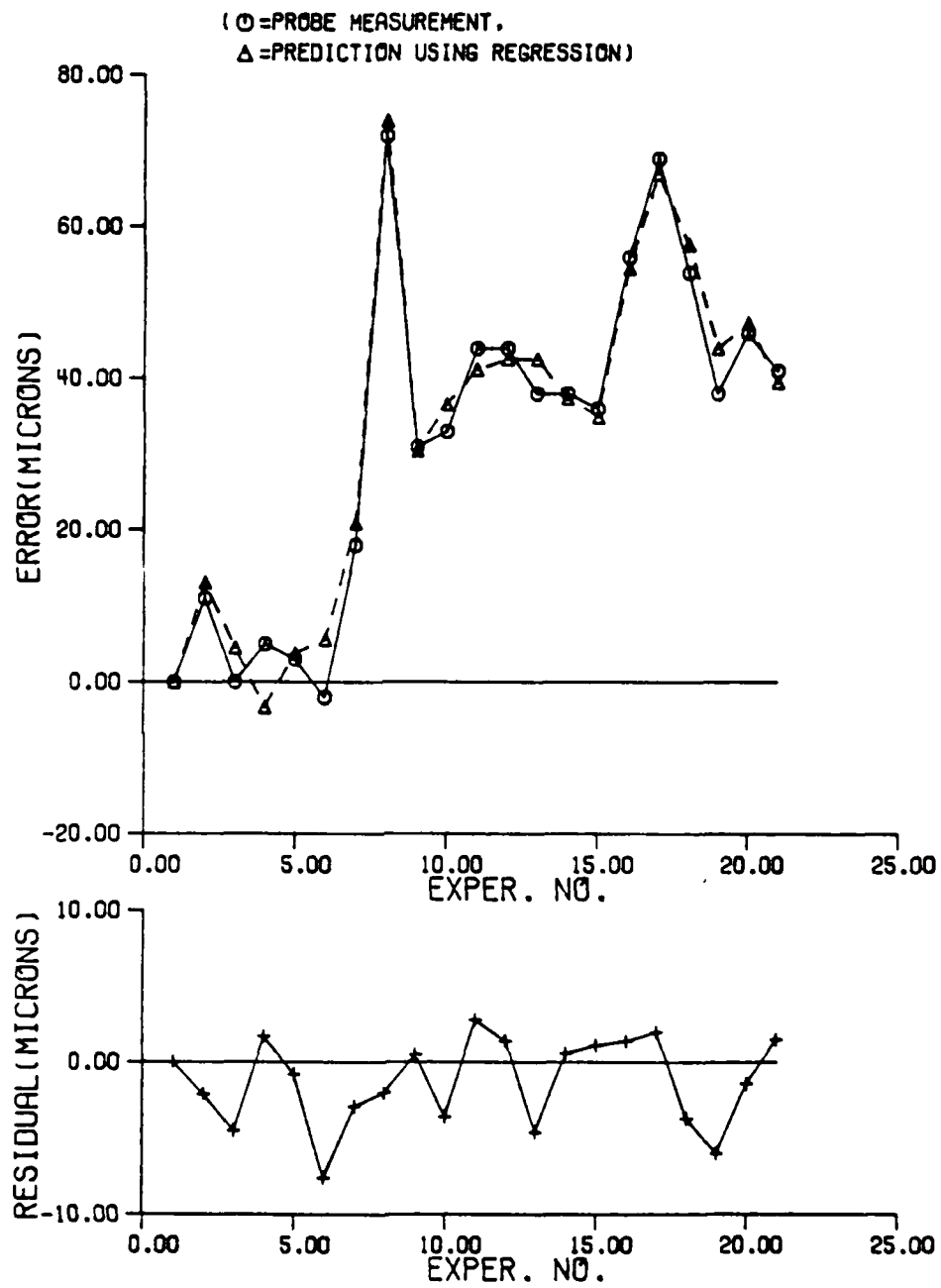


Figure A.4.12 The regression result of y absolute errors of point 1 and residual for long probe.

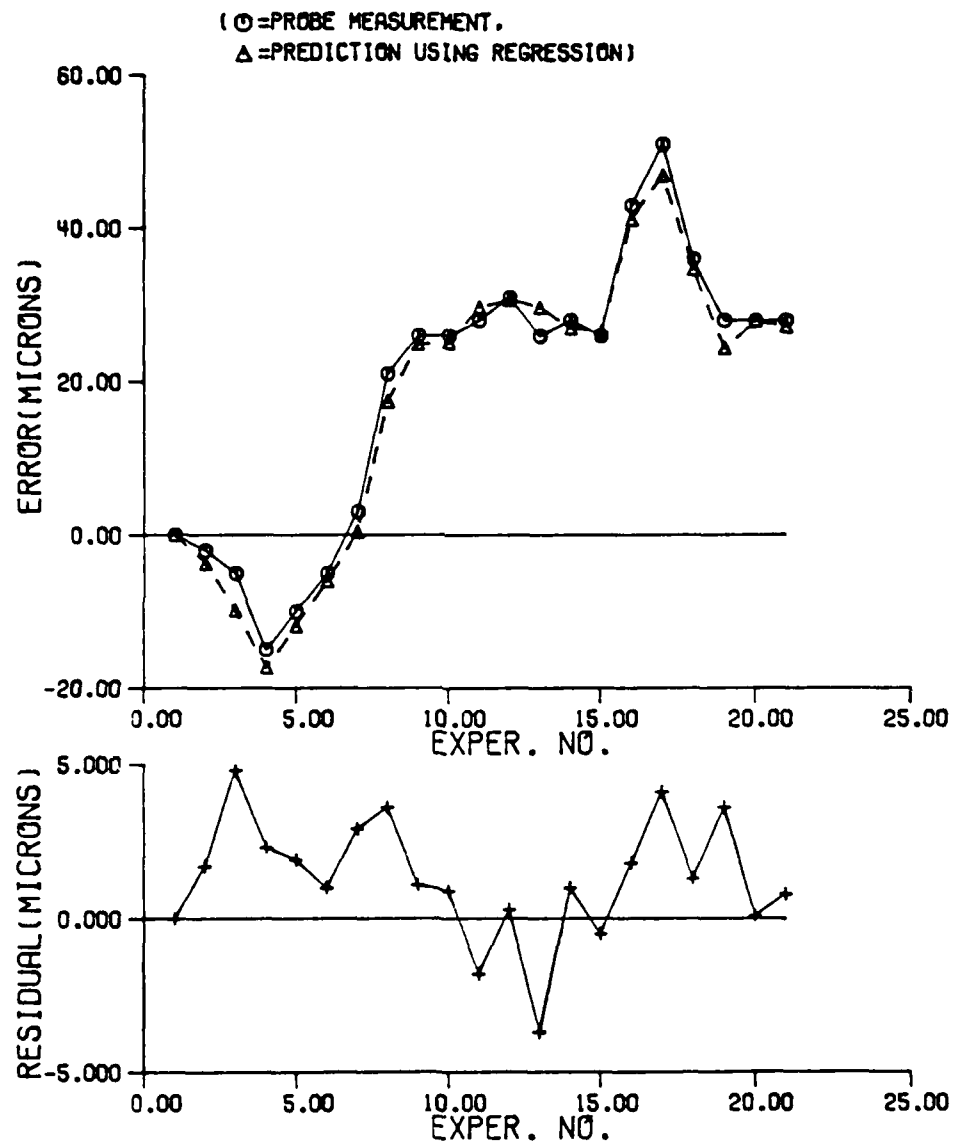


Figure A.4.13 The regression result of y absolute errors of point 1 and residual for two probe.

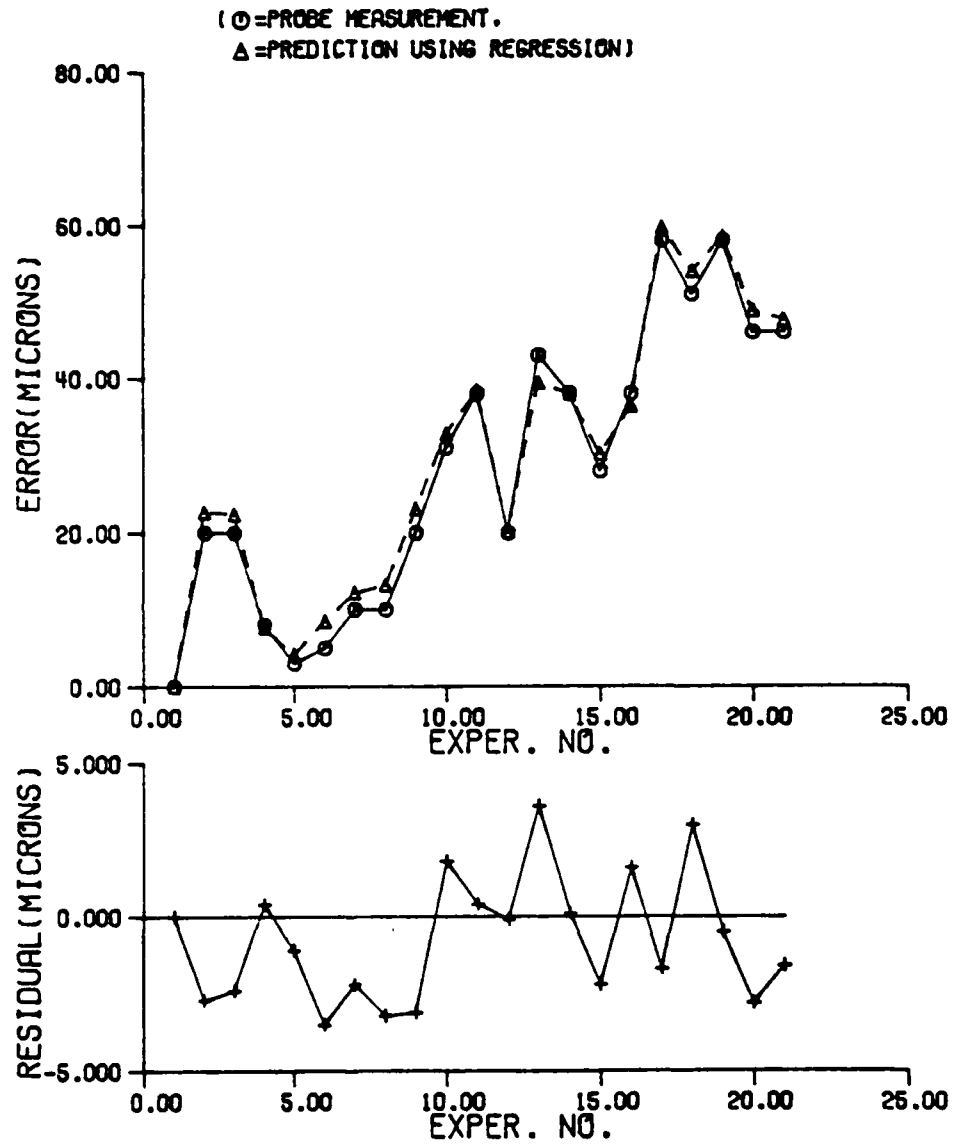


Figure A.4.14 The regression result of z absolute errors of point 1 and residual for short probe.

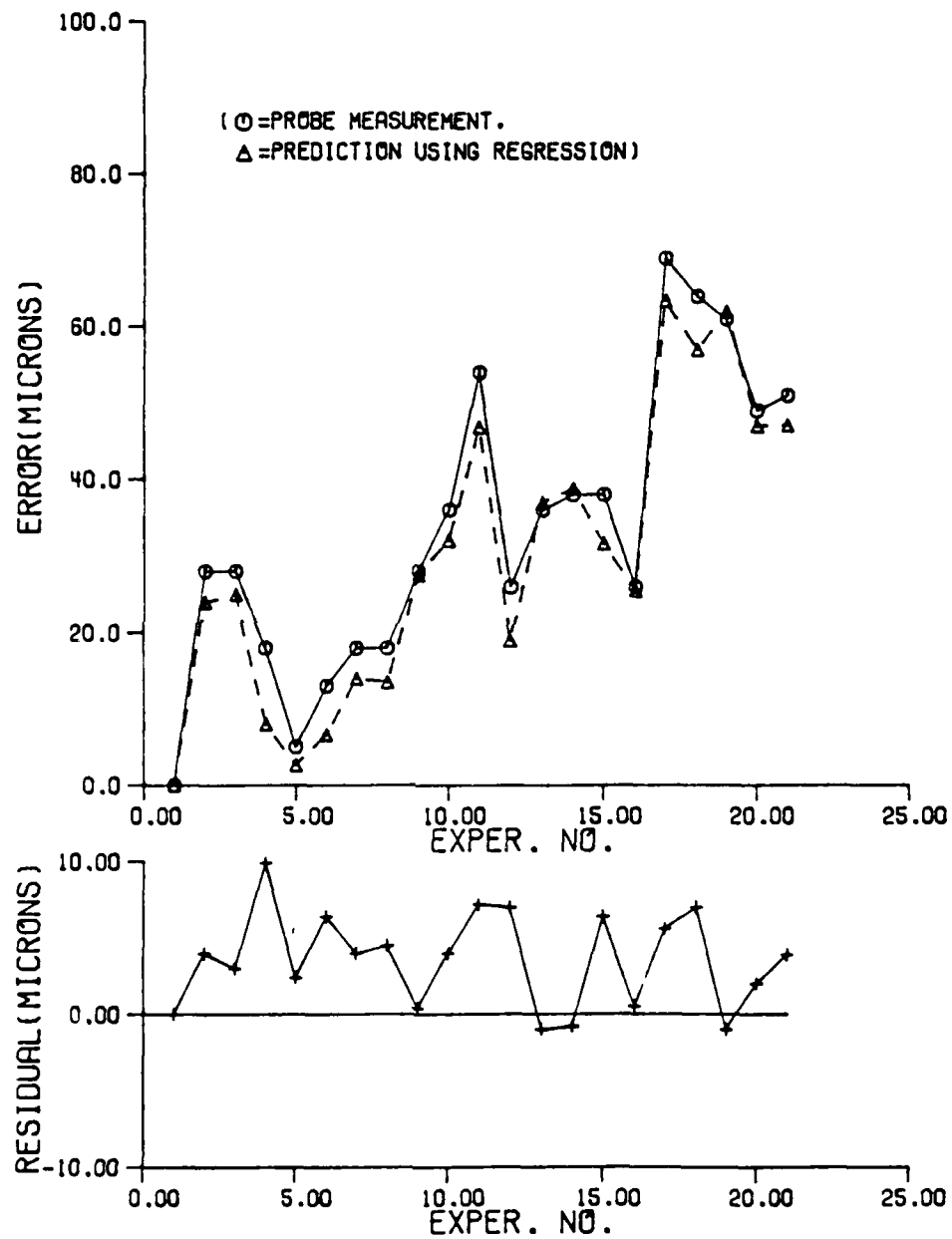


Figure A.4.15 The regression result or z absolute errors of point 1 and residual for long probe.

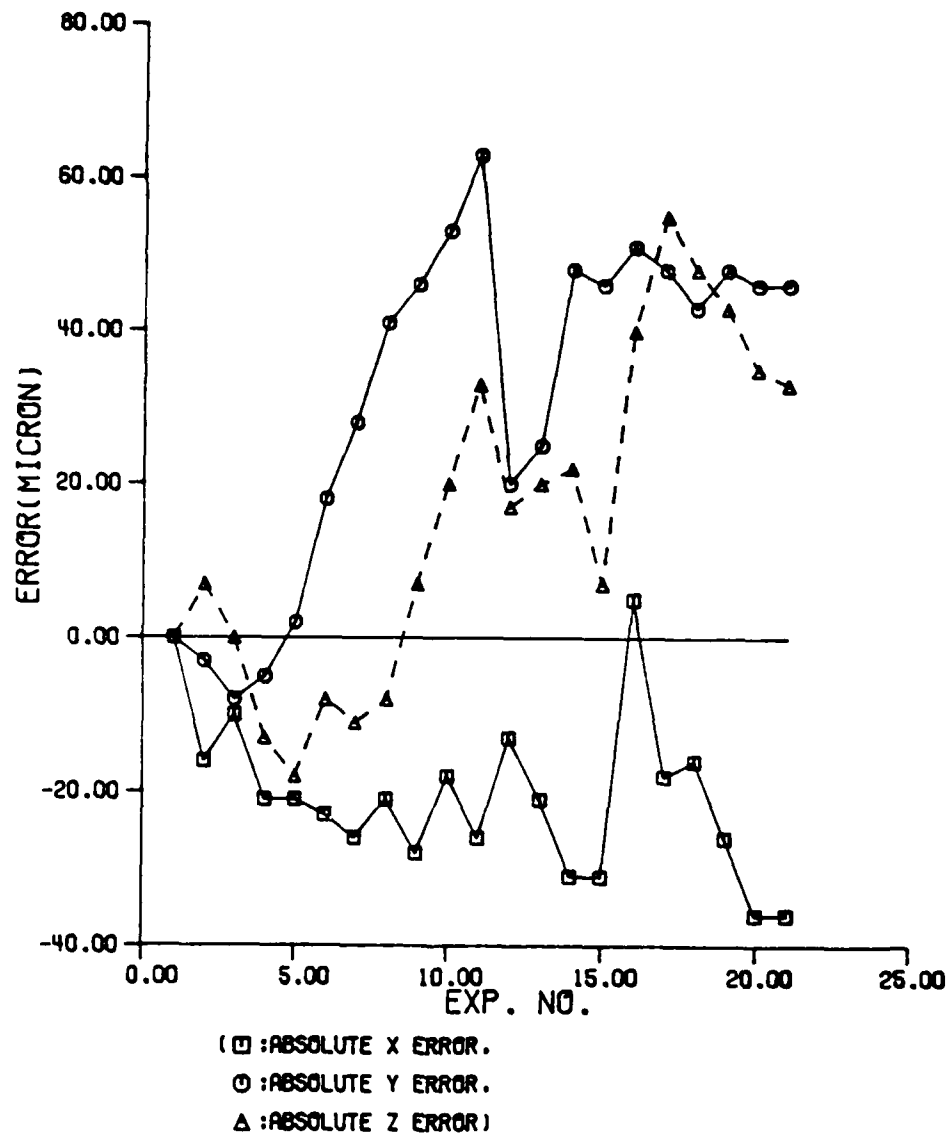


Figure A.4.16 The variation of absolute error for point 11 during experiment.

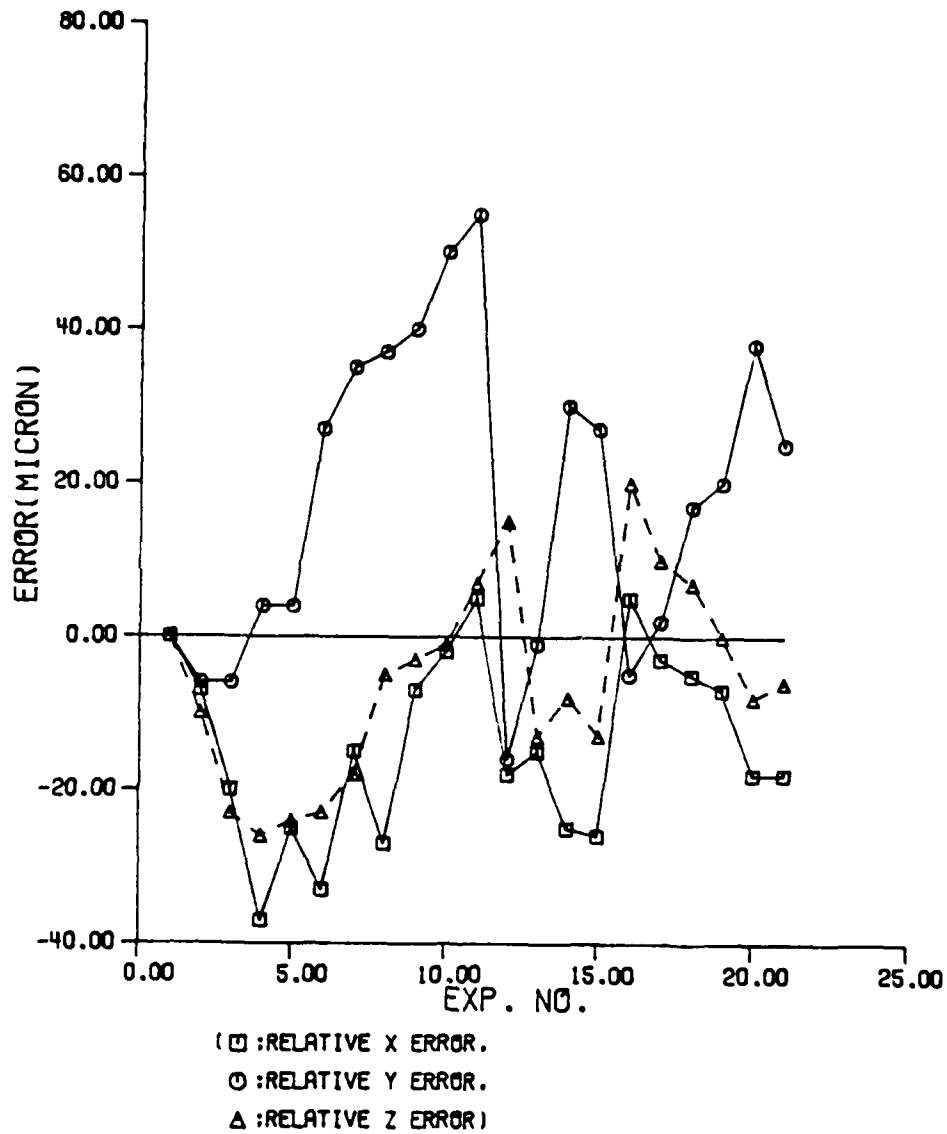


Figure A.4.17 The variation of relative error for point 11 during experiment.

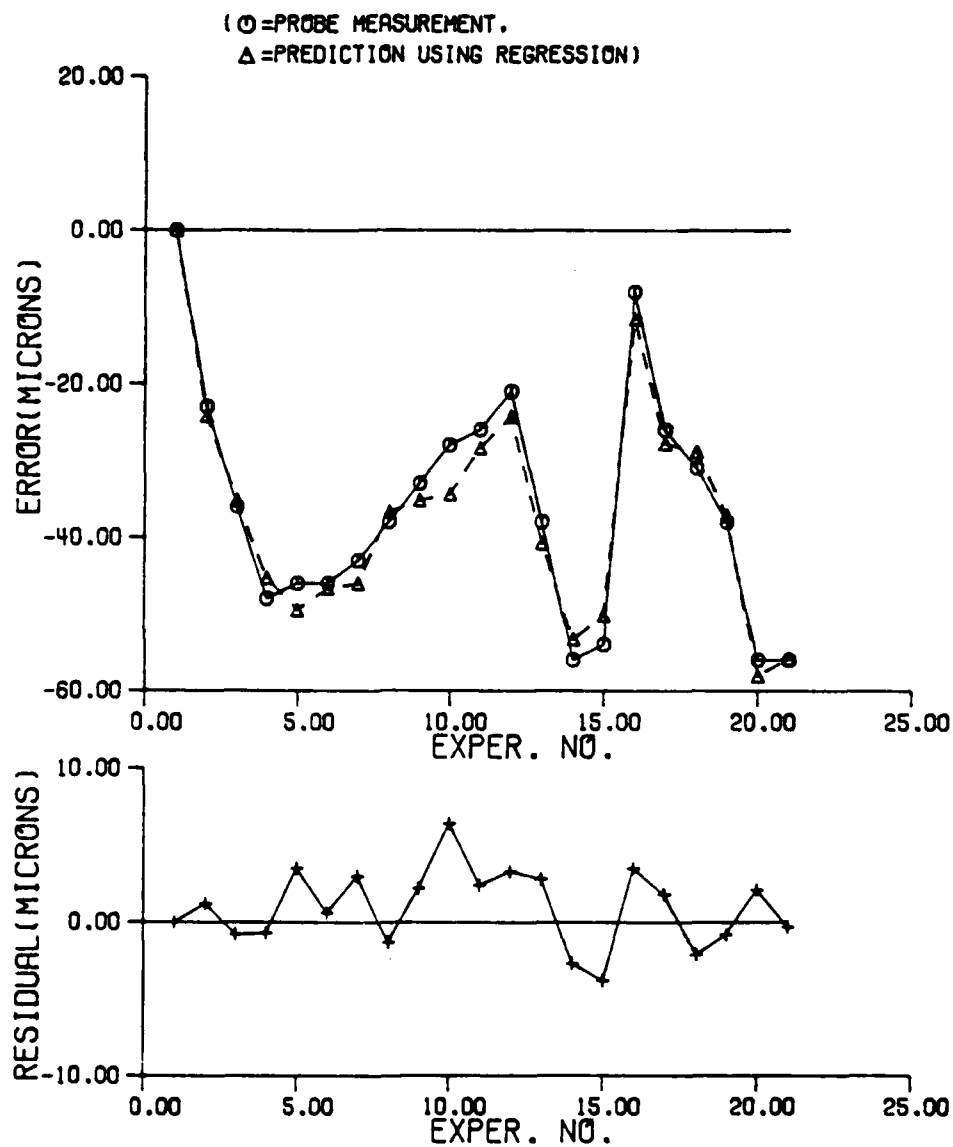


Figure A.4.18 The regression result of x absolute errors of point 11 and residual for short probe.

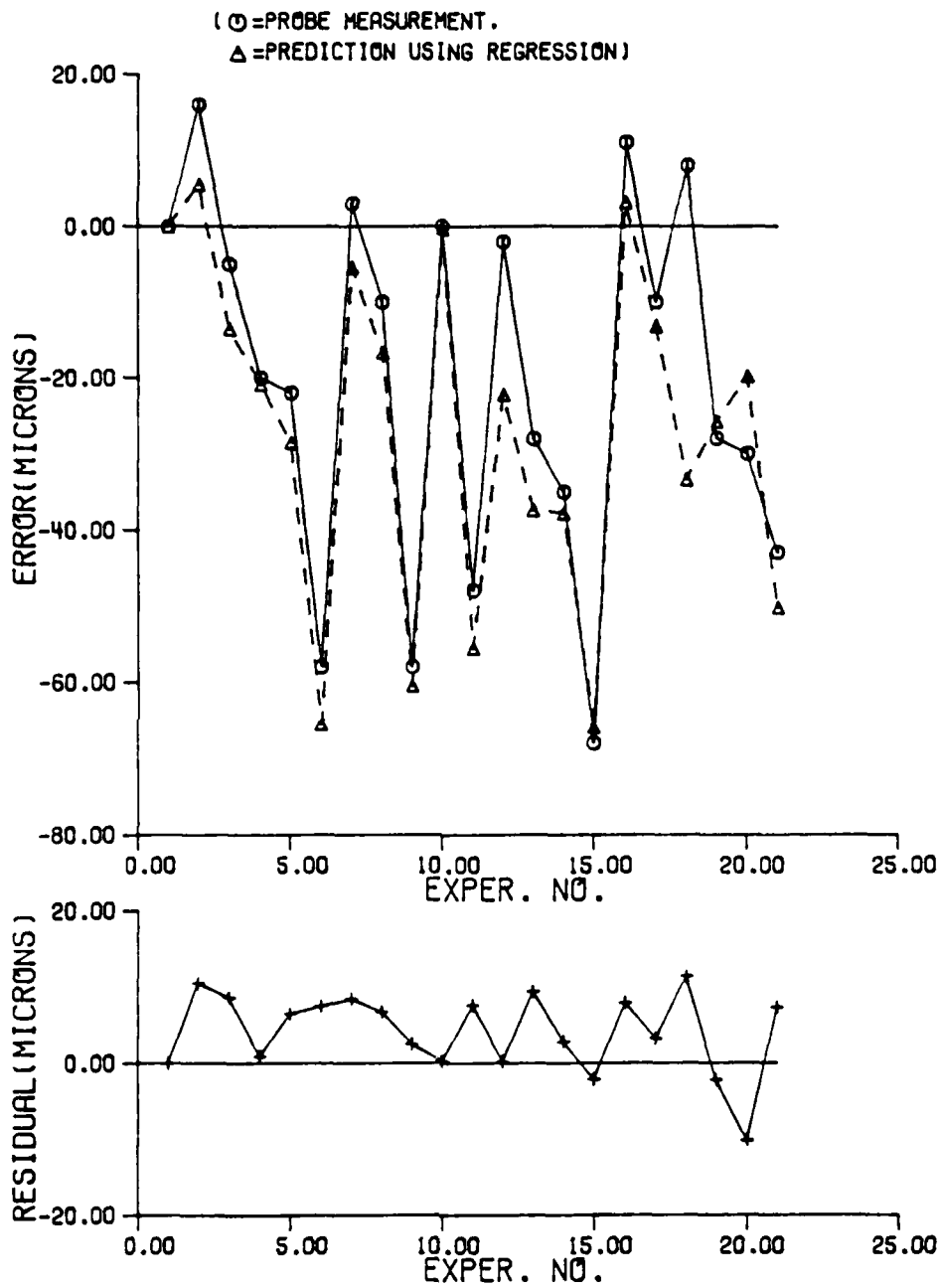


Figure A.4.19 The regression result of x absolute errors of point 11 and residual for long probe.

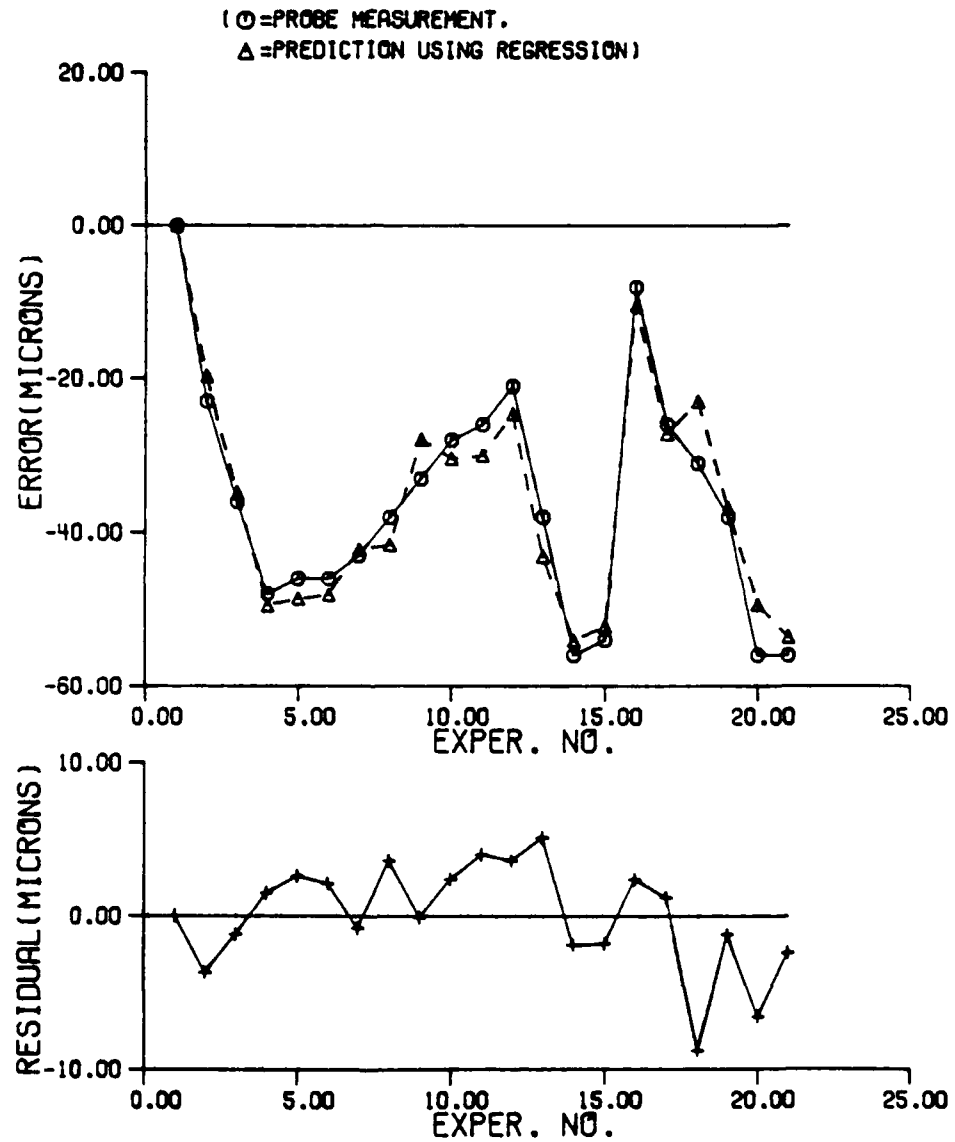


Figure A.4.20 The regression result of x absolute errors of point 11 and residual for two probe.

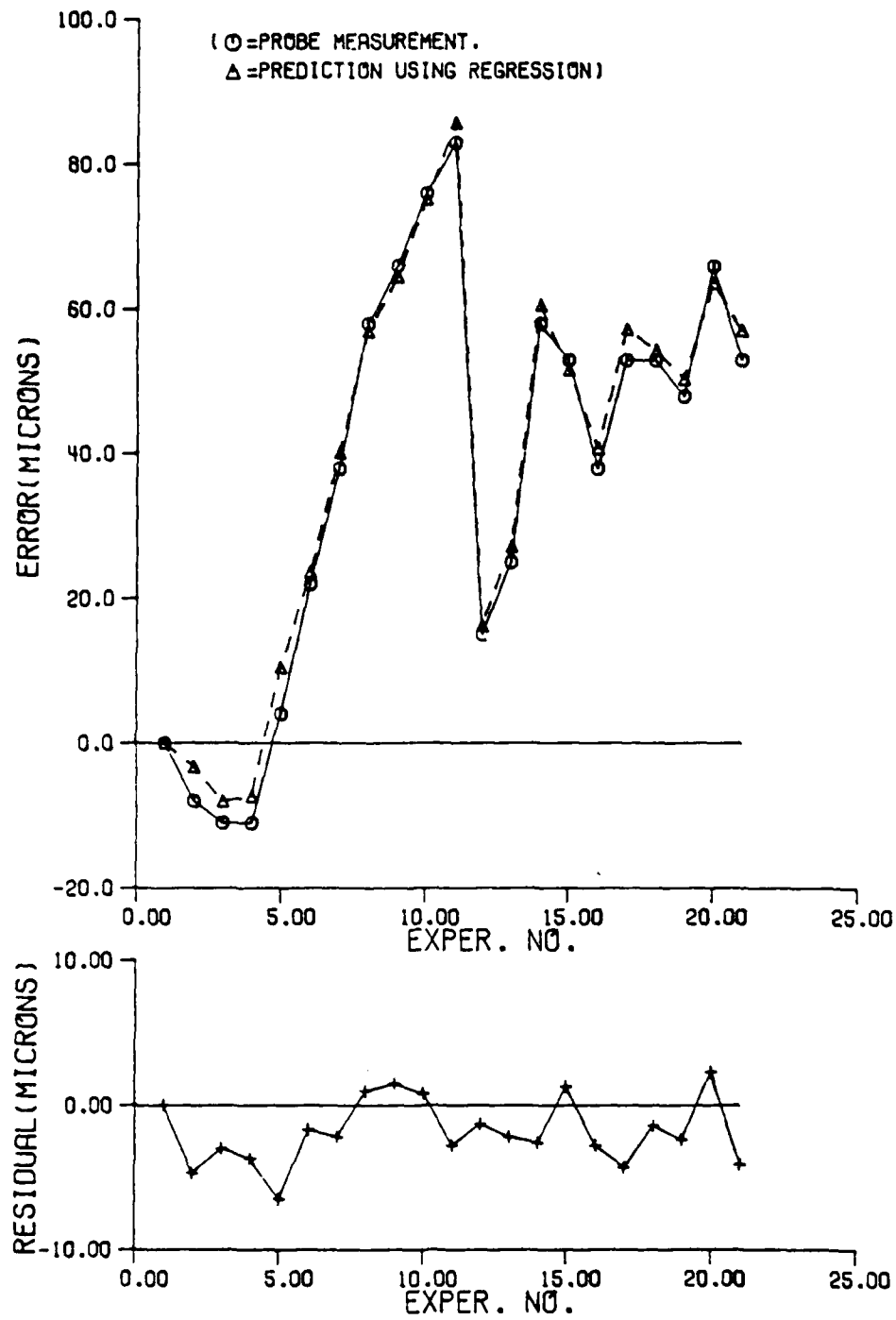


Figure A.4.21 The regression result of y absolute errors of point 11 and residual for short probe.

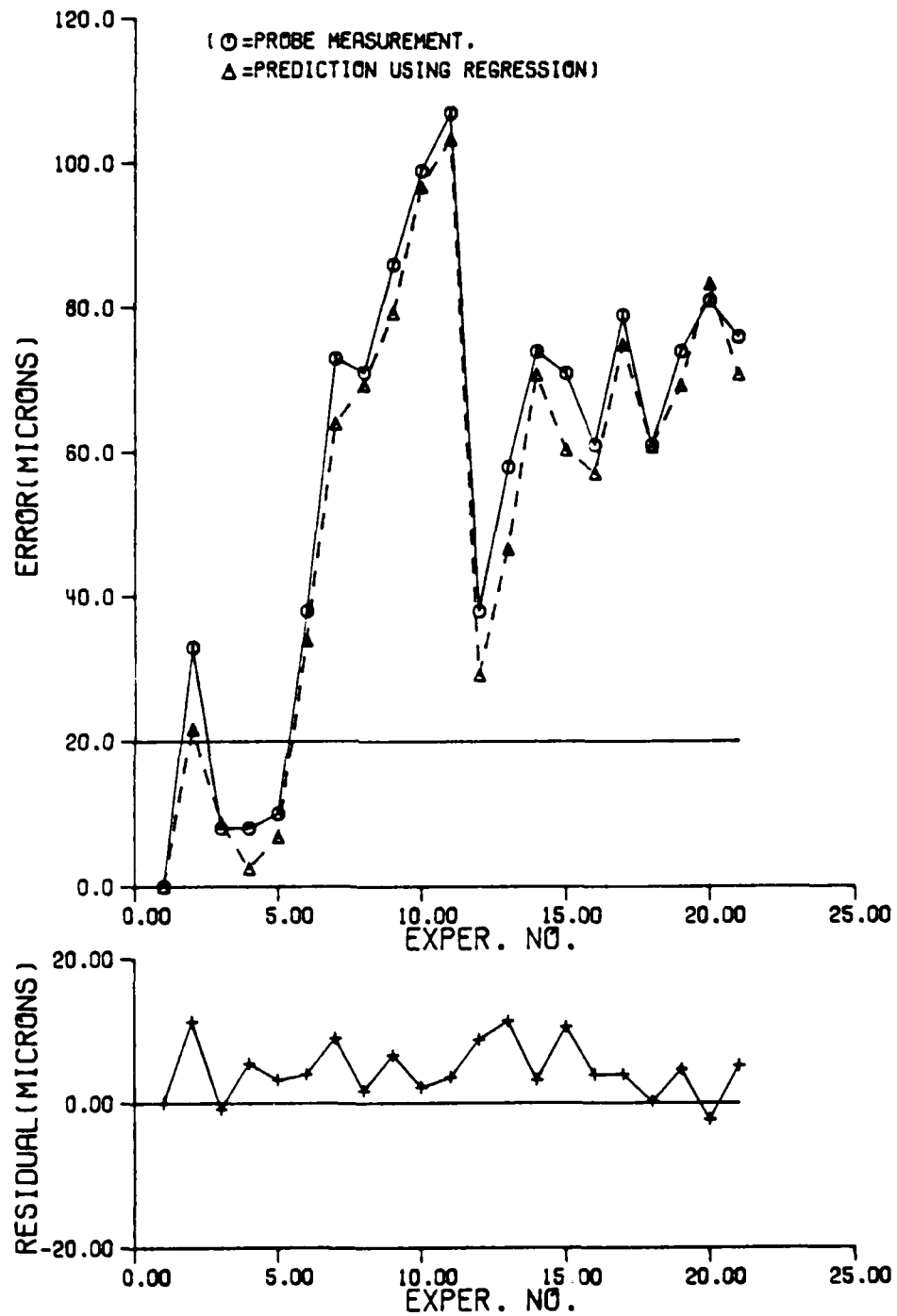


Figure A.4.22 The regression result of y absolute errors of point 11 and residual for long probe.

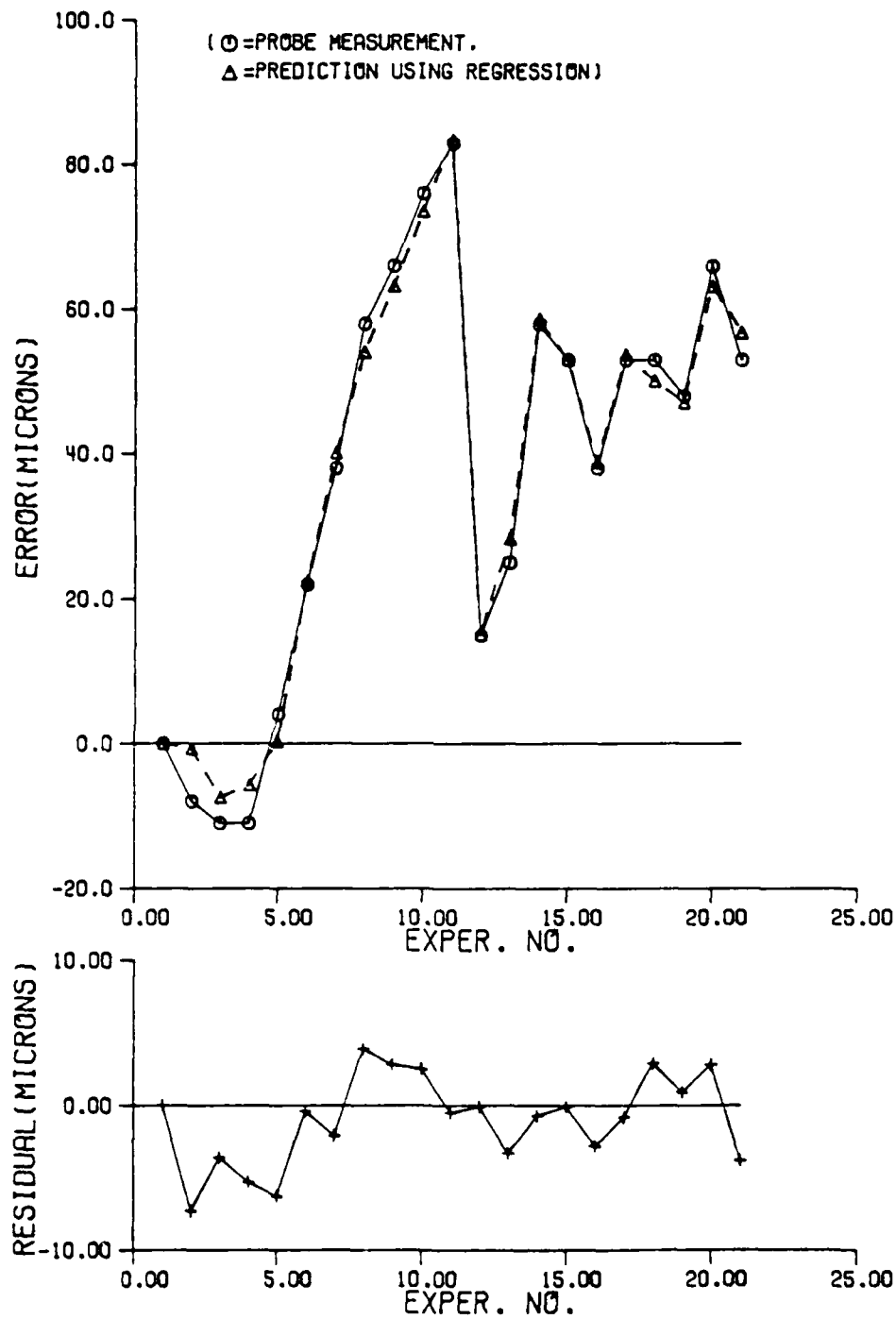


Figure A.4.23 The regression result of y absolute errors of point 11 and residual for two probe.

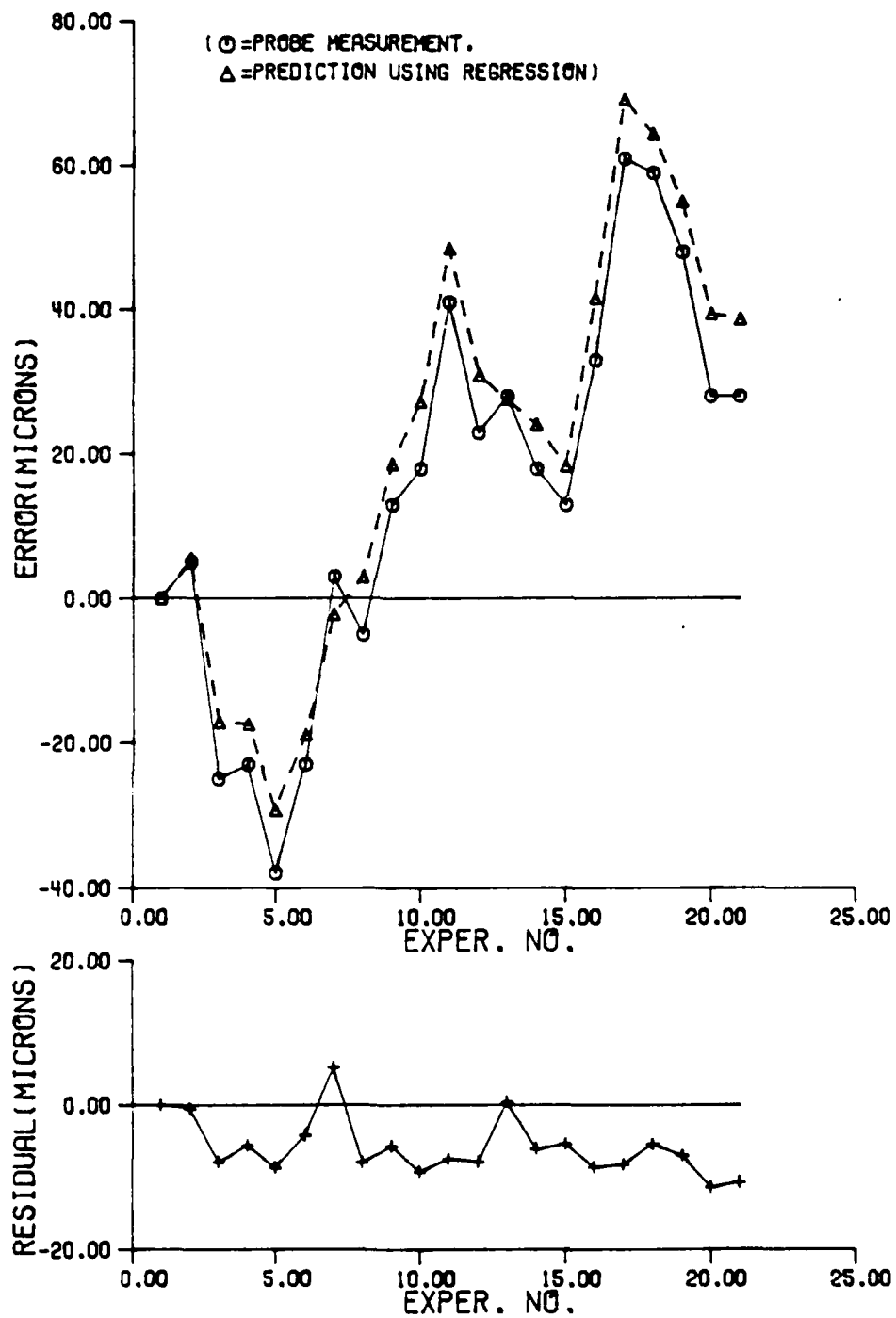


Figure A.4.24 The regression result of z absolute errors of point 11 and residual for long probe.

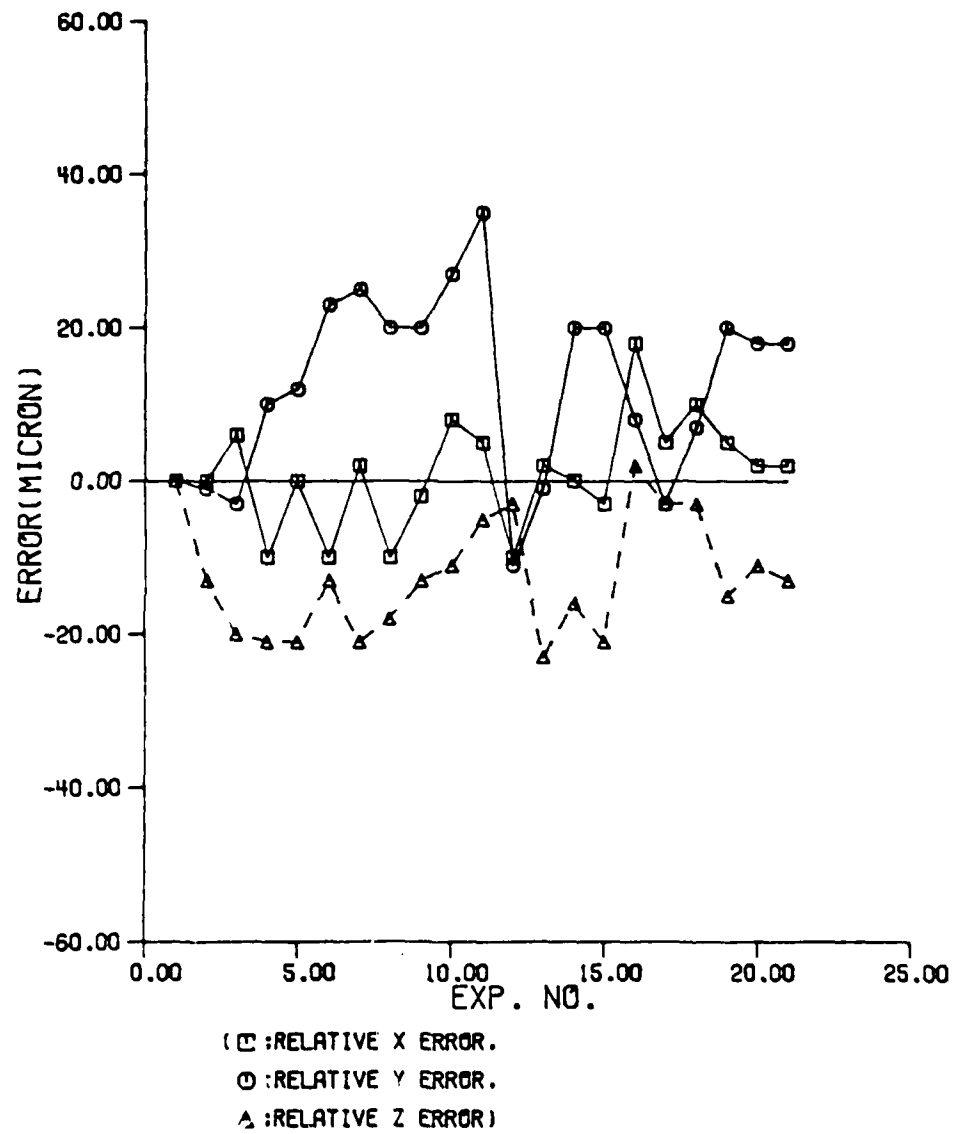
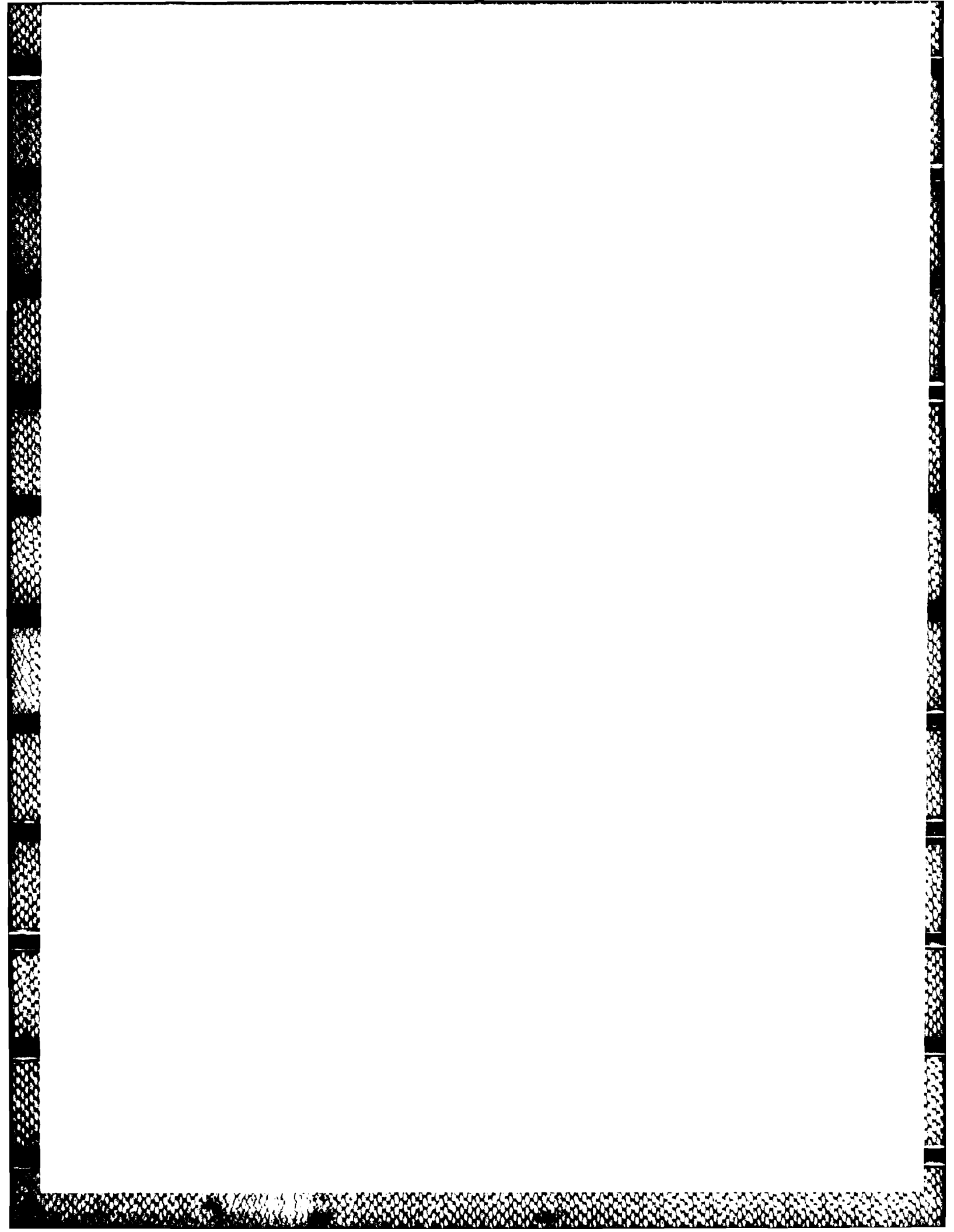


Figure A.4.25 The variation of relative error for point 22 during experiment.



Appendix 5 - Repeatability Data for Probing Experiment

Table A.5.1. Repeatability result of test no. 1 for three positions for a short and a long probes (s.d.=standard deviation,in micro meter)

Posi- tion	Axis	short probe		long probe	
		s.d.	range	s.d.	range
no. 1	x	3.3	13.0	4.1	13.0
	y	1.0	2.0	3.4	12.0
	z	2.3	7.0	3.5	10.0
no. 11	x	3.3	10.0	5.2	17.0
	y	2.5	10.0	2.2	8.0
	z	4.2	15.0	2.6	10.0
no. 18	x	2.8	10.0	6.0	17.0
	y	2.6	8.0	4.5	13.0
	z	3.2	10.0	2.4	7.0

Table A.5.2. Repeatability result of test no. 7 for three positions for a short and a long probes (s.d.=standard deviation,in micro meter)

Posi- tion	Axis	short probe		long probe	
		s.d.	range	s.d.	range
no. 1	x	3.3	12.0	5.6	18.0
	y	4.0	13.0	4.5	15.0
	z	2.7	7.0	2.6	8.0
no. 11	x	5.4	18.0	10.9	28.0
	y	2.1	5.0	5.8	20.0
	z	4.5	15.0	6.3	23.0
no. 18	x	3.4	11.0	9.7	30.0
	y	3.4	13.0	3.9	15.0
	z	3.3	13.0	3.2	8.0

Table A.5.3. Repeatability result of test no. 11 for three positions for a short and a long probes (s.d.=standard deviation,in micro meter)

Posi- tion	Axis	short probe		long probe	
		s.d.	range	s.d.	range
no.	x	3.5	12.0	11.1	33.0
1	y	5.0	18.0	4.4	15.0
	z	1.6	3.1	2.0	8.0
no.	x	4.1	12.0	7.0	25.0
11	y	3.9	13.0	3.5	12.0
	z	3.7	13.0	2.9	7.0
no.	x	3.1	10.0	10.3	35.0
18	y	3.0	8.0	6.9	23.0
	z	3.4	12.0	4.2	13.0

Table A.5.4. Repeatability result of test no. 19 for three positions for a short and a long probes (s.d.=standard deviation,in micro meter)

Posi- tion	Axis	short probe		long probe	
		s.d.	range	s.d.	range
no.	x	2.5	10.0	9.9	28.0
1	y	4.0	12.0	5.5	20.0
	z	2.0	8.1	2.5	7.0
no.	x	5.0	15.0	6.9	23.0
11	y	4.0	13.0	6.6	23.0
	z	2.5	7.0	3.9	12.0
no.	x	4.6	13.0	8.9	31.0
18	y	1.5	5.0	5.0	18.0
	z	2.0	8.0	3.2	12.0

Table A.5.5. Repeatability result of test no. 21 for three positions for a short and a long probes (s.d.=standard deviation,in micro meter)

Position	Axis	short probe		long probe	
		s.d.	range	s.d.	range
no. 1	x	3.8	10.0	6.1	20.0
	y	2.8	10.0	2.5	8.0
	z	2.9	11.0	3.1	8.0
no. 11	x	4.4	13.0	8.3	30.0
	y	3.0	10.0	5.6	21.0
	z	4.1	13.0	3.4	10.0
no. 18	x	3.0	8.0	7.9	25.0
	y	4.3	13.0	3.6	13.0
	z	2.8	10.0	2.8	10.0

Appendix 6 - Result of Decomposition Procedure

Results of decomposition procedure for test number 11 are presented out of those of 21 tests. These include the quadratic and the linear assumption for a short and a long probe approach. Result of two probe approach is also presented. One example of Fortran program to calculate decomposed coefficients of error equations is also presented.

Table A.6.1 The result of decomposition procedure for a short probe of test no. 11 with the quadratic assumption of positioning errors

*** Coefficients of error equations.***

c(2)= -0.50536e-06
 c(4)= 0.26099e-05
 c(6)= 0.55805e-05
 c(7)= 0.10062e-05
 c(11)= -0.71547e-05
 c(14)= 0.19268e-04
 c(17)= 0.28751e-04
 c(18)= 0.79510e-04
 c(21)= 0.72126e-07
 c(23)= 0.13051e-07
 c(25)= -0.13728e-05
 c(29)= -0.15413e-06
 c(30)= 0.78381e-04
 c(32)= 0.55431e-04
 c(33)= -0.22488e-04
 c(34)= 0.40847e-05

Calculation of relative errors using cal. coefficients

no.	rerrorx	cal.ery	rerrory	cal.ery	rerrorz	cal.erz
2	13.0	-36.7	5.0	-141.4	-2.0	-9.3
3	1.0	-37.1	5.0	-136.5	5.0	-4.7
4	8.0	-36.1	26.0	-122.5	3.0	-6.4
5	3.0	-39.4	36.0	-116.0	5.0	6.9
6	-2.0	-40.3	48.0	-96.8	2.0	7.4
7	-7.0	-44.6	61.0	-87.9	21.0	19.8
8	-15.0	-39.1	66.0	-87.9	-5.0	-0.0
9	-9.0	-44.1	58.0	-89.0	18.0	13.6
10	1.0	-38.5	58.0	-88.5	-3.0	-4.4
11	5.0	-42.9	55.0	-89.7	7.0	7.5
12	6.0	-40.7	63.0	-86.5	-5.0	0.1
13	8.0	-37.2	33.0	-118.6	-7.0	-5.8
14	-2.0	-35.4	38.0	-110.0	-12.0	-12.2
15	6.0	-32.3	20.0	-132.1	-18.0	-25.0
16	8.0	-32.9	7.0	-134.9	-17.0	-23.1
17	6.0	-33.6	17.0	-137.9	-20.0	-21.4
18	-2.0	-34.4	10.0	-142.8	-15.0	-19.8
19	10.0	-36.0	5.0	-142.1	-18.0	-13.7
20	6.0	-36.1	23.0	-122.3	-10.0	-9.5
21	3.0	-36.2	32.0	-118.5	-5.0	-8.5
22	5.0	-38.6	35.0	-118.3	-5.0	0.1
23	11.0	-37.2	15.0	-122.0	-5.0	-3.6

Table A.6.2 The result of decomposition procedure for a long probe of test no. 11 with the quadratic assumption of positioning errors

*** Coefficients of error equations.***						
c(2)=	-0.35823e-07					
c(4)=	-0.79234e-05					
c(6)=	0.66461e-05					
c(7)=	-0.31501e-04					
c(11)=	-0.59633e-06					
c(14)=	0.97168e-04					
c(17)=	0.70843e-04					
c(18)=	0.72661e-04					
c(21)=	-0.40682e-07					
c(23)=	0.38246e-07					
c(25)=	0.48120e-07					
c(29)=	-0.46238e-07					
c(30)=	0.33821e-04					
c(32)=	0.37707e-04					
c(33)=	-0.18185e-04					
c(34)=	-0.18201e-04					

Cal. of relative errors using cal. coefficients						
no.	rerrorx	cal.ery	rerrory	cal.ery	rerrorz	cal.ery
2	26.0	-22.9	2.0	-130.3	-11.0	-19.4
3	26.0	-20.3	2.0	-127.1	-12.9	-16.1
4	16.0	-20.5	9.0	-113.7	-8.0	-15.6
5	21.0	-19.9	22.0	-109.3	-13.0	-16.5
6	6.0	-23.9	33.0	-105.6	0.1	-7.8
7	16.0	-31.3	47.0	-83.6	-4.9	-5.6
8	8.0	-33.3	55.0	-75.2	-5.9	-6.0
9	-13.0	-40.5	62.0	-70.8	-7.9	1.9
10	11.0	-35.3	63.0	-72.8	-16.0	-9.1
11	1.0	-29.3	93.0	-75.5	-29.0	-16.0
12	11.0	-23.2	55.0	-88.8	-11.0	-19.8
13	-7.0	-20.5	35.0	-89.0	-19.0	-23.8
14	-17.0	-47.1	63.0	-66.8	2.1	-3.1
15	0.	-40.2	63.0	-70.0	-13.0	-12.7
16	-7.0	-52.7	63.1	-64.0	-12.9	-8.1
17	-2.0	-51.0	65.0	-62.0	-13.0	-11.7
18	-20.0	-37.1	40.0	-99.6	-12.9	-18.2
19	-7.9	-37.1	35.0	-91.8	-25.9	-20.6
20	3.0	-33.4	22.0	-115.7	-29.0	-29.7
21	21.0	-34.1	17.0	-117.8	-34.0	-29.0
22	-10.0	-34.9	34.0	-120.2	-30.9	-28.5
23	2.0	-35.4	4.0	-124.5	-22.9	-28.0
24	15.0	-28.6	2.0	-127.3	-30.9	-23.0
25	8.0	-31.1	30.0	-106.6	-20.9	-19.4
26	8.0	-28.9	20.0	-104.3	-33.9	-17.9
27	18.0	-29.1	34.0	-99.0	-28.9	-18.0
28	5.0	-30.6	38.0	-103.0	-9.0	-13.3
29	11.0	-25.1	15.0	-109.9	-17.9	-14.6

Table A.6.3 The decomposition result for a long probe of test no. 11 with the linear assumption of positioning errors

*** Coefficients of error equations.***						
c(2)=	0.54073e-06					
c(4)=	0.31572e-05					
c(7)=	-0.25589e-04					
c(11)=	0.24532e-06					
c(14)=	0.11262e-03					
c(18)=	0.11537e-03					
c(21)=	0.27687e-08					
c(23)=	0.89962e-07					
c(25)=	0.24665e-06					
c(30)=	0.91149e-05					
c(32)=	0.30545e-04					
c(33)=	-0.19756e-04					
c(34)=	-0.17674e-04					

Calculation of relative errors using calculated coefficient						
no.	rerrorx	cal.erx	rerrory	cal.ery	rerrorz	cal.erz
2	26.0	19.0	2.0	-5.5	-11.0	-20.1
3	26.0	21.4	2.0	-0.5	-12.9	-17.1
4	16.0	21.4	9.0	15.0	-8.0	-15.3
5	21.0	21.9	22.0	19.4	-13.0	-15.1
6	6.0	17.3	33.0	24.7	0.1	-10.4
7	16.0	8.8	47.0	44.8	-4.9	-7.3
8	8.0	6.3	55.0	51.7	-5.9	-6.5
9	-13.0	-1.9	62.0	54.9	-7.9	-2.3
10	11.0	4.4	63.0	54.3	-16.0	-8.9
11	1.0	11.3	93.0	52.0	-29.0	-12.2
12	11.0	18.4	55.0	39.7	-11.0	-15.2
13	-7.0	21.4	35.0	38.8	-19.0	-16.9
14	-17.0	-9.2	63.0	59.8	2.1	-7.8
15	0.	-1.3	63.0	58.3	-13.0	-13.0
16	-7.0	-16.5	63.1	65.3	-12.9	-13.3
17	-2.0	-14.8	65.0	67.4	-13.0	-14.9
18	-20.0	3.3	40.0	34.1	-12.9	-21.6
19	-7.9	2.9	35.0	41.6	-25.9	-22.0
20	3.0	8.7	22.0	14.2	-29.0	-29.3
21	21.0	8.0	17.0	11.9	-34.0	-29.4
22	-10.0	7.3	34.0	9.3	-30.9	-29.5
23	2.0	6.9	4.0	3.7	-22.9	-29.6
24	15.0	13.9	2.0	-1.7	-30.9	-24.1
25	8.0	10.5	30.0	24.7	-20.9	-21.0
26	8.0	12.8	20.0	26.3	-33.9	-18.8
27	18.0	12.4	34.0	31.5	-28.9	-18.1
28	5.0	10.7	38.0	28.2	-9.0	-16.2
29	11.0	16.7	15.0	19.9	-17.9	-16.1

Table A.6.4 The result of decomposition result when
using two probes for test no. 11

```

*** Coefficients of error equations.***
c(2)=      -0.13598e-03
c(11)=     -0.95960e-04
c(21)=     -0.18370e-03
c(23)=       0.18718e-05
c(25)=       0.94848e-04
c(30)=       0.84723e-04
c(32)=       0.15401e-03
c(33)=     -0.27705e-04

**Cal. of error difference using cal. coefficients**
no. diff.rx  cal.drx  diff.ry  cal.dry  diff.rz  cal.drz
1      10.0      5.3    -16.0    -9.7    -16.0    -12.2
2       7.0      9.2    -13.0   -13.6    -11.0     -4.7
3      16.0     13.0    -17.0   -17.4     13.0     2.6
4      18.0     18.5    -21.0   -21.2       0.     2.6
5      22.0     24.0    -24.1   -25.0       4.0     2.7
6      38.0     20.2    -23.0   -21.2    -10.0    -4.8
7       6.0     16.4    -10.0   -17.3     -8.0    -12.1
8       5.0     10.9    -13.0   -13.5     -3.0    -12.1
9      10.0     14.5    -19.0   -17.2    -12.0    -5.0

```

Table A.6.5 FORTRAN program to calculate the coefficients of decomposed error component equations for a short probe approach

```

cccccccccccccccccccccccccccccccccccccccccccccccccccccccccccc
c
c
c   This program is to decompose the rel. resultant errors
c   obtained by probing the metrology pallet into the error
c   component equations only to see the variation of relative
c   error component.
c   Constant terms of angular error eq. are not included.
c   Linear positioning error and the Squareness are included.
c
c
cccccccccccccccccccccccccccccccccccccccccccccccccccccccccccc
      real x,y,z,wk,s,tol
      real xo,yo,zo,errorxo,erroryo,errorzo
      real mat,transmat,fainv,errorx,errory,errorz,c
      real cerrorx,cerrory,cerrorz
      integer np,ia,m,n,iainv,ier,nl
      character * 1 al
      dimension al(80)
      dimension x(100),y(100),z(100),errorx(100),erry(100)
      dimension cerrorx(100),cerrory(100),cerrorz(100),errorz(100)
      dimension s(100),wk(100)
      dimension mat(100,50),transmat(50,100),fainv(50,100),c(50)
      double precision a(13,13), ainv(13,13)
      open(unit=3,file="error6.data")
      open(unit=8,file="decomp6.res")

c
c   read the number of points to be used
c
      np = 22
      np2 = 13
      do 3 i= 1, 26
         read(3,2) al
3      continue
2      format(80al)

c
c   read the coordinates and the errors
c
      read (3,110) nl,xo,yo,zo,errorxo,erroryo,errorzo
      do 100 i = 1, np
      read (3,110) nl,x(i),y(i),z(i),errorx(i),erry(i),errorz(i)
         x(i) = x(i) / 1000.
         y(i) = y(i) / 1000.
         z(i) = z(i) / 1000.
         errorx(i) = errorx(i) / 1000000.
         errory(i) = errory(i) / 1000000.
         errorz(i) = errorz(i) / 1000000.

```

Table A.6.5 Continued.

```

110          format (i5,3f10.3,3f10.1)
100  continue
c
c      set up the matrix from the coordinate data
c
      j=0
      do 200 i=1,np*3,3
      j = j + 1
c
c      for the errorx(i)
c
          mat(i,1) = z(j) * x(j) - zo * xo
          mat(i,2) = -x(j) * y(j) + xo * yo
          mat(i,3) = x(j) - xo
          mat(i,4) = 0.
          mat(i,5) = - y(j) * y(j) + yo * yo
          mat(i,6) = 0.
          mat(i,7) = 0.
          mat(i,8) = z(j) * z(j) - zo * zo
          mat(i,9) = -y(j) * z(j) + yo * zo
          mat(i,10) = 0.
          mat(i,11) = 0.
          mat(i,12) = z(j) - zo
          mat(i,13) = -y(j) + yo
c
c      for the errory(i)
c
          mat(i+1,1) = 0.
          mat(i+1,2) = x(j) * x(j) - xo * xo
          mat(i+1,3) = 0.
          mat(i+1,4) = -y(j) * z(j) + yo * zo
          mat(i+1,5) = 0.
          mat(i+1,6) = y(j) - yo
          mat(i+1,7) = -z(j) * z(j) + zo * zo
          mat(i+1,8) = 0.
          mat(i+1,9) = x(j)*z(j) - xo * zo
          mat(i+1,10) = 0.
          mat(i+1,11) = -z(j) + zo
          mat(i+1,12) = 0.
          mat(i+1,13) = -x(j) + xo
c
c      for the errorz(i)
c
          mat(i+2,1) = -x(j)*x(j) + xo * xo
          mat(i+2,2) = 0.
          mat(i+2,3) = 0.
          mat(i+2,4) = y(j)*y(j) - yo * yo
          mat(i+2,5) = 0.

```


Table A.6.5 Continued.

```

      mat(i+2,6) = 0.
      mat(i+2,7) = y(j)*z(j) - yo * zo
      mat(i+2,8) = -x(j)*z(j) + xo * zo
      mat(i+2,9) = 0.
      mat(i+2,10) = z(j) - zo
      mat(i+2,11) = y(j) - yo
      mat(i+2,12) = x(j) - xo
      mat(i+2,13) = 0.
200  continue
c
c  calculate the transposition of a matrix mat(np*3,np2)
c
      do 210 i=1,np*3
          do 210 j=1,np2
              transmat(j,i) = mat(i,j)
210  continue
c
c  initialize the matrix a(i,k) as 0.
c
      do 300 i = 1,np2
          do 305 j = 1,np2
              a(i,j) = 0.
305  continue
300  continue
c
c  set up the matrix to be inversed
c
      do 250 k=1,np2
          do 320 i=1,np2
              do 330 j = 1,np*3
                  a(i,k) = a(i,k) + transmat(i,j)*mat(j,k)
330  continue
320  continue
250  continue
      ia = np2
      m = np2
      n = np2
      tol = 0.
      iainv = np2
      call lginf(a,ia,m,n,tol,ainv,iainv,s,wk,ier)
c
c  calculate the multiplication of inverse matrix of
c  A'*A and A'
c
c
c  initialize the matrix fainv(i,k) as 0.
c

```

Table A.6.5 Continued.

```

do 500 i = 1,np2
  do 505 j = 1,np*3
    fainv(i,j) = 0.
505   continue
500   continue
c
c   set up the matrix multiplied
c
do 610 k=1,np*3
  do 620 i=1,np2
    do 630 j = 1,np2
      fainv(i,k) = fainv(i,k) + ainv(i,j)*transmat(j,k)
630   continue
620   continue
610   continue
c
c   ---calculate the coefficient vector c(i) by
c       Fainv(np2,3*np)*E(3*np,1)
c
do 700 i= 1,np2
  c(i) = 0.
  do 710 j=1,np
    c(i) = c(i) + fainv(i,3*j-2) * errorx(j)
1    +fainv(i,3*j-1) * errory(j) + fainv(i,3*j)*errorz(j)
710   continue
700   continue
c
c   output the result of decomposed values for coefficients
c   of error equations
c
write(8,*) "    *** Coefficients of error equations.***"
write(8,801) c(1)
801   format(/5x,"c(2)= ", e12.5)
write(8,802) c(2)
802   format(5x,"c(4)= ", e12.5)
write(8,804) c(3)
804   format(5x,"c(7)= ", e12.5)
write(8,805) c(4)
805   format(5x,"c(11)= ", e12.5)
write(8,806) c(5)
806   format(5x,"c(14)= ", e12.5)
write(8,808) c(6)
808   format(5x,"c(18)= ", e12.5)

```

AD-A174 974

THE SCIENCE OF AND ADVANCED TECHNOLOGY FOR
COST-EFFECTIVE MANUFACTURE OF (U) PURDUE UNIV
LAFAYETTE IN SCHOOL OF INDUSTRIAL ENGINEERING

4/4

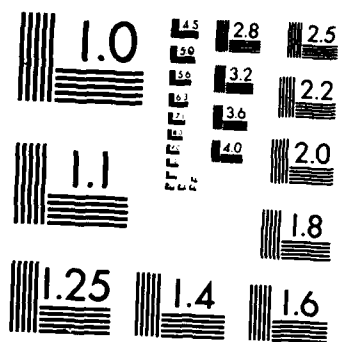
UNCLASSIFIED

S LEE ET AL NOV 86 N00014-83-K-0385

F/G 13/9

NL





MICROCOPY RESOLUTION TEST CHART
NATIONAL BUREAU OF STANDARDS 1963-A

Table A.6.5 Continued.

```

      write(8,809) c(7)
809  format(5x,"c(21)=  ", e12.5)
      write(8,810) c(8)
810  format(5x,"c(23)=  ", e12.5)
      write(8,811) c(9)
811  format(5x,"c(25)=  ", e12.5)
      write(8,813) c(10)
813  format(5x,"c(30)=  ", e12.5)
      write(8,814) c(11)
814  format(5x,"c(32)=  ", e12.5)
      write(8,815) c(12)
815  format(5x,"c(33)=  ", e12.5)
      write(8,816) c(13)
816  format(5x,"c(34)=  ", e12.5)
      write(8,820)
820  format("**Calculation of relative errors using cal.",
1 1 1 'coefficients**")
      write(8,821)
821  format(" no.  rerrorx  cal.ery  rerrory  ",
1 "cal.ery  rerrorz  cal.erz",)
      do 900 i = 1, np

c
c      for the relative errorx(i)
c
      cerrorx(i) =
1      + ( z(i) * x(i) - zo * xo ) * c(1)
1      + ( -x(i) * y(i) + xo * yo ) * c(2)
1      + ( x(i) - xo ) * c(3)
1      + ( -y(i) * y(i) + yo * yo ) * c(5)
1      + ( z(i) * z(i) - zo * zo ) * c(8)
1      + ( -y(i) * z(i) + yo * zo ) * c(9)
1      + ( z(i) - zo ) * c(12)
1      + ( -y(i) + yo ) * c(13)

c
c      for the relative rerrory(i)
c
      cerrory(i) =
1      + ( x(i) * x(i) - xo * xo ) * c(2)
1      + ( -y(i) * z(i) + yo * zo ) * c(4)
1      + ( y(i) - yo ) * c(6)
1      + ( -z(i) * z(i) + zo * zo ) * c(7)
1      + ( x(i)*z(i) - xo * zo ) * c(9)
1      + ( -z(i) + zo ) * c(11)
1      + ( -x(i) + xo ) * c(13)

c
c      for the relative errorz(i)
c

```

Table A.6.5 Continued.

```

      cerrorz(i) =
1      + ( -x(i)*x(i) + xo * xo ) * c(1)
1      + ( y(i)*y(i) - yo * yo ) * c(4)
1      + ( y(i)*z(i) - yo * zo ) * c(7)
1      + ( -x(i)*z(i) + xo * zo ) * c(8)
1      + ( z(i) - zo ) * c(10)
1      + ( y(i) - yo ) * c(11)
1      + ( x(i) - xo ) * c(12)
900  continue
      do 920 i = 1, np
        errorx(i) = errorx(i) * 1000000.
        errory(i) = errory(i) * 1000000.
        errorz(i) = errorz(i) * 1000000.
        cerrorx(i) = cerrorx(i) * 1000000.
        cerrory(i) = cerrory(i) * 1000000.
        cerrorz(i) = cerrorz(i) * 1000000.
        write(8,910)i,errorx(i),ceerrorx(i),errory(i),
1          cerrory(i),errorz(i),ceerrorz(i)
910  format(i3,3x,f6.1,3x,f6.1,2x,f6.1,3x,f6.1,
1        f6.1,3x,f6.1)
920  continue
      endfile(unit=8)
      close(unit=8)
      stop
      end

```

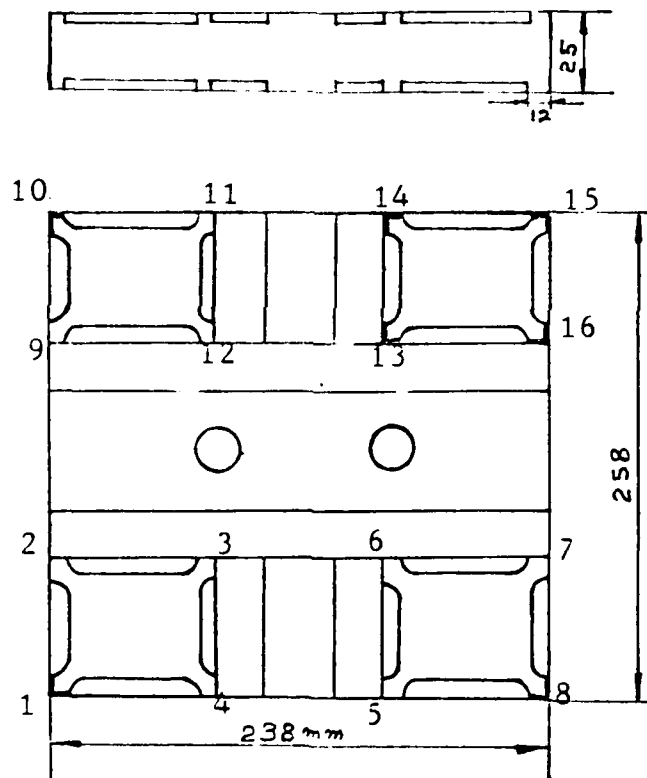
Appendix 7- Analysis Data for Machining Experiment

Figure A.7.1 Numbering system for corners of a work-piece for the machining experiment.

(A) Result for a short probe system:

*Calculated error by probing when the machining experiment is done in the warmed-up condition.

point	x	y	z	errorx	errory	errorz
1	59.691	18.414	498.871	-31.0	23.0	-10.0
2	131.258	18.487	498.775	-28.0	25.0	-25.0
3	61.065	72.765	498.996	-31.0	26.0	-12.0
4	98.231	179.000	415.140	-33.0	46.0	-23.0
5	59.287	291.261	499.021	-31.0	44.0	-15.0
6	97.878	438.903	421.670	-35.0	66.0	-26.0
7	60.197	553.038	498.414	-28.0	71.0	-5.0
8	202.881	480.587	331.381	-26.0	71.0	-25.0
9	331.141	551.981	498.099	-28.0	66.0	-15.0
10	407.694	481.595	332.747	-36.0	66.0	-16.0
11	604.227	551.179	497.581	-33.0	74.0	-38.0
12	630.902	542.698	415.691	-17.0	74.0	-36.0
13	604.130	281.372	497.868	-25.0	45.0	-30.0
14	630.965	315.434	400.878	-26.0	54.0	-43.0
15	631.072	77.527	397.751	-9.9	23.0	-41.0
16	631.074	66.222	430.235	-18.0	31.0	-36.0
17	631.092	51.817	462.120	-26.0	30.0	-33.0
18	601.732	17.819	497.967	-16.0	28.0	-35.0
19	331.997	18.736	498.734	-20.0	25.0	-23.0
20	452.655	215.043	452.618	-28.0	38.0	-28.0
21	363.066	236.793	424.835	-26.0	43.0	-33.0
22	329.495	278.261	498.597	-28.0	46.0	-23.0
23	212.698	215.000	458.922	-28.0	33.0	-15.0

*Calculated coefficients for x error regression function.

c	1	(1)	=	-96.7336
c	1	(2)	=	8.72145
c	1	(3)	=	-2.01300
c	1	(4)	=	26.0379
c	1	(5)	=	-0.390361
c	1	(6)	=	-0.156846
c	1	(7)	=	-1.20160
c	1	(8)	=	-0.105513
c	1	(9)	=	0.560193
c	1	(10)	=	-2.54640

*Calculation of x errors using x error regression function and its residual.

i	errorx(i)	prediction	residual
1	-31.0	-29.2	-1.8
2	-28.0	-27.4	-0.6
3	-31.0	-30.5	-0.5
4	-33.0	-32.6	-0.4
5	-31.0	-32.7	1.7
6	-35.0	-31.4	-3.6
7	-28.0	-28.2	0.2
8	-26.0	-32.3	6.3
9	-28.0	-27.8	-0.2
10	-36.0	-27.7	-8.3
11	-33.0	-28.9	-4.1
12	-17.0	-24.5	7.5
13	-25.0	-27.6	2.6
14	-26.0	-23.4	-2.6
15	-9.9	-16.4	6.4
16	-18.0	-16.8	-1.2
17	-26.0	-17.5	-8.5
18	-16.0	-18.5	2.5
19	-20.0	-23.1	3.1
20	-28.0	-25.4	-2.6
21	-26.0	-26.9	0.9
22	-28.0	-29.4	1.4
23	-28.0	-29.6	1.6

*Calculated coefficients for y error regression function.

c	2	(1)	=	-21.2090
c	2	(2)	=	-13.2845
c	2	(3)	=	13.4810
c	2	(4)	=	29.5681
c	2	(5)	=	2.42012e-02
c	2	(6)	=	-1.46921
c	2	(7)	=	2.18883
c	2	(8)	=	0.457206
c	2	(9)	=	0.384897
c	2	(10)	=	-4.09469

*Calculation of y errors using y error regression function and its residual.

i	errory(i)	prediction	residual
1	23.0	24.3	-1.3
2	25.0	23.2	1.8
3	26.0	27.8	-1.8
4	46.0	41.8	4.2
5	44.0	44.4	-0.4
6	66.0	66.6	-0.7
7	71.0	69.1	2.0
8	71.0	72.0	-1.0
9	66.0	67.8	-1.8
10	66.0	65.8	0.3

11	74.0	73.3	0.8
12	74.0	74.9	-0.9
13	45.0	47.6	-2.6
14	54.0	49.5	4.5
15	23.0	27.2	-4.2
16	31.0	29.0	2.0
17	30.0	29.8	0.2
18	28.0	27.8	0.2
19	25.0	22.8	2.2
20	38.0	39.5	-1.5
21	43.0	41.6	1.4
22	46.0	41.9	4.1
23	33.0	39.8	-6.8

*Calculated coefficients for z error regression function.

c	3	(1)	=	53.6955
c	3	(2)	=	11.0708
c	3	(3)	=	3.41810
c	3	(4)	=	-52.2504
c	3	(5)	=	-0.300667
c	3	(6)	=	-0.461117
c	3	(7)	=	-2.31236
c	3	(8)	=	-0.427376
c	3	(9)	=	9.62395e-02
c	3	(10)	=	7.72286

*Calculation of z errors using z error regression function and its residual.

i	errorz(i)	prediction	residual
1	-10.0	-15.0	5.0
2	-25.0	-16.0	-9.0
3	-12.0	-14.4	2.5
4	-23.0	-26.6	3.6
5	-15.0	-11.6	-3.4
6	-26.0	-21.4	-4.6
7	-5.0	-7.2	2.2
8	-25.0	-21.1	-3.9
9	-15.0	-17.5	2.5
10	-16.0	-22.6	6.6
11	-38.0	-34.2	-3.8
12	-36.0	-37.2	1.2
13	-30.0	-34.5	4.5
14	-43.0	-37.4	-5.6
15	-41.0	-37.3	-3.7
16	-36.0	-38.4	2.3
17	-33.0	-37.7	4.7
18	-35.0	-33.3	-1.7
19	-23.0	-21.0	-2.0
20	-28.0	-30.2	2.2
21	-33.0	-28.6	-4.4

22	-23.0	-19.9	-3.1
23	-15.0	-22.5	7.5

*Calculated error for each corner.

corner	ix3(i)	iy3(i)	ex(i)	ey(i)
1	-13565	-13565	0.0	0.0
2	-13563	83557	-2.1	8.2
3	93564	83559	0.9	5.8
4	93562	-13563	3.4	-2.4
5	149430	-13562	5.0	-3.3
6	149433	83560	2.3	5.0
7	256560	83561	4.9	4.2
8	256557	-13561	8.0	-4.1
9	-13562	174418	-3.1	16.6
10	-13562	271539	-3.1	26.2
11	93566	271541	-1.0	23.9
12	93566	174421	-0.5	14.2
13	149434	174422	0.7	13.4
14	149435	271542	0.1	23.1
15	256563	271543	1.9	22.3
16	256562	174422	2.9	12.6

(B) Result for a two probe system:

*Calculated error by probing when the machining experiment is done in the warmed-up condition.

point	x	y	z	errorx	errory	errorz
1	59.691	18.414	498.871	-31.0	23.0	-10.0
2	59.287	291.261	499.021	-31.0	44.0	-15.0
3	60.197	553.038	498.414	-28.0	71.0	-5.0
4	331.141	551.981	498.099	-28.0	66.0	-15.0
5	604.227	551.179	497.581	-33.0	74.0	-38.0
6	604.130	281.372	497.868	-25.0	45.0	-30.0
7	601.732	17.819	497.967	-16.0	28.0	-35.0
8	331.997	18.736	498.734	-20.0	25.0	-23.0
9	329.495	278.261	498.597	-28.0	46.0	-23.0
10	59.608	18.335	649.123	-20.0	15.0	-7.0
11	59.196	291.184	649.278	-18.0	43.0	-10.0
12	60.100	552.964	648.671	-21.0	68.0	-7.0
13	331.050	551.910	648.348	-35.0	73.0	-31.0
14	604.140	551.103	647.835	-21.0	66.0	-20.0
15	604.041	281.306	648.125	-26.0	40.0	-20.0
16	601.646	17.748	648.224	-33.0	22.0	-25.0
17	331.918	18.660	648.996	-13.0	20.0	-12.0
18	329.404	278.185	648.861	-20.0	46.0	-15.0

*Calculated coefficients for x error regression function.

c	1	(1)	=	20773.9
c	1	(2)	=	-3.24089e-02
c	1	(3)	=	-9.88986e-02
c	1	(4)	=	-73.7476
c	1	(5)	=	-1.17997e-05
c	1	(6)	=	1.64256e-04
c	1	(7)	=	7.84146e-05
c	1	(8)	=	-1.62025e-05
c	1	(9)	=	-2.81256e-06
c	1	(10)	=	6.42564e-02

*Calculation of x errors using x error regression function and its residual.

i	errorx(i)	prediction	residual
1	-31.0	-25.0	-6.0
2	-31.0	-31.5	0.5
3	-28.0	-30.9	2.9
4	-28.0	-29.6	1.5
5	-33.0	-28.6	-4.4
6	-25.0	-24.2	-0.7
7	-16.0	-18.6	2.6

8	-20.0	-23.6	3.7
9	-28.0	-28.0	-0.1
10	-20.0	-21.1	1.1
11	-18.0	-17.9	-0.1
12	-21.0	-22.6	1.6
13	-35.0	-24.2	-10.8
14	-21.0	-30.1	9.1
15	-26.0	-26.7	0.7
16	-33.0	-25.7	-7.3
17	-13.0	-19.1	6.1
18	-20.0	-19.6	-0.4

*Calculated coefficients for y error regression function.

c	2	(1)	=	12489.3
c	2	(2)	=	-4.11034e-02
c	2	(3)	=	4.10085e-03
c	2	(4)	=	-44.1592
c	2	(5)	=	-1.80109e-05
c	2	(6)	=	1.33297e-04
c	2	(7)	=	1.08267e-04
c	2	(8)	=	-1.78512e-05
c	2	(9)	=	2.52873e-05
c	2	(10)	=	3.84182e-02

*Calculation of y errors using y error regression function and its residual.

i	error(y(i))	prediction	residual
1	23.0	22.8	0.2
2	44.0	43.0	0.9
3	71.0	70.3	0.7
4	66.0	70.9	-4.9
5	74.0	70.1	4.0
6	45.0	46.7	-1.7
7	28.0	28.4	-0.4
8	25.0	25.1	-0.1
9	46.0	44.6	1.3
10	15.0	15.8	-0.8
11	43.0	43.3	-0.3
12	68.0	68.8	-0.8
13	73.0	70.1	2.9
14	66.0	67.7	-1.7
15	40.0	42.3	-2.3
16	22.0	19.8	2.2
17	20.0	21.1	-1.1
18	46.0	44.2	1.8

*Calculated coefficients for z error regression function.

c	3	(1)	=	10875.8
c	3	(2)	=	-0.189440

```

c 3 ( 3 ) = 2.29469e-02
c 3 ( 4 ) = -38.5757
c 3 ( 5 ) = -4.85418e-06
c 3 ( 6 ) = -3.76908e-05
c 3 ( 7 ) = 2.49869e-04
c 3 ( 8 ) = 1.91019e-05
c 3 ( 9 ) = -1.70540e-06
c 3 ( 10 ) = 3.36006e-02

```

*Calculation of z errors using z error regression function and its residual.

i	errorz(i)	prediction	residual
1	-10.0	-9.9	-0.1
2	-15.0	-9.8	-5.2
3	-5.0	-6.1	1.1
4	-15.0	-20.8	5.8
5	-38.0	-31.8	-6.2
6	-30.0	-33.2	3.2
7	-35.0	-33.8	-1.2
8	-23.0	-24.9	1.9
9	-23.0	-23.6	0.6
10	-7.0	-8.2	1.2
11	-10.0	-8.0	-2.0
12	-7.0	-12.0	4.9
13	-31.0	-19.7	-11.3
14	-20.0	-25.7	5.6
15	-20.0	-22.6	2.6
16	-25.0	-20.8	-4.2
17	-12.0	-14.2	2.3
18	-15.0	-15.8	0.8

*Calculated error for each corner.

corner	1x3(i)	1y3(i)	ex(i)	ey(i)
1	-13565	-13565	0.	0.
2	-13562	83559	-3.5	5.8
3	93570	83560	-4.6	4.8
4	93566	-13564	-1.0	-0.8
5	149437	-13564	-1.7	-1.4
6	149440	83561	-5.4	4.1
7	256572	83562	-7.1	2.5
8	256568	-13562	-3.3	-2.8
9	-13558	174423	-6.8	11.7
10	-13555	271547	-10.4	18.4
11	93577	271548	-11.7	17.0
12	93573	174424	-8.0	10.5
13	149444	174425	-8.8	9.7
14	149448	271549	-12.6	16.2
15	256580	271551	-14.6	14.2
16	256576	174427	-10.7	8.0

(C) Result for a long probe system:

*Calculated error by probing when the machining experiment is done in the warmed-up condition.

point	x	y	z	errorx	errory	errorz
1	59.608	18.335	649.123	-20.0	15.0	-7.0
2	131.162	18.404	649.029	-10.0	16.0	-12.0
3	60.977	72.686	649.255	-30.0	25.0	-2.0
4	98.134	178.922	565.397	-31.0	41.0	-7.0
5	97.969	203.133	511.823	-31.0	36.0	-18.0
6	59.196	291.184	649.278	-18.0	43.0	-10.0
7	97.784	438.827	571.930	-25.0	63.0	-12.0
8	97.896	483.440	512.687	-25.0	74.0	-5.0
9	60.100	552.964	648.671	-21.0	68.0	-7.0
10	202.792	480.514	481.643	-21.0	79.0	-18.0
11	216.338	422.937	347.757	-8.0	69.0	-28.0
12	200.799	317.225	342.329	0.	77.0	-25.0
13	201.548	287.413	256.081	15.0	33.0	-35.0
14	331.050	551.910	648.348	-35.0	73.0	-31.0
15	407.603	481.524	482.989	-35.0	78.0	-20.0
16	604.140	551.103	647.835	-21.0	66.0	-20.0
17	630.815	542.627	565.943	-3.0	79.0	-28.0
18	604.041	281.306	648.125	-26.0	40.0	-20.0
19	630.374	315.363	551.140	-30.0	51.0	-33.0
20	630.988	77.461	548.010	-21.0	33.0	-31.0
21	631.003	66.151	580.487	0.	23.0	-25.0
22	631.014	51.744	612.374	-20.0	38.0	-31.0
23	601.646	17.748	648.224	-33.0	22.0	-25.0
24	331.918	18.660	648.996	-13.0	20.0	-12.0
25	452.571	214.974	602.872	0.	30.0	-18.0
26	362.983	236.714	575.094	-17.0	38.0	-23.0
27	362.500	270.616	533.532	-15.0	41.0	-22.9
28	329.404	278.185	648.861	-20.0	46.0	-15.0
29	212.615	214.916	609.174	-12.0	26.0	-15.0

*Calculated coefficients for x error regression function.

c	1	(1)	=	93.7982
c	1	(2)	=	13.6196
c	1	(3)	=	-7.30946
c	1	(4)	=	-42.0106
c	1	(5)	=	0.140326
c	1	(6)	=	0.970783
c	1	(7)	=	-1.75095
c	1	(8)	=	-0.378352
c	1	(9)	=	-1.85507e-02
c	1	(10)	=	3.76568

*Calculation of x errors using x error regression function and its residual.

i	errorx(i)	prediction	residual
1	-20.0	-19.2	-0.8
2	-10.0	-18.1	8.1
3	-30.0	-19.7	-10.3
4	-31.0	-23.1	-7.9
5	-31.0	-22.9	-8.1
6	-18.0	-21.9	3.9
7	-25.0	-27.6	2.6
8	-25.0	-29.5	4.5
9	-21.0	-24.7	3.7
10	-21.0	-23.9	2.9
11	-8.0	-7.9	-0.1
12	0.	-4.0	4.0
13	15.0	14.6	0.4
14	-35.0	-20.5	-14.5
15	-35.0	-16.8	-18.2
16	-21.0	-21.9	0.9
17	-3.0	-20.6	17.6
18	-26.0	-21.0	-5.0
19	-30.0	-16.9	-13.0
20	-21.0	-13.9	-7.1
21	0.	-17.0	17.0
22	-20.0	-19.3	-0.7
23	-33.0	-20.4	-12.7
24	-13.0	-17.0	4.0
25	0.	-18.3	18.3
26	-17.0	-18.3	1.3
27	-15.0	-17.1	2.1
28	-20.0	-18.6	-1.4
29	-12.0	-20.3	8.2

*Calculated coefficients for y error regression function.

c	2	(1)	=	-54.1449
c	2	(2)	=	-3.30593
c	2	(3)	=	20.4211
c	2	(4)	=	28.0712
c	2	(5)	=	-0.296058
c	2	(6)	=	-2.25589
c	2	(7)	=	0.466148
c	2	(8)	=	0.238687
c	2	(9)	=	0.737011
c	2	(10)	=	-2.64440

*Calculation of y errors using y error regression function and its residual.

i	errorx(i)	prediction	residual
1	15.0	17.6	-2.6

2	16.0	17.7	-1.7
3	25.0	21.0	4.0
4	41.0	35.2	5.8
5	36.0	40.1	-4.1
6	43.0	39.1	3.9
7	63.0	65.4	-2.4
8	74.0	78.2	-4.2
9	68.0	70.1	-2.2
10	79.0	78.6	0.4
11	69.0	72.6	-3.6
12	77.0	54.3	22.7
13	33.0	43.6	-10.6
14	73.0	67.4	5.6
15	78.0	76.6	1.4
16	66.0	68.2	-2.2
17	79.0	78.4	0.6
18	40.0	40.8	-0.8
19	51.0	51.7	-0.7
20	33.0	30.3	2.7
21	23.0	29.3	-6.3
22	38.0	27.9	10.1
23	22.0	24.4	-2.4
24	20.0	19.3	0.7
25	30.0	36.8	-6.8
26	38.0	39.9	-1.9
27	41.0	45.7	-4.7
28	46.0	37.4	8.6
29	26.0	35.2	-9.2

*Calculated coefficients for z error regression function.

c	3	(1)	=	-76.6257
c	3	(2)	=	-11.2966
c	3	(3)	=	10.6229
c	3	(4)	=	18.3411
c	3	(5)	=	0.112345
c	3	(6)	=	-1.61941
c	3	(7)	=	0.870178
c	3	(8)	=	0.380599
c	3	(9)	=	-0.225330
c	3	(10)	=	-1.05923

*Calculation of x errors using x error regression function and its residual.

i	errorz(i)	prediction	residual
1	-7.0	-5.4	-1.6
2	-12.0	-8.9	-3.0
3	-2.0	-5.5	3.5
4	-7.0	-10.6	3.6
5	-18.0	-12.8	-5.2
6	-10.0	-6.8	-3.2

7	-12.0	-10.1	-1.9
8	-5.0	-10.3	5.3
9	-7.0	-11.3	4.3
10	-18.0	-16.2	-1.8
11	-28.0	-23.7	-4.3
12	-25.0	-26.9	1.9
13	-35.0	-35.9	1.0
14	-31.0	-20.9	-10.1
15	-20.0	-24.9	4.9
16	-20.0	-24.9	4.9
17	-28.0	-26.7	-1.3
18	-20.0	-22.0	2.0
19	-33.0	-28.2	-4.8
20	-31.0	-32.2	1.2
21	-25.0	-28.9	3.9
22	-31.0	-25.9	-5.1
23	-25.0	-22.4	-2.7
24	-12.0	-16.7	4.7
25	-18.0	-22.2	4.2
26	-23.0	-21.2	-1.8
27	-22.9	-23.2	0.3
28	-15.0	-17.1	2.1
29	-15.0	-14.1	-0.9

*Calculated error for each corner.

corner	ix3(i)	iy3(i)	ex(i)	ey(i)
1	-13565	-13565	-0.0	0.
2	-13562	83553	-3.1	12.1
3	93563	83554	2.2	11.3
4	93560	-13565	5.2	-0.5
5	149427	-13564	7.5	-0.5
6	149430	83554	4.7	11.1
7	256556	83554	8.7	11.1
8	256554	-13565	11.4	-0.2
9	-13559	174410	-6.0	24.6
10	-13556	271526	-9.2	39.4
11	93569	271527	-3.6	38.0
12	93566	174411	-0.6	23.5
13	149433	174412	1.9	23.2
14	149436	271528	-1.0	37.5
15	256562	271528	3.3	36.9
16	256559	174412	6.1	22.9

Appendix 8

Project Staff in 1985-1986

Faculty

M. M. Barash, Ransburg Professor of Manufacturing and Professor of Industrial Engineering	Principle Investigator & Project Director
C. R. Liu, Professor of Industrial Engineering	Principal Investigator
K. S. Fu [*] , Goss Distinguished Professor of Engineering (Elec.Eng.)	Faculty Associate
J. Modrey, Professor of Mechanical Engineering	Co-Principal Investigator
A. L. Sweet, Professor of Industrial Engineering	Co-Principal Investigator
W. Stevenson, Professor of Mechanical Engineering	Faculty Associate
W. Johnson ^{**} , Visiting Professor of Industrial Engineering	Faculty Associate
J. L. Batra [†] , Visiting Professor of Industrial Engineering	Faculty Associate

^{*}Deceased April 1985.

^{**}University of Cambridge, England (retired)

[†]Indian Institute of Technology, Kanpur

Graduate Research Assistants

* P. Chen
Y.C. Chou
* G. Eshel
P. Ferreira
* R. Khanna
G. Lang
* S.K. Lee
G.R. Liang
* Y.T. Lin
J. Lopez

A.I. Najashi
* D. Noller
Y.S. Ouyang
U. Roy
S. Shodhan
R. Srinivasan
* R. Venugopal
M.C. Wu
* J. York
Y.C. Yu

* - Graduated

END

1-87

DTIC